Modification and Sequence of tRNAs and mRNAs Impact Translational Speed and Accuracy: Insight into how Purines can Modulate Protein Synthesis

by

Tyler J. Smith

A dissertation submitted in partial fulfillment
of the requirements for the degree of
Doctor of Philosophy
(Chemistry)
in the University of Michigan
2022

Doctoral Committee:

Assistant Professor Kristin Koutmou, Chair
Assistant Professor Sarah Keane
Professor Nils G. Walter
Professor Anthony Antonellis

Tyler J. Smith

Smithtyl@umich.edu

ORCID iD: 0000-0001-8444-6808

Dedication

To my biggest supporter Grace and to all the friends I have made along the way.

Acknowledgements

I would like to acknowledge my partner, Grace Kenney, first and foremost as she kept me motivated and held me accountable through not just my PhD but through life in general. I am a better scientist and human because of her. Working through a graduate career is not always easy and I have had much help, guidance, and support throughout my time at the University of Michigan. In that regard, I would first like to thank my advisor, Professor Kristin Koutmou, who taught me the importance of learning through failure, perseverance, and that it is okay to take ask for help. Without her guidance, I would have drowned in the work a long time ago. I would like to thank the members of my committee, Professor Nils Walter, Professor Sarah Keane, and Professor Anthony Antonellis, who have offered invaluable insight in my PhD work and more importantly reminded me that science is much broader than my little *in vitro* system. Thinking of how my work can fit into the world of translation, cell physiology, and biology as a whole has made my experimental design and analysis all the better.

I would then like to thank all the members of my lab over the years who made my time enjoyable and fruitful, in both academic and personal aspects. Frances, Luke, Laura, Josh, Minli, Rachel, Zezhong, Abby, Olivia, Ryan, Megan, and Julia are among many names who through laughter and camaraderie kept me sane. I would then like to extend personal acknowledgements to a few individuals. Firsty, Dr. Daniel Eyler who taught me how to be a good scientist and whose patience saved me, himself, and everyone else in lab. The knowledge Dan has given me will resound for years to come in my life. Next, I would like to thank Dr. Meredith Purchal who helped me not take life too seriously and to remind me that while science is important – I am

more important. After all, if I cannot laugh at, love, and take care of myself I will not be any use to anyone. Tough love and no shit tolerated go a long way. Then I would like to acknowledge Dr. Jeremy Monroe who suffered through many long days and late nights with me and made it all more bearable. He helped me (and I hope I helped him) think critically and carefully to make sure that our science (in the whole of the lab and field) was transparent and thorough. He also helped me with the trajectory of my life through serious discussions that helped me realize what was important to me. Finally, I would like to thank the person who helped me most of all. My best friend and the greatest scientist I have had the pleasure of working with, Dr. Monika Franco. She kept me sane, kept me happy, and kept me going through "all the things" – big or small. I would not have made it through without her.

On a final personal note, I would like to thank my DnD family, Hannah, Brendan, Emma, Carla, and Monika who let me creatively flourish outside of the lab and not take life seriously. Oh, and of course, as strange as it sounds I would like to thank my cat and dog, Nova and River, who have been the best, most captive audience a candidacy-presentation-poster-seminar-defense preparing scientist could ask for.

Table of Contents

List of Tables

.

List of Figures

List of Appendices

Abstract

The biochemical process of protein synthesis, known as translation, is comprised and dependent upon multiple types of RNA, including ribosomal RNA (rRNA), transfer RNA (tRNA), and messenger RNA (mRNA). While necessary, the importance of structure, sequence, and modification status of these different biomolecules is still being elucidated in the field. This body of work focuses on the roles that sequence and nucleotide modification status, in both tRNAs and mRNAs, have in impacting rates and efficiency of translation to better understand the roles of these biomolecules in peptide synthesis. I developed methodology used through this work, the reconstituted *in vitro* bacterial translation system, which I used to dissect translation down to its components at mechanistic, molecular, and atomic levels. There are known instances of ribosome pausing and slowed elongation rates, involved in protein and mRNA homeostasis, during translation of mRNAs encoding for polybasic peptides. I challenged the dogma that this process was caused by nascent peptide, decoupling and investigating role for individual contributions of mRNA sequence, peptide identity, and tRNA modification status in such synthesis (in the context of poly-lysine synthesis) and I determined that mRNA alone is sufficient to alter elongation rates of the ribosome in these instances. More strikingly, I discovered that when poly(A) is present within such mRNAs the ribosome can exhibit non-canonical translation. I defined a mechanism for this new-found process, deemed ribosome sliding, in which ribosome can lose frame and generating alternative protein products. My work found that this process, as well as other instances of canonical translation, can be perturbed with

either the presence or absence of modifications to mRNA and tRNA species existing at the mRNA-tRNA interfaces within the ribosome. As such, my work serves a solid foundation for probing and investigating the process of translation and other biological process, which is necessary as the field considers the prevalence that RNA sequence and modification have in myriad disease states. To that end, my study of modifications for the purines adenosine (*N6*-methyladenosine [m^6A]) and guanosine (*N1*-methylguanosine [m^1G], *N2*-methylguanosine [m^2G], and *N2,N2*-methylguanosine [m_2^2G]) revealed that modifications to mRNA codons can drastically impact translation rates and efficiency in a position-dependent manner. I found that the presence of m^6A in poly(A) relegates the extent at which the ribosome can slide on the message while guanosine studies suggest that the first two base-pairs between a codon and anticodon need at least 1 either *N1* or *N6* hydrogen bond for effective translation. As such results are also contingent upon the binding capacity of tRNAs, specifically its anticodon, I explored and summarized the known effects that anti-codon stem loop modifications of tRNA have on codon recognition and efficient translation as these concepts had been at a severe deficit in the field and is improved by my work. I specifically detail that ASL modifications are integral for frame maintenance, integral in -1 and +1 programmed ribosomal frameshift (PRF) events, and proper decoding and accommodation during translation. I also show that tRNA modifications are involved in stress-response situations, as is the case of antibiotic stress with hygromycin B, and can impact cross-talk intermolecular tRNA modification levels as well as translocation and cell viability. My work presented highlights the importance that mRNA and tRNA sequence and modification status has in modulating protein synthesis as well as a better understanding of how they do so.

Chapter 1 Assessing the Consequences of mRNA Modifications on Protein Synthesis using *In Vitro* Translation Assays[1]

Work presented in this chapter was published in Methods in Enzymology.

Jeremy G. Monroe[‡], Tyler J. Smith[‡], and Kristin S. Koutmou.

‡ - *The authors contributed equally to this work*

1.1 Introduction

Translation of the genetic code into functional protein molecules is accomplished by the ribosome. The ribosome uses messenger RNAs (mRNAs) as molecular blueprints to direct the rapid and accurate synthesis of proteins. The ability of the cell to faithfully express its genetic code is essential for cellular survival. However, the speed and fidelity of the ribosome is not uniform. Even in healthy cells, amino acids unspecified by the mRNA are incorporated into growing polypeptide chains every 1,000 to 10,000 codons [1]. While most miscoding events are inconsequential for protein function, reductions in translational fidelity can have biological consequences – both perturbing and promoting cellular health. Increases in amino acid substitution levels are deleterious to cellular health and to linked a variety of neurological

[1] In this work, Jeremy Monroe and myself, Tyler Smith, were co-first authors and contributed equally to the conception of this methods paper. The sections (and protocols) I wrote and developed are listed hereafter (with Jeremy's contributions being those not listed – though we both served as general editor's along with our advisor, Kristin Koutmou): *Section 1:* Ribosome Purification, *Section 4:* Preparing aminoacylated tRNA and mRNAs, *Section 5:* Initiation complex formation and amino acid addition reactions, *Section 8:* Quantification and Kinetic Analysis.

disorders (Kapur & Ackerman, 2018)[2,3]. However, under some conditions temporary, modest increases in miscoding transcriptome side enhance cellular fitness under environmental stress [4–6].

Many factors, including the availability of aminoacyl-tRNAs and the post-transcriptional modification status of RNAs in the translational machinery, influence the how accurately ribosomes decode mRNAs [7–11]. Evaluating the impact of individual RNA modifications on translational fidelity is challenging in the context of a cell because modifications are often incorporated into multiple RNAs important for protein synthesis (tRNAs, rRNAs and mRNAs) by the same enzyme. This makes it difficult to deplete RNA modifying enzymes and confidently assign observed changes in protein output to a distinct RNA species. Determining the influence of mRNA modifications on translational fidelity is becoming an important question with the discovery of modifications in mRNA codons, and the incorporation of modified nucleosides into mRNAs in emerging mRNA-based vaccine and therapeutic platforms [12–16].

In vitro and cell free systems to study translation date back to the 1960's when they were used to reveal the triplet codon pattern of the genetic code [17]. Here we discuss the application of a fully reconstituted *E. coli in vitro* translation system to investigate how chemically modified mRNA codons impact ribosome fidelity at the molecular level. This approach has long been used by researchers to discover how the ribosome decodes mRNA codons [18–20]. We present how to purify the individual components required for translation (ribosomes, mRNAs, tRNAs and translation factors), reconstitute active translation complexes from purified components, and perform single turnover assays to assess amino acid incorporation (and misincorporation) by the ribosome (Figure 1).

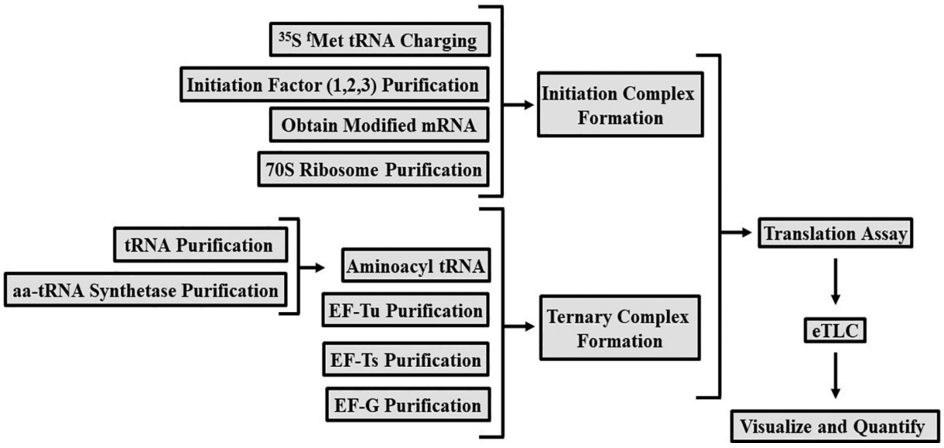

Figure 1.1 *Experimental flowchart for in vitro translation assays.*

While these experiments focus on investigating modifications in mRNAs, the approaches we discuss can also be applied to other aspects of translation.

1.2 In vitro System Chemicals and Equipment and Buffers

Table 1.1 *A table of needed materials both chemical and instrumental in order to prepare and assess miscoding in an prokaryotic in vitro system*

Chemicals	**Equipment**
Tris Base	HPLC (+ Fraction collector)
Luria-Base (LB) Broth	FPLC (+ Fraction collector)
Luria-Base (LB) Agar	Waters XBridge BEH C18 OBD Prep wide pore HPLC column
Luria-Base (LB) Agar	HisTrap FF column, 5 mL
Acetic Acid	Resource Q Column, 5 mL
Magnesium Chloride ($MgCl_2$)	Beckman Coulter Optima XE-90 Ultracentrifuge with zonal setting
Ammonium Chloride (NH_4Cl_2)	Ti-15 Zonal Rotor
Sucrose	Type 45 Ti Fixed-Angle Titanium Rotor
Beta-mercaptoethanol (BME)	Ti45 Polycarbonate Ultracentrifuge tubes
Terrific Base (TB) Broth	Beckman TLA 100 Benchtop Ultracentrifuge (or similar able to spink at 69,000 RPM)
Ethylenediaminetetraacetic acid (EDTA)	TLA-100 Rotor (or comparable)
Pyridine	5 mL polycarbonate Ultracentrifuge tubes
Stoddard Solvent	Teledyne ISCO UA-6 UV/Vis Detector and Type 6 Optical Unit Attachment
Ethanol (EtOH)	French press/Microfluidizer
Liquid Nitrogen	Large Shaking Incubator
Ampicillin	CO8000 Cell Density Meter
E. coli cells with a pUC57 plasmid over expressing tRNA of interest	4 L Erlenmeyer Flasks
E. coli strain MRE600	50 mL conical centrifuge tubes
GTP	15 mL conical centrifuge tubes
Iron (III) Chloride ($FeCl_3$)	Ultracentrifuge tubes
Glycerol	Bio-Rad P6 Spin Columns
Acetic Acid	Micropipettes and filter tips (2, 20, 200, and 1000 µL)

Table 1.2 *Ribosome buffers needed for the purification of 70S ribosomes*

Buffer R-D:

Reagent	Final Concentration
Tris HCl, pH 7.5	20 mM
NH4Cl	500 mM
MgCl2	10 mM
EDTA	0.5 mM
Sucrose	1.1 M

Buffer R-60:

Reagent	Final Concentration
Buffer R-O (10X)	1X
Sucrose	60% (w/v)
BME	3mM

Buffer R-10: 1X Buffer R-O, 10% w/v sucrose, 3 mM BME

Reagent	Final Concentration
Buffer R-O (10X)	1X
Sucrose	10% (w/v)
BME	3mM

Buffer R-O (10X):

Reagent	Final Concentration
Tris HCl, pH 7.5	200 mM
NH4Cl	600 mM
MgCl2	52.5 mM
EDTA	2.5 mM

Buffer R-50:

Reagent	Final Concentration
Buffer R-O (10X)	1X
Sucrose	50% (w/v)
BME	3mM

Buffer R-40:

Reagent	Final Concentration
Buffer R-O (10X)	1X
Sucrose	40% (w/v)
BME	3mM

Buffer R-A

Reagent	Final Concentration
Tris HCl, pH 7.5	20 mM
NH4Cl	100 mM
MgCl2	10 mM
EDTA	0.5 mM
BME	6 mM

Table 1.3 *Buffers required to purify native tRNA*

tRNA Growth Media	
Reagent	Concentration
Terrific Broth (TB)	25 g/L
Glycerol	5 g/L
NH_4Cl	50 mM
$MgSO_4$	2 mM
$FeCl_3$	0.1 mM
Glucose	0.05% (w/v)
Lactose (if using autoinduction)	0.2% (w/v)

Buffer A (IEX)	
Regent	Final Concentration
NH_4OAc	50 mM
NaCl	300 mM
$MgCl_2$	10 mM

Buffer B (IEX)	
Regent	Final Concentration
NH_4OAc	50 mM
NaCl	800 mM
$MgCl_2$	10 mM

HPLC Buffer A, pH 5	
Reagent	Final Concentration
NH_4OAc	20 mM
$MgCl_2$	10 mM
NaCl	400 mM

HPLC Buffer B, pH 5	
Reagent	Final Concentration
NH_4OAc	20 mM
$MgCl_2$	10 mM
NaCl	400 mM
Methanol	60%

5x KF Buffer	
Reagent	Final Concentration
HEPES	0.5 M
KCl	0.05 M
$MgCl_2$	0.1 M
H_2O	to 1 mL

Extraction Buffer, pH 7	
$Mg(OAc)_2$	20 mM
Tris-HCl	20 mM

Table 1.4 *Buffers needed for miscoding assays*

5x Charging Buffer	
Reagent	**Final Concentration**
HEPES	0.5 M
KCl	0.05 M
$MgCl_2$	0.1 M
H_2O	to 1 mL

10x Translation Buffer	
Reagent	**Final Concentration**
Tris-Cl pH 7.5	0.5 M
NH_4Cl	0.7 M
KCl	0.3 M
MgCl2	0.07 M
BME	0.05 M
H_2O	to 1 mL

Table 1.5 *Possible buffers conditions for proper separation in an eTLC system*

eTLC Buffers		
pH	**Contents**	**Volume in 3L (final volume)**
1.9	formic acid/acetic acid	60mL/240mL
2	formic acid	80 mL
2.5	acetic acid	200 mL
2.8	pyridine/acetic acid	15 mL /600 mL
3.5	pyridine/acetic acid	6.6 mL/66 mL
3.6	ammonium formate/formic acid	6.3g/10ml
3.7	2M citric acid/1N sodium hydroxide	40 mL/67 mL
4.5	acetic acid/sodium acetate/EDTA	9.4 mL /10.3g/1.3g
5.3	pyridine/acetic acid	20mL/8mL
6	acetic acid/pyridine	14mL/136mL
6.4	pyridine/acetic acid	200mL/8mL
8.6	barbitone/sodium diethylbarbitone	3.3g/25.5g
9.2	sodium borate	38g

1.3 Section 1: Ribosome Purification

Zonal centrifugation of crude *E. coli* cell lysate yields fractions of 30S and 50S ribosomal subunits, 70S ribosomes and polysomes. We use a linear sucrose gradient to purify coupled 70S ribosomes and separate the 30S and 50S subunits. We find that standard double pelleting ribosomes yields materials of insufficient purity for our assays [21].

1.3.1 Protocol

Day 1

1. Streak MRE 600 cells onto an LB-agar plate without antibiotic and incubate overnight at 37°C. *E. coli* MRE 600 is the strain of choice ribosome growth because it lacks Ribonuclease I and has negligible nuclease activity [22].

Day 2

2. Inoculate 50 mL of LB media with a single MRE600 colony. Grow overnight (~16 hours) in a shaker-incubator at 37ºC, 220 rpm.

Day 3

3. Prewarm 6 x 4L flasks containing 1L of LB media. Add 5 mL of the MRE600 overnight culture to each flask. Shake and incubate at 37°C, 220 rpm.

4. While the cultures grow, prepare an ice bath for the 4 L flasks.

5. Once the cultures reach an OD600 of 0.6, transfer them to the ice bath for 20 minutes.

6. Spin the chilled cultures at in a JLA-8.100 rotor at 4,000 RPM, 4ºC for 15 minutes. Combine the cell pellets in a 50 mL conical tube. Either store at -80°C, or continue to step 7.

7. Resuspend pellet in ~50 mL of cold Buffer R-A. Lyse cells by microfluidizer or French-Press.

8. Clarify lysate by centrifugation. Spin in a JA-20 rotor at 16,000 RPM, 4º C for 30 minutes.

9. While the lysate spins, prepare sucrose cushions by filling 4-6 Ti45 ultracentrifuge tubes with 35 mL of Buffer R-D. Chill on ice.

10. Discard the pellet. Filter supernatant through a 0.22 μM PES syringe filter.

11. Add cold Buffer R-A to bring the filtered supernatant volume to 100 mL.
12. Slowly pour (layer) 25 mL of the supernatant onto the pre-chilled Buffer R-D in Ti45 ultracentrifuge tubes. Balance centrifuge tubes with Buffer R-A.

13. Centrifuge tubes in a Ti45 Ultracentrifuge rotor at 37,000 x RPM, 4°C for 18 hours. Use the slowest acceleration and deceleration setting available on the centrifuge.

Day 4

14. Remove supernatant and rinse each pellet with ~50 □L of cold Buffer R-A.

15. Add 400 µL of Buffer R-A and resuspend pellets in the centrifuge bottles by orbital shaking at 120 rpm, 4ºC for 2 hours.

16. Prepare, filter (0.22 µM PES) and chill (store at 4ºC) Buffer R-O, Buffer R-5, Buffer R-10, Buffer R-40, Buffer R-50, and Buffer R-60. Add BME only after filtering.

> **Note*: make enough R-10 and R-40 to fill your zonal rotor (~1.85 L for the Ti-15 zonal rotor used here).

17. While the pellets resuspend, generate a sucrose gradient in the chilled Ti-15 zonal rotor. Using a gradient maker, begin slowly loading Buffer R-10 via the loading/unloading device (rotor specific). A peristaltic pump can be used to automate buffer loading. After adding ~250 mL of Buffer R-10, begin slowly adding Buffer R-40 into Buffer R-10 to create a 10-40% sucrose gradient. Keep stirring to ensure proper mixing of sucrose to form desired gradient. After R-40 is loaded, add Buffer R-50 (~100 mL) until sucrose solution begins coming out of the top of the rotor or loading device to ensure rotor is completely filled. Keep the rotor and centrifuge

chilled at 4°C and 3,000 RPM.

18. Clarify resuspended pellets (from step 15) by centrifuging in a benchtop microfuge at 14,800 RPM for 1 minute.

19. Combine the ribosome-containing supernatants in a 50 mL conical tube on ice. Make a 1:1,000 dilution of the supernatant and measure (in triplicate) the absorbance readings at 260 nm.

20. Dilute supernatant to ~ 30 mL in cold Buffer R-5. Load onto the top of the sucrose gradient in the zonal rotor (step 17) via the loading/unloading device. For best results, load using a 50 mL syringe.

21. Use a 50 mL syringe to slowly add 30 mL of cold Buffer R-O to the top of the gradient in the zonal rotor via the loading/unloading device. This will fully displace the ribosome suspension onto the sucrose gradient.

22. Spin the zonal rotor at 28,000 RPM, 4°C for 19 hours. After 19 hours the centrifuge should not stop, but be programmed to transition to spin at 3,000 RPM, 4°C.

> *Note:* check if your zonal rotor has different cap components for loading/unloading and higher speed centrifugation, as these caps may need to be changed.

Day 5

23. Attach a UA-6 UV spectrophotometer to the loading/unloading device for the zonal rotor to follow ribosome unloading at 260 nM.

24. Slowly unload the rotor by adding Buffer R-50 (as described in step 17). After adding ~250 mL, begin mixing Buffer R-60. Collect 15-50 mL fractions in conical tubes when UV peaks are observed. Label tubes with fraction number, place on ice.

25. Take 100 µL of each fraction of interest and extract with 500 µL Buffer R-Extraction. Phenol-chloroform extract the solution and ethanol precipitate the aqueous phase samples with 2.5 volumes of ethanol for 15 minutes on ice.

26. Centrifuge samples for 15 minutes in a benchtop microfuge at maximum speed. Remove supernatant and wash pellets with 70% ethanol. Resuspend pelleted fractions in 25 µL of MilliQ H_2O.

27. Mix up to 2 µg from extracted samples with 2X formamide RNA loading dye and heat denature at 95°C for 10 minutes. Run samples on a 5% denaturing PAGE gel and visualize by UV shadowing or methylene blue staining. Fractions containing 70S ribosomes will have 2 predominant bands corresponding to the 16S and 23S rRNA.

28. Pool the fractions (from step 24) that contain 70S ribosomes. Measure and record the absorbance of the pooled sample at 260 nm.

29. Place 70S ribosomes into chilled Ti-45 centrifuge tubes. Balance tubes with Buffer R-A and spin at 37,000 X RPM, 4°C for 18 hours. Use the slowest possible acceleration and deceleration settings.

Day 6

30. Remove the supernatant from tubes, taking care because the ribosome pellet is glassy and not well attached. Gently resuspend the pellets using a total of 2-5 mL of Buffer R-A. Do not pull the ribosome pellet up into the pipette tip, instead repeatedly (~50 times) rinse over the pellet buffer until resuspended.

31. Measure the absorbance of the pooled ribosomes at 260 nm and calculate the concentration ($\varepsilon = 6.94 \times 10^7\ M^{-1}cm^{-1}$). Aliquot (50-100 μL) ribosomes and flash freeze in liquid nitrogen and store at -80°C.

1.4 Section 2: Translation Factor Purification

A single round of translation involves a host of translation factor proteins. At a minimum, initiation factors 1, 2, and 3 (IF1, IF2, IF3), ^{f}methionyl-tRNA formyltransferase (MTF), aminoacyl-tRNA synthetases (AA-RSs) and elongation factor-Tu (EF-Tu) are required for the reconstituted bacterial translation system to function. Additional protein factors, including elongation factor thermal stable (EF-Ts) and elongation factor -G (EF-G), are needed if more than one round of amino acid addition is desired. We purify translation factor proteins from His-tagged plasmids available from AddGene. Multiple expression and purification protocols for translation factors can be found in the literature, and are therefore not included here [9] [23] [24] [25] [26] [27].

1.5 Section 3: Purification of Natively Modified tRNA

Transfer RNAs (tRNAs) contain multiple post-transcriptional modifications important for their function. While T7 transcribed tRNAs can be used for reconstituted translation assays, these tRNAs often exhibit reduced speeds and accuracy in translation reactions compared to their natively modified counterparts [7] [11]. Below we describe the large-scale purification of individual natively modified *E. coli* tRNAs.

1.5.1 Protocol

Day 1 – Transform tRNA plasmid

1. Transform a pUC57 plasmid containing an *E. coli* tRNA sequence of interest (e.g. $tRNA^{Phe}$) into HB101 cells. Grow overnight on an LB-ampicillin agar plate at 37°C.

Day 2 – Overnight culture

2. Inoculate 5 mL of LB-ampicillin media with a single tRNA-expressing colony. Shake for ~16 hours at 37ºC and 220 rpm.

Day 3 – Large scale expression of tRNA

3. Add 400 µg/mL ampicillin to 1 L of enriched TB media. Inoculate TB media with 5 mL of the starter culture from Day 2 (see for details see [28]).

4. Grow cells ~ 16-18 hours in a shaker incubator at 37 °C and 220 rpm.

Day 4 – Isolate tRNA from cells

5. Harvest cells by spinning in a JLA-8.100 rotor at 4,000 RPM, 4 °C for 30 minutes.

6. Pour off supernatant and weigh the cell pellet(s). Pellets can be stored at -80 °C, or extracted as described below.

7. For each cell pellet gather 2 x 250 mL Teflon centrifuge bottles with ETFE O-rings. Label the centrifuge bottles A, B.

8. Resuspend each cell pellet in extraction buffer (200 mL buffer / 25 g cells).

9. Place resuspended cells in Teflon centrifuge bottle A.

10. Add a 1:1 volume ratio of RNase free acid phenol: chloroform (5:1), pH 4.3.

11. Tape centrifuge bottle A horizontally in a shaker-incubator. Shake at 4°C and 200 rpm for 1 hour.

12. Remove the cells from the shaker-incubator. Separate the aqueous and phenol layer by centrifuging the bottles in an A-4-44 swinging bucket rotor with 250 mL bottle adaptors at 5,000 RPM for 1 hour, 4 °C. There will be three layers: brown (bottom, cell debris), thin white (middle, lipids), and transparent (top, aqueous).

13. Use a 25 mL glass pipette to transfer the aqueous layer from tube A to tube B, avoiding the lipid the layer. Add 1:1 ratio of chloroform.

14. Add 100 mL of tRNA extraction buffer to solution remaining in tube A. Shake the tubes for 30 seconds in a fume hood.

15. Spin tubes A and B at A-4-44 swinging bucket rotor at 5,000 RPM, 4° C for 1 hour.

16. Transfer the top layer from tube B to a collection tube. Move the top layer of tube A to tube B.

17. Shake tube B for 30 seconds by hand in a fume hood, then spin in a A-4-44 swinging bucket rotor at 5,000 RPM, 4 °C for 1 hour.

18. Collect the top layer from tube B and combine with the top layer from tube A in a 500 mL JA-10 centrifuge tube.

19. To the contents of the JA-10 tube, add NaOAc, pH 5.2 to 0.3 M (final) and 100% Isopropanol to 20% (final volume). Shake for 30 seconds.

20. Centrifuge in a JA-10 rotor at 9,000 RPM, 4 °C for 1 hour. A small DNA pellet will be visible following centrifugation.

21. Transfer the supernatant to another 500 mL JA-10 tube. Increase the amount of isopropanol in the solution from 20% to 60% (final). Mix by shaking.

22. Precipitate tRNA at -20° C for at least 2 hours.

Day 4 – Deacylated tRNA

23. Centrifuge the tRNA precipitant solution in a JA-10 rotor at 9,000 RPM, 4° C for 1 hour.

24. Discard the supernatant and resuspend the pellet in 10 mL of 200 mM Tris-Acetate, pH 8.0.

25. De-acylate tRNA by taping centrifuge bottles horizontally in a shaker-incubator at 37 °C and 220 rpm for at least 30 minutes.

26. Adding NaOAc to 0.3 M (final concentration) and 2.1 volumes of 100% ethanol to the deacylated tRNA and precipitate overnight at -20ºC.

Day 5 – FPLC purification

27. Spin precipitated deacylated tRNA in a JA-10 rotor at 9,000 RPM, 4°C for 1 hour.

28. Wash the pellets with 70% ethanol. Resuspend tRNA in 5 mL of MilliQ H_2O.

29. Filter tRNA with a 0.22 μm syringe filter.

30. Load the filtered tRNA onto 5 mL ResourceQ ion exchange column equilibrated with Buffer A on an FPLC.

31. Monitor column flow through at multiple absorbance readings (A260, A280 and A230) if possible because the tRNA may saturate the detector. Wash the column with Buffer A until the A260 reading returns to zero.

32. Elute over a linear gradient to 100% Buffer B with >15 column volumes, collecting 1.5 mL fractions.

33. Ethanol precipitate the fractions of interest overnight at -20 °C by adding 1 □L glycoblue/1.5 mL of fraction, 0.3 M NaOAc (final) and 2.1V 100% ethanol.

Day 6 – Selecting tRNA fraction

34. Spin down the ethanol precipitated tRNA at maximum speed in a refrigerated micro-centrifuge set 4°C for 45 minutes.

35. Wash the pellets with 70% ethanol and resuspend in ~20-50 □L MilliQ H_2O.

36. Estimate the tRNA concentration via absorbance at 260 nm (□ = 76,000 $M^{-1} \cdot cm^{-1}$).

37. Since tRNA can distributed throughout the peak, the ability of the components of each fraction to be aminoacylated with the amino acid of interest should be evaluated. An example of a test aminoacylation reaction is given in Table 1 (6) for $tRNA^{Phe}$. A control (null) aminoacylation reaction with no tRNA included should be performed in parallel. Aminoacylation reactions should be run for 30 minutes at 37°C.

Table 1.6 *Example conditions for $tRNA^{Phe}$ aminoacylation reaction*

Reagent	Final concentration
H_2O	to 20 µL
Charging Buffer	1 ×
DTT	1 mM
ATP	10 mM
^{14}C-Phe	19.7 µM
Phe	80 µM
tRNA in fraction (estimated from A260)	5 µM
Phe-RS	1 ×

38. While the aminoacylation reaction is running, chill 50 mL of 10% TCA and 50 mL of 100% ethanol for 30 minutes.

39. After the reactions are complete, remove 1 µL from each reaction and spot on a piece of Whatman paper. Measure the input cpms by scintillation counting.

40. To the reaction mixtures Add 5 µL of heat denatured 10 mg/µL carrier DNA (e.g. calf thymus DNA).

41. Add 500 µL of chilled 10% TCA and pipette to mix. Place the TCA/reaction mixture on ice for 10 minutes.

42. While the TCA/aminoacyl-tRNA reaction mixtures incubate, set up a vacuum flask apparatus with microfiber glass filter paper.

43. After 10 minutes pre-wet the filter with 1 mL of cold 10% TCA and add the TCA/aminoacyl-tRNA reaction mixture to the filter.

44. Wash the precipitated aminoacyl-tRNA twice with 1.5 mL cold 10% TCA.

45. Rinse the filter with 2 mL of cold 100% ethanol.

46. Dry the filter and wash the edges of the filter paper with ethanol to remove any residual contaminates.

47. Remove the filter and measure the output counts (cpms) in a scintillation counter.

48. Use the input cpms and the concentration of unlabeled amino acid (e.g. Phe) added to the reaction to calculate the cpm/pmol for each fraction, in Equation 1.

$$cpm/_{pmol} = \frac{Input\ cpm}{Input\ amino\ acid\ concentration\ (uM)} \quad (1.1)$$

49. Next determine the pmols of Phe in the output, in Equation 2.

$$pmols\ amino\ acid\ output = \frac{(Output\ cpm - Null\ output\ cpm)}{\left(cpm/_{pmol}\right)} \quad (1.2)$$

50. Calculate the concentration of amino acid output by using Equation 3:

$$amino\ acid\ output\ (uM): \frac{pmol\ amino\ acid\ output}{reaction\ volume\ (19\ uL)} \quad (1.3)$$

51. Determine the percent charging with Equation 4:

$$\frac{Output\ amino\ acid\ concentration\ (uM)}{Input\ tRNA\ concentration\ (uM)} \times 100\% \quad (1.4)$$

52. Fractions with greater than 50% charging should be pooled and further purified.

Day 7- HPLC purification

53. Pre-equilibrate a Waters XBridge BEH C18 OBD Prep wide pore column with Buffer A.

54. Inject filtered tRNA sample onto the column on an HPLC.

55. Elute purified tRNA by setting the HPLC to run the program below. Monitor tRNA elution at 260 nm and 280 nm. Set the fraction collector to collect peaks (peak defined as a change of 50 mAU).

- **a)** Flow rate: 3.75 mL/min
- **b)** Inject
- **c)** Linear gradient to 35% buffer B over 35 minutes
- **d)** Linear gradient to 100% B over 5 minutes
- **e)** Hold 100% buffer B for 10 minutes
- **f)** Linear gradient to 0% buffer B over 1 minute

56. Pool the fractions of interest and buffer exchange into water with a 15 mL Amicon Ultra centrifugal filter (10K MWCO).

57. Ethanol precipitate pooled fractions of interest.

58. Estimate concentration via absorbance at A260 (ε = 76,000 $M^{-1} \cdot cm^{-1}$). Concentrate tRNA to ~100 µM by spinning in a 15 mL Amicon Ultra centrifugal filter (10K MWCO) if necessary.

59. Measure the absorbance of 1 µL of purified tRNA at 260 nm – this the A260/µL value required later for the calculation of acceptor activity.

Day 8 – Calculating tRNA acceptor activity

60. Prepare three reactions (Null, S100, and AA-RS) in triplicate to determine the purified tRNA acceptor activity. An acceptor activity greater than 1000 pmols/A260 unit is desired. An A260 unit is the amount of nucleic acid contained in 1 mL and producing an OD of 1 at 260 nm.

Follow the same reaction steps and calculation as a test charging reaction (steps 37-51)

Table 1.7 *tRNA acceptor activity assays. Assays should include a positive control (S100) and a Null control.*

RS Charging reaction		**S100 Charging reaction**		**Null charging reaction**	
Reagent	**Final concentration**	**Reagent**	**Final concentration**	**Reagent**	**Final concentration**
H_2O	to 20 µL	H_2O	to 20 µL	H_2O	to 20 µL
Charging Buffer	1 ×	Charging Buffer	1 ×	Charging Buffer	1 ×
DTT	1 mM	DTT	1 mM	DTT	1 mM
ATP	10 mM	ATP	10 mM	ATP	10 mM
^{14}C-Phe	19.7 µM	^{14}C-Phe	19.7 µM	^{14}C-Phe	19.7 µM
Phe	80 µM	Phe	80 µM	Phe	80 µM
Phe tRNA fraction	5 µM	Phe tRNA fraction	5 µM	Phe tRNA fraction	0 µM
Phe RS	1 ×	S100	1 ×	Phe RS	1 ×

61. Determine aminoacylation acceptor activity for the S100 and RS reactions with Equation 5.

$$Acceptor\ Activity\ = \frac{Average\ pmols\ of\ Phe\ output}{\left(uL\ of\ tRNA\ used\ in\ reaction \times \frac{A260}{1\ uL\ of\ tRNA}\right)} \times 1000 \qquad (1.5)$$

62. Compare extent of the aminoacylation in the RS and S100 reaction. Use the higher value of acceptor activity as the measure of tRNA purity

1.6 Section 4: Preparing Aminoacylated tRNAs and mRNA

Aminoacylated-tRNAs are prepared using purified aminoacyl-tRNA synthetases (AA-RS) as previously described [29]. mRNAs used in these studies have the following sequence: 5' –

GGUGUCUUGCGAGGAUAAGUGCAUUAUGXXXUAA GCCCUUCUGUAGCCA– 3' with XXX denoting the codons positioned in the ribosome A site. Unmodified mRNAs are generated by transcription with T7 polymerase. Chemically modified mRNA can be purchased from Dharmacon, Keck and IDT, or prepared by ligation as previously described [30]. UHPLC MS/MS can be used to verify the abundance but not the position of mRNA modification incorporation in commercially prepared mRNAs [9].

1.7 Section 5: Initiation complex formation and Amino Acid Addition reactions

The first step in assembling active *in vitro* translating ribosomes is to form initiation complexes (ICs). ICs consist of 70S ribosomes bound to mRNA with ^{35}S-^{f}Met-tRNA^{fMet} in the P site and can be stored at -80°C for ~3-6 months. To perform reactions, the ICs are mixed with ternary complexes (TCs) assembled immediately before the translation reactions are started. Reactions can be performed either by hand, or on a rapid quenching device (quench-flow) depending on the time-frame of the experiment. When planning experiments note that different quenching methods consume varying amounts material per timepoint (i.e. ~1 μL of IC/TC mixture per timepoint for benchtop assays vs. ~15 μL per timepoint for quench-flow).

1.7.1 Protocol

Before forming ICs and carrying out translation reactions have following components available: 1M KOH, 10X translation buffer, 10 mM GTP, 70S ribosomes, ^{35}S-^{f}Met-tRNA^{fMet}, aminoacyl-tRNA of interest, IF-1, IF-2, IF-3, EF-Tu, EF-G and mRNAs (see sections 1-4).

Part 1 - Assemble 70S E. coli Initiation Complexes (ICs)

1. Prepare a 10X mix of Initiation Factors (IFs) containing 20 μM (each) of IF-1, IF-2, and IF-3 in 1X Translation buffer. Place the IF mixture on ice.

2. Assemble ICs by mixing components and *gently* pipetting up and down: 1X Translation Buffer, 1 mM GTP, 1X IF mixture, 2 μM mRNA, 1 μM 70S Ribosomes and 2.5 μM ^{35}S-methionine-tRNA^{f}Met. Add ^{35}S-^{f}Met-tRNA^{fMet} and 70S ribosomes to the tube last.

3. Incubate IC mixture at 37ºC for 30 minutes. Pellet ICs for higher concentrations as described below and store at -80°C, or proceed directly to Part 3 – Ternary Complex Formation. Pelleting removes unbound ^{35}S-^{f}Met-tRNA^{fMet} and is recommended.

4. If pelleting ICs, pre-chill TLA 100.3 rotor and benchtop ultracentrifuge (such as a TLA-100) to 4°C. Additionally, add 1 mL cold Buffer R-D to 5 mL polycarbonate ultracentrifuge tubes and chill on ice.

Part 2 (recommended optional step) - Pellet ICs

5. After IC formation, remove 1 μL of IC and dilute in 9 μL of H_2O. Spot 1 μL of the dilution onto Whatman filter paper and measure the ^{35}S counts (cpm) by scintillation counting. This measurement is needed to eventually calculate the final concentration of the pelleted, resuspended ICs.

6. Stabilize ICs for pelleting by raising the final concentration of Mg^{2+} to 12 mM using $MgCl_2$. Remember that 1X Translation Buffer already contains 7 mM Mg^{2+}.

7. Layer IC onto chilled Buffer R-D prepared in step 4. Place tubes in a cold TLA 100.3 rotor and spin at 69,000 X RPM, 4º C for 2 hours in a benchtop ultracentrifuge.

8. Immediately following centrifugation, place the tubes on ice.

9. Gently remove the supernatant. The pellet is glassy, fragile, and often poorly attached to the tube.

10. Resuspend each pellet in the minimum amount of 1x Translation Buffer possible (~20-100 µL). For best results, resuspend pellet by *gently* pipetting the Translation Buffer up and down slowly (up to 50 times). Avoid making the ribosome suspension bubbly.

11. Spot 1 µL of the resuspended IC onto Whatman filter paper and measure the ^{35}S counts (cpm) by scintillation counting. Aliquot the remaining pelleted IC into 5-50 µL samples, freeze in liquid N_2 and store at -80ºC.

12. Calculate percent yield, Equation , for IC formation and pelleting the equation below. A good efficiency to aim for is ≥ 60%.

$$Percent\ Yield = \frac{\left(\frac{cpm\ of\ resuspended\ pellet}{vol.of\ pellet\ counted\ by\ scintillation}\right) * vol.of\ resuspended\ pellet}{\left(\frac{cpm\ of IC\ formation\ reaction}{vol.of\ IC\ counted\ by\ scintillation}\right) * vol.used\ in\ IC\ formation} \quad (1.6)$$

13. Calculate the IC concentration using the following equation:

$$[IC] = \frac{[70S\ Ribosomes]}{\left(\frac{cpm\ of\ IC\ formation\ reaction}{vol.of\ IC\ counted\ by\ scintillation}\right)} * \left(\frac{cpm\ of\ resuspended\ pellet}{vol.of\ pellet\ counted\ by\ resuspension}\right) \quad (1.7)$$

Part 3 - Ternary complex (TC) formation

In contrast to ICs, TCs cannot be preassembled and frozen. The previously prepared protein and

nucleic acid component of TCs (EF-Tu, EF-G and aminoacylated tRNAs) should be thawed on ice.

14. Prepare an "EFTu mix" containing final concentrations of 1X translation buffer, 10 mM GTP and 20 μM EFTu. Incubate EFTu mix at 37°C for 15 minutes. The volume of EFTu mix required will vary depending on the scale of the experiment and should be ~1/3 of the total volume of the planned translation assay.

15. While the EF-Tu mix is incubating, prepare a "tRNA mix" containing final concentrations of 1X translation buffer, 10 mM GTP, 10-20 μM aa-tRNA^{aa}. If your investigations involve the formation of more than a single peptide bond, include 24 μM EFG in the tRNA mix to enable translocation. Keep tRNA mix on ice for 10-15 minutes. The volume of tRNA mix required will vary depending on the scale of the experiment and should be ~1/3 of the total volume of the planned translation assay.

16. Form ternary complexes (TCs) by combining equal volumes of the EFTu mix and tRNA mixes and incubating at 37°C for 10 minutes.

Part 4 - Amino acid addition time courses

17. Before running reactions decide on a set of 8-12 timepoints. If your reaction is are slow enough to stop timepoints by hand (3 seconds or longer) prepare a series of quench tubes containing 1 μL KOH prior to beginning assays. If the timepoints are fast enough to need a quench-flow apparatus (e.g. KinTek Model RQF-3) load 1M KOH as the quench.

18. If using frozen ICs, thaw on ice. Make a 160-180 nM solution of ICs in 1X translation buffer for use in your reaction. Immediately freeze any remaining thawed IC.

19. Initiate translation reactions by mixing equal volumes of ICs and TCs. For reactions performed on the benchtop that is quenched by hand, this usually means mixing 4-6 □L of ICs with TCs to make a 8-12 μL reaction. Much larger volumes (> 120 μL of IC and TC) are required for experiments conducted on the quench flow. Reactions can be carried out at room temperature or 37°C.

20. For slower reactions performed on the bench-top, transfer 1 μL of translation reaction to a KOH quench tube prepared in step 17 at each of the pre-selected time points. Review your quench-flow manual for information about how to quench time points 3 seconds or faster.

22. Quenched timepoints can be stored at -20°C or worked up as described in section 7.

> *Note*: If storing samples for extended periods of time, consider neutralizing timepoints with acetic acid.

1.8 Section 6: Miscoding Screening Assays

Miscoding screening assays use the endpoint level of overall miscoded dipeptide product to evaluate if a modification alters the fidelity of amino acid incorporation. Screening assays are much like the general translation assays described in section 5, only TCs are formed with a mixture of aminoacylated total-tRNA. Controls should be run concurrently to confidently identify the miscoded dipeptide products. Specifically, make sure to include: 1) a null reaction performed with TCs formed without any aminoacyl-total tRNA, 2) a positive control with the correctly charged aminoacyl-tRNA, and 3) a reaction with ICs formed on mRNA with an unmodified codon. These assays only provide qualitative insights and results should be verified with the careful kinetic assays presented in section 6.2.

1.8.1 Protocol

Part 1- Aminoacylate total tRNA

1. Aminoacylate total tRNA by combining, in order, the following reagents (final concentrations given) on ice: MilliQ H_2O, 1X buffer KF, 0.1 mM amino acid mixture (each amino acid is present at 0.1 mM), 3 mM ATP, 8 mM total RNA, 1 X S100.

2. Incubate at 37° C for 20 minutes.

3. Add NaOAc pH 5.2 to a final concentration of 0.3 M.

4. Perform two sequential acid phenol extraction and a chloroform extraction.

5. Desalt the final aqueous layer using a Bio-Rad P6 spin column or equivalent.

6. To precipitate tRNA, add NaOAc to 0.3 M final and 2.3 volumes of 100% ethanol for at least two hours at - 20ºC.

7. Spin the ethanol precipitation at maximum speed in a refrigerated microfuge for 30 minutes at 4°C. Remove the supernatant and resuspend pellet in ~20 μL 20mM KOAc, pH 5.2.

8. Approximate the overall concentration of aminoacyl-total tRNA by absorbance at 260 nm (ε = 76,000 $M^{-1} \cdot cm^{-1}$)

Note: This is an *estimated* concentration, there is no way to determine the charging efficiency of the S100 or acceptor activity of each tRNA.

9. Aliquot aminoacyl-total tRNA and store at -80°C.

Note: Select aliquot sizes keeping in mind that aminoacyl-total tRNA samples can become significantly deacylated after three or more freeze/thaw cycles.

Part 2- Perform miscoding screening assay

10. Assemble total-TCs by combining, in order, the following reagents (final concentrations given) on ice: water, 1X translation buffer, 8 mM GTP, 4 □M aminoacyl-total tRNA, 30 μM EF-Tu. Incubate total-TC reaction at 37 °C for 15 min.

11. While the total-TCs incubate, prepare ICs as in Section 5. If using frozen ICs, thaw on ice. Make a 200 nM solution of ICs in 1X translation buffer for use in your reaction. Immediately freeze any remaining thawed IC.

12. Initiate miscoding screening reaction by mixing equal volumes of total-TCs with ICs (final concentration 100 nM ribosomes, 2 μM aminoacylated-total tRNA). Typically, small volumes (~1-2 μL of total-TC and IC) are used in these reactions. Incubate at 37 °C for 15 minutes. The control reactions discussed above should be set up in parallel.

13. Quench each reaction by adding 1 μL of 1 M KOH. Visualize the resulting peptide products by eTLC as described in section 8.

1.9. Section 7: Measuring Rate constants for Miscoding

To develop an understanding of how different modifications impact miscoding, single turnover kinetic assays should be employed. Due to the ribosome's stringent proofreading mechanisms an energy regeneration mix is used to produce multiple rounds of accommodation, while remaining single turnover with respect to peptidyl transfer, thus producing measurable

amounts of miscoded dipeptide product. The energy regeneration mix consists of the ternary complex with the addition of EFTs, pyruvate kinase (PK) and phosphoenolpyruvate (PEP). This protocol is adapted from previous work [18]. Before starting this miscoding assay, it is important to ensure saturating levels aminoacyl-tRNA are being used (typically 5-10 μM). These reactions have a $t_{1/2}$ of ~2 minutes, permitting reactions to manually quenched.

1.9.1 Protocol

1 As in section 5, determine a time-course and set-up a series of tubes containing 5 μL 1 M KOH.

2 Prepare 1 □M ICs in 1X-translation buffer as described in section 5.

3 Assemble the EF-Tu/Ts mixture by combining the following reagents on ice

Table 1.8 *EF-Tu/Ts mixture for miscoding kinetic assays*

Reagent	Concentration in mixture	Final reaction concentration
Water	–	to 500 µL
10 × Translation Buffer	1.1 ×	1 ×
GTP	1.11 mM	1 mM
$MgCl_2$	7.77 mM	7 mM
EF-Tu	44.44 µM	40 µM
EF-Ts	11.11 µM	10 µM
PEP	3.33 mM	3 mM
PK	0.11 mM	0.1 mM

4 Incubate the EFTu/Ts mixture at 37 °C for 15 min.

5 Add 1.11 µM of the aminoacyl-tRNA of interest. Incubate at 37 °C for 10 minutes to form miscoding ternary complexes (MC-TCs).

6 Initiate translation reactions by adding the MC-TC to IC in a 10:1 ratio at room temperature.

7 For each timepoint, transfer 1 µL of the reaction to a tube containing 1µL 1 M KOH.

8 After approximately 5 minutes, add 2 µL of 5 M acetic acid to each quenched tube.

9 Spot 1 µL of the quenched and neutralized reaction in 0.8-1 cm increments on a cellulose TLC plate to visualize reactions as described in section 8.

1.10 Section 8: Quantification and Kinetic Analysis

Electrophoretic thin layer chromatography (eTLC) separates small charged species by size and charge, similar to isoelectric focusing. Below we describe how to use this method to visualize the

unreacted ^{f}Met and small peptide products in the translation reactions generated in sections 5-7. Following separation, the different ^{35}S-labeled species can be detected via scintillation counting or phosphorescence (as is used in this protocol). Volatile buffers are used for separation so that

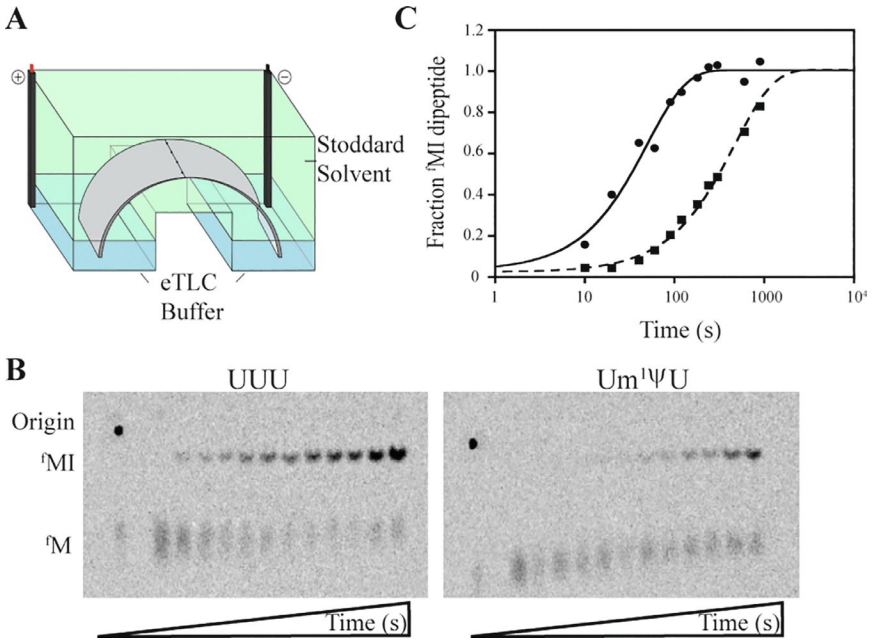

Figure 1.2 *Visualizing translation products by electrophoretic thin-layer chromatography (eTLC). (**A**) TLC electrophoresis tank used in this protocol. (**B**) Example eTLC plate after separation and phosphorimaging. Time courses of miscoding product formed when Ile-tRNA^{Ile} TCs are mixed with ICs programmed with phenylalanine codons (UUU and Um^{1}ΨU) in the A site. (**C**) Representative curves fit of MI dipeptide formed during experiment shown in (**B**). Data from Ile added on UUU [circle] or Um^{1}ΨU [square] are fit with the equation* $[MI]_{Eq} = [M]_0 * e^{-(k_{obs})t}$ *to determine the observed rate constants (k_{obs}).*

the TLC plates are dry prior to exposure to phosphorscreens. Different peptide compositions and charge states affect separation and resolution. Consider the pI of potential peptides to be synthesized and choose an appropriate pH and composition for your eTLC buffer. An example set-up with buffer system is shown in Figure 2A.

1.10.1 Protocol

1. Spot 1.0 □L of each timepoint onto a cellulose eTLC plate, leaving ~1 cm between spots.

2. Wet TLC plate with the selected buffer (most commonly pyridine acetate buffer, pH 2.8).

3. Run TLC for 10-50 minutes in an electrophoresis tank pyridine acetate buffer in the cathode and anode reservoirs and an organic, nonpolar solvent – such as Stoddard Solvent – as a liquid stationary phase (Figure 2A). Peptide charge state and pI affect separation in this system and longer times may be needed for full separation and resolution of peptide products.

4. Remove TLCs from the tank and dry completely with a heat gun.

5. Once dry, wrap TLCs in plastic wrap and expose them against a phosphorscreen for 1-48 hours. The specific activity of the radiolabel and dilution state of samples will dictate exposure time.

6. Scan phosphorscreen in an instrument capable of imaging in a phosphorescence mode, scanning at a voltage of 4000 PMT and a resolution of 100 □m.

7. Using the image analysis software of your choice (e.g. ImageQuant or ImageJ) quantify phosphorescence signals to obtain percent and volume of peptide species at each time point in the assay.

1.11 References

[1] Gromadski KB, Rodnina MV. Kinetic Determinants of High-Fidelity tRNA Discrimination on the Ribosome. Molecular Cell 2004;13:191–200. https://doi.org/10.1016/S1097-2765(04)00005-X.

[2] Steiner RE, Ibba M. Regulation of tRNA-dependent translational quality control. IUBMB Life 2019;71:1150–7. https://doi.org/10.1002/iub.2080.

[3] Kapur M, Ackerman SL. mRNA Translation Gone Awry: Translation Fidelity and Neurological Disease. Trends Genet 2018;34:218–31. https://doi.org/10.1016/j.tig.2017.12.007.

[4] Garrett S, Rosenthal JJC. RNA Editing Underlies Temperature Adaptation in K+ Channels from Polar Octopuses. Science 2012;335:848–51. https://doi.org/10.1126/science.1212795.

[5] Drummond DA, Wilke CO. The evolutionary consequences of erroneous protein synthesis. Nat Rev Genet 2009;10:715–24. https://doi.org/10.1038/nrg2662.

[6] Pan T. Adaptive translation as a mechanism of stress response and adaptation. Annu Rev Genet 2013;47:121–37. https://doi.org/10.1146/annurev-genet-111212-133522.

[7] Jackman JE, Alfonzo JD. Transfer RNA modifications: Nature's combinatorial chemistry playground. Wiley Interdiscip Rev RNA 2013;4:35–48. https://doi.org/10.1002/wrna.1144.

[8] Hudson BH, Zaher HS. Ribosomes Left in the Dust: Diverse Strategies for Peptide-Mediated Translation Stalling. Mol Cell 2014;56:345–6. https://doi.org/10.1016/j.molcel.2014.10.023.

[9] Eyler DE, Franco MK, Batool Z, Wu MZ, Dubuke ML, Dobosz-Bartoszek M, et al. Pseudouridinylation of mRNA coding sequences alters translation. Proc Natl Acad Sci U S A 2019;116:23068–74. https://doi.org/10.1073/pnas.1821754116.

[10] Hoernes TP, Clementi N, Juen MA, Shi X, Faserl K, Willi J, et al. Atomic mutagenesis of stop codon nucleotides reveals the chemical prerequisites for release factor-mediated peptide release. Proc Natl Acad Sci USA 2018;115:E382–9. https://doi.org/10.1073/pnas.1714554115.

[11] Dunkle JA, Dunham CM. Mechanisms of mRNA frame maintenance and its subversion during translation of the genetic code. Biochimie 2015;114:90–6. https://doi.org/10.1016/j.biochi.2015.02.007.

[12] Jones JD, Monroe J, Koutmou KS. A molecular-level perspective on the frequency, distribution, and consequences of messenger RNA modifications. WIREs RNA 2020;11:e1586. https://doi.org/10.1002/wrna.1586.

[13] Andries O, Mc Cafferty S, De Smedt SC, Weiss R, Sanders NN, Kitada T. N1-methylpseudouridine-incorporated mRNA outperforms pseudouridine-incorporated mRNA by providing enhanced protein expression and reduced immunogenicity in mammalian cell lines and mice. Journal of Controlled Release 2015;217:337–44. https://doi.org/10.1016/j.jconrel.2015.08.051.

[14] Sahin U, Karikó K, Türeci Ö. mRNA-based therapeutics — developing a new class of drugs. Nature Reviews Drug Discovery 2014;13:759–80. https://doi.org/10.1038/nrd4278.

[15] Pardi N, Hogan MJ, Porter FW, Weissman D. mRNA vaccines — a new era in vaccinology. Nat Rev Drug Discov 2018;17:261–79. https://doi.org/10.1038/nrd.2017.243.

[16] Karikó K, Muramatsu H, Welsh FA, Ludwig J, Kato H, Akira S, et al. Incorporation of Pseudouridine Into mRNA Yields Superior Nonimmunogenic Vector With Increased Translational Capacity and Biological Stability. Mol Ther 2008;16:1833–40. https://doi.org/10.1038/mt.2008.200.

[17] Nirenberg MW, Matthaei JH. The dependence of cell-free protein synthesis in *E. coli* upon naturally occurring or synthetic polyribonucleotides. PNAS 1961;47:1588–602. https://doi.org/10.1073/pnas.47.10.1588.

[18] Rodnina MV, Wintermeyer W. Fidelity of Aminoacyl-tRNA Selection on the Ribosome: Kinetic and Structural Mechanisms. Annu Rev Biochem 2001;70:415–35. https://doi.org/10.1146/annurev.biochem.70.1.415.

[19] Dever TE, Dinman JD, Green R. Translation Elongation and Recoding in Eukaryotes. Cold Spring Harb Perspect Biol 2018;10. https://doi.org/10.1101/cshperspect.a032649.

[20] Pape T, Wintermeyer W, Rodnina MV. Complete kinetic mechanism of elongation factor Tu-dependent binding of aminoacyl-tRNA to the A site of the *E. coli* ribosome. EMBO J 1998;17:7490–7. https://doi.org/10.1093/emboj/17.24.7490.

[21] Rivera MC, Maguire B, Lake JA. Isolation of Ribosomes and Polysomes. Cold Spring Harb Protoc 2015;2015:pdb.prot081331. https://doi.org/10.1101/pdb.prot081331.

[22] Cammack KA, Wade HE. The sedimentation behaviour of ribonuclease-active and -inactive ribosomes from bacteria. Biochem J 1965;96:671–80.

[23] Rodnina MV, Wintermeyer W. GTP consumption of elongation factor Tu during translation of heteropolymeric mRNAs. Proc Natl Acad Sci U S A 1995;92:1945–9.

[24] Soffientini A, Lorenzetti R, Gastaldo L, Parlett JH, Spurio R, La Teana A, et al. Purification procedure for bacterial translational initiation factors IF2 and IF3. Protein Expr Purif 1994;5:118–24. https://doi.org/10.1006/prep.1994.1018.

[25] Dahlquist KD, Puglisi JD. Interaction of translation initiation factor IF1 with the *E. coli* ribosomal A site. J Mol Biol 2000;299:1–15. https://doi.org/10.1006/jmbi.2000.3672.

[26] Shimizu Y, Inoue A, Tomari Y, Suzuki T, Yokogawa T, Nishikawa K, et al. Cell-free translation reconstituted with purified components. Nat Biotechnol 2001;19:751–5. https://doi.org/10.1038/90802.

[27] Studer SM, Joseph S. Binding of mRNA to the Bacterial Translation Initiation Complex. Methods in Enzymology, vol. 430, Elsevier; 2007, p. 31–44. https://doi.org/10.1016/S0076-6879(07)30002-5.

[28] Studier FW. Protein production by auto-induction in high density shaking cultures. Protein Expr Purif 2005;41:207–34. https://doi.org/10.1016/j.pep.2005.01.016.

[29] Walker SE, Fredrick* K. Preparation and evaluation of acylated tRNAs. Methods 2008;44:81–6. https://doi.org/10.1016/j.ymeth.2007.09.003.

[30] Keedy HE, Thomas EN, Zaher HS. Decoding on the ribosome depends on the structure of the mRNA phosphodiester backbone. PNAS 2018;115:E6731–40. https://doi.org/10.1073/pnas.1721431115.

Chapter 2 mRNA and tRNA Modification States Influence Ribosome Frame Maintenance During Poly(lysine) Peptide Synthesis[2]

Work presented in this chapter was published in
Journal of Biological Chemistry.

Tyler J. Smith[1], Mehmet Tardu[1,2], Hem Raj Khatri[1], and Kristin S. Koutmou[1]
1- Department of Chemistry, University of Michigan, Ann Arbor, Michigan, USA
2- Department of Biology, Istanbul University, Istanbul, Turkey

2.1 Introduction

Translation of the nucleic acid code into protein is catalyzed by the ribosome. During this process, ribosomes use messenger RNAs (mRNAs) as molecular maps to direct the programmed assembly of amino acids into polypeptides. In *E. coli*, growing polypeptide chains are extended by an average of 4 to 22 amino acids per second, though the rate of individual amino acid incorporation by the ribosome is not always uniform [1–3]. Heterogeneity in peptide elongation rates is caused by a number of factors including substrate (e.g. mRNA, aminoacyl-transfer RNAs (aatRNAs), translation factors) availability and modification status, and the formation of stable interactions between the growing polypeptide chain and the ribosome machinery [4, 5]. Although translation initiation rates are responsible for controlling the rate of protein expression in many

[2] In the work presented in this chapter I was the primary author and developer of all the work listed throughout. This includes all work except as indicated hereafter. Kristin Koutmou assisted in editing, as well as conception and motivation of the work. Mehmet Tardu performed bioinformatic analysis to determine frequency of poly(A), m^6A installation, and polybasic peptide iteration and frequency. Hem Raj Khatri synthesized the Valinyl-DBE substrate used in flexizyme mis-acylation assays (assays performed by me, Tyler Smith).

circumstances, situations that alter polypeptide elongation rates can change protein levels, protein folding and mRNA stability to ultimately impact cellular health and fitness [6–8].

Contacts between the ribosome and its nascent peptide products are receiving growing recognition for their role in translationally controlling protein expression [9]. The interactions involving the ribosome and positively charged peptides present a classic example of this phenomenon. There is overwhelming evidence that translating the cationic peptide sequences commonly present in proteins slows the ribosome [10, 11]. In humans there are over 60,000 examples of proteins containing 4 or more consecutive basic amino acids, suggesting that the synthesis of positively charged peptides contributes to the post-transcriptional control of a significant fraction of the proteome (SI Tables 1-2). The observation that ribosomes slow while linking iterated positively charged amino acids has long been attributed to the formation of strong ionic interactions between cationic peptides and the anionic ribosome peptide exit channel [12]. However, several recent reports demonstrate the ribosome produces different amounts of protein from mRNAs encoding identical positively charged poly(lysine) and poly(arginine) peptides [13–15]. Ionic interactions alone cannot explain these findings, suggesting that additional factors in the translation system also contribute to modulating ribosome speed during the synthesis of cationic peptides.

Multiple codons instruct the ribosome to add the positively charged amino acids lysine (AAA and AAG) and arginine (AGA, AGG and CGN (N=U, C, A,G)). The ability of individual arginine codons to differentially impact protein expression largely depends on the availability of tRNA isoacceptors possessing appropriate anti-codon sequences. Some isoacceptors are less abundant, and translation along mRNA sequences containing multiple codons corresponding to these rare tRNAs can slow sufficiently to trigger cellular mechanisms that rescue stalled

ribosomes [16, 17]. The cause of differential protein expression from the two lysine codons appears to differ from that of arginine codons. In the case of lysine, less protein is produced from mRNAs containing consecutive AAA codons than those with consecutive AAG codons in both eukaryotic and bacterial cells [13, 14, 18, 19]. However, differences in substrate tRNA levels are unlikely to account for these codon-specific observations, because AAA and AAG are decoded by a single tRNALys in at least one of the species (*E. coli*) where codon dependent differences in poly(lysine) protein output have been observed. Furthermore, in addition to reducing the rate of protein synthesis, under some conditions the presence of two or more AAA codons in a row can promote an unusual ribosome movement termed 'ribosome sliding' [13]. During sliding, the ribosome loses reading frame and shifts along an mRNA. The ribosome has been captured moving backwards by 1 to 3 nucleotides while translating iterated AAA codons [13, 14], changing the identity of the peptide beings made. These movements activate co-translational surveillance mechanisms that target the translated mRNA and resulting peptide products for degradation [18]. Ribosome sliding differs from other non-canonical ribosome movements, which place the ribosome at a single, discrete location on an mRNA and can produce stable products [20, 21].These data suggest that the influence of mRNA and tRNA sequences on the translation of poly(lysine) peptide regions warrant further examination.

Here, we use a reconstituted *E. coli* translation system to deconvolute the contributions of peptide, mRNA sequence and RNA (mRNA and tRNA) modification to both the speed of amino acid addition and ribosome frame maintenance during the translation of iterated lysine codons. We chose to investigate the role of RNA modifications in addition to peptide and mRNA sequence because these common chemical changes to nucleosides can alter the hydrogen bonding interactions between tRNAs and mRNAs used by the ribosome to ensure the faithful

and rapid translation of the genetic code into protein [22]. Our findings expand the biochemical framework for understanding the contributions of individual components of the translation system to ribosome stalling during cationic peptide synthesis. We demonstrate that in addition to peptide charge, mRNA sequence, along with mRNA and tRNA modification status, are important determinants of ribosome speed during poly(lysine) translation. Additionally, we developed a minimal kinetic mechanism for ribosome sliding on iterated AAA codons in which the ribosome moves along an mRNA in the 3' direction one nucleotide at a time, until it can bind an available cognate aatRNA and resume "normal" translation (though in a different frame). Much like ribosome speed, this series of 1 nucleotide ribosome movements is controlled not only by peptide charge, but also by post-transcriptional modifications to tRNALys and mRNA (N6-methyladenosine (m6A)). While it has been known for decades that tRNA anticodon stem-loop modifications can influence ribosome movements, our data provide the first evidence that mRNA modifications also have the power to impact ribosome reading frame maintenance [23]. Our work presents a molecular level rationalization for how seemingly small changes in the translational machinery (e.g. synonymous codon substitution, single post-transcriptional modifications) can result in different protein production outcomes.

2.2 Results

2.2.1 Ribosomes move backwards 1 nucleotide at a time on poly(A) sequences

There are multiple ways to envision how ribosome sliding on consecutive AAA codons could be achieved. For example, the ribosome might hop directly into the -1 and -3 frames, 'scan' along an mRNA until it reaches a specific, desired frame, or make series of discrete 1 nucleotide frameshifts [13, 14, 24, 25]. We developed a kinetic framework to distinguish between these

possibilities and describe how the ribosome moves during sliding using a fully reconstituted in vitro translation system [26]. To accomplish this we first identified the reading frames the ribosome enters during translation along an mRNA with a AUG-AAA-AAA-UUC-UAA [MK2(AAA)FX; X=stop codon] coding sequence (Fig. 1A). In these assays, 70 nM of *E. coli* 70S ribosome initiation complexes (ICs) containing 35S-labeled formylmethionine-tRNAfMet bound to an AUG in the P site and an AAA codon in the A site were reacted with saturating concentrations of two ternary complexes (10-30 μM TCs; aa-tRNAaa•EF-Tu•GTP) formed with cognate Lys-tRNALys and individual aa-tRNAaa species capable of reacting in each of the reading frames that the ribosome could inhabit on our MK2(AAA)FX mRNA (-2 frame: Asn-tRNAAsn, -1 frame: Ile-tRNAIle, 0 frame: Phe-tRNAPhe, +1 frame: Ser-tRNASer, +2 frame: Leu-tRNALeu) (Fig. 1A). These reactions were conducted in the presence of 0-12 μM EFG•GTP at 37°C. The reactants (fMet), programmed peptides (MK, MK2, MK2F) and peptide products resulting from the ribosome sliding (MK2I, MK2N, MK2S, MK2L, MK3, MK4+) were

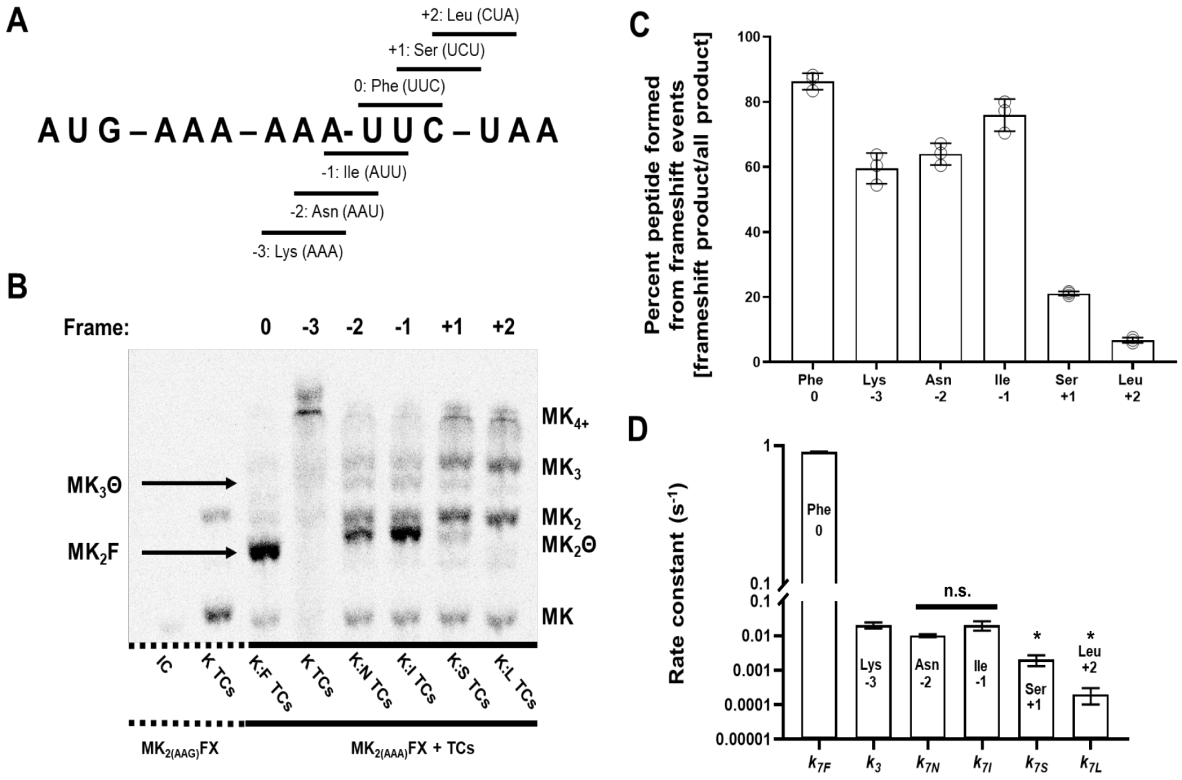

Figure 2.1 *The ribosome moves into multiple frames on poly(A) in absence of next cognate aa-tRNAaa. (A) Possible ribosome sliding events on MK2(AAA)FX mRNA result in new discrete codons positioned in the A-site, allowing for decoding and accommodation of non-coded aa-tRNAaa. (B) Phosphorimage eTLC of 20-minute end-point reactions of frameshift studies during ribosome sliding on MK2(AAA)FX or MK2(AAG)FX mRNA incubated with Lys-tRNALys and aa-tRNAaa TCs. Lanes indicate the aa-tRNAaa TCs used in each reaction, with the numbers correlating to the amino acid identity as indicated in panel A (e.g. -2 indicates reaction with Lys-tRNALys and Asn-tRNAAsn. Θ in short peptide sequences indicate amino acid that would be added upon successful frameshift and incorporation of aa-tRNAaa as indicated per lane and in panel A (e.g. bands for MK2Θ and MK3Θ in -2 lane correspond to the peptides MK2N and MK3N, respectively). (C) Percent of peptide formed due to sliding/frameshifting compared to total peptide synthesized during translation assays, with frame and third amino acid added as signified. Sliding in reactions produce -3 peptide products (incorporating additional lysine) as well as frameshift products (e.g. MK2Θ), resulting in peptides longer than MK2. Peptide products were determined after 20-minute translation assays incubated with Lys-tRNALys and respective aa-tRNAaa TCs as specified with frame corresponding to panel A. Error bars represent standard deviation. (D) Rate constants of frameshift events during ribosome sliding on MK2(AAA)FX mRNA using Lys-tRNALys and aa-tRNAaa TCs as specified with frame (panel A), as defined by the proposed mechanism in Figure 2. Error bars represent standard deviation. When comparing rate constants for -1 (Ile; k7I) and -2 (Asn; k7N) amino acid addition, there is no significant difference when compared to the rate constant for -3 (Lys; k3) amino acid addition when using an unpaired student t-test. For +1 (Ser; k7S) and +2 (Leu; k7L) rate constants, a ' * ' represented a significant alteration with a p-value <0.05 using a unpaired student t-test when compared to the -3 rate constant (Lys; k3).*

visualized by electrophoretic TLC (eTLC; Figure 1B). In our assays, the ribosome generated products in five different reading frames (0, -1, -2, -3 and +1; Figs. 1A-C). We find that

movement of the ribosome into non-0 frames is EF-G dependent, much like canonical -1 frameshifting ribosome movements (SI Fig. 1) [24, 27–29].

After establishing which frames the ribosome inhabits during sliding, we measured the extent of amino acid incorporation in each of these frames at discrete time points (0-1200 seconds, Fig. 1C, SI Fig. 2). These data were used to develop a minimal kinetic mechanism for ribosome sliding by globally fitting our experimental observations with KinTek Explorer (SI Figure 2). We examined a series of possible mechanisms (SI Fig. 3), and selected the model that best fit our data to ascertain the rate constants for each step in the mechanism. Our fits indicate that the ribosome undergoes a series of progressive -1 nucleotide movements from the 0-frame into the -1, -2 and -3 frames during ribosome sliding (Fig. 2, SI Fig. 4). The rate constants for amino acid addition in the -1, -2 and -3 frames are relatively uniform (k7 values range between 0.01-0.02 s-1) (Fig. 1D, Table 1).

Table 2.1 *Rate constants for frameshift and amino acid addition during ribosome sliding*

Frameshift position	**0 frame**	**-2 frame**	**-1 frame**	**+1 frame**	**+2 frame**
tRNA TCs	Lys + Phe	Lys + Asn	Lys + Ile	Lys + Ser	Lys + Leu
Rate constants (s^{-1})					
k_1	11.7 ± 0.01	13.1 ± 0.01	15.3 ± 0.82	12.7 ± 0.66	13.3 ± 0.74
k_2	1.5 ± 0.002	1.6 ± 0.002	1.4 ± 0.19	1.5 ± 0.15	1.2 ± 0.26
k_3	-	0.005 ± 0.0002	0.008 ± 0.0015	0.008 ± 0.0012	0.02 ± 0.0041
$k_{4:6,\ obs}$	-	0.006 ± 0.0015	0.003 ± 0.0016	0.007 ± 0.0027	0.002 ± 0.009
k_5	-	0.0008 ± 0.00004	0.0007 ± 0.00026	0.002 ± 0.0005	0.017 ± 0.0087
k_7	0.9 ± 0.0007	0.01 ± 0.0009	0.02 ± 0.006	0.002 ± 0.0007	0.0002 ± 0.00097

Furthermore, a subset of ribosomes (~10%) appear unable to extend the growing polypeptide following each progressive -1 nucleotide ribosome movement (Figs. 1B and 2 (k5, k4:6,obs), SI Figs. 3 and 5B). While we do observe a small amount of product formation in the +1 frame, both

the endpoint and rate constant for this reaction are diminished relative to the same values for the ribosome reacting in the -1, -2, and -3 frames (Figs. 1C, D). These observations lead us to propose a model for ribosome sliding in which a small (< 5% of ribosomes) can undergo a +1 frameshift, while most ribosomes move in the 3' direction by one nucleotide a time until they enter a reading frame that can react with an available aminoacyl-tRNA species (Fig. 2).

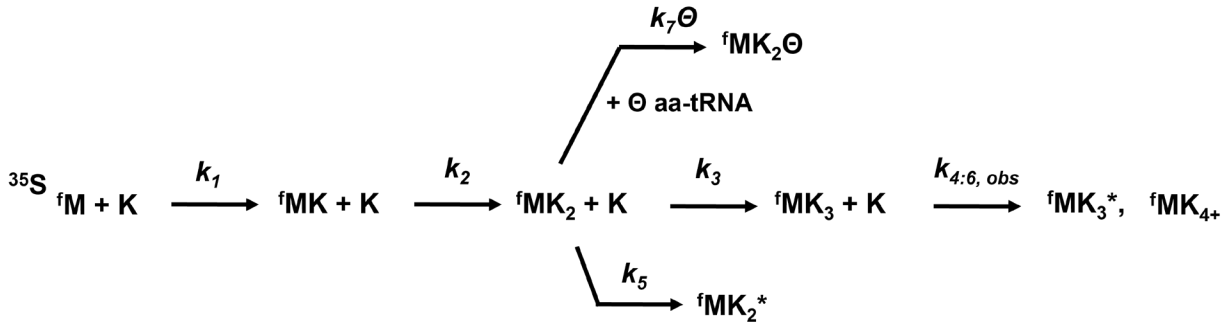

Figure 2.2 *Proposed general scheme for frameshift events during ribosome sliding on poly(A). In the case where available aa-tRNAs are incorporated via frameshift, as indicated by Θ, this scheme describes subsequent amino acid additions by a ribosome translating on a poly(A) containing mRNA – as displayed in Fig. 1. The scheme contains parameters obtainable from the experiments presented here. Rate constants refer to amino-acid addition and peptide length: dipeptide formation (k1), tripeptide formation (k2), ribosome sliding and frameshift events (k3 – first -3 sliding/frameshift event generating tetrapeptide [MK3] ; k5 – first sliding/frameshift event resulting in unproductive ribosome(s); k7Θ – first sliding/frameshift of ribosome moving into new coding frame [MK2Θ]), and secondary/tertiary sliding events capable of occurring following first sliding/frameshift event (k4:6,obs).*

2.2.2 tRNALys modifications moderate ribosome sliding during poly-lysine synthesis

Native tRNAs possess post-transcriptional chemical modifications essential to their stability, structure and function [30, 31]. Modifications located in tRNA anticodon stem loops have the capacity to modulate -1 and +1 ribosomal frameshifts and enhance ribosome reading frame maintenance [32, 33]. Since the tRNALys N6-threonylcarbamoyladenosine (t6A37) (and 5-methoxycarbonylmethyl2-thiouridine (mcm5S2U34) modifications in yeast tRNALys,UUU influence tRNA decoding, we speculated that analogous *E. coli* tRNALys modifications, such as 5- methylaminocarbonylmethyluridine (mnm5s2U34), might suppress ribosome sliding and

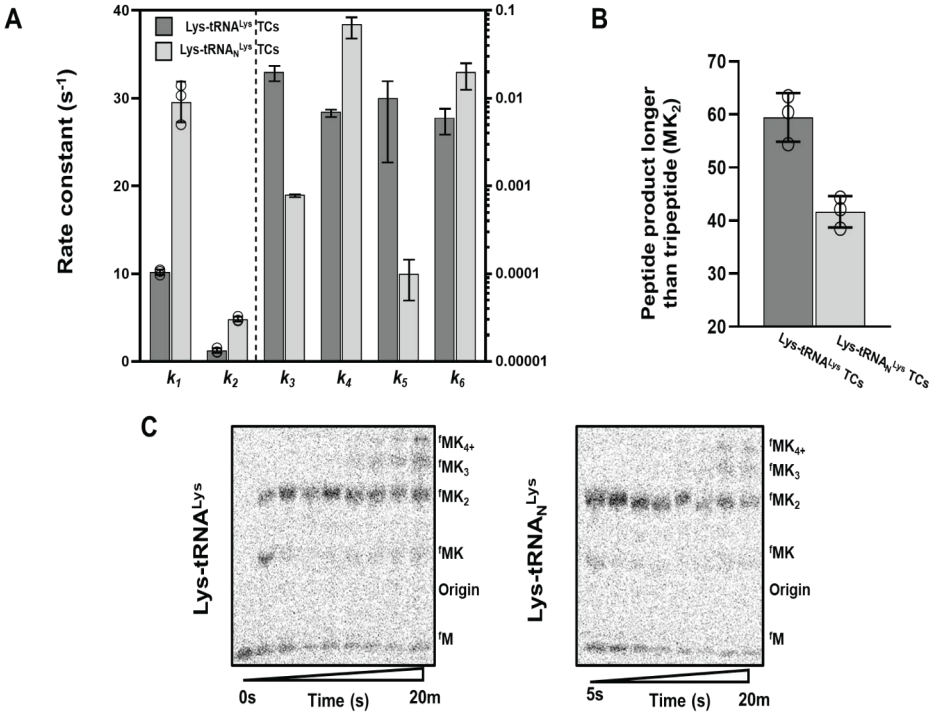

Figure 2.3 *Modifications on tRNALys regulate extent of frame loss on poly(A) mRNA. (A) Rate constants of ribosome sliding on MK2(AAA)FX mRNA using either Lys-tRNALys or Lys-tRNANLys TCs, as defined by the proposed mechanism in Supplemental Figure 3A. Error bars represent standard deviation. (B) Percent of total peptide formed as a result of ribosome sliding (longer than MK2 tri-peptide) on MK2(AAA)FX mRNA after 20 minute translation assays incubated with Lys-tRNALys or Lys-tRNANLys TCs. Error bars represent standard deviation. (C) Phosphorimage eTLCs of 20-minute time course reactions of ribosome sliding on MK2(AAA)FX mRNA, incubated with either Lys-tRNALys TCs(left) or Lys-tRNANLys TCs (right).*

enhance poly(lysine) translation (34, 35). To test this idea, we compared the rate constants for lysine addition during the translation of AUG-AAA-AAA-UUC-UAA [MK2(AAA)FX] and AUG-AAG-AAG-UUC-UAA [MK2(AAG)FX] messages using saturating levels (20-30 μM) of unmodified T7 transcribed Lys-tRNALys and natively modified Lys-tRNANLys purified from *E. coli* cells (Fig. 3A, SI Fig. 6). We find that the rate constants for programmed MK and MK2 peptide formation are 2- to 4-fold faster when ribosome complexes are reacted with TCs containing modified Lys-tRNANLys than with unmodified Lys-tRNALys. These moderate enhancements in lysine addition rate constants are observed when either AAG or AAA containing mRNAs are translated (Table 2). The modifications have a larger role on frame

maintenance than on programmed lysine addition; the rate constants for forming ribosome sliding products (MK3 and MK4+) on AAA codons are decreased by up to 25-fold when natively modified Lys-tRNANLys is used (Fig. 3B). Despite the slowed formation of these sliding products, the percentage of peptides that are eventually extended and generated sliding products is only slightly reduced by the inclusion of modifications on tRNALys (Lys-tRNALys = 60% ± 3% vs. Lys-tRNANLys = 40% ± 6%) (Fig. 3B-C, SI Fig. 6). Our data suggest that tRNANLys modifications likely limit the extent of ribosome sliding in cells.

2.2.3 Ribosomes slow and slide when synthesizing poly(Valine) peptides from lysine-encoding mRNAs

Regardless of tRNALys modification status, we observed that after the first lysine is added into a peptide, the rate constant for adding subsequent lysines on AAA-codons are reduced (Table 2, Fig. 3A). This is consistent with a large body of evidence from cellular reporter and ribosome profiling studies indicating that the translation of iterated positive charges slows the ribosome [36].

Table 2.2 *Rate constants for lysine addition during ribosome sliding*

mRNA construct	$MK_{2(AAA)}FX$		$MK_{2(AAG)}FX$	
tRNA TCs	Lys-$tRNA^{Lys}$	Lys-$tRNA_N^{Lys}$	Lys-$tRNA^{Lys}$	Lys-$tRNA_N^{Lys}$
Rate constants (s^{-1})				
k_1	10.2 ± 0.3	28.9 ± 1.9	2.7 ± 0.5	12.7 ± 0.4
k_2	1.2 ± 0.4	4.8 ± 0.4	2.1 ± 0.7	4.4 ± 0.33
k_3	0.02 ± 0.004	0.0008 ± 0.000008	0.006 ± 0.002	0.002 ± 0.001
k_4 (or $k_{4,obs}$)	0.007 ± 0.001	0.07 ± 0.02	0.0004 ± 0.0001	0.00009 ± 0.00002
k_5	0.01 ± 0.008	0.0001 ± 0.00005	0.001 ± 0.0001	0.001 ± 0.0002
k_6	0.006 ± 0.002	0.02 ± 0.007	-	-

However, the observation that different poly(lysine) encoding mRNA sequences differentially impact translation lead us to wonder if mRNA sequence, and therefore also structure, contribute to ribosome slowing and during poly(lysine) translation [13, 14]. To de-convolute the effects of peptide charge from mRNA sequence, we mis-charged unmodified tRNALys and natively modified tRNANLys sequences with the small non-polar amino acid Valine (Val-tRNALys, Val-tRNANLys) (Fig. 4A). Mis-acylation was accomplished using a small RNA microhelix (fleixzyme) capable of attaching an esterified amino acid acyl-donor to virtually any tRNA of interest [37]. ICs containing mRNAs encoding consecutive lysines (AUG-AAA-AAA-UUC-UAA and AUG-AAG-AAG-UUC-UAA) were reacted with TCs possessing mischarged tRNAs (Val-tRNALys•EF-Tu•GTP, Val-tRNANLys•EF-Tu•GTP). Because the translation factor EF-Tu selects for correct tRNA and amino-acyl donor pairings, we titrated EF-Tu with each aminoacyl-tRNA to ensure saturating conditions for incorporating these species (SI Fig. 7) [38, 39]. Concurrent control assays with TCs containing Val-tRNAVal and ICs formed on an mRNA encoding consecutive valines (AUG-GUG-GUG-UUC-UAA) were also performed. The rate

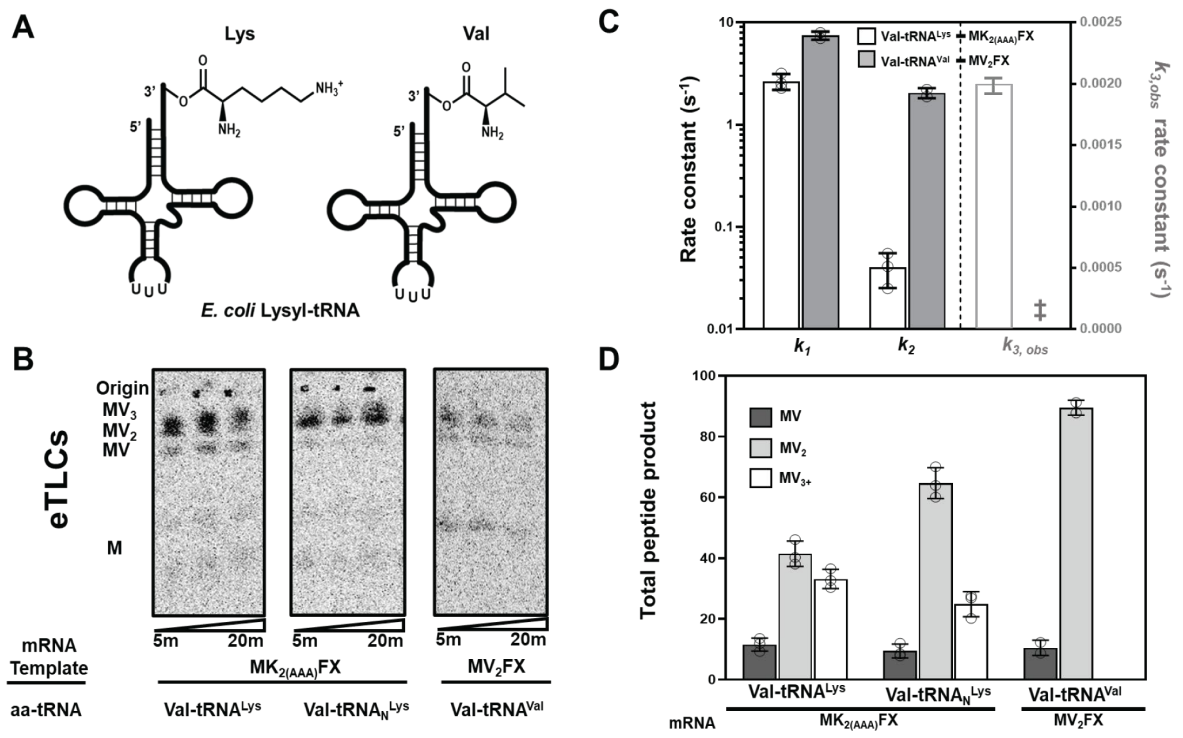

Figure 2.4 *Neutral amino acid and tRNA pairing effect ribosome sliding on poly(A) mRNA. (A) Lysyl E. coli tRNAUUU can be acylated with positive charge lysine or misacyalted with neutral charge valine, via dFx flexizyme, to be used in studies to asses influence of amino acid charge on lysine addition during translation. (B) Phosphorimage eTLCs of time course reactions of amino acid addition and ribosome sliding on mRNA. These reactions were incubated with either Val-tRNALys (left) or Val-tRNANLys TCs (middle) on MK2(AAA)FX mRNA, or incubated with Val-tRNAVal (transcribed) on MV2FX mRNA. (C) Rate constants of amino acid addition on MK2(AAA)FX mRNA using Val-tRNALys and MV2FX mRNA using Val-tRNAVal TCs as defined by the proposed mechanism in Supplemental Figure 3A. k3,obs rate constant is presented on the right Y-axis with no rate constant obtainable for peptide synthesis on MV2FX mRNA (‡) as no sliding is observed in these assays. Error bars represent standard deviation. (D) Percent of peptide products formed during assays on MK2(AAA)FX or MV2FX mRNAs after 20 minute translation assays incubated with Val-tRNALys , Val-tRNANLys , or Val-tRNAVal TCs as shown in panel B. Error bars represent standard deviation.*

constants for MV and MV2 formation are 3- and 5-fold slower (respectively) on AUG-AAA-AAA-UUC-UAA [MK2(AAA)FX] mRNA than AUG-GUG-GUG-UUC-UAA GUG [MV2FX] mRNA regardless of the modification status of tRNALys (Fig. 4C, SI Table 3). In contrast, the rate constants for synthesizing MV and MV2 on AUG-AAG-AAG-UUC-UAA [MK2(AAG)FX] mRNA are reduced by less than 2-fold relative to [MV2FX] mRNA when modified Val-tRNANLys is included in the translation reaction. However, when unmodified Val-tRNALys is used instead the ability of the ribosome to add Val to a growing polypeptide on an AAG codon is

dramatically slowed, and the rate constants for MV and MV2 synthesis are diminished by >1000-fold (SI Fig. 8, SI Table 3).

In addition to impacting ribosome speed, our investigations with Val-tRNALys and Val-tRNANLys revealed that peptide charge also contributes to ribosome frame maintenance on lysine encoding messages. We find that extended MV3+ peptides, analogous to the MK3+ peptides made during ribosome sliding (Fig. 4B), are generated from the AAA, but not AAG or GUG containing messages. While unprogrammed MV3+ peptides can still be generated on consecutive AAA codons, the incorporation of additional valines is ~10-fold slower than unprogrammed lysine addition on the same message. Our findings suggest that peptide charge and mRNA sequence make independent contributions to ribosome speed and frame maintenance during poly(lysine) peptide synthesis.

2.2.4 m6A mRNA modifications suppress sliding on consecutive AAA codons in a position dependent manner

Our data indicate that iterated AAA, but not AAG, lysine encoding codons promote a series of consecutive -1 movements by the ribosome (ribosome sliding). We hypothesized that poly(A) regions might form a unique structure within the ribosome mRNA channel that promotes these loss of frame events. Recent cryo-EM structures of the yeast ribosome translating an mRNA sequence with six consecutive A nucleosides supports this idea, revealing that stacked As can adopt a single-stranded helix in the ribosome decoding center [40, 41]. In these structures there are three As in the mRNA are positioned in A site, where they form a helical stack with residues in the 18S rRNA [41]. To test the possibility that such a helical structure might enhance frame loss on poly(A) sequences, we performed translation assays on AUG-AAA-AAA-UUC-UAA

[MK2(AAA)FX] messages with various A-nucleosides substituted with N6-methyladenosine (m6A) (Fig. 5A) to perturb the structure of this poly(A) helix. We selected m6A as a probe

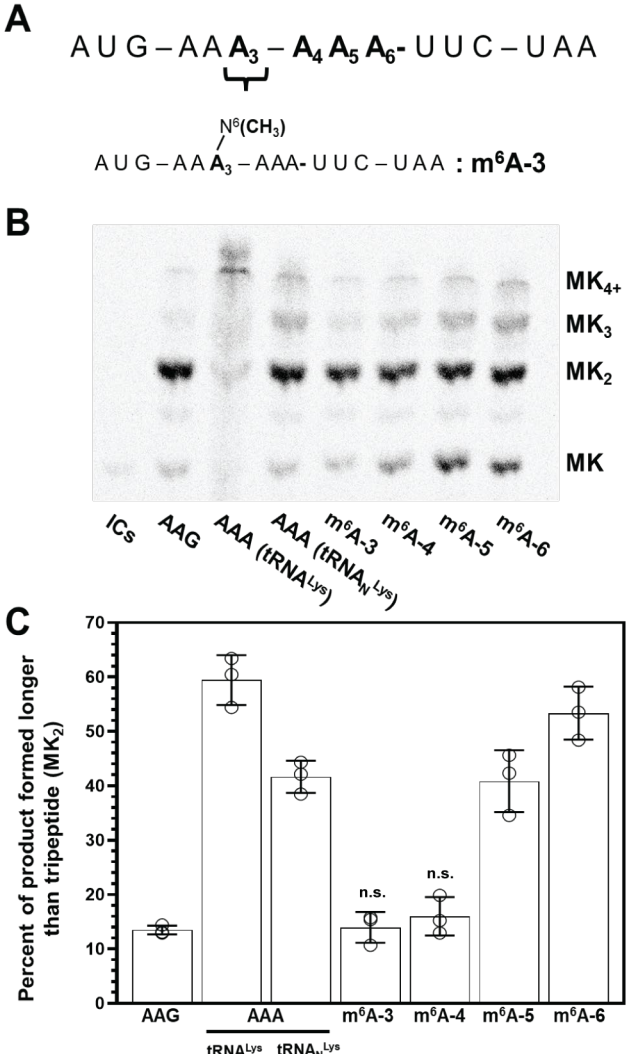

Figure 2.5 *m6A modification to single nucleotides in poly(A) modulate ribosome frame loss. (A) MK2(AAA)FX mRNA was chemically modified with a single m6A on one of the six consecutive As. Specifically at positions A3, A4, A5, and A6 with position 3, m6A-3, shown. (B) Phosphorimage eTLC of 20-minute end-point reactions of sliding studies on MK2(AAA)FX harboring a single m6A modification at nucleotide specified. (C) Percent of total peptide formed as a result of ribosome sliding (longer than MK2 tri-peptide) on MK2(AAA)FX mRNAs harboring one or no m6A modification after 20 minute translation assays incubated with Lys-tRNANLys TCs. Error bars represent standard deviation. There is no significant difference observed for peptide product formed on messages containing m6A at either position A3 or A4 using Lys-tRNANLys TCs when compared to peptide product formed on MK2(AAG)FX using Lys-tRNANLys TCs when using an unpaired student t-*

because it has been shown to change RNA structure and dynamics [42–44]. We find that when m6A is positioned in the middle of a 6 consecutive A nucleosides (at the third and fourth adenosine in the message), where they presumably could disrupt helix formation, very little extended peptide product is formed (Figs. 5B-C, SI Table 4). In contrast, when the m6A is positioned at the 5th or 6th adenosine in the poly(A) sequence, sliding levels are comparable to those on an unmodified message (Fig. 5C). We examined the location of m6A in two available datasets that mapped m6A transcriptome wide to begin evaluating if our observation that m6A can promote frame maintenance could have relevance in endogenous A-rich mRNA coding sequences [45, 46]. Our bioinformatic analyses reveal that m6A exists both in AAA codons and in iterated A (5 or more As) stretches found in the coding region of over 80 mRNAs (SI Table 5). These findings together suggest that one consequence of m6A might be to prevent the ribosome from losing frame on consecutive AAA codons.

2.3 Discussion

The elongation of cationic peptides slows the ribosome and can impact the expression of thousands of proteins (SI Table 1-2) (36, 47). Available evidence suggests that ionic interactions between positively charged peptides and the ribosome account for reducing translation speed on these sequences [40, 48, 49]. We directly tested this model by comparing the rate constants for amino acid incorporation on MK2 encoding mRNAs using tRNALys aminoacylated with either a positively charged (Lys-tRNALys) or neutral (Val-tRNALys) amino acid (Fig. 4). Our investigations reveal that ribosomes translating consecutive AAA codons add a second amino acid (V or K) more slowly. The extent of slowing amino is not dependent on amino acid identity (Val-tRNALys k1/k2 = 6, Lys-tRNALys k1/k2 = 8). In contrast, on consecutive AAG lysine codons the rate constants for adding the first and second lysine are equivalent (Lys-tRNALys

k1/k2 = 1), while a second valine is added substantially more slowly (Val-tRNALys k1/k2 = 20) (SI Table 3). The inclusion of modifications into tRNANLys diminished the differences we observed in the rate constants for adding consecutive lysines and valines on AAG and AAA codons (on AAG: Val-tRNANLys k1/k2 = 4, Lys-tRNANLys k1/k2 = 3; on AAA: Val-tRNANLys k1/k2 = 2, Lys-tRNANLys k1/k2 = 6) (Table 2, SI Table 3). Our results indicate that both peptide charge and codon:tRNALys interactions have significant roles in controlling poly(lysine) peptide synthesis rates. These factors play similarly important roles in ribosome frame maintenance during poly(lysine) peptide translation. While we observe ribosome sliding when Val-tRNALys/Val-tRNANLys are used (Fig. 4), the rate and extent of sliding on AAA codons are both modestly enhanced by Lys-tRNALys/Lys-tRNANLys. mRNA sequence (AAA vs AAG) and the post-transcriptional modification status of tRNALys have larger impacts on frame maintenance than peptide charge. As previously reported, we find that ribosome sliding is only prevalent on lysine encoding mRNAs with consecutive AAA codons (Fig. 3, SI Fig. 1) [13]. We also noticed that the presence of tRNALys modifications significantly reduces the rate constant (25-fold) for sliding associated frame loss events (Fig. 3, Table 2). The strong influence of tRNANLys modifications on frame maintenance is consistent with previous observations that both bacterial and yeast tRNA with these modifications also promote mRNA-tRNA interactions [34, 50–52]. In addition to enhancing frame maintenance, tRNANLys modifications appear to be especially important for the addition of valine on AAG, but not AAA, codons by mischarged Val-tRNALys. The rate constant for Val insertion increases by 70 to >1000-fold when fully-modified Val-tRNANLys is reacted on AAG codons (SI Fig. 8, SI Table 3). These findings collectively help to rationalize why loss of tRNANLys modifications is lethal in yeast, and the

observation that mutations in the tRNANLys modification machinery are linked to disease [23, 53–57].

mRNA:tRNA interactions can be controlled not only by tRNA modifications, but also by the post-transcriptional modification of mRNAs. Emerging evidence suggests that mRNA modifications can slow the ribosome, and influence the extent of amino acid mis-incorporation into peptides [22, 58–60]. However, the impact of mRNA modifications on ribosome frame maintenance has not been explored. This question is especially relevant in the context of ribosome sliding because the most common mRNA modification, m6A, is present in AAA codons in cells [45, 46]. Our analysis of available datasets that map the location of m6A transcriptome-wide reveals that m6A is included into > 80 mRNAs containing 5 or more consecutive As (SI Table 5). While m6A disrupts both RNA base-pairing and tRNA selection by the ribosome, the influence of m6A , or any other mRNA modification, on ribosome frame maintenance is not known [42, 61, 62]. Our results demonstrate that m6A can suppress frame loss events. We find that ribosome sliding is limited when m6A is positioned to break up stretches of iterative adenosines (Fig. 5). Together, our biochemical and bioinformatic findings suggest that one consequence of having m6A present in these mRNA sequences could be to prevent ribosome sliding in homopolymeric A-rich stretches [63].

While previous studies revealed that the ribosome moves robustly into multiple frames on poly(A) sequences in vitro, the mechanism by which this occurs was not known [13, 24, 25]. Here, we measured the rate constants for the ribosome moving into five different reading frames while translating an AUG-AAA-AAA-UUC-UAA [MK2(AAA)FX] mRNA sequence. These data lead us to propose a model for ribosome sliding in which the ribosome moves backwards, one nucleotide at a time, along a homopolymeric(A) sequence until it either encounters a aa-

tRNAaa that it can react with or enters an unproductive state (Fig. 2, SI Fig 3). We find that the rate constants for backward movements by the ribosome are reduced by 50-fold relative to 0-frame amino acid addition, and that the greatest levels of non-productive complex formation are observed following the first -1 movement (Fig. 1D and Table 1). The rate constants for these movements, collectively referred to as ribosome sliding, are reduced relative to normal amino acid addition, amino acid mis-incorporation and -1 programmed frame shifting [22, 64, 65]. While we do observe some amino acid addition in the +1 frame, these events are less robust than their -1 counterparts and we believe that the +1 frameshifts are not a product of sliding, but rather the result of an empty A site [66].

The slow nature of the progressive -1 movements and formation of non-productive complexes can help explain why it is possible to capture the ribosome in multiple frames in vitro, but only visualize ribosome stalling and the first -1 movements in cells. Following the first -1 movement on poly(A) sequence, our results suggest that the ribosome is capable of adding the amino acid in the -1 frame, likely leading to the creation of a pre-maturely truncated protein product and triggering non-sense mediated decay (NMD). Indeed, there is evidence that NMD occurs on following -1 frameshifts on poly(A) containing reporters in human cells [14, 67]. Additionally, the -1 movement is quite slow (longer than 1 min), giving time for ribosome collisions to occur and a co-translational quality control mechanism targeting the stalled ribosome complex to be activated [68–70]. Together, this work quantitatively describes how the ribosome translates mRNAs containing poly(A) regions, and reveals the important contributions of tRNA:mRNA interactions to ribosome slowing during cationic peptide. Our results suggest that post-transcriptional mRNA modifications provide cells with a previously unrecognized for

cells for ensuring that the ribosome remains in the correct mRNA reading frame during translation of slippery sequences.

2.4 Experimental Procedures

2.4.1 In vitro translation assays

70S initiation complexes (ICs) were prepared using *E. coli* ribosomes programmed with various mRNAs and f-[35S]-Met-tRNAMet in the P site [71]. Translation was initiated by mixing equal volumes of ternary complex (20–60 μM aminoacyl-tRNA(s), 24 μM EF-G, 60 μM EF-Tu) with ICs (140 nM) in 219-Tris buffer (50 mM Tris pH 7.5, 70 mM NH4Cl, 30 mM KCl, 7 mM MgCl2, 5 mM βME). All initiation factors (IF-1, IF-2, and IF-3), translation factors (EF-Tu and EF-G) used were His-tag purified from *E. coli* using plasmids available from AddGene [26]. The reactions were quenched with equal volume of 1 M KOH at discrete time points (0 s–20 min) by hand (5 s – 20 min) or using a KinTek RQF-3 quench flow apparatus (0.001 – 5 s) [72]. Each sample was diluted 1:10 in nuclease free water and the reactants, intermediates and products were separated by electrophoretic TLC (eTLC), visualized by phosphorimaging and quantified with ImageQuant as previously described [26]. Depending on the expected peptide products, eTLCs were run in different running buffer conditions to improve separation [26]. eTLCs analyzing peptides containing one or more lysines were run in pyridine acetate buffer, pH 2.8, while eTLCs separating peptides with valine (but no lysine) were run in pyridine acetate buffer, pH 5.2. For m6A studies in this work, all m6A mRNA constructs were purchased from Dharmacon – Horizon Discovery.

2.4.2 tRNA aminoacylation by synthetases and flexizyme

tRNAs used in experiments were either transcribed with T7 polymerase or were overexpressed and purified from using a pCWAug vector. tRNAs were then aminoacylated using either purified, bacterial lysine aminoacyl tRNA synthetase (LysRS) or misacylated using the dFx flexizyme as described previously [37, 73]. In the case of native tRNANLys, a pUC57 plasmid containing the *E. coli* tRNANLysUUU sequence for study was transformed in HB101 cells. These were then grown, purified, and tRNA de-acylated for use in synthetase and flexizyme amino-acylation assays, as described previously [26]. All other T7 transcribed tRNAs used in this study were aminoacylated using their cognate aminoacyl-tRNA synthetase (AsnRS, IleRS, PheRS, SerRS, and ValRS) and were His-tag purified from *E. coli* using plasmids available from AddGene [26]. *E. coli* tRNANfMet was natively purified from a pCWAug vector and methionine was formylated and installed on tRNANfMet using MTF and MetRS enzymes, which were His-tag purified from *E. coli* using plasmids available from AddGene [26, 74].

2.4.3 Global analysis simulations of amino acid addition

The reactions used to fit and model our data are displayed in SI Fig. 3. The fits used to obtain k1 and k2 were modeled using differential equations in Kaleidagraph. Subsequent rate constants (k3+) were modeled against simulations using KinTek Explorer. Simulations in KinTek Explorer were run against different potential mechanisms of ribosome sliding (SI Fig. 3) using data from quantified peptide formation.

2.4.4 Homopolymeric A sequences in human coding sequences

Homo sapiens genome assembly GRCh37 (hg19 release 75, cds.fa) data was used to identify the consecutive As in human coding sequences. Consecutive As were counted using in-house R scripts. Then, we analyzed single nucleotide resolution m6A mapping studies in different tissues

[45, 46] to find out whether any of these consecutive As have at least one installed m6A modification. This analysis yielded m6A frequencies that were reported in SI Table 5.

2.5 References

1. Wohlgemuth, I., Pohl, C., Mittelstaet, J., Konevega, A. L., and Rodnina, M. V. (2011) Evolutionary optimization of speed and accuracy of decoding on the ribosome. Philos. Trans. R. Soc. B Biol. Sci. 366, 2979–2986

2. Pedersen, S. (1984) *Escherichia coli* ribosomes translate in vivo with variable rate. EMBO J. 3, 2895–2898

3. Siller, E., DeZwaan, D. C., Anderson, J. F., Freeman, B. C., and Barral, J. M. (2010) Slowing bacterial translation speed enhances eukaryotic protein folding efficiency. J. Mol. Biol. 396, 1310–1318

4. Qian, W., Yang, J.-R., Pearson, N. M., Maclean, C., and Zhang, J. (2012) Balanced Codon Usage Optimizes Eukaryotic Translational Efficiency. PLoS Genet. 8, e1002603

5. Ban, N., Nissen, P., Hansen, J., Moore, P. B., and Steitz, T. A. (2000) The Complete Atomic Structure of the Large Ribosomal Subunit at 2.4 Å Resolution. Science. 289, 905–920

6. Jacobs, W. M., and Shakhnovich, E. I. (2017) Evidence of evolutionary selection for cotranslational folding. Proc. Natl. Acad. Sci. U. S. A. 114, 11434–11439

7. Hanson, G., Alhusaini, N., Morris, N., Sweet, T., and Coller, J. (2018) Translation elongation and mRNA stability are coupled through the ribosomal A-site. RNA. 24, 1377–1389

8. Presnyak, V., Alhusaini, N., Chen, Y.-H., Martin, S., Morris, N., Kline, N., Olson, S., Weinberg, D., Baker, K. E., Graveley, B. R., and Coller, J. (2015) Codon optimality is a major determinant of mRNA stability. Cell. 160, 1111–1124

9. Choi, J., Grosely, R., Prabhakar, A., Lapointe, C. P., Wang, J., and Puglisi, J. D. (2018) How mRNA and nascent chain sequences regulate translation elongation. Annu. Rev. Biochem. 87, 421–449

10. Lu, J., and Deutsch, C. (2008) Electrostatics in the Ribosomal Tunnel Modulate Chain Elongation Rates. J. Mol. Biol. 384, 73–86

11. Brandman, O., Stewart-Ornstein, J., Wong, D., Larson, A., Williams, C. C., Li, G.-W., Zhou, S., King, D., Shen, P. S., Weibezahn, J., Dunn, J. G., Rouskin, S., Inada, T., Frost, A., and Weissman, J. S. (2012) A Ribosome-Bound Quality Control Complex Triggers Degradation of Nascent Peptides and Signals Translation Stress. Cell. 151, 1042–1054

12. Charneski, C. A., and Hurst, L. D. (2013) Positively Charged Residues Are the Major Determinants of Ribosomal Velocity. PLoS Biol. 10.1371/journal.pbio.1001508

13. Koutmou, K. S., Schuller, A. P., Brunelle, J. L., Radhakrishnan, A., Djuranovic, S., and Green, R. Ribosomes slide on lysine-encoding homopolymeric A stretches. eLife. 10.7554/eLife.05534

14. Arthur, L. L., Pavlovic-Djuranovic, S., Koutmou, K. S., Green, R., Szczesny, P., and Djuranovic, S. (2015) Translational control by lysine-encoding A-rich sequences. Sci. Adv. 10.1126/sciadv.1500154

15. Rosenberg, A. H., Goldman, E., Dunn, J. J., Studier, F. W., and Zubay, G. (1993) Effects of consecutive AGG codons on translation in *Escherichia coli*, demonstrated with a versatile codon test system. J. Bacteriol. 175, 716–722

16. Sørensen, M. A., Kurland, C. G., and Pedersen, S. (1989) Codon usage determines translation rate in *Escherichia coli*. J. Mol. Biol. 207, 365–377

17. Liu, Y., Yang, Q., and Zhao, F. (2021) Synonymous but not Silent: The Codon Usage Code for Gene Expression and Protein Folding. Annu. Rev. Biochem. 90, 375–401

18. Ito-Harashima, S., Kuroha, K., Tatematsu, T., and Inada, T. (2007) Translation of the poly(A) tail plays crucial roles in nonstop mRNA surveillance via translation repression and protein destabilization by proteasome in yeast. Genes Dev. 21, 519–524

19. Release Factor eRF3 Mediates Premature Translation Termination on Polylysine-Stalled Ribosomes in *Saccharomyces cerevisiae* | Molecular and Cellular Biology [online] https://journals.asm.org/doi/10.1128/MCB.00799-14 (Accessed October 8, 2021)

20. Agirrezabala, X., Samatova, E., Klimova, M., Zamora, M., Gil-Carton, D., Rodnina, M. V., and Valle, M. (2017) Ribosome rearrangements at the onset of translational bypassing. Sci. Adv. 3, e1700147

21. Dinman, J. D. (2012) Mechanisms and implications of programmed translational frameshifting. Wiley Interdiscip. Rev. RNA. 3, 661–673

22. Jones, J. D., Monroe, J., and Koutmou, K. S. (2020) A molecular-level perspective on the frequency, distribution, and consequences of messenger RNA modifications. Wiley Interdiscip. Rev. RNA. 11, e1586

23. Ranjan, N., and Rodnina, M. V. (2016) tRNA wobble modifications and protein homeostasis. Translation. 4, e1143076

24. Tsai, T.-W., Yang, H., Yin, H., Xu, S., and Wang, Y. (2017) High-Efficiency "–1" and "–2" Ribosomal Frameshiftings Revealed by Force Spectroscopy. ACS Chem. Biol. 12, 1629–1635

25. Yan, S., Wen, J.-D., Bustamante, C., and Tinoco, I. (2015) Ribosome Excursions during mRNA Translocation Mediate Broad Branching of Frameshift Pathways. Cell. 160, 870–881

26. Monroe, J. G., Smith, T. J., and Koutmou, K. S. (2021) Investigating the consequences of mRNA modifications on protein synthesis using in vitro translation assays, Methods in Enzymology, Academic Press, https://doi.org/10.1016/bs.mie.2021.06.011

27. Kim, H.-K., and Tinoco, I. (2017) EF-G catalyzed translocation dynamics in the presence of ribosomal frameshifting stimulatory signals. Nucleic Acids Res. 45, 2865–2874

28. Klimova, M., Senyushkina, T., Samatova, E., Peng, B. Z., Pearson, M., Peske, F., and Rodnina, M. V. (2019) EF-G–induced ribosome sliding along the noncoding mRNA. Sci. Adv. 10.1126/sciadv.aaw9049

29. Chen, J., Petrov, A., Johansson, M., Tsai, A., O'Leary, S. E., and Puglisi, J. D. (2014) Dynamic pathways of -1 translational frameshifting. Nature. 512, 328–332

30. Lorenz, C., Lünse, C. E., and Mörl, M. (2017) tRNA Modifications: Impact on Structure and Thermal Adaptation. Biomolecules. 7, 35

31. Agris, P. F., Narendran, A., Sarachan, K., Väre, V. Y. P., and Eruysal, E. (2017) The Role of RNA Modifications in Translational Fidelity. The Enzymes. 41, 1–50

32. Bekaert, M., and Rousset, J.-P. (2005) An extended signal involved in eukaryotic -1 frameshifting operates through modification of the E site tRNA. Mol. Cell. 17, 61–68

33. Maehigashi, T., Dunkle, J. A., Miles, S. J., and Dunham, C. M. (2014) Structural insights into +1 frameshifting promoted by expanded or modification-deficient anticodon stem loops. Proc. Natl. Acad. Sci. U. S. A. 111, 12740–12745

34. Rezgui, V. A. N., Tyagi, K., Ranjan, N., Konevega, A. L., Mittelstaet, J., Rodnina, M. V., Peter, M., and Pedrioli, P. G. A. (2013) tRNA tKUUU, tQUUG, and tEUUC wobble position modifications fine-tune protein translation by promoting ribosome A-site binding. Proc. Natl. Acad. Sci. U. S. A. 110, 12289–12294

35. Ranjan, N., and Rodnina, M. V. (2017) Thio-Modification of tRNA at the Wobble Position as Regulator of the Kinetics of Decoding and Translocation on the Ribosome. J. Am. Chem. Soc. 139, 5857–5864

36. Ahmed, N., Friedrich, U. A., Sormanni, P., Ciryam, P., Altman, N. S., Bukau, B., Kramer, G., and O'Brien, E. P. (2020) Pairs of amino acids at the P- and A-sites of the ribosome predictably and causally modulate translation-elongation rates. J. Mol. Biol. 432, 166696

37. Goto, Y., Katoh, T., and Suga, H. (2011) Flexizymes for genetic code reprogramming. Nat. Protoc. 6, 779–790

38. Dale, T., Sanderson, L. E., and Uhlenbeck, O. C. (2004) The Affinity of Elongation Factor Tu for an Aminoacyl-tRNA Is Modulated by the Esterified Amino Acid. Biochemistry. 43, 6159–6166

39. Yikilmaz, E., Chapman, S. J., Schrader, J. M., and Uhlenbeck, O. C. (2014) The Interface between *Escherichia coli* Elongation Factor Tu and Aminoacyl-tRNA. Biochemistry. 53, 5710–5720

40. Tesina, P., Lessen, L. N., Buschauer, R., Cheng, J., Wu, C. C.-C., Berninghausen, O., Buskirk, A. R., Becker, T., Beckmann, R., and Green, R. (2020) Molecular mechanism of translational stalling by inhibitory codon combinations and poly(A) tracts. EMBO J. 39, e103365

41. Chandrasekaran, V., Juszkiewicz, S., Choi, J., Puglisi, J. D., Brown, A., Shao, S., Ramakrishnan, V., and Hegde, R. S. (2019) Mechanism of ribosome stalling during translation of a poly(A) tail. Nat. Struct. Mol. Biol. 26, 1132–1140

42. Liu, B., Shi, H., Rangadurai, A., Nussbaumer, F., Chu, C.-C., Erharter, K. A., Case, D. A., Kreutz, C., and Al-Hashimi, H. M. (2021) A quantitative model predicts how m6A reshapes the kinetic landscape of nucleic acid hybridization and conformational transitions. Nat. Commun. 12, 5201

43. Shi, H., Liu, B., Nussbaumer, F., Rangadurai, A., Kreutz, C., and Al-Hashimi, H. M. (2019) NMR chemical exchange measurements reveal that N6-methyladenosine slows RNA annealing. J. Am. Chem. Soc. 141, 19988–19993

44. Roost, C., Lynch, S. R., Batista, P. J., Qu, K., Chang, H. Y., and Kool, E. T. (2015) Structure and Thermodynamics of N6-Methyladenosine in RNA: A Spring-Loaded Base Modification. J. Am. Chem. Soc. 137, 2107–2115

45. Linder, B., Grozhik, A. V., Olarerin-George, A. O., Meydan, C., Mason, C. E., and Jaffrey, S. R. (2015) Single-nucleotide resolution mapping of m6A and m6Am throughout the transcriptome. Nat. Methods. 12, 767–772

46. Zhang, Z., Chen, L.-Q., Zhao, Y.-L., Yang, C.-G., Roundtree, I. A., Zhang, Z., Ren, J., Xie, W., He, C., and Luo, G.-Z. (2019) Single-base mapping of m6A by an antibody-independent method. Sci. Adv. 5, eaax0250

47. Leininger, S. E., Rodriguez, J., Vu, Q. V., Jiang, Y., Li, M. S., Deutsch, C., and O'Brien, E. P. (2021) Ribosome Elongation Kinetics of Consecutively Charged Residues Are Coupled to Electrostatic Force. Biochemistry. 60, 3223–3235

48. Lu, J., and Deutsch, C. (2008) Electrostatics in the Ribosomal Tunnel Modulate Chain Elongation Rates. J. Mol. Biol. 384, 73–86

49. Dimitrova, L. N., Kuroha, K., Tatematsu, T., and Inada, T. (2009) Nascent Peptide-dependent Translation Arrest Leads to Not4p-mediated Protein Degradation by the Proteasome. J. Biol. Chem. 284, 10343–10352

50. Licznar, P., Mejlhede, N., Prère, M.-F., Wills, N., Gesteland, R. F., Atkins, J. F., and Fayet, O. (2003) Programmed translational –1 frameshifting on hexanucleotide motifs and the wobble properties of tRNAs. EMBO J. 22, 4770–4778

51. Johansson, M. J. O., Esberg, A., Huang, B., Björk, G. R., and Byström, A. S. (2008) Eukaryotic Wobble Uridine Modifications Promote a Functionally Redundant Decoding System. Mol. Cell. Biol. 28, 3301–3312

52. Rozov, A., Demeshkina, N., Khusainov, I., Westhof, E., Yusupov, M., and Yusupova, G. (2016) Novel base-pairing interactions at the tRNA wobble position crucial for accurate reading of the genetic code. Nat. Commun. 10.1038/ncomms10457

53. Karlsborn, T., Tükenmez, H., Chen, C., and Byström, A. S. (2014) Familial dysautonomia (FD) patients have reduced levels of the modified wobble nucleoside mcm5s2U in tRNA. Biochem. Biophys. Res. Commun. 454, 441–445

54. Björk, G. R., Huang, B., Persson, O. P., and Byström, A. S. (2007) A conserved modified wobble nucleoside (mcm5s2U) in lysyl-tRNA is required for viability in yeast. RNA. 13, 1245–1255

55. Suzuki, T. (2021) The expanding world of tRNA modifications and their disease relevance. Nat. Rev. Mol. Cell Biol. 22, 375–392

56. Torres, A. G., Batlle, E., and Ribas de Pouplana, L. (2014) Role of tRNA modifications in human diseases. Trends Mol. Med. 20, 306–314

57. Yasukawa, T., Suzuki, T., Ishii, N., Ohta, S., and Watanabe, K. (2001) Wobble modification defect in tRNA disturbs codon–anticodon interaction in a mitochondrial disease. EMBO J. 20, 4794–4802

58. Hoernes, T. P., Heimdörfer, D., Köstner, D., Faserl, K., Nußbaumer, F., Plangger, R., Kreutz, C., Lindner, H., and Erlacher, M. D. (2019) Eukaryotic Translation Elongation is Modulated by Single Natural Nucleotide Derivatives in the Coding Sequences of mRNAs. Genes. 10.3390/genes10020084

59. Hoernes, T. P., Faserl, K., Juen, M. A., Kremser, J., Gasser, C., Fuchs, E., Shi, X., Siewert, A., Lindner, H., Kreutz, C., Micura, R., Joseph, S., Höbartner, C., Westhof, E., Hüttenhofer, A., and Erlacher, M. D. (2018) Translation of non-standard codon nucleotides reveals minimal requirements for codon-anticodon interactions. Nat. Commun. 10.1038/s41467-018-07321-8

60. You, C., Dai, X., and Wang, Y. (2017) Position-dependent effects of regioisomeric methylated adenine and guanine ribonucleosides on translation. Nucleic Acids Res. 45, 9059–9067

61. Choi, J., Ieong, K.-W., Demirci, H., Chen, J., Petrov, A., Prabhakar, A., O'Leary, S. E., Dominissini, D., Rechavi, G., Soltis, S. M., Ehrenberg, M., and Puglisi, J. D. (2016) N 6 -methyladenosine in mRNA disrupts tRNA selection and translation-elongation dynamics. Nat. Struct. Mol. Biol. 23, 110–115

62. Ieong, K.-W., Indrisiunaite, G., Prabhakar, A., Puglisi, J. D., and Ehrenberg, M. (2021) N 6-Methyladenosines in mRNAs reduce the accuracy of codon reading by transfer RNAs and peptide release factors. Nucleic Acids Res. 49, 2684–2699

63. Kladwang, W., Topkar, V. V., Liu, B., Rangan, R., Hodges, T. L., Keane, S. C., al-Hashimi, H., and Das, R. (2020) Anomalous reverse transcription through chemical modifications in polyadenosine stretches. Biochemistry. 59, 2154–2170

64. Caliskan, N., Katunin, V. I., Belardinelli, R., Peske, F., and Rodnina, M. V. (2014) Programmed –1 Frameshifting by Kinetic Partitioning during Impeded Translocation. Cell. 157, 1619–1631

65. Eyler, D. E., Franco, M. K., Batool, Z., Wu, M. Z., Dubuke, M. L., Dobosz-Bartoszek, M., Jones, J. D., Polikanov, Y. S., Roy, B., and Koutmou, K. S. (2019) Pseudouridinylation of mRNA coding sequences alters translation. Proc. Natl. Acad. Sci. U. S. A. 116, 23068–23074

66. Liao, P.-Y., Gupta, P., Petrov, A. N., Dinman, J. D., and Lee, K. H. (2008) A new kinetic model reveals the synergistic effect of E-, P- and A-sites on +1 ribosomal frameshifting. Nucleic Acids Res. 36, 2619–2629

67. Sitron, C. S., and Brandman, O. (2020) Detection and Degradation of Stalled Nascent Chains via Ribosome-Associated Quality Control. Annu. Rev. Biochem. 89, 417–442

68. Meydan, S., and Guydosh, N. R. (2020) Disome and trisome profiling reveal genome-wide targets of ribosome quality control. Mol. Cell. 79, 588-602.e6

69. Juszkiewicz, S., and Hegde, R. S. (2017) Initiation of Quality Control during Poly(A) Translation Requires Site-Specific Ribosome Ubiquitination. Mol. Cell. 65, 743-750.e4

70. Guydosh, N. R., and Green, R. (2017) Translation of poly(A) tails leads to precise mRNA cleavage. RNA. 23, 749–761

71. Youngman, E. M., Brunelle, J. L., Kochaniak, A. B., and Green, R. (2004) The Active Site of the Ribosome Is Composed of Two Layers of Conserved Nucleotides with Distinct Roles in Peptide Bond Formation and Peptide Release. Cell. 117, 589–599

72. Zaher, H. S., and Green, R. (2009) Quality control by the ribosome following peptide bond formation. Nature. 457, 161–166

73. Murakami, H., Ohta, A., Ashigai, H., and Suga, H. (2006) A highly flexible tRNA acylation method for non-natural polypeptide synthesis. Nat. Methods. 3, 357–359

74. Walker, S.E., and Fredrick, K. (2008) Preparation and evaluation of acylated tRNAs. Methods 44, 81–86

Chapter 3 Anticodon Stem-Loop --tRNA Modifications Influence Codon Decoding and Frame Maintenance During Translation[3]

Work presented in this chapter was submitted for publication in
Seminars in Cell and Developmental Biology.

Tyler J. Smith and Kristin S. Koutmou

3.1 Introduction

Transfer RNAs (tRNAs) are key adaptor molecules in protein synthesis, shuttling amino acids into the ribosome in an order dictated by the genetic code. The ability of tRNAs to "read" mRNA blueprints during translation is essential for ensuring that amino acids are linked together in the correct order to generate functional proteins. One feature that distinguishes tRNAs from other types of RNA molecules is the large number and variety of post-transcriptional modifications enzymatically incorporated into their scaffolds. Typically, 10-20% of tRNA nucleobases are modified, and the chemical diversity of these modifications range broadly in complexity from methyl additions (e.g. 1-methyladenosine) incorporated by a single enzyme, to entire ring additions that require multiple enzymes to install (e.g. Wybutosine (yW) is added in a 7-step enzymatic pathway) [1]. Given the substantial effort that biology makes to incorporate and maintain modifications in all organisms, it is unsurprising that post-transcriptional modifications

[3] The work presented in this chapter was to review what is known about how modifications to the Anti-Codon Stem Loop (ASL) of tRNAs impact translation rates, fidelity, and frame maintenance. While the referenced work throughout are the motivation and proof of the role these modifications have in such factors, I was the primary author and editor for assembling such work in this review. Kristin Koutmou provided writing and editing assistance after completion of the main body of this work/review.

play essential roles in tRNA function – affecting their structure, stability, aminoacylation, and decoding capabilities [2].

The significance of modifications in tRNAs is underscored by wide-spread observations that alterations in the tRNA modification status can drastically impact protein homeostasis [3], [4]. This is exemplified during cellular stress, when changes to the overall modification landscape of tRNAs can have important downstream consequences, including the reprogramming of tRNAs to control selective translation as well as cell and protein homeostasis [5], [6]. There is a wealth of rapidly expanding literature supporting notion that the dysregulation tRNA modifications has deleterious outcomes on cellular and human health [1], [3], [7], [8]. Depletion of tRNA modifications and the enzymes that install them result in a wide range of pathological consequences, or 'RNA modopathies', such as cancer, neurological disorders, and mitochondrial diseases [9], [10]. In light of their central role in maintaining protein levels, it is important to understand how tRNA modifications impact protein synthesis at the molecular level. This is a complicated endeavor given the sheer variety of tRNA modifications reported in biology (> 90), but a clear picture is beginning to emerge about how a limited subset of modifications influence translation. While chemically altered nucleosides are incorporated throughout the tRNA structure (Figure 1A), modifications localized in the anticodon stem loop (ASL) region (Figure 1B) near the site of mRNA:tRNA interaction are particularly notable because they often essential for guaranteeing that the translational machinery rapidly and faithfully decodes mRNA sequences [11]. In this review, we discuss the current state of the molecular-level knowledge surrounding how tRNA ASL modifications influence codon recognition, translational fidelity, and ribosome reading frame maintenance.

3.2 tRNA modifications impact codon decoding during translation

Aminoacylated tRNAs (aa-tRNAs) must faithfully decode messenger RNA (mRNA) codon sequences to ensure that the ribosome rapidly and accurately synthesizes proteins. For the 61 sense codons, there are over 1000 known tRNA sequences across phylogeny, most of which share a high level of structural conservation [12]. Despite their shared structures, different tRNAs and their isoacceptors (tRNAs that encode for the same amino acid but recognize different codons) recognize between one and four codon sequences. Codon recognition requires the formation of stable interactions between mRNA nucleobases and the ASL region of tRNAs. The ability of a given tRNA sequence to interact (or not) with a variety of codons is largely dictated by the modification status of the tRNA anti-codon stem loop (ASL; as reviewed in (Figure 1A,B) [13].

The ASL contains the highest density of modifications within tRNA sequences. Over 20 varieties of modifications have been reported within tRNA ASLs (Figure 1), and tRNA positions 32, 34, 37, 38, and 39 are most commonly modified. These modifications typically enhance stem-

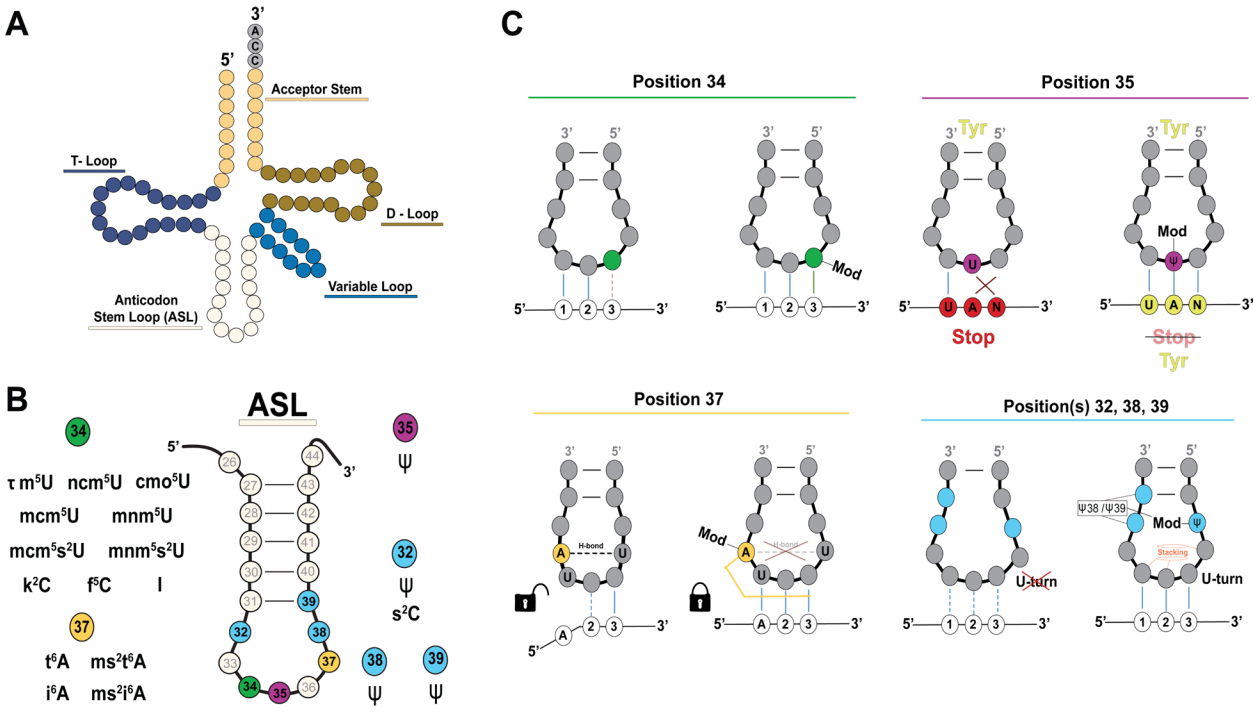

Figure 3.1 *Modifications to the anticodon stem loop of tRNAs impact ability to recognize codons. (A) Cloverleaf representation of a tRNA, in 5' to 3' directionality, with regions highlighted. (B) Isolated Anticodon stem loop from (A) consisting of nucleotides 26-44 with modifications that impact translation listed. Modifications discussed in this work are installed at positions 34 (green), 35 (purple), and 37 (yellow) as part of, or just adjacent to, the anticodon which impact direct codon recognition. Othe modifications are installed as part of, or just adjacent to, the stem loop and impact ASL stability. (C) Summaries of numbered positions modifications and their general effect to the ASL and codon recognition. Modifications at position 34 (green) stabilize the N1-N34 codon-anticodon base pair and often expand degeneracy. Pseudouridine, ψ, at position 35 (purple) in tRNATyr in eukaryotes allows for UA(A/G) stop codon suppression. Modifications at position 37 (yellow) serve a dual purpose based on extent of modification (i.e. t6A37 vs ms2t6A37). These can be broadly summarized as stabilizing and decreasing flexibility of the ASL by preventing intra-loop H-bond and improving N1-N34 codon-anticodon A-U base pairs via mRNA-tRNA cross-strand stacking, both of which improve codon recognition. Modifications at the base and adjacent to the stem loop (blue) improve ASL stability and codon recognition by allowing for additional H-bonding in the stem-loop or ASL, or by introducing base-stacking elements to reduce flexibility – often being integral in formation of the U-turn motif in tRNAs which improves decoding. ψ can be installed at one or more of the following positions in a single: 32, 38, and/or 39.*

loop stability and mRNA recognition, though their identity at each ASL position varies between organisms and tRNA isoacceptors (Figure 1B) [2], [14], [15]. Positions 34 and 37 tend to have the most chemically complex modifications on tRNAs (and more broadly within RNA biology). These modifications are generally important for crucial steps in translation, namely elongation and termination. The significance of these modifications is underscored by the observation that some of the enzymes that incorporate them are essential for cell viability – for example, the

tRNA-specific adenosine deaminase 2 (ADAT2)-ADAT3 complex in humans responsible for catalyzing the conversion of adenosine to inosine at position 34. [9]. However, while genetic studies reveal the importance of many ASL modifications to cellular health, our understanding of precisely how individual modifications assert their function rely on molecular level biochemical and/or structural investigations. Below we examine how modifications in the ASL impacting amino acid addition, codon recognition, and mRNA-tRNA interactions, with an emphasis on their mechanism of action.

3.2.1 Position 34 modifications enhance (and sometimes expand) codon decoding by tRNAs

Position 34 in tRNAs base pairs with the 3rd nucleotide in a codon, and referred to as the "wobble position". A wider variety of interactions are permitted between tRNA 34 and the wobble position, and can include several types of non-Watson–Crick base pairs. While position 34 is not always modified, non-canonical interactions are largely facilitated by tRNA modifications to all four nucleotides at position 34. Uracil bases at this position commonly possess the largest, most diverse modifications and tend to be essential for mRNA decoding. For example, tRNAs are commonly post-transcriptionally modified with xm5 (5-methylaminomethyl [mnm5] and 5-methylaminomethyl-2-thio [mnm5s2] in bacteria, and 5-carbamoylmethyl [ncm5], 5-carbamoylmethyl-2-thio [ncm5s2], 5-methoxycarbonylmethyl [mcm5], 5-methoxycarbonylmethyl-2-thio [mcm5s2] in yeast and higher eukaryotes) at the U34 wobble base [16], [17]. This class of modifications is important for association and accommodation in the A-site of the ribosome, among other elongation events, and loss of U34 modifications results in cellular dysfunction as a consequence of changes in rates of decoding and altered protein homeostasis [10], [18], [19]. In vitro and cell-based studies of tRNALys(UUU), tRNAGln(UUG), and tRNAGlu(UUC) demonstrate that mcm5 and s2 at U34

stabilize binding to mRNA substrates and are indispensable for efficient translation on mRNAs enriched with AAA, CAA, or GAA codons [19]–[22]. Although presence of mcm5, mcm5s2, or ncm5s2 promote the decoding of codons ending in either A or G, the modifications do not appear to be required (at least in yeast) for U-G wobble decoding for AAG, CAG, and GAG codons as protein homeostasis is largely unaffected when they are missing [22]–[24].

High resolution NMR and x-ray structural studies support biochemical and cellular findings that tRNALys(UUU) xm5s2U34 modifications increase the ability of the tRNA to decode multiple codons. These investigations reveal that in humans tRNALys(UUU) mcm5s2 is able to undergo a tautomerization to form a U-G Watson-Crick like base-pair, and *E. coli* tRNALys(UUU) mnm5s2 is similarly capable of adapting a zwitterionic form that allows for reading of AAG codons [25]–[27]. The s2 modification appears to be particularly important in tRNALys decoding as it is involved in H-bonding when pairing with G and increases binding affinity of tRNALys when pairing with A [27]–[29]. In addition, kinetic studies of the translation pathway indicate that tRNALys(UUU) possessing hypomodified mcm5U34 (lacking s2) have slower EF-Tu rearrangement and Pi release following GTP hydrolysis (~6-fold), exhibit faster dissociation between the codon-recognition complex (~5-fold), and increase the rate constant for tRNALys(UUU) rejection (~3-fold). Additionally, s2-deplete tRNALys(UUU) also modestly impede translocation of the ribosome when compared to natively mcm5s2U34 modified tRNALys(UUU) [29], [30]. Similar work investigating the impact of mnm5s2U34 on *E. coli* tRNAGln(UUG) function discovered through mass spectrometry that the mcm5 moiety at position 34 is actually cmnm5s2U and that the s2 modification in this context also enhances binding affinity to cognate codons (CAA and CAG) as well as increases the rate of GTP hydrolysis of EF-Tu during translation (~5-fold) [31]. Furthermore, xm5s2U34 modifications are

essential in frameshifting/frame maintenance, as we discuss in the subsequent -1 programmed frame shifting (PRF) focused portion of this review.

Uridine modifications beyond the xm5s2U34 also have similar effects, enhancing weaker mRNA:tRNA basepairing interactions to allow for expanded codon decoding by a single tRNA species. Examples include τm5U34, found in mitochondrial *E. coli* tRNALeu(UUR), and cmo5U34, one of the most prevalent modifications in tRNA. Mitochondrial *E. coli* tRNALeu(UUR) decodes both UUA and UUG codons, and UUG (but not UUA) decoding strictly requires the τm5U34 modification because it enables the tRNA to form a non-wobble Watson-Crick like U-G base pair [32]–[34]. cmo5U34 also enables tRNAs to decode a wide array of codons, as highlighted by the observation that *E. coli* and S. typhirium tRNA species possessing cmo5U34 all recognize four codons in their four-fold degenerate codon boxes (tRNAAla, tRNASer, tRNAThr, tRNAPro, tRNAVal, with tRNALeu having six codon degeneracy), while those lacking the modification are not [35], [36]. In vitro studies in *E. coli* have shown that the cmo5U34 modification of the tRNA1BAla(CGU) allows for efficient recognition of its cognate codon (GCA) as well as of the non-cognate Ala codon (GCG), with the U-G pairing treated as an almost-correct base-pair versus a mismatch [28], [37], [38]. NMR studies further reveal that cmo5 is important for pre-ordering the anticodon stem loop to promote the binding of *E. coli* tRNAVal3(UAC) to all four valine codons, further suggesting that the modification may be important in both stabilizing and expanding codon reading [39].

Other support for wobble position expanding genetic code that does not involve modified uridine is the 5-formylcytidine (f5C34) modification on mitochondrial human tRNAMet(CAU). Prokaryotes and eukarytotes tend to have two isoacceptors for tRNAMet(CAU) to distinguish between AUG initiator and elongator methionine. However, human mitochondria only have a

single modified isoacceptor to decode AUG, which is not present in cytosolic human tRNAMet(CAU) [40]. Instead, hmtRNAMet(CAU) has an f5C34 in its ASL which allows for initiator Met decoding at AUG as well as elongator Met decoding at the universal Ile codon, AUA, with 80% of elongator Met installed at these Ile codons in mitochondrial tRNA [41]. The f5C34 hmtRNA is capable of decoding at both P- and A-sites of the ribosome through prototropic tautomerization, allowing for a Watson-Crick f5C-A base-pair as well as proper ASL U-turn formation for A-site binding on AUA codons [42]. Interestingly, cytidine at position 34 is also found to be modified with lysidine (k2C34) on tRNA2Ile(CAU) in *E. coli* which seemingly functions in the opposite manner of f5C34, enhancing decoding AUA and restricting AUG decoding [43], [44]. The k2C34, in conjunction with a t6A37, facilitate base stacking and stability of the ASL, which shift codon recognition from AUG to AUA for decoding [43], [45]. Comparing the effects wobble f5C and k2C have in expanding or restricting codon recognition highlights the unique role tRNA ASL modifications have in adapting to evolution of genetic code.

Inosine, formed by the deamination of adenosine, was the first modification discovered within the anticodon and allows for expanded degeneracy by reading A, U, and C, serving as another wobble nucleobase when at position 34 of tRNAs [46]. While it is widely considered a standard Crick nucleotide, inosine has only been reported in two *E. coli* tRNAs (tRNA1Arg(ACG) and tRNA2Arg(ACG)), and 8 cytosolic eukaryotic tRNAs [1], [47], [48]. When harboring just a single I34 modification both *E. coli* tRNAArg(ACG) isoacceptors in are able to decode all three synonymous codons for arginine (CGU, CGA, and CGG), whereas the unmodified versions can only bind CGU [49]. Notably, tRNA1,2Arg(AGC) possess additional modifications, s2C32 and m2A37, within their ASL which that drive them to prefer either CGU

or CGC binding but drastically reducing CGA decoding [13], [49], [50]. The combinatorial effect of modifications may explain codon bias against CGA in mRNAs as well as begin to highlight the interplay that tRNA modifications have in evolution of genetic code degeneracy [51], [52]. When combined, such structural and biochemical studies suggest that modifications, especially those at U34, are imperative in proper ASL formation and accurate decoding of mRNA (Figure 1C).

3.2.2 Position 37 modifications form hydrogen bonding interactions that promote base-stacking to stabilize codon-anticodon interactions

Nucleotides at position 37 of tRNAs are adjacent to the 3' of the anticodon, and not directly involved in making mRNA:tRNA hydrogen bonding interactions (Figure 1). Nonetheless, these nucleotides, which are universally purines, are often modified and can modulate ASL structure to stabilize codon-anticodon interactions. N6-threonylcarbamoyladenosine (t6A) is among modifications most commonly found on A37 of tRNAs decoding ANN codons in all domains of life. t6A promotes efficient tRNA binding and decoding of codons in the ribosome A site, as well as helps to maintain both efficient translocation and frame maintenance [53], [54]. This is accomplished through a network of intra-ASL hydrogen bonding interactions that promote base-stacking to promote tRNA:mRNA associations [2], [55]. t6A modification can be found alone or in conjunction with additional chemical moieties, as is the case in the human tRNA3Lys(UUU), which contains an ms2 group to generate ms2t6A37 [56]. In either state (t6A or ms2t6A), this modification stabilizes the A-U base pair formed between the mRNA and tRNA (A1 – U36 or U1 – A36) in the A-site by stacking over this codon-anticodon base-pair, with the stacking then propagating up the 3' side of the ASL necessary to form initial cross-strand stack to increase ASL flexibility, though it should be noted that mnm5s2U34 (or mcm5s2 in eukaryotes) must also

be present for proper decoding of AAA or AAG codons as binding is weaker with the UUU anticodon when either modification is absent [25], [57], [58]. The ms2 modification is not present on all t6A37 modifications in tRNAs, however it appears to improve decoding of AAG by tRNA3Lys(UUU) through dehydration of the ASL as well as the codon-anticodon interaction when it is installed [27], [59], [60]. In *E. coli* and yeast, t6A37 can also be further cyclized to an oxazolone ring (ct6A37) that enhances decoding efficiency by generating an additional H-bond with an A1 codon nucleotide in addition to the stacking effect the modification provides [61], [62]. Interestingly, t6A has been found to be universal and essential in many bacteria and eukaryotes but the enzyme orthologs responsible for the modification function in distinct complexes and it is unclear how cellular environments have involved to maintain the modification [58], [63].

Isopentyladenosine (i6A) and its ms2i6A counterpart are also frequently found on A37 of tRNAs. Much like t6A, i6A modifications act to stabilize U1 - A36 base pairing when decoding UNN codons [64]. Lack of (ms2)i6A in *E. coli* tRNAPhe(GAA), tRNALeu(UUR) tRNACys(GCA) and tRNATyr(QUA) decreases the recognition efficiency of cognate tRNAs for their codons [65]–[68]. In eukaryotes (ms2)i6A37 modification appears to ensure both accurate decoding in manners detailed above, as well as efficiency of suppressor tRNAs on the UGA stop codon [69], [70]. Whether (ms2)t6A or (ms2)i6A are installed on A37, the modifications are important in maintain ASL structure by preventing H-bonding between U33 and A37 in addition to stabilizing their adjacent A-U Watson-Crick base pair of the codon's first position [2]. The other purine, guanosine, is frequently modified to wyosine (imG) and its derivatives at position 37 in tRNAs (e.g. tRNAPhe(GAA)) and is important for proper decoding and maintaining mRNA-tRNA interactions in the both the P- and A-sites of the ribosome (Konevega et al., 2006;

Soboleva et al., 2003). The complex modification enhances base stacking with adjacent bases to prevent flexibility in the ASL, further supporting the role that modification to purines at position 37 in tRNAs have in the pre-structuring and decoding capability of the ASL (Figure 1C) [73], [74].

3.2.3 Modifications at further positions within the ASL make diverse contributions to tRNA maturation and function

Many modifications within tRNA ASLs act synergistically to impact decoding, such as s2C32 and I34 of tRNA(ACG) discussed above, or have been found to affect protein homeostasis (as reviewed in Lateef et al., 2022). Additionally, many modifications in this region of tRNA are responsible for directing efficient installation of other ASL modifications. As is the case for yeast tRNASer in which i6A37 appears as a pre- or co-requisite of successful m3C32 modification [76]–[78]. Direct structural and biochemical investigations of other ASL modifications in translation remain limited, though interest in these modifications is receiving growing attention. Currently, pseudouridine (ψ), an isomer of uridine, is among the most well studied modifications with the ASL region of tRNAs. It can be incorporated throughout the ASL, but regardless of its location ψ appears to be important for pre-structuring the ASL and to enhance tRNA decoding. For example, ψ modifications are frequently incorporated on *E. coli* and eukaryotic tRNAs at U32, U38 and U39 of tRNAs and are involved in proper intra-ASL base-pairing and structuring of the stem-loop (Figure 1C) [79], [80]. On *E. coli* tRNAPhe(GAA), ψ39 base-pairs with A31 and allows for strengthening of the stem-loop while ψ32 forms a bifurcated H-bond with A38 which promotes the U-turn motif and open-loop structure required for efficient decoding of the ribosomal A-site [27], [81]–[83]. More directly involved in codon recognition, the U35ψ substitution in tRNATyr(GψA) from multiple various organisms appears

to be indispensable for both UAA and UAG stop codon suppression. Strikingly, this modification does not impact normal UAU and UAC decoding by tRNATyr(GUA), suggesting that the U35ψ modification is important for genetic code expansion – a similar situation observed for a tRNAAsn(GψU) capable of decoding a near cognate lysine codon (AAA) while not affecting normal asparagine decoding (AAC/U) (Figure 1C) [69], [84]. While clear that ψ throughout the ASL are important for structure and codon recognition, continuing mechanistic studies of other modifications is important to understand the role that the stem-loop and modification cross-talk have in altering tRNA decoding.

3.3 tRNA Modifications in frame maintenance

Since codons of mRNA are comprised of 3 nucleotides, there are inherently 3 potential translation reading frames the ribosome can decode. As such, it is important to understand how the ribosome chooses and the maintains proper reading frame during elongation to ensure the correct gene-encoded protein. While this is generally the case, altering frameshifting can be situationally advantageous as is the case of many viruses which use programmed shifts to move into different reading frames in order to recognize alternative start sites and bypass or recode termination sites [85] (Figure 2A). mRNA:tRNA interactions are integral to maintain proper frame, and it stands to reason that tRNA ASL modifications affect decoding, but also the ability of frameshift.

3.3.1 ASL modifications can alternatively promote and limit -1 frameshifting events

Programmed ribosomal frameshifting (PRF) into the -1 frame requires mRNA elements to improve frequency of frameshift compared to spontaneous ribosome slippage (once in every 104-105 codons) [86], [87]. These elements often include a 5'-Shine Dalgarno sequence (in

bacterial systems) and a 3'- mRNA structural element such as a hairpin or pseudoknot, that position and pause the ribosome over a 'slippery' heptanucleotide sequence: X XXY YYZ (in which XXX and YYY are triplets of the same nucleotide, but different codons) [88], [89]. The efficiency of any given -1 PRF in cells often depends on the availability of cognate tRNAs and, sometimes, the nutrient levels of cells [90]. The site of -1 PRF occurs when the ribosome has the Y(YY/Z) split-box codon positioned in the A-site and the anticodon of the aa-tRNA dissociating before recognizing the new -1 frame [91], [92]. The ability of the aa-tRNA to dissociate from YYZ and instead decode the -1 frame, YYY, can be influenced by the modification state of the tRNA's anti-codon ASL at positions 34 and 37 (Table 1, Figure 2A). tRNAs involved in these -1 frameshifting

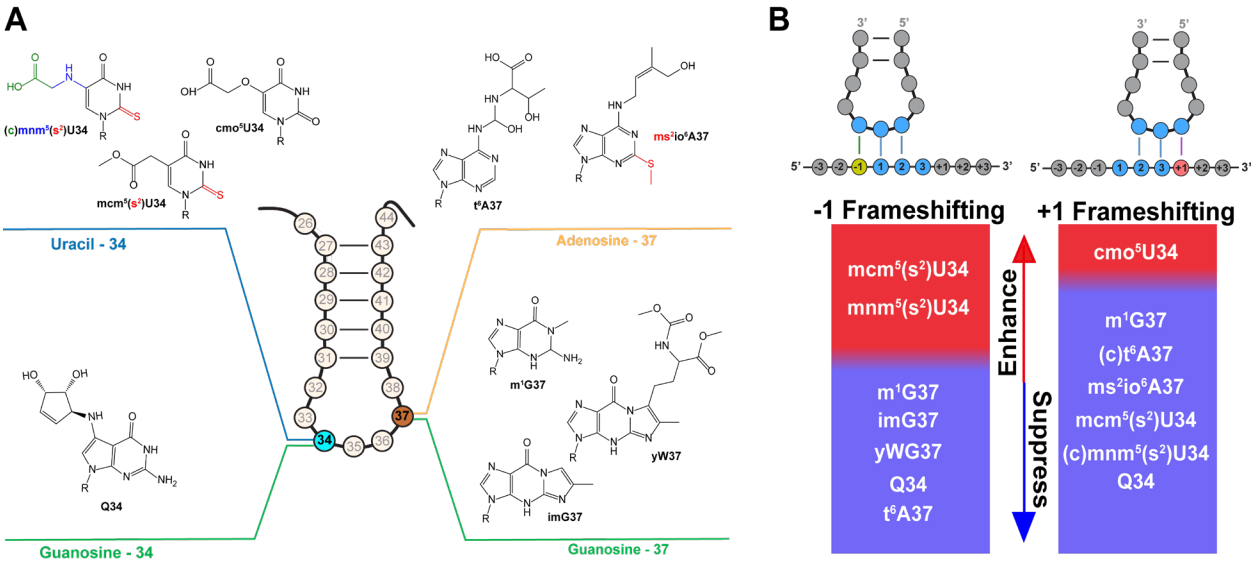

Figure 3.2 *Modifications at position 34 and 37 are important in directing -1 and +1 frameshifts (A) Isolated anticodon stem loop which with nucleobase modifications involved in enhancing or suppressing frameshifting when installed at positions 34 or 37. Colored sections of nucleobases and their abbreviations indicate that various levels of complexity of that modification are involved in directing frameshifting events. (i.e. (c)mnm5s2U34 has three possible modification states which impart frameshifting – green: cmnm5s2U34, red: mnm5s2U34, blue: mnm5U34 – as shown in (B). (B) Modifications at position 34 or 37 which enhance or suppress frameshift.*

events are commonly post-transcriptionally modified at the U34 wobble base with xm5 (mnm5, mnm5s2 in bacteria, and ncm5, ncm5s2, mcm5, mcm5s2 in yeast and higher eukaryotes) [16],

[17]. In bacteria, loss of the either the mnm5 or s2 modification on U34 of tRNALys(UUU) impedes -1 frameshifting by the ribosome on the AAA/G split codon box, because the hypomodified state has increased affinity for U-G binding for the A-site tRNA, limiting potential dissociation and recoding (Figure 2B) [93]–[95]. However, when looking at individual lysine codon-anticodon interactions, tRNALys with mnm5s2 forms a unique zwitterionic U-G base pair that is comparable to the U-A pairing when allowed opportunity to change 'shape' of the wobble [26]. This highlights an interplay between U34 modification state and mRNA context as the modifications shift the tRNALys to preferentially form U-A instead of U-G pairings although a single isoacceptor is used to decode both AAA and AAG codons [25]. It may also help to rationalize why many eukaryotes possess two distinct isoacceptors for lysine codons (tRNALys(UUU) and tRNALys(UUC)), because in order to (limit such frameshifting events / more finely control fidelity) [96]. mcm5s2 U34 is found in other split-box codon tRNAs (e.g. tRNAArg(UCU), tRNAGln(UUG), and tRNAGlu(UUC)) and has the potential to influence fidelity and frameshifting. Indeed, tRNAGlu(UUC) has been found to also have -1 frameshifting in *S. cerevisiae* strains lacking Trm9, which is responsible for the formation of mcm5U (Figure 2B) [97]–[99].

While some modifications are enhance -1 PRF, there are others that exhibit the opposite effect. In particular, there is class of guanosine modifications at positions 34 and 37 of some tRNAs reported to prevent or suppress potential frameshifting (Figure 2B). Wybutosine (yW) and its derivatives incrementally reduce -1 PRF when installed at position 37 in tRNAPhe, depending on the stage of modification (m1G > imG > yW) [100]–[102]. Queuosine (Q) shows a similar effect when installed on position 34 of the "shifty" tRNAAsn, although it seems compounded with distal alterations to tRNA sequence as well. Queuosine has been observed to

Table 3.1 Summary of tRNA modifications in the anticodon stem loop of tRNAs and their impact on translation

ASL Position	Modification	Enzyme(s)	Reported roles in Frame Maintenance and/or Translation		Refs
32	s^2C	IscS[a], TtcA[a]	Prevents I34 wobble with adenosine and limits CGA decoding of $tRNAArg_{1,2}^{(ICG)}$		[49], [50]
	ψ	RluA[a] ; Pus9p[b]	H-bonding and U-turn formation for ASL stability and improved decoding		[79], [121]
34	ncm^5U	Elp complex[b]	———	Promote decoding of NNA and NNG codons ; Suppress -1 frameshifting at split-box codons ; Suppress +1 frameshifting	[16], [17], [23]
	mcm^5U	Elp complex[b], Trm9[b]	———		[16], [17], [23], [98], [99]
	mcm^5s^2U	Elp complex[b], Trm9[b], Ncs2-6[b]	Increases rates of association and translocation		[16], [25], [57], [98], [99], [122], [123]
	mnm^5U	MnmE[a]	———		[25]–[27], [93], [94]
	mnm^5s^2U	MnmA[a], MnmE[a]	Increases rate of GTP hydrolysis of EF-Tu		[27], [93], [94], [124]
	$cmnm^5s^2U$	MnmA[a], MnmE-G[a]			[31], [125]
	cmo^5U	CmoA[a]* ; CmoB[b]*	Expands codon degeneracy - pairing with NN(U/A/C/G) ; Pre-orders ASL ; enhances +1 frameshifting (in absence of m^1G)		[36]–[38], [113]
	τm^5U	Mto1[c]‡	Improves decoding of UUA and UUG codons		[34], [126]
	I	TadA[a] ; Tad2,3[b]	Expands codon degeneracy - pairing with NNU, NNA, and NNG codons		[47], [48]
	f^5C	hmtRNA[d]‡	Allows $hmtRNA^{Met(CAU)}$ to decode AUG (Met) and AUA (Ile)		[41], [42]
	k^2C	TilS[a]	Restricts AUG (Met) decoding of tRNAIle(CAU) in bacteria ; Enhances base-stacking to stabilize ASL		[43]–[45]
	Q	Tgt[a] ; Qtrt1,2[c]	Suppresses -1 frameshifting		[103], [104], [127]
35	ψ	Pus7[b]	Allows $tRNATyr^{(GψA)}$ to function as a UAA/UAG nonsense suppressor		[69], [84]
37	t^6A	TsaC[a], TsaD[a] ; Tcs1-7[b]	Suppresses -1 frameshifting on (AAA)n codons	Stabilize A-U base pair between N1 of codon and N34 of anticodon	[63], [105], [124]
	ct^6A	TsaC[a], TsaD[a], TcdA[a] ; Tcd1,2[b]	———		[61], [62]
	ms^2t^6A	TsaC[a], TsaD[a], TrmO[a] ; Cdka1[c]	Improves decoding of AAG ; stabilizes ASL		[27], [59], [60], [128]
	i^6A	MiaA[a], MiaB[a] ; Mod5p[b]	Enhance decoding of cognate codons		[65], [67], [69], [70]
	ms^2i^6A	MiaA[a], MiaB[a]			[68], [129]
	ms^2io^6A	MiaA[a], MiaB[a], MiaE[a]			[120]
	m^1G	TrmD[a] ; Trm5[b]	Suppresses +1 frameshifting ; stabilizes ASL	Suppress -1 frameshifting	[100]–[102], [116]
	imG	Trm5[b], Tyw1[b]	Enhance codon recognition ; Enhance base-stacking to stabilize ASL		[100], [102], [130]
	yW	Trm5[b], Tyw1-4[b]			[100], [102], [130]
38	ψ	TruA[a] ; Deg1[b]	Increases ASL stability and improves decoding		[80], [131]
39	ψ	TruA[a] ; Deg1[b]	H-bonding with position 31 and stem-loop formation for ASL stability and improved decoding		[80], [124], [131]

a - Known enzyme(s) for installation of modification in *Escherichia coli*
b - Known enzyme(s) for installation of modification in Saccharomyces Cerevisiae
c - Enzyme(s) for installation in eukaryotes
d - Modifications that have been chemically synthesized

* - Enzyme is part of a pathway for installation that has not been fully elucidated
‡ - Currently unknown what enzymes are involved in installation of modification..

repress -1 PRF in eukaryotic retroviruses when present, and enhance -1 PRF, as observed in yeast, when the modification is absent from the tRNAAsn. [103], [104]. The adenosine modification t6A on position 37 of tRNALys has also been reported to suppress -1 PRF in *S. cerevisiae*, specifically in the case of tandem AAA codons [105]. Compared to other tRNALys modifications (as discussed above) which increase -1 PRF, this showcases interplay of modifications across the tRNA's ASL, and likely across its entire sequence. This is further highlighted when comparing frame maintenance of tRNALys on tandem AAAs in vitro when *E. coli* tRNALys lacks all modifications, as -1 frameshifting (among -2 and +1 frameshifts as well) is much greater compared to natively modified tRNALys [106].

3.3.2 ASL modifications generally suppress +1 frameshifting events

Alterations to mRNA sequence and secondary structure are not the only way that organisms accomplish the programmed expansion of their genetic code. Bacteria provide a prime example using +1 frameshift suppressor tRNAs for recoding, in which the ribosome recognizes a codon with 'four nucleotides' as a result of the tRNA recognizing four instead of three nucleotides [107], [108]. Typically, these +1 frameshift tRNAs have an additional nucleotide inserted into their ASL which allows for the hypothesized quadruplet-pairing model to restore proper translation product from genes which have had single-nucleotide insertion or deletion mutations. Classic examples of +1 frameshift suppressors include tRNASufD, a derivative of tRNAGly(GGC), and tRNASufA6 , a derivative of tRNAPro(GGG), in Salmonella which themselves have a mutation insertion in their ASL adjacent to position 37: C and G, respectively [109], [110]. While such suppressors were originally thought to decode 4 nucleotide codons, biochemical and structural studies revealed that the frameshift suppressor tRNA is still recognizing a 3 nucleotide codon, but in a different frame [111], [112]. Interestingly, the

frameshift tRNAPro(GGG) and the tRNASufA6 mutant are dependent on a m1G modification – at position 37 or 37.5, respectively – with the m1G programmed in position 37 of tRNAPro isoacceptors across all three domains of life [1], [100]. Lack of this m1G modification at this site result in increased +1 frameshifts which can be a consequence of destabilization of a A-U base-pair in the ASL (as is the case with tRNAPro(CGG)), expanded codon recognition from the wobble position in frameshift prone tRNAs (seen in tRNA(UGG)), or weakened mRNA-tRNA base-pairing (tRNAPro(GGG) has the most modest effect with only up to ~50% frameshift efficiency) [113]–[117]. While it is clear that the m1G modification is essential to allow for proper +1 frameshift suppression it is of interest to note the presence of the cmo5U34 modification on tRNAPro(UGG) which actually promotes +1 and +2 frameshift in the absence of m1G37 [113]. This example highlights the interplay of cross-tRNA modifications in expanding codon recognition (cmo5U34 allows tRNAPro(UGG) to recognize all 4 proline encoding codons) while guaranteeing proper frame maintenance.

Unlike -1 PRF, which can have enhanced or suppressed frameshift with modified tRNA nucleotides, almost all +1 PRF events are suppressed by tRNA modifications on the ASL (Figure 2B). Lack of modifications to positions 34 and 37 result in increased frameshifting in a wide range of tRNAs beyond the classic tRNAPro detailed above, showcasing that nucleotide modification has much broader impact than just the incorporation of proline. As discussed with -1 PRF, xm5 modifications presence are important for tRNAs to maintain proper frame and the same is observed regarding +1 frameshifting events. Loss of either mcm5 or s2 at U34 in yeast tRNA (tRNALys(UUU), tRNAArg(UCU), tRNAGly(UCC), tRNAGlu(UUC)), or (c)mnm5s2U34 in prokaryotes, leads to an increase in +1 frameshifting events [115], [118], [119]. Loss of other modifications at position 34 of tRNA frameshift suppressors, such as the

hypermodified guanosine modification queuosine in tRNATyr(GUA), are also shown to increase +1 frameshift[120]. As position 34 is known to impact decoding capabilities of tRNA, it can be rationalized that modifications at this position may also be involved in maintaining proper frame on an mRNA. Similarly, position 37 reflects its importance in codon recognition as modifications at position 37 of tRNA anticodons also result in increased +1 frameshift, as is the case of ms2io637 of tRNAPhe(GAA) or tRNA(GUA) in *E. coli*, t6A37 in bulk yeast tRNA, and (c)t6A in yeast tRNALys(UUU) [105], [132], [133]. It is important to note that many of the modifications effecting +1 frameshifting are generally not involved in effecting -1 frameshifting, despite being observed on some of the same isoacceptors [134]. When compared alongside structure and dynamic studies that highlight difficulty of the ribosome to adopt canonical interactions with mRNA-tRNA on frameshift elements, it can be reasoned that modifications to tRNA are essential to disrupting the ribosome from more readily losing frame [91], [116], [135], [136].

3.4 Conclusion

It is evident that tRNA modifications are important, and often essential, in maintaining translation efficiency and fidelity across all domains of life. However, understanding the discrete, molecular level roles many tRNA modifications have to improve codon recognition is still underdeveloped at this point in time, though rapidly growing. The potential diversity that modifications allow tRNA in decoding and recoding is tremendous, especially since presence of modifications can influence intra- and intercellular signaling or further modification [77], [137]. Despite this potential diversity, it is interesting to observe the persistence of many modifications across all domains of life. Understanding how such modifications work on a molecular level may

begin to provide insight into the evolution of gene expression as a consequence of RNA modification state.

3.5 References

[1] P. Boccaletto et al., "MODOMICS: a database of RNA modification pathways. 2017 update," Nucleic Acids Res., vol. 46, no. D1, Art. no. D1, Jan. 2018, doi: 10.1093/nar/gkx1030.

[2] M. D. Berg and C. J. Brandl, "Transfer RNAs: diversity in form and function," RNA Biol., vol. 18, no. 3, pp. 316–339, doi: 10.1080/15476286.2020.1809197.

[3] V. de Crécy-Lagard and M. Jairoch, "Functions of bacterial tRNA modifications: from ubiquity to diversity," Trends Microbiol., vol. 29, no. 1, pp. 41–53, Jan. 2021, doi: 10.1016/j.tim.2020.06.010.

[4] L. Pollo-Oliveira et al., "Loss of Elongator- and KEOPS-Dependent tRNA Modifications Leads to Severe Growth Phenotypes and Protein Aggregation in Yeast," Biomolecules, vol. 10, no. 2, p. 322, Feb. 2020, doi: 10.3390/biom10020322.

[5] C. T. Y. Chan et al., "Reprogramming of tRNA modifications controls the oxidative stress response by codon-biased translation of proteins," Nat. Commun., vol. 3, p. 937, Jul. 2012, doi: 10.1038/ncomms1938.

[6] A. Dannfald, J.-J. Favory, and J.-M. Deragon, "Variations in transfer and ribosomal RNA epitranscriptomic status can adapt eukaryote translation to changing physiological and environmental conditions," RNA Biol., vol. 18, no. Suppl 1, pp. 4–18, doi: 10.1080/15476286.2021.1931756.

[7] P. Barraud and C. Tisné, “To be or not to be modified: Miscellaneous aspects influencing nucleotide modifications in tRNAs,” Iubmb Life, vol. 71, no. 8, pp. 1126–1140, Aug. 2019, doi: 10.1002/iub.2041.

[8] V. de Crécy-Lagard et al., “Matching tRNA modifications in humans to their known and predicted enzymes,” Nucleic Acids Res., vol. 47, no. 5, pp. 2143–2159, Mar. 2019, doi: 10.1093/nar/gkz011.

[9] T. Suzuki, “The expanding world of tRNA modifications and their disease relevance,” Nat. Rev. Mol. Cell Biol., vol. 22, no. 6, Art. no. 6, Jun. 2021, doi: 10.1038/s41580-021-00342-0.

[10] A. G. Torres, E. Batlle, and L. Ribas de Pouplana, “Role of tRNA modifications in human diseases,” Trends Mol. Med., vol. 20, no. 6, pp. 306–314, Jun. 2014, doi: 10.1016/j.molmed.2014.01.008.

[11] W. Zhang, M. Foo, A. M. Eren, and T. Pan, “tRNA modification dynamics from individual organisms to metaepitranscriptomics of microbiomes,” Mol. Cell, vol. 82, no. 5, pp. 891–906, Mar. 2022, doi: 10.1016/j.molcel.2021.12.007.

[12] R. Giegé, F. Jühling, J. Pütz, P. Stadler, C. Sauter, and C. Florentz, “Structure of transfer RNAs: similarity and variability,” WIREs RNA, vol. 3, no. 1, pp. 37–61, 2012, doi: 10.1002/wrna.103.

[13] P. F. Agris, E. R. Eruysal, A. Narendran, V. Y. P. Väre, S. Vangaveti, and S. V. Ranganathan, “Celebrating wobble decoding: Half a century and still much is new,” RNA Biol., vol. 15, no. 4–5, pp. 537–553, Sep. 2017, doi: 10.1080/15476286.2017.1356562.

[14] L. Lei and Z. F. Burton, "'Superwobbling' and tRNA-34 Wobble and tRNA-37 Anticodon Loop Modifications in Evolution and Devolution of the Genetic Code," Life, vol. 12, no. 2, p. 252, Feb. 2022, doi: 10.3390/life12020252.

[15] P. J. McCown et al., "Naturally occurring modified ribonucleosides," WIREs RNA, vol. 11, no. 5, Art. no. 5, 2020, doi: 10.1002/wrna.1595.

[16] B. Huang, J. Lu, and A. S. Byström, "A genome-wide screen identifies genes required for formation of the wobble nucleoside 5-methoxycarbonylmethyl-2-thiouridine in *Saccharomyces cerevisiae*," RNA, vol. 14, no. 10, pp. 2183–2194, Oct. 2008, doi: 10.1261/rna.1184108.

[17] B. HUANG, M. J. O. JOHANSSON, and A. S. BYSTRÖM, "An early step in wobble uridine tRNA modification requires the Elongator complex," RNA, vol. 11, no. 4, pp. 424–436, Apr. 2005, doi: 10.1261/rna.7247705.

[18] N. T. Ingolia, S. Ghaemmaghami, J. R. S. Newman, and J. S. Weissman, "Genome-Wide Analysis in Vivo of Translation with Nucleotide Resolution Using Ribosome Profiling," Science, vol. 324, no. 5924, pp. 218–223, Apr. 2009, doi: 10.1126/science.1168978.

[19] D. D. Nedialkova and S. A. Leidel, "Optimization of Codon Translation Rates via tRNA Modifications Maintains Proteome Integrity," Cell, vol. 161, no. 7, pp. 1606–1618, Jun. 2015, doi: 10.1016/j.cell.2015.05.022.

[20] V. A. N. Rezgui et al., "tRNA tKUUU, tQUUG, and tEUUC wobble position modifications fine-tune protein translation by promoting ribosome A-site binding," Proc. Natl. Acad. Sci. U. S. A., vol. 110, no. 30, pp. 12289–12294, Jul. 2013, doi: 10.1073/pnas.1300781110.

[21] C. Yarian et al., “Modified Nucleoside Dependent Watson−Crick and Wobble Codon Binding by tRNA Lys UUU Species,” Biochemistry, vol. 39, no. 44, pp. 13390–13395, Nov. 2000, doi: 10.1021/bi001302g.

[22] B. Zinshteyn and W. V. Gilbert, “Loss of a Conserved tRNA Anticodon Modification Perturbs Cellular Signaling,” PLoS Genet., vol. 9, no. 8, p. e1003675, Aug. 2013, doi: 10.1371/journal.pgen.1003675.

[23] M. J. O. Johansson, A. Esberg, B. Huang, G. R. Björk, and A. S. Byström, “Eukaryotic Wobble Uridine Modifications Promote a Functionally Redundant Decoding System,” Mol. Cell. Biol., vol. 28, no. 10, pp. 3301–3312, May 2008, doi: 10.1128/MCB.01542-07.

[24] T. Yasukawa, T. Suzuki, N. Ishii, S. Ohta, and K. Watanabe, “Wobble modification defect in tRNA disturbs codon–anticodon interaction in a mitochondrial disease,” EMBO J., vol. 20, no. 17, pp. 4794–4802, Sep. 2001, doi: 10.1093/emboj/20.17.4794.

[25] F. V. Murphy, V. Ramakrishnan, A. Malkiewicz, and P. F. Agris, “The role of modifications in codon discrimination by tRNA(Lys)UUU,” Nat. Struct. Mol. Biol., vol. 11, no. 12, pp. 1186–1191, Dec. 2004, doi: 10.1038/nsmb861.

[26] A. Rozov, N. Demeshkina, I. Khusainov, E. Westhof, M. Yusupov, and G. Yusupova, “Novel base-pairing interactions at the tRNA wobble position crucial for accurate reading of the genetic code,” Nat. Commun., vol. 7, Jan. 2016, doi: 10.1038/ncomms10457.

[27] F. A. P. Vendeix et al., “Human tRNALys3UUU is Pre-Structured by Natural Modifications for Cognate and Wobble Codon Binding through Keto-EnolTautomerism,” J. Mol. Biol., vol. 416, no. 4, pp. 467–485, Mar. 2012, doi: 10.1016/j.jmb.2011.12.048.

[28] E. M. Nilsson and R. W. Alexander, “Bacterial Wobble Modifications of NNA-Decoding tRNAs,” IUBMB Life, vol. 71, no. 8, pp. 1158–1166, Aug. 2019, doi: 10.1002/iub.2120.

[29] N. Ranjan and M. V. Rodnina, “Thio-Modification of tRNA at the Wobble Position as Regulator of the Kinetics of Decoding and Translocation on the Ribosome,” J. Am. Chem. Soc., vol. 139, no. 16, pp. 5857–5864, Apr. 2017, doi: 10.1021/jacs.7b00727.

[30] K. B. Gromadski and M. V. Rodnina, “Kinetic Determinants of High-Fidelity tRNA Discrimination on the Ribosome,” Mol. Cell, vol. 13, no. 2, pp. 191–200, Jan. 2004, doi: 10.1016/S1097-2765(04)00005-X.

[31] A. Rodriguez-Hernandez et al., “Structural and mechanistic basis for enhanced translational efficiency by 2-thiouridine at the tRNA anticodon wobble position,” J. Mol. Biol., vol. 425, no. 20, pp. 3888–3906, Oct. 2013, doi: 10.1016/j.jmb.2013.05.018.

[32] Y. Kirino et al., “Codon-specific translational defect caused by a wobble modification deficiency in mutant tRNA from a human mitochondrial disease,” Proc. Natl. Acad. Sci. U. S. A., vol. 101, no. 42, pp. 15070–15075, Oct. 2004, doi: 10.1073/pnas.0405173101.

[33] S. Kurata et al., “Modified Uridines with C5-methylene Substituents at the First Position of the tRNA Anticodon Stabilize U·G Wobble Pairing during Decoding*,” J. Biol. Chem., vol. 283, no. 27, pp. 18801–18811, Jul. 2008, doi: 10.1074/jbc.M800233200.

[34] A. S. Kamble, B. V. Kumbhar, S. B. Sambhare, R. S. Bavi, and K. D. Sonawane, “Conformational Preferences of Modified Nucleoside 5-Taurinomethyluridine, τm5U Occur at ‘wobble’ 34th Position in the Anticodon Loop of tRNA,” Cell Biochem. Biophys., vol. 71, no. 3, pp. 1589–1603, Apr. 2015, doi: 10.1007/s12013-014-0382-x.

[35] P. F. Agris, F. A. P. Vendeix, and W. D. Graham, “tRNA’s wobble decoding of the genome: 40 years of modification,” J. Mol. Biol., vol. 366, no. 1, pp. 1–13, Feb. 2007, doi: 10.1016/j.jmb.2006.11.046.

[36] A. Weixlbaumer et al., “Mechanism of expanding the decoding capacity of tRNAs by modification of uridines,” Nat. Struct. Mol. Biol., vol. 14, no. 6, pp. 498–502, Jun. 2007, doi: 10.1038/nsmb1242.

[37] U. Kothe and M. V. Rodnina, “Codon Reading by tRNAAla with Modified Uridine in the Wobble Position,” Mol. Cell, vol. 25, no. 1, pp. 167–174, Jan. 2007, doi: 10.1016/j.molcel.2006.11.014.

[38] S. S. Phelps, A. Malkiewicz, P. F. Agris, and S. Joseph, “Modified Nucleotides in tRNALys and tRNAVal are Important for Translocation,” J. Mol. Biol., vol. 338, no. 3, pp. 439–444, Apr. 2004, doi: 10.1016/j.jmb.2004.02.070.

[39] F. A. P. Vendeix et al., “Anticodon Domain Modifications Contribute Order to tRNA for Ribosome-Mediated Codon Binding,” Biochemistry, vol. 47, no. 23, pp. 6117–6129, Jun. 2008, doi: 10.1021/bi702356j.

[40] H. Lusic et al., “Synthesis and investigation of the 5-formylcytidine modified, anticodon stem and loop of the human mitochondrial tRNAMet,” Nucleic Acids Res., vol. 36, no. 20, pp. 6548–6557, Nov. 2008, doi: 10.1093/nar/gkn703.

[41] C. Takemoto, L. L. Spremulli, L. A. Benkowski, T. Ueda, T. Yokogawa, and K. Watanabe, “Unconventional decoding of the AUA codon as methionine by mitochondrial

tRNAMet with the anticodon f5CAU as revealed with a mitochondrial in vitro translation system," Nucleic Acids Res., vol. 37, no. 5, pp. 1616–1627, Apr. 2009, doi: 10.1093/nar/gkp001.

[42] W. A. Cantara, F. V. Murphy, H. Demirci, and P. F. Agris, "Expanded use of sense codons is regulated by modified cytidines in tRNA," Proc. Natl. Acad. Sci. U. S. A., vol. 110, no. 27, pp. 10964–10969, Jul. 2013, doi: 10.1073/pnas.1222641110.

[43] C. Fabret et al., "Life without the essential bacterial tRNA Ile2-lysidine synthetase TilS: a case of tRNA gene recruitment in Bacillus subtilis," Mol. Microbiol., vol. 80, no. 4, pp. 1062–1074, May 2011, doi: 10.1111/j.1365-2958.2011.07630.x.

[44] T. Muramatsu et al., "Codon and amino-acid specificities of a transfer RNA are both converted by a single post-transcriptional modification," Nature, vol. 336, no. 6195, pp. 179–181, Nov. 1988, doi: 10.1038/336179a0.

[45] S. B. Sambhare, B. V. Kumbhar, A. D. Kamble, R. S. Bavi, N. M. Kumbhar, and K. D. Sonawane, "Structural significance of modified nucleosides k2C and t6A present in the anticodon loop of tRNAIle," RSC Adv., vol. 4, no. 27, pp. 14176–14188, Mar. 2014, doi: 10.1039/C3RA47335J.

[46] R. W. Holley et al., "Structure of a Ribonucleic Acid," Science, vol. 147, no. 3664, pp. 1462–1465, Mar. 1965, doi: 10.1126/science.147.3664.1462.

[47] À. Rafels-Ybern et al., "The Expansion of Inosine at the Wobble Position of tRNAs, and Its Role in the Evolution of Proteomes," Mol. Biol. Evol., vol. 36, no. 4, pp. 650–662, Apr. 2019, doi: 10.1093/molbev/msy245.

[48] A. G. Torres, D. Piñeyro, L. Filonava, T. H. Stracker, E. Batlle, and L. Ribas de Pouplana, “A-to-I editing on tRNAs: Biochemical, biological and evolutionary implications,” FEBS Lett., vol. 588, no. 23, pp. 4279–4286, 2014, doi: 10.1016/j.febslet.2014.09.025.

[49] W. A. Cantara et al., “Modifications Modulate Anticodon Loop Dynamics and Codon Recognition of *E. coli* tRNAArg1,2,” J. Mol. Biol., vol. 416, no. 4, pp. 579–597, Mar. 2012, doi: 10.1016/j.jmb.2011.12.054.

[50] S. Vangaveti et al., “A structural basis for restricted codon recognition mediated by 2-thiocytidine in tRNA containing a wobble position inosine,” J. Mol. Biol., vol. 432, no. 4, pp. 913–929, Feb. 2020, doi: 10.1016/j.jmb.2019.12.016.

[51] T. Ikemura, “Codon usage and tRNA content in unicellular and multicellular organisms.,” Mol. Biol. Evol., vol. 2, no. 1, pp. 13–34, Jan. 1985, doi: 10.1093/oxfordjournals.molbev.a040335.

[52] T. E. F. Quax, N. J. Claassens, D. Söll, and J. van der Oost, “Codon Bias as a Means to Fine-Tune Gene Expression,” Mol. Cell, vol. 59, no. 2, pp. 149–161, Jul. 2015, doi: 10.1016/j.molcel.2015.05.035.

[53] P. F. Agris, A. Narendran, K. Sarachan, V. Y. P. Väre, and E. Eruysal, “Chapter One - The Importance of Being Modified: The Role of RNA Modifications in Translational Fidelity,” in The Enzymes, vol. 41, G. F. Chanfreau, Ed. Academic Press, 2017, pp. 1–50. doi: 10.1016/bs.enz.2017.03.005.

[54] F. Jühling, M. Mörl, R. K. Hartmann, M. Sprinzl, P. F. Stadler, and J. Pütz, "tRNAdb 2009: compilation of tRNA sequences and tRNA genes," Nucleic Acids Res., vol. 37, no. Database issue, pp. D159–D162, Jan. 2009, doi: 10.1093/nar/gkn772.

[55] V. Dao et al., "Ribosome binding of DNA analogs of tRNA requires base modifications and supports the 'extended anticodon'.," Proc. Natl. Acad. Sci. U. S. A., vol. 91, no. 6, pp. 2125–2129, Mar. 1994.

[56] Z. Zhou, B. Sun, S. Huang, W. Jia, and D. Yu, "The tRNA-associated dysregulation in diabetes mellitus," Metabolism, vol. 94, pp. 9–17, May 2019, doi: 10.1016/j.metabol.2019.01.017.

[57] J. W. Stuart et al., "Functional Anticodon Architecture of Human tRNALys3 Includes Disruption of Intraloop Hydrogen Bonding by the Naturally Occurring Amino Acid Modification, t6A," Biochemistry, vol. 39, no. 44, pp. 13396–13404, Nov. 2000, doi: 10.1021/bi0013039.

[58] P. C. Thiaville et al., "Essentiality of threonylcarbamoyladenosine (t6A), a universal tRNA modification, in bacteria," Mol. Microbiol., vol. 98, no. 6, pp. 1199–1221, 2015, doi: 10.1111/mmi.13209.

[59] P. C. Durant, A. C. Bajji, M. Sundaram, R. K. Kumar, and D. R. Davis, "Structural Effects of Hypermodified Nucleosides in the Escherichia *coli* and Human tRNALys Anticodon Loop: The Effect of Nucleosides s2U, mcm5U, mcm5s2U, mnm5s2U, t6A, and ms2t6A," Biochemistry, vol. 44, no. 22, pp. 8078–8089, Jun. 2005, doi: 10.1021/bi050343f.

[60] S. Vangaveti, S. V. Ranganathan, and P. F. Agris, “Physical Chemistry of a Single tRNA-Modified Nucleoside Regulates Decoding of the Synonymous Lysine Wobble Codon and Affects Type 2 Diabetes,” J. Phys. Chem. B, vol. 126, no. 6, pp. 1168–1177, Feb. 2022, doi: 10.1021/acs.jpcb.1c09053.

[61] M. Matuszewski and E. Sochacka, “Stability studies on the newly discovered cyclic form of tRNA N6-threonylcarbamoyladenosine (ct6A),” Bioorg. Med. Chem. Lett., vol. 24, no. 12, pp. 2703–2706, Jun. 2014, doi: 10.1016/j.bmcl.2014.04.048.

[62] K. Miyauchi, S. Kimura, and T. Suzuki, “A cyclic form of N6-threonylcarbamoyladenosine as a widely distributed tRNA hypermodification,” Nat. Chem. Biol., vol. 9, no. 2, Art. no. 2, Feb. 2013, doi: 10.1038/nchembio.1137.

[63] J. Beenstock and F. Sicheri, “The structural and functional workings of KEOPS,” Nucleic Acids Res., vol. 49, no. 19, pp. 10818–10834, Oct. 2021, doi: 10.1093/nar/gkab865.

[64] U. Schweizer, S. Bohleber, and N. Fradejas-Villar, “The modified base isopentenyladenosine and its derivatives in tRNA,” RNA Biol., vol. 14, no. 9, pp. 1197–1208, Feb. 2017, doi: 10.1080/15476286.2017.1294309.

[65] J. I. Aubee, M. Olu, and K. M. Thompson, “The i6A37 tRNA modification is essential for proper decoding of UUX-Leucine codons during rpoS and iraP translation,” RNA, vol. 22, no. 5, pp. 729–742, May 2016, doi: 10.1261/rna.053165.115.

[66] F. Bouadloun, T. Srichaiyo, L. A. Isaksson, and G. R. Björk, “Influence of modification next to the anticodon in tRNA on codon context sensitivity of translational suppression and accuracy.,” J. Bacteriol., vol. 166, no. 3, pp. 1022–1027, Jun. 1986.

[67] J. Cabello-Villegas, M. E. Winkler, and E. P. Nikonowicz, “Solution Conformations of Unmodified and A37N6-dimethylallyl Modified Anticodon Stem-loops of *Escherichia coli* tRNAPhe,” J. Mol. Biol., vol. 319, no. 5, pp. 1015–1034, Jun. 2002, doi: 10.1016/S0022-2836(02)00382-0.

[68] R. K. Wilson and B. A. Roe, “Presence of the hypermodified nucleotide N6-(delta 2-isopentenyl)-2-methylthioadenosine prevents codon misreading by *Escherichia coli* phenylalanyl-transfer RNA.,” Proc. Natl. Acad. Sci. U. S. A., vol. 86, no. 2, pp. 409–413, Jan. 1989.

[69] S. Blanchet, D. Cornu, I. Hatin, H. Grosjean, P. Bertin, and O. Namy, “Deciphering the reading of the genetic code by near-cognate tRNA,” Proc. Natl. Acad. Sci. U. S. A., vol. 115, no. 12, pp. 3018–3023, Mar. 2018, doi: 10.1073/pnas.1715578115.

[70] T. N. Lamichhane et al., “Lack of tRNA Modification Isopentenyl-A37 Alters mRNA Decoding and Causes Metabolic Deficiencies in Fission Yeast,” Mol. Cell. Biol., vol. 33, no. 15, pp. 2918–2929, Aug. 2013, doi: 10.1128/MCB.00278-13.

[71] A. L. Konevega, N. G. Soboleva, V. I. Makhno, A. V. Peshekhonov, and V. I. Katunin, “Effect of modification of tRNA nucleotide 37 on the tRNA interaction with the A and P sites of the *Escherichia coli* 70S ribosome,” Mol. Biol., vol. 40, no. 4, pp. 597–610, Jul. 2006, doi: 10.1134/S0026893306040121.

[72] N. G. Soboleva, V. I. Makhno, A. L. Konevega, Yu. P. Semenkov, and V. I. Katunin, “The Effect of Modification of Nucleotide-37 on the Interaction of Aminoacyl-tRNA with the A Site of the 70S Ribosome,” Mol. Biol., vol. 37, no. 1, pp. 110–115, Jan. 2003, doi: 10.1023/A:1022345115927.

[73] A. L. KONEVEGA et al., “Purine bases at position 37 of tRNA stabilize codon–anticodon interaction in the ribosomal A site by stacking and Mg2+-dependent interactions,” RNA, vol. 10, no. 1, pp. 90–101, Jan. 2004, doi: 10.1261/rna.5142404.

[74] J. W. Stuart, K. M. Koshlap, R. Guenther, and P. F. Agris, “Naturally-occurring Modification Restricts the Anticodon Domain Conformational Space of tRNAPhe,” J. Mol. Biol., vol. 334, no. 5, pp. 901–918, Dec. 2003, doi: 10.1016/j.jmb.2003.09.058.

[75] O. M. Lateef, M. O. Akintubosun, O. T. Olaoba, S. O. Samson, and M. Adamczyk, “Making Sense of ‘Nonsense’ and More: Challenges and Opportunities in the Genetic Code Expansion, in the World of tRNA Modifications,” Int. J. Mol. Sci., vol. 23, no. 2, p. 938, Jan. 2022, doi: 10.3390/ijms23020938.

[76] A. G. Arimbasseri et al., “Evolving specificity of tRNA 3-methyl-cytidine-32 (m3C32) modification: a subset of tRNAsSer requires N6-isopentenylation of A37,” RNA, vol. 22, no. 9, pp. 1400–1410, Sep. 2016, doi: 10.1261/rna.056259.116.

[77] L. Han and E. M. Phizicky, “A rationale for tRNA modification circuits in the anticodon loop,” RNA, vol. 24, no. 10, pp. 1277–1284, Oct. 2018, doi: 10.1261/rna.067736.118.

[78] N. Kleiber et al., “The RNA methyltransferase METTL8 installs m3C32 in mitochondrial tRNAsThr/Ser(UCN) to optimise tRNA structure and mitochondrial translation,” Nat. Commun., vol. 13, p. 209, Jan. 2022, doi: 10.1038/s41467-021-27905-1.

[79] I. Behm-Ansmant, H. Grosjean, S. Massenet, Y. Motorin, and C. Branlant, “Pseudouridylation at Position 32 of Mitochondrial and Cytoplasmic tRNAs Requires Two

Distinct Enzymes in *Saccharomyces cerevisiae**," J. Biol. Chem., vol. 279, no. 51, pp. 52998–53006, Dec. 2004, doi: 10.1074/jbc.M409581200.

[80] F. Lecointe, O. Namy, I. Hatin, G. Simos, J.-P. Rousset, and H. Grosjean, "Lack of Pseudouridine 38/39 in the Anticodon Arm of Yeast Cytoplasmic tRNA Decreases in Vivo Recoding Efficiency*," J. Biol. Chem., vol. 277, no. 34, pp. 30445–30453, Aug. 2002, doi: 10.1074/jbc.M203456200.

[81] D. R. Davis, "Stabilization of RNA stacking by pseudouridine," Nucleic Acids Res., vol. 23, no. 24, Art. no. 24, Dec. 1995, doi: 10.1093/nar/23.24.5020.

[82] I. Tworowska and E. P. Nikonowicz, "Base Pairing within the ψ32,ψ39-Modified Anticodon Arm of *Escherichia coli* tRNAPhe," J. Am. Chem. Soc., vol. 128, no. 49, pp. 15570–15571, Dec. 2006, doi: 10.1021/ja0659368.

[83] C. S. Yarian et al., "Structural and functional roles of the N1- and N3-protons of psi at tRNA's position 39.," Nucleic Acids Res., vol. 27, no. 17, pp. 3543–3549, Sep. 1999.

[84] H. Beier and M. Grimm, "Misreading of termination codons in eukaryotes by natural nonsense suppressor tRNAs," Nucleic Acids Res., vol. 29, no. 23, pp. 4767–4782, Dec. 2001, doi: 10.1093/nar/29.23.4767.

[85] J. D. Dinman, "Mechanisms and implications of programmed translational frameshifting," Wiley Interdiscip. Rev. RNA, vol. 3, no. 5, pp. 661–673, 2012, doi: 10.1002/wrna.1126.

[86] C. G. Kurland, "Translational accuracy and the fitness of bacteria," Annu. Rev. Genet., vol. 26, pp. 29–50, 1992, doi: 10.1146/annurev.ge.26.120192.000333.

[87] J. Parker, “Errors and alternatives in reading the universal genetic code.,” Microbiol. Rev., vol. 53, no. 3, pp. 273–298, Sep. 1989.

[88] J. Atkinson, M. Dodge, and J. Gallant, “Secondary structures and starvation-induced frameshifting,” Mol. Microbiol., vol. 26, no. 4, pp. 747–753, 1997, doi: 10.1046/j.1365-2958.1997.6101959.x.

[89] B. Larsen, N. M. Wills, R. F. Gesteland, and J. F. Atkins, “rRNA-mRNA base pairing stimulates a programmed -1 ribosomal frameshift,” J. Bacteriol., vol. 176, no. 22, pp. 6842–6851, Nov. 1994, doi: 10.1128/jb.176.22.6842-6851.1994.

[90] M. V. Rodnina et al., “Translational recoding: canonical translation mechanisms reinterpreted,” Nucleic Acids Res., vol. 48, no. 3, pp. 1056–1067, Feb. 2020, doi: 10.1093/nar/gkz783.

[91] N. Caliskan, V. I. Katunin, R. Belardinelli, F. Peske, and M. V. Rodnina, “Programmed –1 Frameshifting by Kinetic Partitioning during Impeded Translocation,” Cell, vol. 157, no. 7, pp. 1619–1631, Jun. 2014, doi: 10.1016/j.cell.2014.04.041.

[92] J. Chen, A. Petrov, M. Johansson, A. Tsai, S. E. O’Leary, and J. D. Puglisi, “Dynamic pathways of -1 translational frameshifting,” Nature, vol. 512, no. 7514, pp. 328–332, Aug. 2014, doi: 10.1038/nature13428.

[93] L. V. Bock, N. Caliskan, N. Korniy, F. Peske, M. V. Rodnina, and H. Grubmüller, “Thermodynamic control of −1 programmed ribosomal frameshifting,” Nat. Commun., vol. 10, Oct. 2019, doi: 10.1038/s41467-019-12648-x.

[94] P. Licznar et al., “Programmed translational –1 frameshifting on hexanucleotide motifs and the wobble properties of tRNAs,” EMBO J., vol. 22, no. 18, pp. 4770–4778, Sep. 2003, doi: 10.1093/emboj/cdg465.

[95] N. D. Maynard, D. N. Macklin, K. Kirkegaard, and M. W. Covert, “Competing pathways control host resistance to virus via tRNA modification and programmed ribosomal frameshifting,” Mol. Syst. Biol., vol. 8, p. 567, Jan. 2012, doi: 10.1038/msb.2011.101.

[96] M. Raba et al., “Nucleotide Sequence of Three Isoaccepting Lysine tRNAs from Rabbit Liver and SV40-Transformed Mouse Fibroblasts,” Eur. J. Biochem., vol. 97, no. 1, pp. 305–318, 1979, doi: 10.1111/j.1432-1033.1979.tb13115.x.

[97] H. R. Kalhor and S. Clarke, “Novel Methyltransferase for Modified Uridine Residues at the Wobble Position of tRNA,” Mol. Cell. Biol., vol. 23, no. 24, pp. 9283–9292, Dec. 2003, doi: 10.1128/MCB.23.24.9283-9292.2003.

[98] J. LU, B. HUANG, A. ESBERG, M. J. O. JOHANSSON, and A. S. BYSTRÖM, “The Kluyveromyces lactis γ-toxin targets tRNA anticodons,” RNA, vol. 11, no. 11, pp. 1648–1654, Nov. 2005, doi: 10.1261/rna.2172105.

[99] A. Patil, C. T. Y. Chan, M. Dyavaiah, J. P. Rooney, P. C. Dedon, and T. J. Begley, “Translational infidelity-induced protein stress results from a deficiency in Trm9-catalyzed tRNA modifications,” RNA Biol., vol. 9, no. 7, pp. 990–1001, Jul. 2012, doi: 10.4161/rna.20531.

[100] G. R. Björk, P. M. Wikström, and A. S. Byström, “Prevention of Translational Frameshifting by the Modified Nucleoside 1-Methylguanosine,” Science, vol. 244, no. 4907, pp. 986–989, May 1989, doi: 10.1126/science.2471265.

[101] B. A. Carlson et al., “1-Methylguanosine in Place of Y Base at Position 37 in Phenylalanine tRNA Is Responsible for Its Shiftiness in Retroviral Ribosomal Frameshifting,” Virology, vol. 279, no. 1, pp. 130–135, Jan. 2001, doi: 10.1006/viro.2000.0692.

[102] W. F. Waas, Z. Druzina, M. Hanan, and P. Schimmel, “Role of a tRNA Base Modification and Its Precursors in Frameshifting in Eukaryotes*,” J. Biol. Chem., vol. 282, no. 36, pp. 26026–26034, Sep. 2007, doi: 10.1074/jbc.M703391200.

[103] B. A. Carlson, S. Y. Kwon, B. J. Lee, and and D. Hatfield, “Yeast Asparagine (Asn) tRNA without Q Base Promotes Eukaryotic Frameshifting More Efficiently Than Mammalian Asn tRNAs with or without Q Base,” Mol. Cells, vol. 10, no. 1, pp. 113–118, Feb. 2000.

[104] B. A. Carlson, S. Y. Kwon, M. Chamorro, S. Oroszlan, D. L. Hatfield, and B. J. Lee, “Transfer RNA Modification Status Influences Retroviral Ribosomal Frameshifting,” Virology, vol. 255, no. 1, pp. 2–8, Mar. 1999, doi: 10.1006/viro.1998.9569.

[105] B. El Yacoubi et al., “A role for the universal Kae1/Qri7/YgjD (COG0533) family in tRNA modification,” EMBO J., vol. 30, no. 5, pp. 882–893, Mar. 2011, doi: 10.1038/emboj.2010.363.

[106] T. J. Smith, M. Tardu, H. R. Khatri, and K. Koutmou, “mRNA and tRNA modification states influence ribosome speed and frame maintenance during poly(lysine) peptide synthesis,” J. Biol. Chem., p. 102039, May 2022, doi: 10.1016/j.jbc.2022.102039.

[107] J. F. Atkins, G. Loughran, P. R. Bhatt, A. E. Firth, and P. V. Baranov, “Ribosomal frameshifting and transcriptional slippage: From genetic steganography and cryptography to

adventitious use," Nucleic Acids Res., vol. 44, no. 15, pp. 7007–7078, Sep. 2016, doi: 10.1093/nar/gkw530.

[108] J. F. Atkins and G. R. Björk, "A Gripping Tale of Ribosomal Frameshifting: Extragenic Suppressors of Frameshift Mutations Spotlight P-Site Realignment," Microbiol. Mol. Biol. Rev. MMBR, vol. 73, no. 1, pp. 178–210, Mar. 2009, doi: 10.1128/MMBR.00010-08.

[109] J. N. Li and G. R. Björk, "Structural alterations of the tRNA(m1G37)methyltransferase from Salmonella typhimurium affect tRNA substrate specificity.," RNA, vol. 5, no. 3, pp. 395–408, Mar. 1999.

[110] D. L. Riddle and J. Carbon, "Frameshift Suppression: a Nucleotide Addition in the Anticodon of a Glycine Transfer RNA," Nature. New Biol., vol. 242, no. 121, Art. no. 121, Apr. 1973, doi: 10.1038/newbio242230a0.

[111] S. Hong, S. Sunita, T. Maehigashi, E. D. Hoffer, J. A. Dunkle, and C. M. Dunham, "Mechanism of tRNA-mediated +1 ribosomal frameshifting," Proc. Natl. Acad. Sci. U. S. A., vol. 115, no. 44, pp. 11226–11231, Oct. 2018, doi: 10.1073/pnas.1809319115.

[112] Q. Qian, J. Li, H. Zhao, T. G. Hagervall, P. J. Farabaugh, and G. R. Björk, "A New Model for Phenotypic Suppression of Frameshift Mutations by Mutant tRNAs," Mol. Cell, vol. 1, no. 4, pp. 471–482, Mar. 1998, doi: 10.1016/S1097-2765(00)80048-9.

[113] H. B. Gamper, I. Masuda, M. Frenkel-Morgenstern, and Y.-M. Hou, "The UGG Isoacceptor of tRNAPro Is Naturally Prone to Frameshifts," Int. J. Mol. Sci., vol. 16, no. 7, pp. 14866–14883, Jul. 2015, doi: 10.3390/ijms160714866.

[114] E. D. Hoffer et al., “Structural insights into mRNA reading frame regulation by tRNA modification and slippery codon–anticodon pairing,” eLife, vol. 9, p. e51898, doi: 10.7554/eLife.51898.

[115] G. Jäger, K. Nilsson, and G. R. Björk, “The Phenotype of Many Independently Isolated +1 Frameshift Suppressor Mutants Supports a Pivotal Role of the P-Site in Reading Frame Maintenance,” PLoS ONE, vol. 8, no. 4, p. e60246, Apr. 2013, doi: 10.1371/journal.pone.0060246.

[116] T. Maehigashi, J. A. Dunkle, S. J. Miles, and C. M. Dunham, “Structural insights into +1 frameshifting promoted by expanded or modification-deficient anticodon stem loops,” Proc. Natl. Acad. Sci. U. S. A., vol. 111, no. 35, pp. 12740–12745, Sep. 2014, doi: fle.

[117] H. A. Nguyen, E. D. Hoffer, and C. M. Dunham, “Importance of a tRNA anticodon loop modification and a conserved, noncanonical anticodon stem pairing in tRNACGGPro for decoding,” J. Biol. Chem., vol. 294, no. 14, pp. 5281–5291, Apr. 2019, doi: 10.1074/jbc.RA119.007410.

[118] R. Klassen, P. Grunewald, K. L. Thüring, C. Eichler, M. Helm, and R. Schaffrath, “Loss of Anticodon Wobble Uridine Modifications Affects tRNALys Function and Protein Levels in *Saccharomyces cerevisiae*,” PLoS ONE, vol. 10, no. 3, Mar. 2015, doi: 10.1371/journal.pone.0119261.

[119] H. Tükenmez, H. Xu, A. Esberg, and A. S. Byström, “The role of wobble uridine modifications in +1 translational frameshifting in eukaryotes,” Nucleic Acids Res., vol. 43, no. 19, pp. 9489–9499, Oct. 2015, doi: 10.1093/nar/gkv832.

[120] J. Urbonavičius, Q. Qian, J. M. B. Durand, T. G. Hagervall, and G. R. Björk, "Improvement of reading frame maintenance is a common function for several tRNA modifications," EMBO J., vol. 20, no. 17, pp. 4863–4873, Sep. 2001, doi: 10.1093/emboj/20.17.4863.

[121] J. Wrzesinski, K. Nurse, A. Bakin, B. G. Lane, and J. Ofengand, "A dual-specificity pseudouridine synthase: an *Escherichia coli* synthase purified and cloned on the basis of its specificity for psi 746 in 23S RNA is also specific for psi 32 in tRNA(phe).," RNA, vol. 1, no. 4, pp. 437–448, Jun. 1995.

[122] S. Leidel et al., "Ubiquitin-related modifier Urm1 acts as a sulphur carrier in thiolation of eukaryotic transfer RNA," Nature, vol. 458, no. 7235, Art. no. 7235, Mar. 2009, doi: 10.1038/nature07643.

[123] P. C. Thiaville and V. Crécy-Lagard, "The emerging role of complex modifications of tRNALysUUU in signaling pathways," Microb. Cell, vol. 2, no. 1, pp. 1–4, doi: 10.15698/mic2015.01.185.

[124] M. Sundaram, P. C. Durant, and D. R. Davis, "Hypermodified Nucleosides in the Anticodon of tRNALys Stabilize a Canonical U-Turn Structure," Biochemistry, vol. 39, no. 41, pp. 12575–12584, Oct. 2000, doi: 10.1021/bi0014655.

[125] I. Moukadiri, M.-J. Garzón, G. R. Björk, and M.-E. Armengod, "The output of the tRNA modification pathways controlled by the *Escherichia coli* MnmEG and MnmC enzymes depends on the growth conditions and the tRNA species," Nucleic Acids Res., vol. 42, no. 4, pp. 2602–2623, Feb. 2014, doi: 10.1093/nar/gkt1228.

[126] M. Fakruddin et al., “Defective Mitochondrial tRNA Taurine Modification Activates Global Proteostress and Leads to Mitochondrial Disease,” Cell Rep., vol. 22, no. 2, pp. 482–496, Jan. 2018, doi: 10.1016/j.celrep.2017.12.051.

[127] C. Fergus, D. Barnes, M. A. Alqasem, and V. P. Kelly, “The Queuine Micronutrient: Charting a Course from Microbe to Man,” Nutrients, vol. 7, no. 4, Art. no. 4, Apr. 2015, doi: 10.3390/nu7042897.

[128] F.-Y. Wei et al., “Deficit of tRNA(Lys) modification by Cdkal1 causes the development of type 2 diabetes in mice,” J. Clin. Invest., vol. 121, no. 9, pp. 3598–3608, Sep. 2011, doi: 10.1172/jci58056.

[129] L. A. Petrullo and D. Elseviers, “Effect of a 2-methylthio-N6-isopentenyladenosine deficiency on peptidyl-tRNA release in *Escherichia coli*,” J. Bacteriol., vol. 165, no. 2, pp. 608–611, Feb. 1986, doi: 10.1128/jb.165.2.608-611.1986.

[130] A. P. Young and V. Bandarian, “TYW1: A radical SAM enzyme involved in the biosynthesis of wybutosine bases,” Methods Enzymol., vol. 606, pp. 119–153, 2018, doi: 10.1016/bs.mie.2018.04.024.

[131] R. Klassen and R. Schaffrath, “Role of Pseudouridine Formation by Deg1 for Functionality of Two Glutamine Isoacceptor tRNAs,” Biomolecules, vol. 7, no. 1, p. 8, Jan. 2017, doi: 10.3390/biom7010008.

[132] R. Klassen, A. Bruch, and R. Schaffrath, “Independent suppression of ribosomal +1 frameshifts by different tRNA anticodon loop modifications,” RNA Biol., vol. 14, no. 9, pp. 1252–1259, Dec. 2016, doi: 10.1080/15476286.2016.1267098.

[133] J. Urbonavičius, Q. Qian, J. M. B. Durand, T. G. Hagervall, and G. R. Björk, "Improvement of reading frame maintenance is a common function for several tRNA modifications," EMBO J., vol. 20, no. 17, pp. 4863–4873, Sep. 2001, doi: 10.1093/emboj/20.17.4863.

[134] J. Urbonavicius et al., "Transfer RNA modifications that alter +1 frameshifting in general fail to affect -1 frameshifting," RNA N. Y. N, vol. 9, no. 6, pp. 760–768, Jun. 2003, doi: 10.1261/rna.5210803.

[135] J. A. Dunkle and C. M. Dunham, "Mechanisms of mRNA frame maintenance and its subversion during translation of the genetic code," Biochimie, vol. 114, pp. 90–96, Jul. 2015, doi: 10.1016/j.biochi.2015.02.007.

[136] H.-K. Kim, F. Liu, J. Fei, C. Bustamante, R. L. Gonzalez, and I. Tinoco, "A frameshifting stimulatory stem loop destabilizes the hybrid state and impedes ribosomal translocation," Proc. Natl. Acad. Sci. U. S. A., vol. 111, no. 15, pp. 5538–5543, Apr. 2014, doi: 10.1073/pnas.1403457111.

[137] J. Li, W.-Y. Zhu, W.-Q. Yang, C.-T. Li, and R.-J. Liu, "The occurrence order and cross-talk of different tRNA modifications," Sci. China Life Sci., vol. 64, no. 9, pp. 1423–1436, Sep. 2021, doi: 10.1007/s11427-020-1906-4.

Chapter 4 Methylated Guanosine and Uridine Modifications in *S. cerevisiae* mRNAs Modulate Translation Elongation[4]

Work presented in this chapter was submitted for publication in
RSC Chemical Biology.

Joshua D. Jones[1], Monika K. Franco[2], Tyler J. Smith[1], Laura R. Snyder[1], Anna G. Anders[1], Brandon T. Ruotolo[1], Robert T. Kennedy[1,2], Kristin S. Koutmou[1,2]*

[1]University of Michigan, Department of Chemistry. [2]University of Michigan, Program in Chemical Biology. 930 N University, Ann Arbor, MI 48109, * corresponding author

4.1 Introduction

Post-transcriptional modifications to RNA molecules can change their structure, localization, stability, and function [1], [2]. To date, over 150 different nucleoside chemical modifications have been identified within non-coding RNAs (ncRNA), and many are important, or even

[4] In the work presented in this chapter I performed all translation assays for peptide synthesis on mRNAs that contained m^1G or m^2G in their sequence. I also assisted Joshua Jones on the development of the mRNA purification and enrichment pipeline as well as wrote and advised on the methods for translation using the reconstituted *in vitro* translation system. Finally, I served as a writer and editor for this work which has been uploaded to *BioRxiv*. The briefly summarized work of other authors are as follows:
- Joshua Jones was responsible for developing the LC-MS/MS pipeline as well as mRNA purification methods. He was also involved in the assay development for the modification enzymes studies conducted. Finally, he served as the primary author and editor.
- Monika Franco performed translation studies for mRNAs containing m^5U, assisted with *in vitro* translation system utilization, and served as a secondary author and editor.
- Laura Snyder was responsible for testing of wild-type and mutant *S. cerevisiae* cultures containing modification enzyme knockout strains as well as for RNA purification, extraction, and preparation prior and during to characterization and LC-MS/MS steps.
- Anna Anders helped perform and optimize LC-MS/MS assays and analysis.

essential, for a myriad of cellular processes [1], [3]. The significance of RNA modifications to cellular health is underscored by decades of observations implicating the mis-regulation of ncRNA modifying enzymes in cancer and other diseases [4]–[9]. Recent advances in next generation RNA sequencing (RNA-seq) [10]–[19] and liquid chromatography coupled to tandem mass spectrometry (LC-MS/MS) technologies [20]–[24] enabled the detection of chemical modifications in protein encoding messenger RNAs (mRNA). Over 15 mRNA modifications have been reported, including N6-methyladensoine (m^6A), inosine (I), N7-methylguanosine (m^7G), and pseudouridine (Ψ) [1], [12], [13], [22], [25]–[28]. There are >10-fold more types of modifications reported in ncRNA than in mRNA, raising the possibility that the diversity of mRNA modifications has not yet been revealed.

While the biological significance of ncRNA modifications has been extensively studied, the consequences of mRNA modifications on gene expression are just beginning to be explored. Modified nucleosides resulting from RNA damage (e.g. oxidation, alkylation, or UV) commonly perturb protein synthesis and can trigger RNA degradation pathways [29], [30]. Despite typically being present at lower levels than their enzymatically incorporated counterparts [31], there is evidence that oxidized mRNAs can accumulate in neurodegenerative diseases [31]–[33]. The most abundant and well-studied modification added by enzymes into mRNA coding regions, m6A, has been implicated as a key modulator of multiple facets of the mRNA lifecycle including nuclear expor t[34]–[36], mRNA stability [37]–[39], and translational efficiency [19], [38], [40]–[43]. Given these potential contributions to mRNA function, it is unsurprising that the mis-regulation of m6A is linked to a host of diseases such as endometrial cancer [44] and type 2 diabetes [45]. While initial studies of m6A provide an example of the biological impact mRNA modifications can have, most other mRNA modifications have been minimally investigated. The

development of additional sensitive and quantitative techniques to comprehensively evaluate the mRNA modification landscape will be essential to direct future investigations that characterize the molecular level consequence of emerging mRNA modifications.

LC-MS/MS has been a powerful approach to characterize chemical modifications of all three major classes of biomolecules central to protein synthesis (DNA, RNA, and protein). In particular, the sensitivity and specificity of LC-MS/MS methodologies have enabled the identification and extensive characterization of post-translational protein modifications [46]. While post-transcriptional modifications of ncRNA have been studied for decades using 2D thin layer chromatography [47] and LC coupled to ultraviolet detection [48], [49], recent developments in LC-MS/MS analyses provided some of the first insight into RNA modification abundance and dynamics under cellular stress [50]–[56]. Such methods can broadly detect and provide absolute quantification of modifications in any purified RNA sample [25]. These features have made LC-MS/MS an attractive technology to adopt for mRNA modification discovery. Currently, published methods can assay up to 40 ribonucleosides in a single analysis and use calibration curves from standards to enable quantification with high accuracy and selectivity [20]. However, despite these advantages and the proven utility of LC-MS/MS methodologies for investigating ncRNA modifications, LC-MS/MS has yet to be widely used to study mRNA modifications unlike the comprehensive characterization of post-translational protein modifications by LC-MS/MS technologies over the past few decades.

Here, we identify two factors that have impeded application of LC-MS/MS to mRNA modification analysis: the quantity of mRNA required for current LC-MS/MS sensitivities, and the difficulty to obtain highly pure mRNA. We integrated an improved chromatographic approach with an enhanced mRNA purification and validation process to overcome these

limitations and develop a robust workflow for mRNA modification characterization. Our method is capable of quantifying 50 ribonucleoside variants in a single analysis. Analysis of purified *S. cerevisiae* mRNA samples reveals that 1-methylguanosine (m1G), N2-methylguanosine (m2G), N2, N2-dimethylguanosine (m22G), and 5-methyluridine (m5U) are likely incorporated into mRNAs both enzymatically (Trm10, Trm11, Trm1, and Trm2) and non-enzymatically. We also use a fully purified in vitro translation system to demonstrate that the inclusion of these methylated nucleosides into mRNA codons can slow amino acid addition by the ribosome. Together, our findings advance available chromatography and mRNA purification and validation methods to enhance the high-confidence and high-throughput detection of modified nucleosides by LC-MS/MS and support a growing body of evidence that the inclusion of mRNA modifications commonly alters the peptide elongation during protein synthesis.

4.2 Results

4.2.1 Development of highly sensitive LC-MS/MS method for simultaneously quantifying 50 ribonucleosides

RNA-seq based technologies capable of identifying the location of RNA modifications have revealed that modified nucleosides can be found in thousands of mRNAs [57]. These powerful methodologies have enabled the widespread study of mRNA modifications, but are computationally laborious, not generally quantitative, and typically detect a single modification at a time. In contrast, LC-MS/MS analyses rapidly and quantitatively identify the presence of RNA modifications but cannot report on where they exist throughout the transcriptome[25]. Therefore, the integration of orthogonal LC-MS/MS and RNA-seq based methodologies is required to develop robust platforms for detecting mRNA modifications [57]–[66]. However, the

application of LC-MS/MS for nucleoside discovery has been limited by lingering questions regarding mRNA purity, as many reports do not present the comprehensive quality controls necessary for confident mRNA modification analysis. Indeed, a few reported mRNA modifications have not yet been mapped to discrete mRNAs in the transcriptome by RNA-seq based methodologies (e.g., m1G), likely due to their low abundance and/or possible non-specific incorporation. While there is evidence that the insertion of some mRNA modifications are programmed, suggesting a biological function, other modifications are likely added in a less specific manner (e.g., RNA damage, off target modification by ncRNA enzymes). Modifications incorporated at lower levels are unlikely to be detected by sequencing-based methods, but can have consequences for cellular health, as illustrated by links between RNA-damage and disease. Therefore, regardless of why a modification is present, it is still essential for us to fully elucidate the mRNA modification landscape and interrogate how these modifications affect cellular function.

Ribonucleosides are most commonly separated using reversed phase chromatography and quantified using multiple reaction monitoring (MRM) on a triple quadrupole mass spectrometer [20], [50], [52], [67], [68]. These methods have reported limits of detection (LODs) down to ~60 attomole for select ribonucleosides using standard mixtures with canonical and modified nucleosides at equal concentrations[50]. However, the abundance of unmodified and modified nucleosides in RNAs are not equivalent in cells, with canonical bases existing in 20- to 10,000-fold higher concentrations than RNA modifications (Figure 1A). In currently available chromatography methods, modified nucleosides (e.g., m5U, m1G, m1□, and s2U) commonly coelute with canonical nucleosides, reducing the detectability of some modified bases [50], [52], [53]. Coelution limits the utility of available LC-MS/MS methods because it results in ion

suppression of modified nucleoside signals, with abundant canonical nucleosides outcompeting modified nucleosides for electrospray droplet surface charge. Additionally, this phenomenon makes calibration curves non-linear and worsens the quantifiability of modifications at concentrations necessary for mRNA modification analyses. Recent efforts have been made to derivatize ribonucleosides prior to LC-MS/MS analysis to increase sensitivity and retention on reversed-phase chromatography [21], [69]–[71]. The analogous benzoyl chloride derivatization of neurochemicals has previously been an important separation strategy for many neurochemical monitoring applications [72], [73]. However, labeling strategies are unlikely to prove as useful for

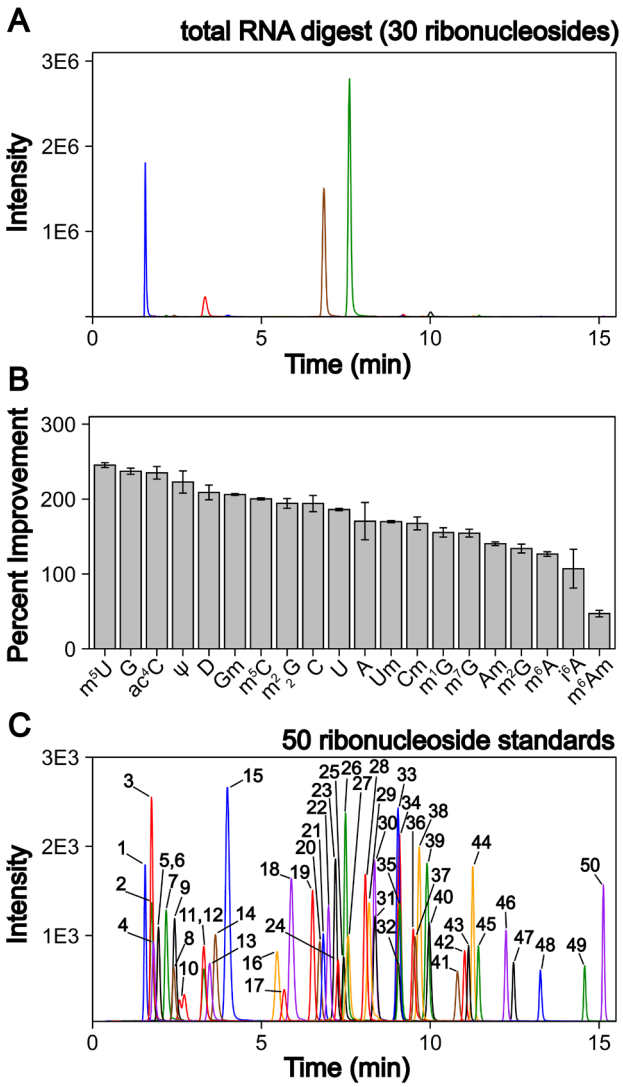

Figure 4.1 *LC-MS/MS method development to quantify 50 ribonucleosides in a single analysis. A) Extracted ion chromatogram for the 30 ribonucleosides (4 canonical bases and 26 naturally occurring modifications) detected in a S. cerevisiae total RNA digestion displaying that the canonical bases exist at much larger levels than the ribonucleoside modifications. B) LC-MS/MS signal percent improvement using 1 mm chromatography at 100 μL/min compared to 2 mm chromatography at 400 μL/min. C) Extracted ion chromatogram for 50 ribonucleoside standards (4 canonical bases, 45 naturally occurring modifications, and 1 non-natural modifications). The concentrations of each ribonucleoside standards within the standard mix and their corresponding peak numbers are displayed in Supplemental Table S2. For the chromatograms, each color peak represents a separate ribonucleoside in the method, and the colors are coordinated between panel A and C.3*

investigating mRNA modifications because derivatizing agents are typically nucleobase specific,

limiting the ability of LC/MS-MS assays to be multiplexed [21], [69], [70]. Furthermore, labeling increases the amount of mRNA sample required due to additional sample preparation steps following derivatization. This is an important consideration given that mRNAs represent only ~1-2% of the total RNAs in a cell, and it is already challenging to purify sufficient quantities of mRNA for LC-MS/MS analysis. We addressed these limitations by first improving upon existing chromatography techniques. Current methods typically utilize 2 mm internal diameter (I.D.) columns that require higher flow rates (300 to 400 μL/min), which worsens ionization efficiencies than smaller I.D. chromatography with lower flow rates. We utilized a 1 mm I.D. column with flow rates at 100 μL/min to lessen these effects. In principle, even smaller bore columns (i.e., "nano-LC"), which are commonly used in in proteomics [74], could be used. Indeed, some studies have shown their effectiveness for nucleosides [75], [76]; however, smaller bore columns can suffer from robustness issues in some conditions. Also, low binding capacity of more polar nucleosides results in poor peak shapes in nano-LC because of relatively large injection volumes. Another limitation has been the stationary phases used, where porous graphitic carbon columns yield poor chromatographic performance for some ribonucleosides (e.g., methylated guanosine modifications) and many C18 phases have low binding capacity for some ribonucleosides (e.g., cytidine and pseudouridine) making them difficult to retain. We used a polar endcapped C18 column to provide more retention and good performance for all nucleosides. We also used mobile phase buffers which have previously been shown to provide high ESI-MS sensitivity for modified ribonucleosides [50]. These alterations combined increased the sensitivity of the assay by 50 to 250% for all nucleosides tested compared to standard 2 mm I.D. chromatography at 400 μL/min (Figure 1B) while maintaining adequate ribonucleoside binding capacity for early eluting ribonucleosides. We also altered the chromatographic

conditions including increased temperature (35℃ vs 25℃) and modified mobile phase gradients to prevent coelution of the highly abundant canonical nucleosides with the modified nucleosides. Notably, in contrast to most available methods, m5U, m1G, m1□ do not coelute with unmodified nucleosides in our method (Figure 1C). This improved separation greatly reduced ionization suppression of these nucleosides. Together, these advancements led to a wider linear dynamic range than previous reports with over four orders of magnitude for most modifications and LODs down to 3 amol (0.6 pM) using a single internal standard and no derivatization steps. Our method represents at least a 10-fold improvement over previous ultrahigh-performance LC (UHPLC) and nano-LC analyses for most modifications analyzed (Supplemental Table S1 and Supplemental Figures S1 through S4). Therefore, the method described here provides a linear dynamic range and LODs capable of analyzing both highly modified ncRNA in addition to the less modified mRNA without large sample requirements. To perform an in-depth RNA modification analysis, approximately 50 to 200 ng of total RNA or mRNA is required per replicate which is achievable using standard eukaryotic and bacterial cell culture techniques. Overall, this assay can quantify the 4 canonical nucleosides, 45 naturally occurring modified nucleosides, and 1 non-natural modified nucleoside (internal control) (Figure 1C, Supplemental Table S2). This work ameliorates current quantitative ribonucleoside LC-MS/MS methodologies by improving chromatographic conditions and characterizing quantifiability at nucleoside concentrations representative of typical RNA digest samples to enable higher confidence total RNA and mRNA modification analyses.

4.2.2 Three-stage mRNA purification and validation pipeline provides highly pure S. cerevisiae mRNA

Total RNA is mainly comprised of the highly modified transfer RNA (tRNA) and ribosomal RNA (rRNA) with a small percentage of mRNA. Unlike RNA-seq, LC-MS/MS assays are unable to distinguish between modifications arising from ncRNA or mRNA. In total RNA digestions, mRNA modifications typically exist at least 100X lower concentrations than in the corresponding total RNA samples [20]. Thus, even low-level contamination of tRNA and rRNA in purified mRNA samples can lead to inaccurate quantifications as well as false mRNA modifications discoveries. Most of the published mRNA purification pipelines use a combination of poly(A) enrichment and rRNA depletion steps to obtain mRNA [10], [12], [20], [22], [24], [77], [78]. However, previously this was found to be insufficient for removing all signal from contaminating ncRNA modifications during LC-MS/MS analyses, especially from contaminating tRNA [20], [79]. The inability to obtain convincingly pure mRNA samples has long limited the utility of LC-MS/MS for studying these molecules. Recently, small RNA depletion steps have begun to be incorporated into mRNA purification pipelines to remove residual tRNA contamination[80]; however, the highest efficiency purifications typically require expensive instrumentation and materials (liquid chromatograph and size exclusion column) [23] or expertise in RNA gel purification [21]. Despite these improvements, most reports do not provide adequate mRNA purity quality control to confirm removal of ncRNA for confident mRNA modification analyses. In order to apply our LC-MS/MS assay to studying mRNAs, we developed and implemented a three-stage purification pipeline comprised of a small RNA depletion step, two consecutive poly(A) enrichment steps, and ribosomal RNA depletion to selectively deplete the small ncRNA (e.g., tRNA and 5S rRNA) in addition to the 18S rRNA and 28S rRNA using fully commercial kits (Figure 2).

Additionally, we performed extensive quality control on our mRNA samples prior to LC-MS/MS analysis – assessing the purity of our mRNA following the three-stage purification pipeline using chip electrophoresis (Bioanalyzer), RNA-seq, and qRT-PCR. The highly purified mRNA contained no detectable tRNA and rRNA peaks based on our Bioanalyzer electropherograms (Figure 3A).

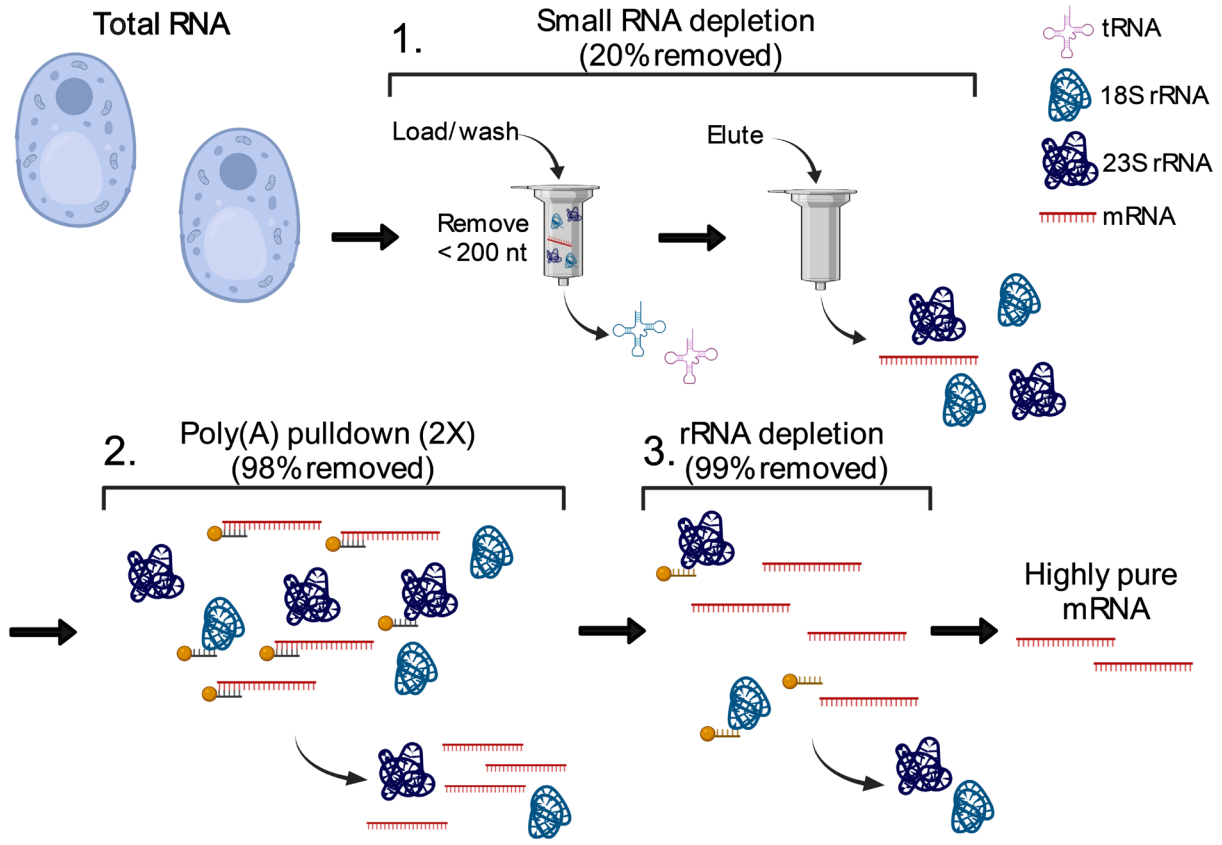

Figure 4.2 *Three-stage mRNA purification pipeline. Total RNA from S. cerevisiae is purified to mRNA using a three-stage purification pipeline: 1. Small RNA (e.g., tRNA and 5S rRNA) is depleted; 2. mRNA is enriched from the small RNA depleted fraction through two consecutive poly(A) enrichment steps; 3. Remaining rRNA is depleted to result in highly purified mRNA. The displayed percent removed is the additive percent of total RNA removed throughout the three-stage purification pipeline.*

The Bioanalyzer RNA 6000 pico assay provides an LOD of 25 pg/uL for a single RNA [81]; thus, the maximum theoretical tRNA or rRNA contamination would be 0.8% if it was just below

our detection limit (3000 pg/uL sample analyzed). Similarly, RNA-seq indicated the mRNA is enriched from 4.1% in our total RNA to to 99.8% purified mRNA samples **(Figure 3B, Supplemental Table S3)**. Additionally, we observed a >3000-fold depletion of 25S and 18S rRNAs and an >9-fold enrichment of actin mRNA based on qRT-PCR **(Supplemental Figure S5)**.

Despite recent improvements in RNA-seq technologies and reverse transcriptases, the ability to accurately measure tRNA abundance by RNA-seq remains a struggle due to RNA modifications

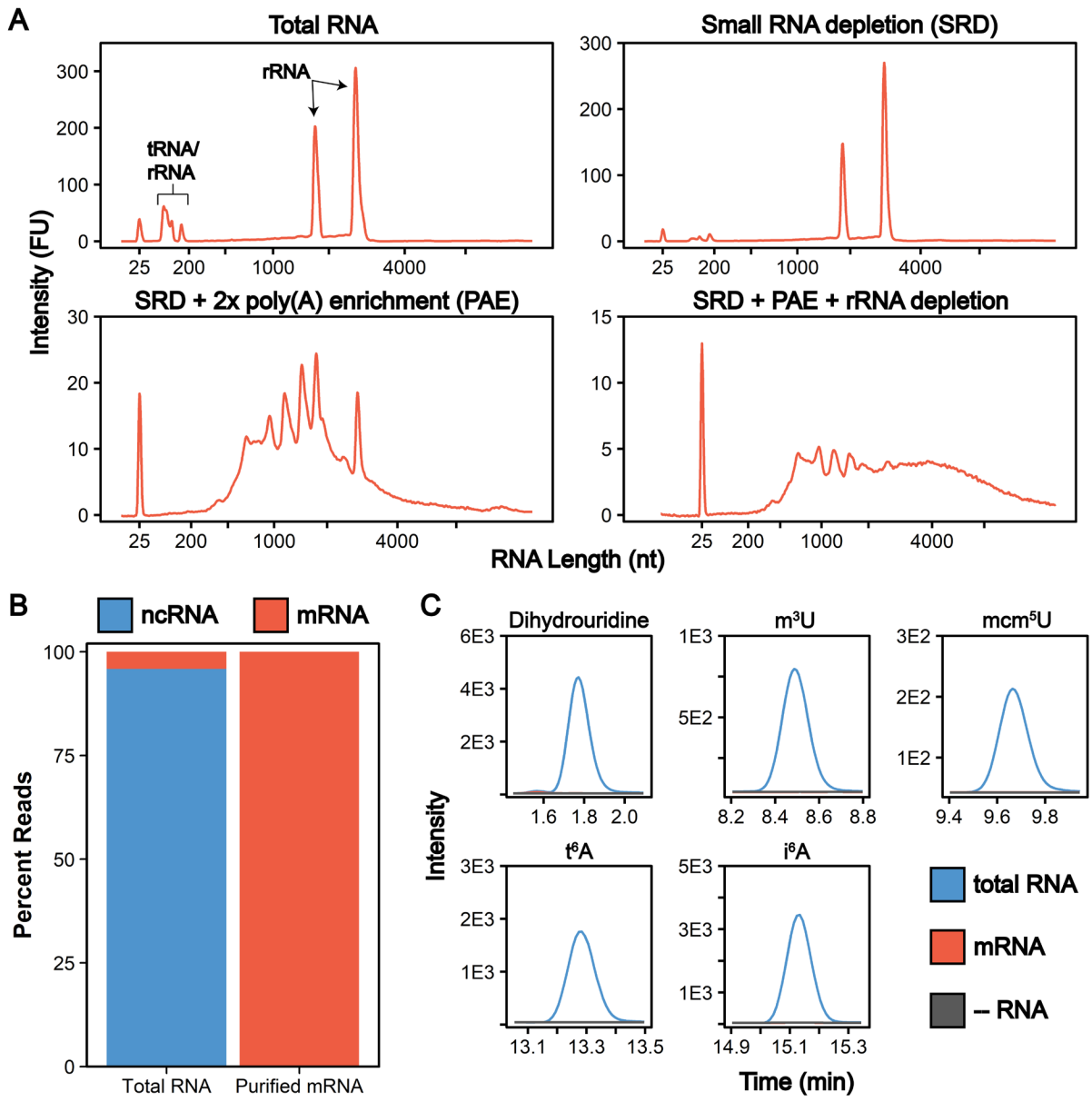

Figure 4.3 *mRNA purity following three-stage purification pipeline. A) Bioanalyzer electropherograms displaying the RNA distribution following each stage of our purification pipeline. B) Average percentage of reads mapping to ncRNA (rRNA, tRNA, snRNA, etc.) and mRNA determined by RNA-seq of two biological replicate total RNA and purified mRNA samples. C) Representative overlaid extraction ion chromatograms for five RNA modifications that exist solely in ncRNA. These five modifications, in addition to eight additional ncRNA modifications, were detected in our total RNA samples (blue) while not detected in our mRNA samples (red) above our control digestions without RNA added (grey).*

in these highly structured RNAs. While similar purities by RNA-seq have been achieved without a small RNA depletion step [20], [78], we previously found that this protocol was insufficient at removing all contaminating ncRNA signals by LC-MS/MS[20] since RNA-seq does not

accurately report on tRNA contamination [82]. Thus, quality control analyses in addition to RNA-seq are necessary to judge tRNA contamination in purified mRNA.

Since our highly multiplexed LC-MS/MS methodology is capable of quantifying known ncRNA and mRNA modifications in a single analysis, we can use this assay to further confirm the purity of our mRNA from the three-stage purification pipeline **(Figure 2)**. In these assays, total RNA and purified mRNA are degraded to ribonucleosides using a two-stage enzymatic digestion with Nuclease P1 and bacterial alkaline phosphatase **(Figure 4A)**.

The resulting modified ribonucleosides are quantified and their concentrations are normalized to their corresponding canonical nucleosides (e.g., m^6A/A) to account for variations in RNA quantities digested. In our total RNA samples, we detected 26 out of 30 known *S. cerevisiae* ribonucleoside modifications that we assayed for, where f^5C, s^2U, $m^{2,7}G$, and m_3G were not detected **(Figure 4B, Supplemental Table S4)**. This was expected because these modifications likely exist at levels below our LOD in our total RNA samples as they either arise from oxidative damage of m^5C (f^5C) [83], [84], are present at very low levels on *S. cerevisiae* tRNA (s^2U) [85]–[87], or are only found in low abundance snRNA and snoRNA ($m^{2,7}G$ and m_3G) [88]–[90]. Additionally, we do not detect the 16 ribonucleoside modifications in our assay that have never been reported in *S. cerevisiae* (1 non-natural and 15 natural) **(Figure 4B, Supplemental Table S4)**. Our purified mRNA samples contained markedly fewer modifications than total RNA, as expected. In addition to the 16 non-*S. cerevisiae* modifications, we do not detect 13 *S. cerevisiae* non-coding RNA modifications that were present in our total RNA samples **(Figure 3C and Supplemental Table S4)**. All modifications not detected in the purified mRNA are reported to be exclusively located in *S. cerevisiae* tRNAs or rRNAs (e.g., i^6A, m^3C) [3], result from

oxidative damage (f^5C) [64], or were only previously detected in *S. cerevisiae* mRNAs purified from cells in

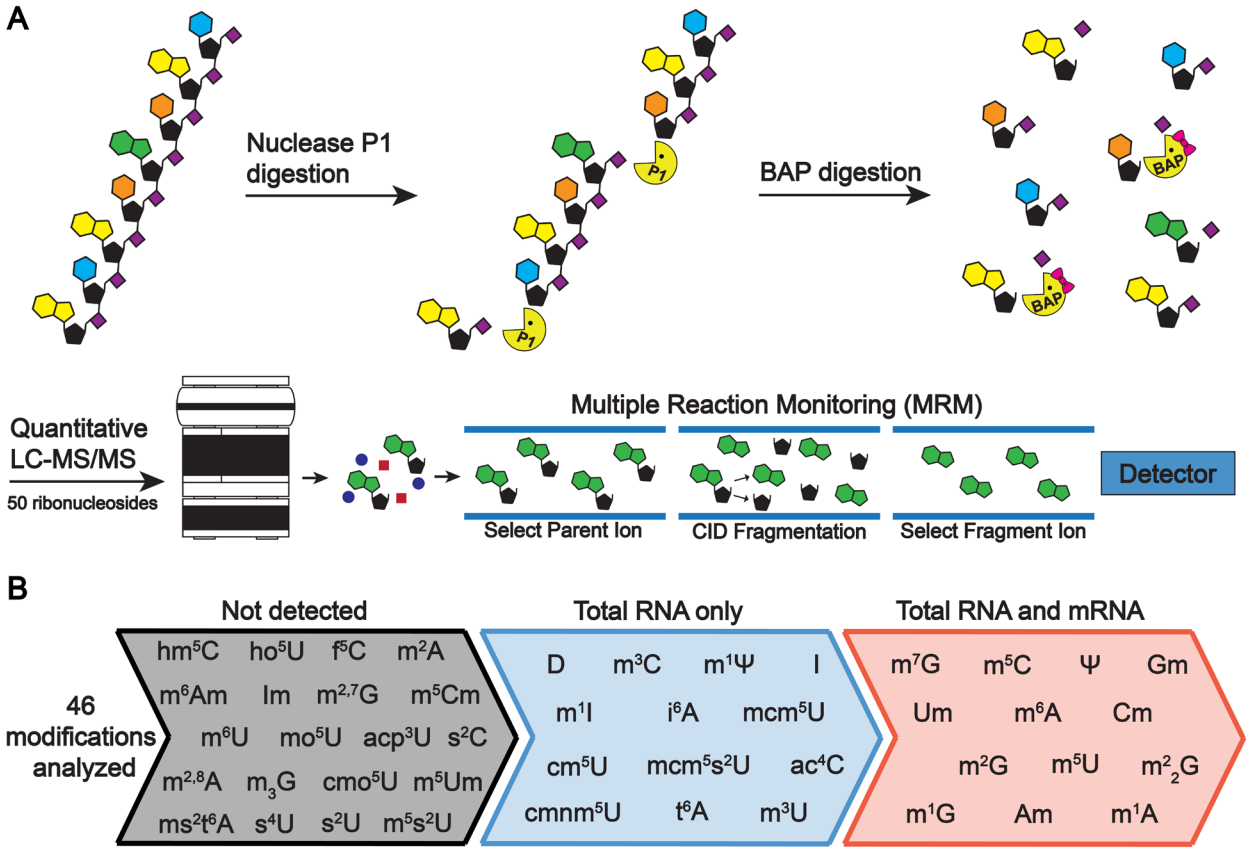

Figure 4.4 *Enzymatic digestion and LC-MS/MS analysis of S. cerevisiae total RNA and mRNA. A) RNA is enzymatic digested to ribonucleosides through a two-stage process. RNA is first digested to nucleotide monophosphates by nuclease P1 and then dephosphorylated to ribonucleosides by bacterial alkaline phosphatase. The resulting ribonucleosides are separated using reverse phase chromatography and then quantified using MRM on a triple quadrupole mass spectrometer. B) S. cerevisiae total RNA and mRNA were analyzed using the LC-MS/MS method developed to quantify 46 modifications in a single analysis. In total RNA, 26 modifications were detected while 13 ribonucleosides were detected in the highly purified mRNA.*

grown under H_2O_2 stress (ac^4C) [20]. The highly abundant dihydrouridine (DHU) modification provides a key example of such a common ncRNA modification that is not detected in our purified samples. DHU is located at multiple sites on every *S. cerevisiae* tRNA and is present at high levels (1.9 DHU/U%) in our total RNA samples **(Supplemental Table S5 and S6)**. However, we do not detect DHU above our LOD in our purified mRNA **(Figure 3C)**. The

inability of our assay to detect highly abundant ncRNA modifications such as DHU provides further evidence that our three-stage purification pipeline produces highly pure mRNA. Commonly, mRNA modification LC-MS/MS analyses characterize only a select few target modifications, which prevents the utilization of LC-MS/MS to judge purity of mRNA. The LC-MS/MS assay described here quantifies up to 46 ribonucleoside modifications in a single analysis, enabling us to use our method to thoroughly characterize mRNA purity. Our analyses ensure that rRNA and tRNA specific modifications are not present at a detectable level in our highly purified mRNA. This highly sensitive corroboration of our Bioanalyzer findings is essential because RNA-seq is not able to sufficiently report on tRNA contamination.

Since all RNA present in our samples will be enzymatically degraded to ribonucleosides during sample preparation **(Figure 4A)**, contaminating highly modified ncRNA will lead to inaccurate modifications quantification in mRNA samples. Thus, extensive quality control for mRNA purity is necessary to give us confidence in downstream LC-MS/MS analyses; however, such data are rarely provided in previous mRNA modification LC-MS/MS studies. Together, we provide four types of evidence (Bioanalyzer, RT-qPCR, RNA-seq, and LC-MS/MS) that our protocol yields highly pure mRNA appropriate for LC-MS/MS analysis. While previous mRNA purification pipelines may inaccurately portray the modification landscape, this pipeline will enable the accurate characterization and quantification of mRNA modifications by providing highly purified mRNA for the analysis using solely commercial kits. We believe that our purification and rigorous purity assessment pipeline could provide a standard method to purify polyadenylated mRNA from total RNA for LC-MS/MS analysis.

4.2.3 m1G, m2G, m22G, and m5U detected in S. cerevisiae mRNA

In our purified mRNA samples, we detected 13 ribonucleoside modifications that ranged in abundance from pseudouridine (0.023 Ψ/U%) to 1-methyladenosine (0.00014 m^1A/A%) **(Figure 4B, Supplemental Figure S6 and Supplemental Tables S5 and S6)**. These abundances are lower than other previous mRNA modification LC-MS/MS analyses, including a previous *S. cerevisiae* study [20]. We attribute this to the fact that our mRNA is more pure than the mRNA used in previous studies, which leads to lower modification abundances in our samples since there is less contaminating highly modified ncRNA. Most of these modifications we observed in our samples are known to be present in *S. cerevisiae* mRNA; however, we detected four modifications for the first time in *S. cerevisiae* (m^1G, m^2G, $m^2{}_2G$, and m^5U) **(Figure 5A)**. This finding corroborates previous studies that detected m^1G [24] and m^5U [15], [21], [91] in *Arabidopsis thaliana* and multiple mammalian cell lines at similar levels, respectively.

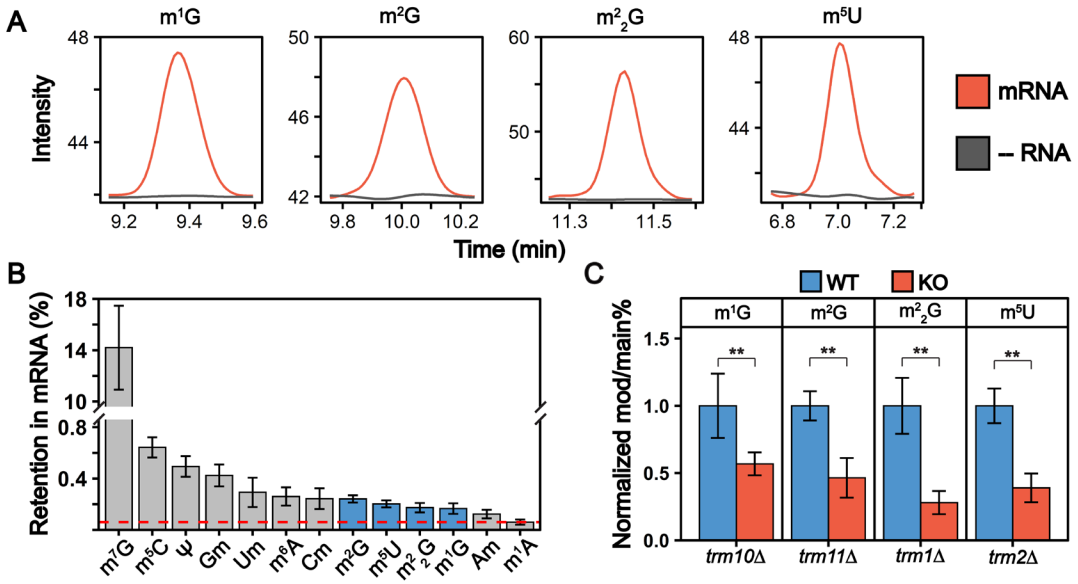

Figure 4.5 *m1G, m2G, m22G, and m5U are present in S. cerevisiae mRNA. A) Overlaid extracted ion chromatograms displaying m1G, m2G, m22G, and m5U are detected in our mRNA samples (red) above our digestion control samples without RNA added (grey). B) m1G, m2G, m22G, and m5U are only present in S. cerevisiae tRNA; thus, we reasoned that they would be retained at a higher percentage than other highly abundant tRNA modifications if they are present in mRNA. Dihydrouridine, which is the most abundant non-mRNA modification in tRNA, was not detected in our purified mRNA samples. If dihydrouridine existed at levels just below our limit of detection (530 amol), the maximum retention of solely tRNA modifications would be 0.06% (red dashed*

*line). The four new mRNA modifications we detect, along with all other known mRNA modifications, are retained at greater extents which proves these modifications exist in S. cerevisiae mRNA. The error bars are the standard deviation of the percent retention. C) m1G, m2G, m22G, and m5U are incorporated into S. cerevisiae mRNA by their corresponding tRNA modifying enzymes (Trm10, trm11, Trm1, and Trm2 respectively). The modification/main base% (e.g., m1G/G%) were normalized to their levels in the average WT mRNA levels. A significant decrease (**p < 0.01) was detected for all cases. The error bars are the standard deviation of the normalized mod/main base%.*

We next critically considered our findings and contemplated the possibility that the signals we detect originated from minor contaminations of tRNA. Prior to this study, in *S. cerevisiae* m^1G, m^2G, $m^2{}_2G$, and m^5U have only been reported in tRNA [3], [92]. Therefore, we reasoned that if these methylated nucleosides are present in *S. cerevisiae* mRNA, they must be retained at higher levels than other tRNA modifications that are not found in mRNA. DHU is the second most abundant RNA modification in *S. cerevisiae* tRNA and thus provides a measure of maximum tRNA contamination **(Supplemental Table S6)**. We did not detect any DHU in our purified mRNA samples. Recent sequencing based studies have reported the presence of DHU in mammalian and *S. pombe* mRNA [15], [16], but our findings indicate DHU either does not exist within *S. cerevisiae* mRNA or is incorporated at levels below our limit of detection. If dihydrouridine existed at levels just below our limit of detection (530 amol), **(Supplemental Table S1)** the maximum extent of DHU/U% retention in our purified mRNA would be 0.06% when calculated using the average digest uridine concentration in a sample of digested mRNA. We find that m^1G, m^2G, $m^2{}_2G$ and m^5U (in addition to all other modifications) were retained to a greater extent than the maximum theoretical retention of level of DHU (>2.5-fold more) in our purified mRNA **(Figure 5B and Supplemental Table S7)**.

Since all contaminating ncRNA species will be digested to ribonucleosides along with mRNA, it is essential to carefully assess our mRNA purity quality controls and the retention of known exclusive ncRNA modifications in our mRNA modification LC-MS/MS data. In this work, our extensive mRNA purity quality control by Bioanalyzer, RNA-seq, RT-qPCR, and LC-

MS/MS in conjunction with there being no other exclusive highly abundant tRNA and rRNA modifications detected in our purified mRNA samples confirms that these modifications are present in *S. cerevisiae* mRNA.

4.2.4 Trm1, Trm2, Trm10 and Trm11 incorporate methylated guanosine and uridine modifications into S. cerevisiae mRNA

Many of the reported mRNA modifications are incorporated by the same enzymes that catalyze their addition into tRNAs and rRNAs [3]. We investigated if the enzymes responsible for inserting m^1G, m^2G, $m^2{}_2G$, and m^5U into *S. cerevisiae* tRNAs (Trm10, Trm11, Trm1, and Trm2 respectively) also incorporate them into *S. cerevisiae* mRNA. We compared the levels of m^1G, m^2G, $m^2{}_2G$, and m^5U in mRNA purified from wild-type and mutant (*trm10*Δ, *trm11*Δ, *trm1*Δ, and *trm2*Δ) *S. cerevisiae.* The abundance of all four modifications decreased significantly in mRNAs purified from the knockout cell lines **(Figure 5C and Supplemental Tables S6)**. While this demonstrates that the tRNA modifying enzymes incorporate these modifications into *S. cerevisiae* mRNA, low levels of m^1G, m^2G, $m^2{}_2G$, and m^5U modifications are still detected in the mRNAs from knockout cell lines **(Figure 5C)**. Several explanations could account for this. A second enzyme, Trm5, also catalyzes m^1G addition into tRNAs and could possibly explain the remaining mRNA m^1G signals. However, given that m^1G and m^2G were previously found as minor products of methylation damage in DNA and RNA [31], [93]–[99], it is perhaps more likely that the remaining low-level signals that we detect arise from methylation associated RNA damage or minor off target methylation by other enzymes. Regardless of how they are incorporated, when present, these modifications have the potential to impact mRNA function.

4.2.5 m1G, m2G and m5U containing mRNA codons slow amino acid addition by the ribosome in a position dependent manner

While our LC-MS/MS assays indicate that m^1G, m^2G, $m^2{}_2G$ and m^5U modifications exist within *S. cerevisiae* mRNA, no previous work has revealed the location or biological consequence of these modifications in mRNA. Despite their low abundance compared to ncRNA modifications (typically significantly lower than 1% modified), evidence that mRNA modifications can alter the chemical and topological properties of modified transcripts which resultingly affect their stability and function continues to increase. Analogously, N-linked and O-linked glycosylations of proteins occur at rates less than approximately 1% and 0.04% per target amino acid, respectively [100]; however, these post-translational modifications play important biological roles, such protein localization and receptor interaction [101], [102], and their misregulation is linked to multiple diseases [103] despite their low abundance. mRNAs are all substrates for the ribosome, and post-transcriptional modifications can change how the ribosome decodes a message by altering the hydrogen bonding patterns between the mRNA codons and aminoacylated-tRNAs [104]–[109]. Indeed, several mRNA modifications have been shown to alter the overall rate and fidelity of protein synthesis in a modification and codon-position dependent manner [40], [41], [110]–[115]. Such perturbations to protein synthesis can have significant consequences even when modifications are incorporated into mRNAs transcripts at very low levels, as exemplified by the biological consequences of oxidatively damaged mRNAs, which exist at levels similar to m^1G, m^2G, $m^2{}_2G$ and m^5U [31], [116]. We investigated how the insertion of m^5U, m^1G, and m^2G into mRNA codons impacts translation using a well-established reconstituted *in vitro* translation system[40] **(Figure 6A)**. This system has long been used to investigate how the ribosome decodes mRNAs because it can be purified in sufficient quantities

to conduct high-resolution kinetic studies. Translation elongation is well conserved between bacteria and eukaryotes [117], and prior studies demonstrate that mRNA modifications (e.g. pseudouridine, N6-methyladenosine and 8-oxo-G) that slow elongation and/or change mRNA

decoding elongation in the reconstituted *E. coli* system [40], [41], [110], [118] also do so in eukaryotes [40], [119]–[121]. $m^2{}_2G$ was not selected for study because the phosphoramidite required for mRNA oligonucleotide synthesis is not commercially available.

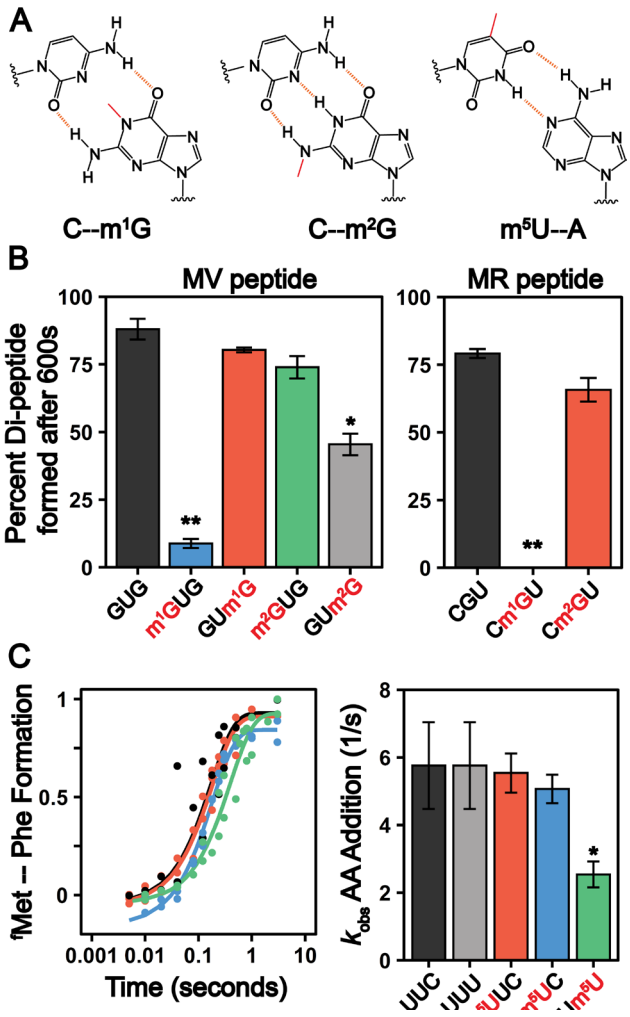

Figure 4.6 *Methylated guanosine and uridine modifications alter amino acid addition. A) Watson-Crick base pairing of m1G, m2G and m5U. The added methylation is displayed in red and the hydrogen bond interactions displayed as a dashed orange line. B) Total peptide formation of translation reactions after 600 seconds using transcribed or single-nucleotide modified mRNAs encoding for either (Left Panel) Met-Val (GUG) or (Right Panel) Met-Arg (CGU) dipeptide. Error bars are the standard deviation. B) Time courses displaying the formation of fMet-Phe dipeptide on an unmodified and singly modified UUC or UUU codons (left panel). Observed rate constants (right panel) were determined from the fit data. The error bars are the standard deviation of the fitted value of kobs. m5U has a minor affect on translation in a position dependent manner in mRNA and no major observed affectt in tRNA. (A) LC-MS/MS analysis showing that our tRNAphe purified from trmA KO cells does not contain m5U modfications. (B) Bar graph showing the formation of misocded Met-Ile product. (C) Kobs Curves and bar plots showing observered rates constant for met-phe dipeptide formation using the KO tRNAphe. panel) were determined from the fit data. The error bars are the standard deviation of the fitted value of kobs. m5U has a minor affect on translation in a position dependent manner in mRNA and no major observed affectt in tRNA.*

In our assays, 70S ribosome initiation complexes (ICs) containing ^{35}S-^{f}Met-tRNA^{fmet} programmed in the A site are formed on transcripts encoding Met-Phe, Met-Arg, or Met-Val dipeptides. Ternary complexes comprised of aminoacyl-tRNA:EF-Tu:GTP are added to the ICs to begin translation. Reactions are quenched as desired timepoints by KOH, and the unreacted ^{35}S-^{f}Met-tRNA^{fmet} and dipeptide translation products are visualized by electrophoretic TLC (eTLC) **(Supplementary Figures S7 through S10)**. We evaluated the extent of total dipeptide synthesis and/or the rate constants (k_{obs}) for amino acid incorporation on unmodified (CGU, GUG, UUC, UUU) and modified (Cm^{1}GU, Cm^{2}GU, m^{1}GUG, m^{2}GUG, GUm^{1}G, GUm^{2}G, m^{5}UUC, Um^{5}UC, Uum^{5}U) codons. The presence of modifications in the codons were verified by direct infusion ESI-MS or nanoelectrospray ionization (nESI)-MS **(Supplemental Figures S11 to S13)**. We observed that the extent of amino acid addition is drastically reduced when m^{1}G is present at the first or second position in a codon but is restored to normal levels when m^{1}G is at the third nucleotide **(Figure 6B and Supplemental Figures S7 through S9)**. Codons containing m^{2}G show a more modest defect in dipeptide production, only significantly impeding dipeptide synthesis (1.9 ± 0.2-fold) when m^{2}G is in the third position of a codon **(Figure 6B and Supplemental Figures S7 through S9)**. These findings are consistent with a previous report indicating that insertion of a single m^{1}G and m^{2}G modification into an mRNA codon reduces the overall protein production and translation fidelity in a position and codon dependent manner [115]. m^{1}G and m^{2}G should both disrupt Watson-Crick base pairing between mRNAs and tRNAs **(Figure 6A)** and might be expected to alter amino acid addition in similar ways. However, our results reveal that the insertion of m^{1}G has a much larger consequence than m^{2}G on peptide production. This can be partially rationalized by the fact that m^{1}G would impede canonical Watson-Crick base-pairing by eliminating a central H-bond interaction, while m^{2}G

disrupts only peripheral interactions **(Figure 6A)**. Additionally, the methylation of the analogous position of adenosine (m^1A) similarly abolishes the ability of the ribosome to add amino acids [30], suggesting that the conserved N1 position on purine nucleobases is particularly crucial to tRNA decoding. The hydrogen bonding patterns possible between m^2G and other nucleosides would be expected to closely resemble those of another well studied modification, inosine. Inosine also has a moderate (if any) impact on the rates of protein synthesis, though it can promote amino acid mis-incorporation [122], [123]. The limited consequence of both inosine and m^2G on overall peptide production indicates that purine peripheral amines on the Watson-Crick face are less important than the N1 position for ensuring the rapid addition of amino acids by the ribosome.

In contrast to the guanosine modifications that we investigated, transcripts containing m^5U Phe-encoding codons did not reduce the total amount of dipeptide produced **(Figure 6C)**. However, the insertion of m^5U into codons can reduce the rate constants for amino acid addition (k_{obs}) in a position dependent manner, similar to Ψ modified transcripts [40]. The rate constant for Phe incorporation on an unmodified and modified codons at the 1st and 2nd position were comparable to an unmodified codon, with a k_{obs} of ~ $5s^{-1}$ **(Figure 6C and Supplemental Figure S10)**. However, when m^5U is in the 3rd position we see a 2-fold decrease in the k_{obs} at ~ $2.5s^{-1}$ **(Figure 6C and Supplemental Figure S10)**. This is the first evidence that m^5U can influence amino acid addition when encountered by the ribosome. It is less clear how m^5U and other modifications that do not change the Watson-Crick face of nucleobases (e.g., Ψ and 8-oxoG) impact translation [124]. It is possible that such modifications alter nucleobase ring electronics to perturb the strength of the hydrogen bond donors and acceptors involved in base pairing.

While the levels of the mRNA modifications we identified are lower than that of more well-established modifications (m^6A and Ψ), our findings suggest that they still have potential to impact biology. Although our data do not report on the ability of the modifications that we uncover to control gene expression or identify the number of mRNAs that they are in, they do suggest that there will be consequences for translation when these modifications are encountered by the ribosome. It is also important to note that the levels and distributions of mRNA modifications (enzymatic and RNA damage) can change significantly in response to different environmental conditions, so the low levels of modification that we measure in healthy, rapidly growing yeast have the potential to significantly increase under stress [20], [28], [116], [125]. The three modifications we investigated alter translation differently depending on their location within a codon. Such a context dependence has been observed for every mRNA modification investigated to date [124]. Modifications have the capacity to change intra-molecular interactions with an mRNA, or interactions between rRNA and mRNA within the A site. There is growing evidence that such factors, and not only anticodon:codon interactions, have a larger contribution to translation elongation than previously recognized. For example, ribosome stalling induced by the rare 8-oxo-guanosine damage modification has the potential to perturb ribosome homeostasis or even the small pauses in elongation induced by mRNA pseudouridine modifications can impact levels of protein expression in a gene specific manner [31], [121]. Additionally, transient ribosome pauses have the potential modulate co-translational protein folding or provide time for RNA binding proteins to interact with a transcript [126], [127]. Future systematic biochemical and computational studies are needed to uncover the causes of the context dependence. Additionally, the continued development of RNA-seq technologies is needed to locate these modifications throughout the transcriptome. This information will be broadly useful as

researchers seek to identify which of the modified mRNA codons are the most likely to have molecular level consequences when encountered by a translating ribosome.

4.3 Conslusions

Mass spectrometry based approaches are widely used to study protein post-translational modifications, but the application of similar techniques to investigate mRNA post-transcriptional modifications has not been widely adopted. The current LC-MS/MS workflows for discovering and studying mRNA modifications are hindered by either low-throughput method development, inadequate mRNA purification, or insufficient sensitivities to detect low level mRNA modifications. This study presents mRNA purification, validation, and LC-MS/MS pipelines that enable the sensitive and highly multiplexed analysis of mRNA and ncRNA modifications. These developments enable us to confidently identify four previously unreported mRNA modifications in *S. cerevisiae* (m^1G, m^2G, $m^2{}_2G$ and m^5U), demonstrating the utility of applying LC-MS/MS to discover and quantify mRNA modifications. In addition to revealing the enzymes that incorporate these modifications, we also demonstrate that the presence of m^1G, m^2G, and m^5U in mRNA can impede translation. However, the impacts of the modifications on amino acid addition are not uniform, with the position and identity of each modification resulting in a different outcome on dipeptide production. This work suggests that the ribosome will regularly encounter a variety of modified codons in the cell and that depending on the identity and position of the modification, these interactions can alter the elongation step in protein synthesis.

4.4 Methods

4.4.1 S. cerevisiae Cell Growth and mRNA Purification

Wild-type, Δtrm1, Δtrm2, Δtrm10 and Δtrm11 BY4741 *S. cerevisiae* (Horizon Discovery) were grown in YPD medium as previously described [20]. Knockout cells lines were grown with 200 µg/mL Geneticin. Briefly, 100 mL of YPD medium was inoculated with a single colony selected from a plate and allowed to grow overnight at 30°C and 250 RPM. The cells were diluted to an OD600 of 0.1 with 300 mL of YPD medium and were grown to an OD600 of 0.6-0.8 at 30°C and 250 RPM. The cell suspension was pelleted at 3,220 x g at 4°C and used for the RNA extraction.

S. cerevisiae cells were lysed as previously described with minor alterations [20], [128]. The 300 mL cell pellet was resuspended in 12 mL of lysis buffer (60 mM sodium acetate pH 5.5, 8.4 mM EDTA) and 1.2 mL of 10% SDS. One volume (13.2 mL) of acid phenol:chloroform:isoamyl alcohol (125:24:1; Sigma-Aldrich, USA; P1944) was added and vigorously vortexed. The mixture was incubated in a water bath at 65°C for five min and was again vigorously vortexed. The incubation at 65°C and vortexing was repeated once. Then, the mixture was rapidly chilled in an ethanol/dry ice bath until lysate was partially frozen. The lysate was allowed to thaw and then centrifuged for 15 min at 15,000 x g. The upper layer containing the total RNA was washed three additional times with 13.2 mL phenol and the phenol was removed using two chloroform extractions of the same volume. The resulting RNA was ethanol precipitated in the presence of 1/10th volume of 3 M sodium acetate and then a second time in the presence of 1/2 volume of 7.5 M ammonium acetate. The extracted total RNA was treated with 140 U RNase-free DNase I (Roche, 10 U/µL) in the supplied digestion buffer at 37°C for 30 min. The DNase I was removed through an acid phenol-chloroform extraction. The resulting RNA was ethanol precipitated in the presence of 1/10th volume of 3 M sodium acetate pH 5.2 and then a second time in the presence of 1/2 volume of 7.5 M ammonium acetate. The

precipitated RNA was pelleted and resuspended in water. The resulting total RNA was used for our LC-MS/MS, bioanalyzer, and RNA-seq analyses.

mRNA was purified through a three-stage purification pipeline. First, small RNA (tRNA and 5S rRNA) was diminished from 240 μg of total RNA using a Zymo RNA Clean and Concentrator-100 kit to purify RNA > 200nt. Two consecutive poly(A) enrichment steps were applied to 125 μg of the resultant small RNA diminished samples using Dynabeads oligo-dT magnetic beads (Invitrogen, USA). The resulting poly(A) RNA was ethanol precipitated using 1/10th volume of 3 M sodium acetate pH 5.2 and resuspended in 14 μL of water. Then, we removed the residual 5S, 5.8S, 18S, and 28S rRNA using the commercial riboPOOL rRNA depletion kit (siTOOLs Biotech). The Bioanalyzer RNA 6000 Pico Kit (Agilent) was used to evaluate the purity of the mRNA prior to LC-MS/MS analysis.

4.4.2 qRT-PCR

DNase I treated total RNA and three-stage purified mRNA (200 ng) were reverse transcribed using the RevertAid First Strand cDNA Synthesis Kit (Thermo Scientific) using the random hexamer primer. The resulting cDNA was diluted 5000-fold and 1 μL of the resulting mixture was analyzed using the Luminaris Color HiGreen qPCR Master Mix (Thermo Scientific) with gene-specific primers (**Supplemental Table S8**).

4.4.3 RNA-Seq

The WT *S. cerevisiae* mRNA was analyzed by RNA-seq as previously described with minimal alterations [20]. Briefly, 50 ng of DNase I treated total RNA and three-stage purified mRNA from the two biological replicates were fragmented using the TruSeq RNA Library Prep Kit v2 fragmentation buffer (Illumina). First-strand cDNA synthesis was performed using the random

hexamer primer, and the second strand was synthesized using the Second Strand Master Mix. The resulting cDNA was purified with AMPure XP beads (Beckman Coulter), the ends were repaired, and the 3' end was adenylated. Lastly, indexed adapters were ligated to the DNA fragments and amplified using 15 PCR cycles. Paired-end sequencing was performed for the cDNA libraries using 2.5% of an Illumina NovaSeq (S4) 300 cycle sequencing platform flow cell (0.625% of flow cell for each sample). All sequence data are paired-end 150 bp reads.

FastQC (v0.11.9) [129] was used to evaluate the quality of the raw and trimmed reads. Then, cutadapt (v1.18) [130] was used to trim to paired-end 50 bp reads and obtain high quality clean reads with the arguments -u 10 -U 10 -l 50 -m 15 -q 10. Following, Bowtie2 (v2.2.5) [131] was used to align the forward strand reads to *S. cerevisiae* reference genome (R64-1-1) with the default parameters. Following alignment, Rmmquant tool R package (v1.6.0) [132] and the gene_biotype feature in the *S. cerevisiae* GTF file was used to count the number of mapped reads for each transcript and classify the RNA species, respectively.

4.4.4 RNA digestions and LC-MS/MS analysis

RNA (200 ng) was hydrolyzed to composite mononucleosides using a two-step enzymatic digestion. The RNA was first hydrolyzed overnight to nucleotide monophosphates using 300 U/ µg Nuclease P1 (NEB, 100,000 U/mL) at 37°C in 100 mM ammonium acetate (pH 5.5) and 100 µM $ZnSO_4$. Following, the nucleotides were dephosphorylated using 50 U/µg bacterial alkaline phosphatase (BAP, Invitrogen, 150U/µL) for 5 hrs at 37°C in 100 mM ammonium bicarbonate (pH 8.1) and 100 µM $ZnSO_4$. Prior to each reaction, the enzymes were buffer exchanged into their respective reaction buffers above using a Micro Bio-Spin 6 size exclusion spin column (Biorad) to remove glycerol and other ion suppressing constituents. After

the reactions, the samples were lyophilized and resuspended in 9 µL of water and 1 µL of 400 nM $^{15}N_4$-inosine internal standard.

The resulting ribonucleosides were separated using a Waters Acquity HSS T3 column (1 x 100 mm, 1.8 µm, 100 Å) with a guard column at 100 µL/min on a Agilent 1290 Infinity II liquid chromatograph interfaced to a Agilent 6410 triple quadrupole mass spectrometer. Mobile phase A was 0.01% (v/v) formic acid in water and mobile phase B was 0.01% (v/v) formic acid in acetonitrile. The gradient is displayed in **Supplemental Table S9**. The autosampler was held at 4°C, and 5 µL was injected for each sample. The eluting ribonucleosides were quantified using MRM and ionized using electrospray ionization in positive mode at 4 kV **(Supplemental Table S10)**. The electrospray ionization conditions were optimized by infusing 500 nM uridine at 100 µL/min at 5% mobile phase B. The gas temperature was 350°C, the gas flow rate was 10 L/min, and the nebulizer gas pressure was 25 psi. After each RNA digestion sample, a wash gradient injection was performed to eliminate any column carryover of late eluting nucleosides (e.g., i^6A) **(Supplemental Table S9)**.

To compare the sensitivity between the 1 mm and 2 mm I.D. column chromatographies, a 2.1 mM Waters Acquity HSS T3 column (2.1 x 100 mm, 1.8 µm, 100A) with a guard column was used at 400 uL/min using the same gradient and mobile phases described above. The source conditions for the 2.1 mm I.D. column were optimized by infusing 500 nM uridine at 400 µL/min at 5% mobile phase B. The gas temperature was 350°C, the gas flow rate was 10 L/min, and the nebulizer gas pressure was 55 psi. For both analyses, 5 uL of ribonucleoside standard mixes containing 1.4 µM canonical nucleosides and 72 nM modifications was injected.

To quantify RNA nucleosides calibration curves were created for the four main bases, 45 natural modified nucleosides, and 1 non-natural modified nucleoside using seven calibration points ranging over four orders of magnitude. $^{15}N_4$-inosine (40 nM) was used as the internal standard for all ribonucleosides. The concentrations of ribonculeoside in the calibration curves standards can be found in **Supplemental Table 11.** Suppliers for ribonucleoside standards can be found in **Supplemental Table 12**. Automated peak integration was performed using the Agilent MassHunter Workstation Quantitative Analysis Software. All peaks were visually inspected to ensure proper integration. The calibration curves were plotted as the $\log_{10}$(response ratio) versus the $\log_{10}$(concentration (pM)) and the RNA sample nucleoside levels were quantified using the resulting linear regression. The limits of detection were calculated using:

$$LOD\ (pM) = 10^{\frac{(3 \times standard\ error\ of\ regression) + (\log_{10} average\ response\ ratio\ of\ blank) - (y\ intercept)}{Slope\ of\ linear\ regression}} \quad (4.1)$$

The calculated LOD was then converted to amol. For each RNA enzymatic digestion samples, the respective calibration curve was used to calculate nucleoside concentrations in the samples.

The retention of modifications in mRNA was calculated using the following equation:

$$Retention\% = \frac{mod/main\%\ in\ mRNA}{mod/main\%\ in\ total\ RNA} x100\% \quad (4.2)$$

4.4.5 E. coli ribosomes and translation factor purification

Ribosomes were purified from *E. coli* MRE600 as previously described[40]. All constructs for translation factors were provided by the Green lab unless specifically stated otherwise. The expression and purification of translation factors were carried out as previously described[40].

4.4.6 tRNA and mRNA for in vitro translation assay

Unmodified transcripts were prepared using run-off T7 transcription of Ultramer DNA templates that were purchased from Integrated DNA Technologies **(Supplemental Table S13)**. HPLC purified modified mRNA transcripts containing 5-methyluridine, 1-methylguanosine, and N2-methylguanosine were purchased from Dharmacon **(Supplemental Table S14)**. The homogeneity and accurate mass for most of the purchased modified oligonucleotides were confirmed by direct infusion ESI-MS prior to use by Dharmacon **(Supplementary Figure S11 through S13)**. For the remaining purchased oligonucleotides lacking Dharmacon spectra, they were analyzed on a ThermoFisher Q-Exactive UHMR Hybrid Quadrupole-Orbitrap Mass Spectrometer in a negative ionization polarity. Samples were buffer exchanged into 100 mM ammonium acetate (AmOAc) using Micro Bio-Spin P-6 gel columns and directly infused via nanoelectrospray ionization (nESI). nESI was performed using borosilicate needles pulled and coated in-house with a Sutter p-97 Needle Puller and a Quorum SCX7620 mini sputter coater, respectively. The acquired native mass spectra were deconvoluted using UniDec [133] in negative polarity **(Supplementary Figure S11)**.

Native tRNA was purified as previously described with minor alterations [134]. Bulk *E. coli* tRNA was either bought in bulk from Sigma-Aldrich or purified from a HB101 *E. coli* strain containing pUC57-tRNA that we obtained from Prof. Yury Polikanov (University of Illinois, Chicago). Two liters of media containing Terrific Broth (TB) media (TB, 4 mL glycerol/L, 50

mM NH_4Cl, 2 mM $MgSO_4$, 0.1 mM $FeCl_3$, 0.05% glucose and 0.2% lactose (if autoinduction media was used)) were inoculated with 1:400 dilution of a saturated overnight culture and incubated with shaking at 37℃ overnight with 400 mg/ml of ampicillin. Cells were harvested the next morning by 30 min centrifugation at 5000 RPM and then stored at -80℃. Extraction of tRNA was done by first resuspending the cell pellet in 200 mL of resuspension buffer (20 mM Tris-Cl, 20 mM $Mg(OAc)_2$ pH 7.) The resuspended cells were then placed in Teflon centrifuge tubes with ETFE o-rings containing 100 mL acid phenol/chloroform/isoamyl alcohol mixture. The tubes were placed in a 4℃ incubator and left to shake for 1 hr. After incubation, the lysate was centrifuged for 60 min at 3,220 x g at 4℃. The supernatant was transferred to another container and the first organic phase was then back-extracted with 100mL resuspension buffer and centrifuged down for 60 min at 3,220 x g at 4℃. Aqueous solutions were then combined and a 1/10 volume of 3 M sodium acetate pH 5.2 was added and mixed well. Isopropanol was added to 20% and after proper mixing was centrifuged to remove DNA at 13,700 x g for 60 min at 4℃. The supernatant was collected, and isopropanol was added to 60% and was left to precipitate at -20℃ overnight. The precipitated RNA was pelleted at 13,700 x g for 60 min at 4℃ and resuspended with approximately 10 mL 200 mM Tris-Acetate, pH 8.0. The RNA was incubated at 37℃ for at least 30 min to deacylate the tRNA. After incubation $1/10^{th}$ volume of 3 M sodium acetate pH 5.2 and 2.5 volumes of ethanol was added to precipitate the RNA. Then, the mixture was centrifuged at 16,000 x g for 60 min at 4℃. The pellet was washed with 70% ethanol, resuspended in water, and desalted using an Amicon 10 kDa MWCO centrifugal filter prior to purification (Millipore-Sigma, USA).

Next, the tRNA was isolated using a Cytiva Resource Q column (6 mL) on a AKTA Pure 25M FPLC. Mobile phase A was 50 mM NH_4OAc, 300 mM NaCl, and 10 mM $MgCl_2$. Mobile

phase B was 50 mM NH_4OAc, 800 mM NaCl, 10 mM $MgCl_2$. The resuspended RNA was filtered, loaded on the Resource Q column, and eluted with a linear gradient from 0-100% mobile phase B over 18 column volumes. Fractions were pulled and ethanol precipitated overnight at -20°C.

The precipitated RNA was resuspended in water and filtered prior to purification on a Waters XBridge BEH C18 OBD Prep wide pore column (10 x 250 mm, 5 μm). Mobile phase A was 20 mM NH_4OAc, 10 mM $MgCl_2$, and 400 mM NaCl at pH 5 in 100% water. Mobile phase B was 20 mM NH_4OAc, 10 mM $MgCl_2$, and 400 mM NaCl at pH 5 in 60% methanol. The injection volume was 400 μl. A linear gradient of mobile phase B from 0-35% was done over 35 min. After 35 min, the gradient was increased to 100% mobile phase B over 5 min and held at 100% for 10 min, column was then equilibrated for 10 column volumes before next injection with mobile phase A. TCA precipitations were performed on the fractions to identify fractions containing the phenylalanine tRNA as well as measuring the A_{260} and amino acid acceptor activity.

4.4.7 Formation of E. coli ribosome initiation complexes

Initiation complexes (ICs) were formed in 1X 219-Tris buffer (50 mM Tris pH 7.5, 70 mM NH_4Cl, 30 mM KCl, 7 mM $MgCl_2$, 5 mM β-ME) with 1 mM GTP as previously described [134]. 70S ribosomes were incubated with 1 μM mRNA (with or without modification), initiation factors (1, 2, and 3) all at 2 μM final, and 2 μM of radiolabeled ^{35}S-^{f}Met-$tRNA^{fMet}$ for 30 min at 37°C. After incubation, $MgCl_2$ was added to a final concentration of 12 mM. The ribosome mixture was then layered onto 1 mL cold buffer D (20 mM Tris-Cl, 1.1 M sucrose, 500 mM NH_4Cl, 10 mM $MgCl_2$, 0.5 mM disodium EDTA, pH 7.5) and centrifuged at 69,000 rpm for

2 hrs at 4°C. After pelleting, the supernatant was discarded into radioactive waste, and the pellet was resuspended in 1X 219-tris buffer and stored at -80°C.

4.4.8 In vitro amino acid addition assays

IC complexes were diluted to 140 nM with 1X 219-Tris buffer. Ternary complexes (TCs) were formed by first incubating the EF-Tu pre-loaded with GTP (1X 219-Tris buffer, 10 mM GTP, 60 μM EFTu, 1 μM EFTs) at 37°C for 10 min. The EF-Tu mixture was incubated with the tRNA mixture (1X 219-Tris buffer, Phe-tRNA^{Phe} (1-10 μM), 1 mM GTP) for another 15 min at 37°C. After TC formation was complete, equal volumes of IC complexes (70 nM) and ternary complex (1 μM) were mixed either by hand or using a KinTek quench-flow apparatus. Discrete time-points (0-600 seconds) were taken as to obtain observed rate constants on m^{5}U-containing mRNAs. Each time point was quenched with 500 mM KOH (final concentration). Time points were then separated by electrophoretic TLC and visualized using phosphorescence as previously described [40], [134]. Images were quantified with ImageQuant. The data were fit using Equation 1:

$$Fraction\ product\ = A \cdot (\ 1 - e^{k_{obs}t}) \tag{4.3}$$

4.5 References

[1] P. J. McCown et al., "Naturally occurring modified ribonucleosides," WIREs RNA, vol. 11, no. 5, p. e1595, 2020, doi: https://doi.org/10.1002/wrna.1595.

[2] R. J. Ontiveros, J. Stoute, and K. F. Liu, "The chemical diversity of RNA modifications," Biochemical Journal, vol. 476, no. 8, pp. 1227–1245, Apr. 2019, doi: 10.1042/BCJ20180445.

[3] P. Boccaletto et al., “MODOMICS: a database of RNA modification pathways. 2017 update,” Nucleic Acids Res, vol. 46, no. Database issue, pp. D303–D307, Jan. 2018, doi: 10.1093/nar/gkx1030.

[4] N. Jonkhout, J. Tran, M. A. Smith, N. Schonrock, J. S. Mattick, and E. M. Novoa, “The RNA modification landscape in human disease,” RNA, vol. 23, no. 12, pp. 1754–1769, Dec. 2017, doi: 10.1261/rna.063503.117.

[5] X. Zhang et al., “Small RNA modifications in Alzheimer’s disease,” Neurobiology of Disease, vol. 145, p. 105058, Nov. 2020, doi: 10.1016/j.nbd.2020.105058.

[6] M. Pereira, S. Francisco, A. S. Varanda, M. Santos, M. A. S. Santos, and A. R. Soares, “Impact of tRNA Modifications and tRNA-Modifying Enzymes on Proteostasis and Human Disease,” International Journal of Molecular Sciences, vol. 19, no. 12, Art. no. 12, Dec. 2018, doi: 10.3390/ijms19123738.

[7] J. Ramos et al., “Identification and rescue of a tRNA wobble inosine deficiency causing intellectual disability disorder,” RNA, vol. 26, no. 11, pp. 1654–1666, Nov. 2020, doi: 10.1261/rna.076380.120.

[8] J. T. Lant, M. D. Berg, I. U. Heinemann, C. J. Brandl, and P. O’Donoghue, “Pathways to disease from natural variations in human cytoplasmic tRNAs,” J. Biol. Chem., vol. 294, no. 14, pp. 5294–5308, Apr. 2019, doi: 10.1074/jbc.REV118.002982.

[9] H. Lin et al., “CO2-sensitive tRNA modification associated with human mitochondrial disease,” Nature Communications, vol. 9, no. 1, Art. no. 1, May 2018, doi: 10.1038/s41467-018-04250-4.

[10] D. Dominissini et al., “Topology of the human and mouse m6A RNA methylomes revealed by m6A-seq,” Nature, vol. 485, no. 7397, pp. 201–206, May 2012, doi: 10.1038/nature11112.

[11] C. Enroth, L. D. Poulsen, S. Iversen, F. Kirpekar, A. Albrechtsen, and J. Vinther, “Detection of internal N7-methylguanosine (m7G) RNA modifications by mutational profiling sequencing,” Nucleic Acids Research, p. gkz736, Aug. 2019, doi: 10.1093/nar/gkz736.

[12] L. S. Zhang et al., “Transcriptome-wide Mapping of Internal N7-Methylguanosine Methylome in Mammalian mRNA,” Mol Cell, vol. 74, no. 6, Art. no. 6, Jun. 2019, doi: 10.1016/j.molcel.2019.03.036.

[13] T. M. Carlile, M. F. Rojas-Duran, B. Zinshteyn, H. Shin, K. M. Bartoli, and W. V. Gilbert, “Pseudouridine profiling reveals regulated mRNA pseudouridylation in yeast and human cells,” Nature, vol. 515, no. 7525, pp. 143–146, Nov. 2014, doi: 10.1038/nature13802.

[14] A. F. Lovejoy, D. P. Riordan, and P. O. Brown, “Transcriptome-Wide Mapping of Pseudouridines: Pseudouridine Synthases Modify Specific mRNAs in *S. cerevisiae*,” PLOS ONE, vol. 9, no. 10, p. e110799, Oct. 2014, doi: 10.1371/journal.pone.0110799.

[15] W. Dai et al., “Activity-based RNA-modifying enzyme probing reveals DUS3L-mediated dihydrouridylation,” Nat Chem Biol, vol. 17, no. 11, pp. 1178–1187, Nov. 2021, doi: 10.1038/s41589-021-00874-8.

[16] O. Finet et al., “Transcription-wide mapping of dihydrouridine reveals that mRNA dihydrouridylation is required for meiotic chromosome segregation,” Molecular Cell, vol. 82, pp. 1–16, Nov. 2021, doi: 10.1016/j.molcel.2021.11.003.

[17] Q. Dai et al., “Nm-seq maps 2′O-methylation sites in human mRNA with base precision,” Nature Methods, vol. 14, no. 7, pp. 695–698, Jul. 2017, doi: 10.1038/nmeth.4294.

[18] S. Okada, H. Ueda, Y. Noda, and T. Suzuki, “Transcriptome-wide identification of A-to-I RNA editing sites using ICE-seq,” Methods, vol. 156, pp. 66–78, Mar. 2019, doi: 10.1016/j.ymeth.2018.12.007.

[19] D. Arango et al., “Acetylation of Cytidine in mRNA Promotes Translation Efficiency,” Cell, vol. 175, no. 7, pp. 1872-1886.e24, Dec. 2018, doi: 10.1016/j.cell.2018.10.030.

[20] M. Tardu, J. D. Jones, R. T. Kennedy, Q. Lin, and K. S. Koutmou, “Identification and quantification of modified nucleosides in *Saccharomyces cerevisiae* mRNAs,” ACS Chem Biol, vol. 14, no. 7, Art. no. 7, Jul. 2019, doi: 10.1021/acschembio.9b00369.

[21] Q.-Y. Cheng et al., “Chemical tagging for sensitive determination of uridine modifications in RNA,” Chem. Sci., vol. 11, no. 7, pp. 1878–1891, 2020, doi: 10.1039/C9SC05094A.

[22] J.-M. Chu et al., “Existence of Internal N7-Methylguanosine Modification in mRNA Determined by Differential Enzyme Treatment Coupled with Mass Spectrometry Analysis,” ACS Chem. Biol., vol. 13, no. 12, pp. 3243–3250, Dec. 2018, doi: 10.1021/acschembio.7b00906.

[23] L. Xu et al., “Three distinct 3-methylcytidine (m3C) methyltransferases modify tRNA and mRNA in mice and humans,” J. Biol. Chem., vol. 292, no. 35, pp. 14695–14703, Sep. 2017, doi: 10.1074/jbc.M117.798298.

[24] H.-C. Duan et al., “ALKBH10B Is an RNA N6-Methyladenosine Demethylase Affecting Arabidopsis Floral Transition,” Plant Cell, vol. 29, no. 12, pp. 2995–3011, Dec. 2017, doi: 10.1105/tpc.16.00912.

[25] J. D. Jones, J. Monroe, and K. S. Koutmou, “A molecular-level perspective on the frequency, distribution, and consequences of messenger RNA modifications,” WIREs RNA, p. e1586, Jan. 2020, doi: 10.1002/wrna.1586.

[26] D. P. Morse and B. L. Bass, “Detection of Inosine in Messenger RNA by Inosine-Specific Cleavage,” Biochemistry, vol. 36, no. 28, pp. 8429–8434, Jul. 1997, doi: 10.1021/bi9709607.

[27] R. Desrosiers, K. Friderici, and F. Rottman, “Identification of Methylated Nucleosides in Messenger RNA from Novikoff Hepatoma Cells,” Proceedings of the National Academy of Sciences, vol. 71, no. 10, pp. 3971–3975, Oct. 1974, doi: 10.1073/pnas.71.10.3971.

[28] S. Schwartz et al., “Transcriptome-wide Mapping Reveals Widespread Dynamic-Regulated Pseudouridylation of ncRNA and mRNA,” Cell, vol. 159, no. 1, pp. 148–162, Sep. 2014, doi: 10.1016/j.cell.2014.08.028.

[29] C. L. Simms, B. H. Hudson, J. W. Mosior, A. S. Rangwala, and H. S. Zaher, “An Active Role for the Ribosome in Determining the Fate of Oxidized mRNA,” Cell Reports, vol. 9, no. 4, pp. 1256–1264, Nov. 2014, doi: 10.1016/j.celrep.2014.10.042.

[30] E. N. Thomas, K. Q. Kim, E. P. McHugh, T. Marcinkiewicz, and H. S. Zaher, “Alkylative damage of mRNA leads to ribosome stalling and rescue by trans translation in bacteria,” eLife, vol. 9, p. e61984, Sep. 2020, doi: 10.7554/eLife.61984.

[31] L. L. Yan and H. S. Zaher, “How do cells cope with RNA damage and its consequences?,” J. Biol. Chem., vol. 294, no. 41, pp. 15158–15171, Oct. 2019, doi: 10.1074/jbc.REV119.006513.

[32] X. Shan and C. G. Lin, “Quantification of oxidized RNAs in Alzheimer’s disease,” Neurobiology of Aging, vol. 27, no. 5, pp. 657–662, May 2006, doi: 10.1016/j.neurobiolaging.2005.03.022.

[33] Y. Chang et al., “Messenger RNA Oxidation Occurs Early in Disease Pathogenesis and Promotes Motor Neuron Degeneration in ALS,” PLOS ONE, vol. 3, no. 8, p. e2849, Aug. 2008, doi: 10.1371/journal.pone.0002849.

[34] I. A. Roundtree et al., “YTHDC1 mediates nuclear export of N6-methyladenosine methylated mRNAs,” eLife, vol. 6, p. e31311, Oct. 2017, doi: 10.7554/eLife.31311.

[35] X. Yang et al., “5-methylcytosine promotes mRNA export - NSUN2 as the methyltransferase and ALYREF as an m5C reader,” Cell Res., vol. 27, no. 5, pp. 606–625, May 2017, doi: 10.1038/cr.2017.55.

[36] G. Zheng et al., “ALKBH5 Is a Mammalian RNA Demethylase that Impacts RNA Metabolism and Mouse Fertility,” Molecular Cell, vol. 49, no. 1, pp. 18–29, Jan. 2013, doi: 10.1016/j.molcel.2012.10.015.

[37] D. Dominissini and G. Rechavi, “N4-acetylation of Cytidine in mRNA by NAT10 Regulates Stability and Translation,” Cell, vol. 175, no. 7, pp. 1725–1727, Dec. 2018, doi: 10.1016/j.cell.2018.11.037.

[38] X. Wang et al., “N6-methyladenosine-dependent regulation of messenger RNA stability,” Nature, vol. 505, no. 7481, pp. 117–120, Jan. 2014, doi: 10.1038/nature12730.

[39] Y. Wang, Y. Li, J. I. Toth, M. D. Petroski, Z. Zhang, and J. C. Zhao, “N6-methyladenosine modification destabilizes developmental regulators in embryonic stem cells,” Nat Cell Biol, vol. 16, no. 2, Art. no. 2, Feb. 2014, doi: 10.1038/ncb2902.

[40] D. E. Eyler et al., “Pseudouridinylation of mRNA coding sequences alters translation,” PNAS, vol. 116, no. 46, pp. 23068–23074, Nov. 2019, doi: 10.1073/pnas.1821754116.

[41] T. P. Hoernes et al., “Nucleotide modifications within bacterial messenger RNAs regulate their translation and are able to rewire the genetic code,” Nucleic Acids Research, vol. 44, no. 2, pp. 852–862, Jan. 2016, doi: 10.1093/nar/gkv1182.

[42] K. D. Meyer et al., “5′ UTR m6A Promotes Cap-Independent Translation,” Cell, vol. 163, no. 4, pp. 999–1010, Nov. 2015, doi: 10.1016/j.cell.2015.10.012.

[43] J. Zhou, J. Wan, X. Gao, X. Zhang, S. R. Jaffrey, and S.-B. Qian, “Dynamic m6A mRNA methylation directs translational control of heat shock response,” Nature, vol. 526, no. 7574, pp. 591–594, Oct. 2015, doi: 10.1038/nature15377.

[44] X. Lin et al., “RNA m6A methylation regulates the epithelial mesenchymal transition of cancer cells and translation of Snail,” Nat Commun, vol. 10, p. 2065, May 2019, doi: 10.1038/s41467-019-09865-9.

[45] D. F. De Jesus et al., “m 6 A mRNA methylation regulates human β-cell biology in physiological states and in type 2 diabetes,” Nature Metabolism, vol. 1, no. 8, pp. 765–774, Aug. 2019, doi: 10.1038/s42255-019-0089-9.

[46] Y. Zhang, B. R. Fonslow, B. Shan, M.-C. Baek, and J. R. Yates, “Protein Analysis by Shotgun/Bottom-up Proteomics,” Chem. Rev., vol. 113, no. 4, pp. 2343–2394, Apr. 2013, doi: 10.1021/cr3003533.

[47] H. Grosjean, L. Droogmans, M. Roovers, and G. Keith, “Detection of Enzymatic Activity of Transfer RNA Modification Enzymes Using Radiolabeled tRNA Substrates,” in Methods in Enzymology, vol. 425, Academic Press, 2007, pp. 55–101. doi: 10.1016/S0076-6879(07)25003-7.

[48] C. W. Gehrke and K. C. Kuo, “Ribonucleoside analysis by reversed-phase high-performance liquid chromatography,” Journal of Chromatography A, vol. 471, pp. 3–36, Jun. 1989, doi: 10.1016/S0021-9673(00)94152-9.

[49] M. Buck, M. Connick, and B. N. Ames, “Complete analysis of tRNA-modified nucleosides by high-performance liquid chromatography: The 29 modified nucleosides of Salmonella typhimurium and *Escherichia coli* tRNA,” Analytical Biochemistry, vol. 129, no. 1, pp. 1–13, Feb. 1983, doi: 10.1016/0003-2697(83)90044-1.

[50] M. Basanta-Sanchez, S. Temple, S. A. Ansari, A. D’Amico, and P. F. Agris, “Attomole quantification and global profile of RNA modifications: Epitranscriptome of human neural stem cells,” Nucleic Acids Res, vol. 44, no. 3, p. e26, Feb. 2016, doi: 10.1093/nar/gkv971.

[51] C. T. Y. Chan, M. Dyavaiah, M. S. DeMott, K. Taghizadeh, P. C. Dedon, and T. J. Begley, “A Quantitative Systems Approach Reveals Dynamic Control of tRNA Modifications during Cellular Stress,” PLoS Genet, vol. 6, no. 12, p. e1001247, Dec. 2010, doi: 10.1371/journal.pgen.1001247.

[52] D. Su et al., “Quantitative analysis of tRNA modifications by HPLC-coupled mass spectrometry,” Nat Protoc, vol. 9, no. 4, pp. 828–841, Apr. 2014, doi: 10.1038/nprot.2014.047.

[53] M. Heiss, F. Hagelskamp, V. Marchand, Y. Motorin, and S. Kellner, “Cell culture NAIL-MS allows insight into human tRNA and rRNA modification dynamics in vivo,” Nature Communications, vol. 12, no. 1, Art. no. 1, Jan. 2021, doi: 10.1038/s41467-020-20576-4.

[54] V. F. Reichle, S. Kaiser, M. Heiss, F. Hagelskamp, K. Borland, and S. Kellner, “Surpassing limits of static RNA modification analysis with dynamic NAIL-MS,” Methods, vol. 156, pp. 91–101, Mar. 2019, doi: 10.1016/j.ymeth.2018.10.025.

[55] K. D. Clark, C. Lee, R. Gillette, and J. V. Sweedler, “Characterization of Neuronal RNA Modifications during Non-associative Learning in Aplysia Reveals Key Roles for tRNAs in Behavioral Sensitization,” ACS Cent. Sci., vol. 7, no. 7, pp. 1183–1190, Jul. 2021, doi: 10.1021/acscentsci.1c00351.

[56] K. D. Clark, S. S. Rubakhin, and J. V. Sweedler, “Single-Neuron RNA Modification Analysis by Mass Spectrometry: Characterizing RNA Modification Patterns and Dynamics with Single-Cell Resolution,” Anal. Chem., vol. 93, no. 43, pp. 14537–14544, Nov. 2021, doi: 10.1021/acs.analchem.1c03507.

[57] Y. Motorin and M. Helm, “Methods for RNA Modification Mapping Using Deep Sequencing: Established and New Emerging Technologies,” Genes, vol. 10, no. 1, p. 35, Jan. 2019.

[58] W. V. Gilbert, T. A. Bell, and C. Schaening, “Messenger RNA modifications: Form, distribution, and function,” Science, vol. 352, no. 6292, pp. 1408–1412, Jun. 2016, doi: 10.1126/science.aad8711.

[59] M. Helm and Y. Motorin, “Detecting RNA modifications in the epitranscriptome: predict and validate,” Nat Rev Genet, vol. 18, no. 5, Art. no. 5, May 2017, doi: 10.1038/nrg.2016.169.

[60] S. Zaccara, R. J. Ries, and S. R. Jaffrey, “Reading, writing and erasing mRNA methylation,” Nat Rev Mol Cell Biol, vol. 20, pp. 608–624, Sep. 2019, doi: 10.1038/s41580-019-0168-5.

[61] S. Schwartz and Y. Motorin, “Next-generation sequencing technologies for detection of modified nucleotides in RNAs,” RNA Biol, vol. 14, no. 9, pp. 1124–1137, Oct. 2016, doi: 10.1080/15476286.2016.1251543.

[62] S. Thalalla Gamage, A. Sas-Chen, S. Schwartz, and J. L. Meier, “Quantitative nucleotide resolution profiling of RNA cytidine acetylation by ac4C-seq,” Nature Protocols, vol. 16, no. 4, Art. no. 4, Apr. 2021, doi: 10.1038/s41596-021-00501-9.

[63] A. V. Grozhik and S. R. Jaffrey, “Distinguishing RNA modifications from noise in epitranscriptome maps,” Nature Chemical Biology, vol. 14, no. 3, pp. 215–225, Feb. 2018, doi: 10.1038/nchembio.2546.

[64] Y. Wang et al., “Single-Base Resolution Mapping Reveals Distinct 5-Formylcytidine in *Saccharomyces cerevisiae* mRNAs,” ACS Chem. Biol., vol. 17, no. 1, pp. 77–84, Nov. 2021, doi: 10.1021/acschembio.1c00633.

[65] J. Cui, Q. Liu, E. Sendinc, Y. Shi, and R. I. Gregory, “Nucleotide resolution profiling of m3C RNA modification by HAC-seq,” Nucleic Acids Research, vol. 49, no. 5, p. e27, Mar. 2021, doi: 10.1093/nar/gkaa1186.

[66] V. Khoddami, A. Yerra, T. L. Mosbruger, A. M. Fleming, C. J. Burrows, and B. R. Cairns, “Transcriptome-wide profiling of multiple RNA modifications simultaneously at single-base resolution,” PNAS, vol. 116, no. 14, pp. 6784–6789, Apr. 2019, doi: 10.1073/pnas.1817334116.

[67] S. Kellner et al., “Profiling of RNA modifications by multiplexed stable isotope labelling,” Chem. Commun., vol. 50, no. 26, pp. 3516–3518, Mar. 2014, doi: c.

[68] S. P. Russell and P. A. Limbach, “Evaluating the reproducibility of quantifying modified nucleosides from ribonucleic acids by LC–UV–MS,” Journal of Chromatography B, vol. 923–924, pp. 74–82, Apr. 2013, doi: 10.1016/j.jchromb.2013.02.010.

[69] Y. Feng et al., “Chemical labeling – Assisted mass spectrometry analysis for sensitive detection of cytidine dual modifications in RNA of mammals,” Analytica Chimica Acta, vol. 1098, pp. 56–65, Feb. 2020, doi: 10.1016/j.aca.2019.11.016.

[70] Y. Dai et al., “Sensitive and Simultaneous Determination of Uridine Thiolation and Hydroxylation Modifications in Eukaryotic RNA by Derivatization Coupled with Mass Spectrometry Analysis,” Anal. Chem., vol. 93, no. 18, pp. 6938–6946, May 2021, doi: 10.1021/acs.analchem.0c04630.

[71] Y. Xie, K. A. Janssen, A. Scacchetti, R. Bonasio, and B. A. Garcia, “Permethylation of ribonucleosides provides enhanced mass spectrometry quantification of post-transcriptional modifications,” bioRxiv, 2022, doi: 10.1101/2022.01.26.477959.

[72] P. Song, O. S. Mabrouk, N. D. Hershey, and R. T. Kennedy, “In Vivo Neurochemical Monitoring Using Benzoyl Chloride Derivatization and Liquid Chromatography–Mass Spectrometry,” Anal. Chem., vol. 84, no. 1, pp. 412–419, Jan. 2012, doi: 10.1021/ac202794q.

[73] J.-M. T. Wong, P. A. Malec, O. S. Mabrouk, J. Ro, M. Dus, and R. T. Kennedy, “Benzoyl chloride derivatization with liquid chromatography–mass spectrometry for targeted metabolomics of neurochemicals in biological samples,” Journal of Chromatography A, vol. 1446, pp. 78–90, May 2016, doi: 10.1016/j.chroma.2016.04.006.

[74] S. R. Wilson, T. Vehus, H. S. Berg, and E. Lundanes, “Nano-LC in proteomics: recent advances and approaches,” Bioanalysis, vol. 7, no. 14, pp. 1799–1815, 2015, doi: 10.4155/bio.15.92.

[75] L. P. Sarin et al., “Nano LC-MS using capillary columns enables accurate quantification of modified ribonucleosides at low femtomol levels,” RNA, vol. 24, no. 10, pp. 1403–1417, Jul. 2018, doi: 10.1261/rna.065482.117.

[76] L. Fu, N. J. Amato, P. Wang, S. J. McGowan, L. J. Niedernhofer, and Y. Wang, “Simultaneous Quantification of Methylated Cytidine and Adenosine in Cellular and Tissue RNA by Nano-Flow Liquid Chromatography–Tandem Mass Spectrometry Coupled with the Stable Isotope-Dilution Method,” Anal. Chem., vol. 87, no. 15, pp. 7653–7659, Aug. 2015, doi: 10.1021/acs.analchem.5b00951.

[77] D. Dominissini et al., “The dynamic N1-methyladenosine methylome in eukaryotic messenger RNA,” Nature, vol. 530, no. 7591, pp. 441–446, Feb. 2016, doi: 10.1038/nature16998.

[78] X. Li et al., “Chemical pulldown reveals dynamic pseudouridylation of the mammalian transcriptome,” Nature Chemical Biology, vol. 11, no. 8, pp. 592–597, Aug. 2015, doi: 10.1038/nchembio.1836.

[79] C. Legrand et al., “Statistically robust methylation calling for whole-transcriptome bisulfite sequencing reveals distinct methylation patterns for mouse RNAs,” Genome Res., vol. 27, no. 9, pp. 1589–1596, Sep. 2017, doi: 10.1101/gr.210666.116.

[80] M.-Y. Cheng, W.-B. Tao, B.-F. Yuan, and Y.-Q. Feng, “Methods for isolation of messenger RNA from biological samples,” Anal. Methods, vol. 13, pp. 289–298, 2021, doi: 10.1039/D0AY01912G.

[81] Agilent Technologies, Inc, “Agilent RNA Kits for the Agilent 2100 Bioanalyzer System,” Agilent Technologies, Inc, Feb. 01, 2019. https://www.agilent.com/cs/library/datasheets/public/datasheet-rna-kits-bioanalyzer-5991-7891en-agilent.pdf

[82] A. Behrens, G. Rodschinka, and D. D. Nedialkova, “High-resolution quantitative profiling of tRNA abundance and modification status in eukaryotes by mim-tRNAseq,” Molecular Cell, vol. 81, no. 8, pp. 1802-1815.e7, Apr. 2021, doi: 10.1016/j.molcel.2021.01.028.

[83] B. Chen, B.-F. Yuan, and Y.-Q. Feng, “Analytical Methods for Deciphering RNA Modifications,” Anal. Chem., vol. 91, no. 1, pp. 743–756, Jan. 2019, doi: 10.1021/acs.analchem.8b04078.

[84] S. M. Huber et al., “Formation and Abundance of 5-Hydroxymethylcytosine in RNA,” ChemBioChem, vol. 16, no. 5, pp. 752–755, 2015, doi: 10.1002/cbic.201500013.

[85] S. Laxman et al., “Sulfur Amino Acids Regulate Translational Capacity and Metabolic Homeostasis through Modulation of tRNA Thiolation,” Cell, vol. 154, no. 2, pp. 416–429, Jul. 2013, doi: 10.1016/j.cell.2013.06.043.

[86] C. Chen, B. Huang, M. Eliasson, P. Rydén, and A. S. Byström, “Elongator Complex Influences Telomeric Gene Silencing and DNA Damage Response by Its Role in Wobble Uridine tRNA Modification,” PLOS Genetics, vol. 7, no. 9, p. e1002258, Sep. 2011, doi: 10.1371/journal.pgen.1002258.

[87] N. Shigi, “Biosynthesis and functions of sulfur modifications in tRNA,” Front Genet, vol. 5, p. 67, Apr. 2014, doi: 10.3389/fgene.2014.00067.

[88] J. Mouaikel, C. Verheggen, E. Bertrand, J. Tazi, and R. Bordonné, “Hypermethylation of the Cap Structure of Both Yeast snRNAs and snoRNAs Requires a Conserved Methyltransferase that Is Localized to the Nucleolus,” Molecular Cell, vol. 9, no. 4, pp. 891–901, Apr. 2002, doi: 10.1016/S1097-2765(02)00484-7.

[89] J. Mouaikel, J. M. Bujnicki, J. Tazi, and R. Bordonné, “Sequence–structure–function relationships of Tgs1, the yeast snRNA/snoRNA cap hypermethylase,” Nucleic Acids Res, vol. 31, no. 16, pp. 4899–4909, Aug. 2003.

[90] S. Hausmann and S. Shuman, “Specificity and Mechanism of RNA Cap Guanine-N2 Methyltransferase (Tgs1),” Journal of Biological Chemistry, vol. 280, no. 6, pp. 4021–4024, Feb. 2005, doi: 10.1074/jbc.C400554200.

[91] J.-M. Carter et al., “FICC-Seq: a method for enzyme-specified profiling of methyl-5-uridine in cellular RNA,” Nucleic Acids Res, vol. 47, no. 19, p. e113, Nov. 2019, doi: 10.1093/nar/gkz658.

[92] J. Yang, S. Sharma, P. Watzinger, J. D. Hartmann, P. Kötter, and K.-D. Entian, “Mapping of Complete Set of Ribose and Base Modifications of Yeast rRNA by RP-HPLC and Mung Bean Nuclease Assay,” PLOS ONE, vol. 11, no. 12, p. e0168873, Dec. 2016, doi: 10.1371/journal.pone.0168873.

[93] D. J. Ashworth, W. M. Baird, C.-J. Chang, J. D. Ciupek, K. L. Busch, and R. G. Cooks, “Chemical modification of nucleic acids. Methylation of calf thymus DNA investigated by mass spectrometry and liquid chromatography,” Biomedical Mass Spectrometry, vol. 12, no. 7, pp. 309–318, 1985, doi: https://doi.org/10.1002/bms.1200120703.

[94] C.-J. Chang and C.-G. Lee, “Chemical modification of ribonucleic acid. A direct study by carbon-13 nuclear magnetic resonance spectroscopy,” Biochemistry, vol. 20, no. 9, pp. 2657–2661, Apr. 1981, doi: 10.1021/bi00512a046.

[95] C. J. Chang, J. D. Gomes, and S. R. Byrn, “Chemical modification of deoxyribonucleic acids: a direct study by carbon-13 nuclear magnetic resonance spectroscopy,” J. Org. Chem., vol. 48, no. 26, pp. 5151–5160, Dec. 1983, doi: 10.1021/jo00174a002.

[96] J. C. Delaney and J. M. Essigmann, “Mutagenesis, genotoxicity, and repair of 1-methyladenine, 3-alkylcytosines, 1-methylguanine, and 3-methylthymine in alkB *Escherichia coli*,” PNAS, vol. 101, no. 39, pp. 14051–14056, Sep. 2004, doi: 10.1073/pnas.0403489101.

[97] P. Ø. Falnes, “Repair of 3-methylthymine and 1-methylguanine lesions by bacterial and human AlkB proteins,” Nucleic Acids Research, vol. 32, no. 21, pp. 6260–6267, Nov. 2004, doi: 10.1093/nar/gkh964.

[98] P. J. Holland and T. Hollis, “Structural and Mutational Analysis of *Escherichia coli* AlkB Provides Insight into Substrate Specificity and DNA Damage Searching,” PLOS ONE, vol. 5, no. 1, p. e8680, Jan. 2010, doi: 10.1371/journal.pone.0008680.

[99] J. O. Kang, “Methylated Purine Bases in Hepatic and Colonic RNA of Rats Treated with 1,2-Dimethylhydrazine,” Biochemical Medicine and Metabolic Biology, vol. 53, no. 1, pp. 52–57, Oct. 1994, doi: 10.1006/bmmb.1994.1057.

[100] G. A. Khoury, R. C. Baliban, and C. A. Floudas, “Proteome-wide post-translational modification statistics: frequency analysis and curation of the swiss-prot database,” Sci Rep, vol. 1, no. 1, Art. no. 1, Sep. 2011, doi: 10.1038/srep00090.

[101] E. Bieberich, “Synthesis, Processing, and Function of N-glycans in N-glycoproteins,” in Glycobiology of the Nervous System, R. K. Yu and C.-L. Schengrund, Eds. New York, NY: Springer, 2014, pp. 47–70. doi: 10.1007/978-1-4939-1154-7_3.

[102] H. H. Wandall, M. A. I. Nielsen, S. King-Smith, N. de Haan, and I. Bagdonaite, “Global functions of O-glycosylation: promises and challenges in O-glycobiology,” The FEBS Journal, vol. 288, no. 24, pp. 7183–7212, 2021, doi: 10.1111/febs.16148.

[103] C. Reily, T. J. Stewart, M. B. Renfrow, and J. Novak, “Glycosylation in health and disease,” Nat Rev Nephrol, vol. 15, no. 6, Art. no. 6, Jun. 2019, doi: 10.1038/s41581-019-0129-4.

[104] Y. Fan et al., “Heterogeneity of Stop Codon Readthrough in Single Bacterial Cells and Implications for Population Fitness,” Molecular Cell, vol. 67, no. 5, pp. 826-836.e5, Sep. 2017, doi: 10.1016/j.molcel.2017.07.010.

[105] Y. Fan, J. Wu, M. H. Ung, N. De Lay, C. Cheng, and J. Ling, “Protein mistranslation protects bacteria against oxidative stress,” Nucleic Acids Research, vol. 43, no. 3, pp. 1740–1748, Feb. 2015, doi: 10.1093/nar/gku1404.

[106] T. Pan, “Modifications and functional genomics of human transfer RNA,” Cell Research, vol. 28, no. 4, Art. no. 4, Apr. 2018, doi: 10.1038/s41422-018-0013-y.

[107] E. M. Phizicky and A. K. Hopper, “tRNA processing, modification, and subcellular dynamics: past, present, and future,” RNA, vol. 21, no. 4, pp. 483–485, Apr. 2015, doi: 10.1261/rna.049932.115.

[108] N. Ranjan and M. V. Rodnina, “Thio-Modification of tRNA at the Wobble Position as Regulator of the Kinetics of Decoding and Translocation on the Ribosome,” J. Am. Chem. Soc., vol. 139, no. 16, pp. 5857–5864, Apr. 2017, doi: 10.1021/jacs.7b00727.

[109] M. H. Schwartz and T. Pan, “Temperature dependent mistranslation in a hyperthermophile adapts proteins to lower temperatures,” Nucleic Acids Research, vol. 44, no. 1, pp. 294–303, Jan. 2016, doi: 10.1093/nar/gkv1379.

[110] J. Choi et al., “N(6)-methyladenosine in mRNA disrupts tRNA selection and translation-elongation dynamics,” Nat. Struct. Mol. Biol., vol. 23, no. 2, pp. 110–115, Feb. 2016, doi: 10.1038/nsmb.3148.

[111] J. Choi et al., “2′- O -methylation in mRNA disrupts tRNA decoding during translation elongation,” Nature Structural & Molecular Biology, vol. 25, no. 3, Art. no. 3, Mar. 2018, doi: 10.1038/s41594-018-0030-z.

[112] T. P. Hoernes et al., “Atomic mutagenesis of stop codon nucleotides reveals the chemical prerequisites for release factor-mediated peptide release,” PNAS, vol. 115, no. 3, pp. E382–E389, Jan. 2018, doi: 10.1073/pnas.1714554115.

[113] T. P. Hoernes et al., “Eukaryotic Translation Elongation is Modulated by Single Natural Nucleotide Derivatives in the Coding Sequences of mRNAs,” Genes, vol. 10, no. 2, Art. no. 2, Feb. 2019, doi: 10.3390/genes10020084.

[114] B. H. Hudson and H. S. Zaher, “O6-Methylguanosine leads to position-dependent effects on ribosome speed and fidelity,” RNA, vol. 21, no. 9, pp. 1648–1659, Sep. 2015, doi: 10.1261/rna.052464.115.

[115] C. You, X. Dai, and Y. Wang, “Position-dependent effects of regioisomeric methylated adenine and guanine ribonucleosides on translation,” Nucleic Acids Research, vol. 45, no. 15, pp. 9059–9067, Sep. 2017, doi: 10.1093/nar/gkx515.

[116] Z. Shen, W. Wu, and S. L. Hazen, “Activated Leukocytes Oxidatively Damage DNA, RNA, and the Nucleotide Pool through Halide-Dependent Formation of Hydroxyl Radical,” Biochemistry, vol. 39, no. 18, pp. 5474–5482, May 2000, doi: 10.1021/bi992809y.

[117] T. E. Dever, J. D. Dinman, and R. Green, “Translation Elongation and Recoding in Eukaryotes,” Cold Spring Harb Perspect Biol, vol. 10, no. 8, p. a032649, Aug. 2018, doi: 10.1101/cshperspect.a032649.

[118] E. N. Thomas, C. L. Simms, H. E. Keedy, and H. S. Zaher, “Insights into the base-pairing preferences of 8-oxoguanosine on the ribosome,” Nucleic Acids Research, vol. 47, no. 18, pp. 9857–9870, Oct. 2019, doi: 10.1093/nar/gkz701.

[119] B. Slobodin et al., “Transcription Impacts the Efficiency of mRNA Translation via Co-transcriptional N6-adenosine Methylation,” Cell, vol. 169, no. 2, pp. 326-337.e12, 06 2017, doi: 10.1016/j.cell.2017.03.031.

[120] L. L. Yan, C. L. Simms, F. McLoughlin, R. D. Vierstra, and H. S. Zaher, “Oxidation and alkylation stresses activate ribosome-quality control,” Nat Commun, vol. 10, no. 1, Art. no. 1, Dec. 2019, doi: 10.1038/s41467-019-13579-3.

[121] O. Levi and Y. S. Arava, “Pseudouridine-mediated translation control of mRNA by methionine aminoacyl tRNA synthetase,” Nucleic Acids Research, vol. 49, no. 1, pp. 432–443, Jan. 2021, doi: 10.1093/nar/gkaa1178.

[122] T. P. Hoernes et al., “Translation of non-standard codon nucleotides reveals minimal requirements for codon-anticodon interactions,” Nat Commun, vol. 9, p. 4865, Nov. 2018, doi: 10.1038/s41467-018-07321-8.

[123] K. Licht, M. Hartl, F. Amman, D. Anrather, M. P. Janisiw, and M. F. Jantsch, “Inosine induces context-dependent recoding and translational stalling,” Nucleic Acids Res, vol. 47, no. 1, pp. 3–14, Jan. 2019, doi: 10.1093/nar/gky1163.

[124] M. K. Franco and K. S. Koutmou, “Chemical modifications to mRNA nucleobases impact translation elongation and termination,” Biophysical Chemistry, vol. 285, p. 106780, Jun. 2022, doi: 10.1016/j.bpc.2022.106780.

[125] M. K. Purchal et al., “Pseudouridine synthase 7 is an opportunistic enzyme that binds and modifies substrates with diverse sequences and structures,” Proceedings of the National Academy of Sciences, vol. 119, no. 4, p. e2109708119, Jan. 2022, doi: 10.1073/pnas.2109708119.

[126] R. Rauscher and Z. Ignatova, “Timing during translation matters: synonymous mutations in human pathologies influence protein folding and function,” Biochemical Society Transactions, vol. 46, no. 4, pp. 937–944, Jul. 2018, doi: 10.1042/BST20170422.

[127] A. Re, T. Joshi, E. Kulberkyte, Q. Morris, and C. T. Workman, “RNA–Protein Interactions: An Overview,” in RNA Sequence, Structure, and Function: Computational and Bioinformatic Methods, J. Gorodkin and W. L. Ruzzo, Eds. Totowa, NJ: Humana Press, 2014, pp. 491–521. doi: 10.1007/978-1-62703-709-9_23.

[128] M. E. Schmitt, T. A. Brown, and B. L. Trumpower, “A rapid and simple method for preparation of RNA from *Saccharomyces cerevisiae*.,” Nucleic Acids Res, vol. 18, no. 10, pp. 3091–3092, May 1990.

[129] S. Andrews, “FastQC: a quality control tool for high throughput sequence data,” 2010. https://www.bioinformatics.babraham.ac.uk/projects/fastqc/ (accessed May 27, 2021).

[130] M. Martin, “Cutadapt removes adapter sequences from high-throughput sequencing reads,” EMBnet.journal, vol. 17, no. 1, Art. no. 1, May 2011, doi: 10.14806/ej.17.1.200.

[131] B. Langmead and S. L. Salzberg, “Fast gapped-read alignment with Bowtie 2,” Nature Methods, vol. 9, no. 4, Art. no. 4, Apr. 2012, doi: 10.1038/nmeth.1923.

[132] M. Zytnicki, “mmquant: how to count multi-mapping reads?,” BMC Bioinformatics, vol. 18, no. 1, p. 411, Sep. 2017, doi: 10.1186/s12859-017-1816-4.

[133] M. T. Marty, A. J. Baldwin, E. G. Marklund, G. K. A. Hochberg, J. L. P. Benesch, and C. V. Robinson, “Bayesian Deconvolution of Mass and Ion Mobility Spectra: From Binary Interactions to Polydisperse Ensembles,” Anal. Chem., vol. 87, no. 8, pp. 4370–4376, Apr. 2015, doi: 10.1021/acs.analchem.5b00140.

[134] J. G. Monroe, T. J. Smith, and K. S. Koutmou, “Chapter Sixteen - Investigating the consequences of mRNA modifications on protein synthesis using in vitro translation assays,” in Methods in Enzymology, vol. 658, J. E. Jackman, Ed. Academic Press, 2021, pp. 379–406. doi: 10.1016/bs.mie.2021.06.011.

Chapter 5 Modulation of tRNA Modification Landscape Alters the Efficacy of Hygromycin B Translation Inhibition[5]

Monika K Franco[1], Joshua D Jones[2], Tyler J. Smith[2], Mehmet Tardu[2], Laura R Snyder[2], Robert T Kennedy[2]*, Kristin S Koutmou[1,2]*

[1]University of Michigan Program in Chemical Biology. [2]University of Michigan, Department of Chemistry.

* Corresponding authors

5.1 Introduction

Post-transcriptional modifications to RNA impact the structure, function, stability and dynamics of cellular RNAs. Thus, it is unsurprising that the dysregulation of RNA modifications is linked to a myriad of pathologies including diabetes, neurological disorders, and many cancers

[5] In the work presented in this chapter I served as a secondary writer, editor, and motivator for the experiments and validation. I provided much of the intellectual discourse surrounding Hygromycin B's effect on translation in the absence or presence of $tRNA^{Phe}$ modifications (namely m^5U) and how modification landscape is dynamic during stress. In addition, I assisted in translation assays for tripeptide synthesis (translocation) and amino acid addition in the presence of m^5U on $tRNA^{Phe}$ in conjunction with Monika Franco. The briefly summarized work of other authors are as follows:
- Monika Franco served as the primary investigator (and whom I assisted) in the translation studies for $tRNA^{Phe}$ species containing or missing m^5U under Hygromycin stress. In addition, she was involved in experimental execution of yeast culture assays for wild-type and mutant Trm2 strains under stress conditions. She also served as the primary author and editor for this work.
- Joshua Jones was responsible for using the LC-MS/MS pipeline to asses modification landscape of $tRNA^{Phe}$ in this work. He was also involved in detecting m^5U levels under stress conditions. Finally, he served as a secondary author and editor.
- Mehmet Tardu was responsible for the experimental design and execution of yeast culture assays for wild-type and mutant Trm2 strains under stress conditions.
- Laura Snyder was responsible for construction growth curves of wildtype and Trm2 knockout yeast under various stress conditions.

[1]–[6]. To date, over 150 different ribonucleoside modifications have been reported over the last 50 years within all three kingdoms of life and all RNA species [7]. However, the precise contribution of only a modest subset of these modifications to discrete biological processes has been established. Here, we identify the affect that a prevalent non-coding RNA (ncRNA) modification, 5-methyluridine (m^5U), has under translational inhibition.

m^5U was originally discovered in 1963 and has since been detected in ncRNAs from all phylogenies and eukaryotic mRNAs [8]. Initial studies of m^5U in tRNAs revealed that it is incorporated into the T-loop of tRNAs by the conserved bacterial and eukaryotic enzyme tRNA (uracil-5-)-methyltransferase (Trm2), and more recent work has detected m^5U in eukaryotic rRNA and most recently the large subunit of bacterial and archaeon rRNAs [9]–[11], [12], [13]. In tRNAs, the tertiary interaction between the T-loop structural motif in tRNAs and the D-loop is known to play an important role in tRNA structure and stability, and the addition of m^5U54 into the T-loop is increases the stability of tRNAs [14]. However, m^5U does not significantly alter the hydrogen bonding pattern in the T-loop. Thus, it is not known whether this stabilizing effect comes from the presence of m^5U54 in the T-loop, however Trm2 and the *E. coli* homologue (TrmA) were found to act as a tRNA folding chaperones which could cause the stabilizing effect [15]. Despite this, the role of m^5U in tRNA and the enzymes that incorporate it have been difficult to define. When a tRMA enzyme is mutated to expunge methyltransferase activity, there were no observed changes in translation in vivo [16]. Nonetheless, cells containing uracil-5-methyltransferase outcompete those without [16], [17]. Additionally, m^5U54 is a highly conserved modification, which suggests that there is an evolutionary significance to the addition of this modifications. Despite its conservation and apparent contributions to tRNA structure, the

overall biological significance of the tRNA m^5U modification and its contributions (if any) to protein translation remains unclear.

Recently, modulation of tRNA modification landscapes has been implicated in the bacterial resistance to antibiotics [18]–[21]. For example, it has been reported that the 1-methylguanosine at the 37 position (m^1G37) methylation of tRNA helps produce strong gram-negative OM membrane proteins in *E. coli* and *salmonella* that promote multi drug resistance [21]. Thus, TrmD, the enzyme that catalyzes m^1G37 incorporation, has now become a target for drug development [19]. There are three targeted mechanisms of action that antibiotics typically take: (1) attacking the cell wall or membrane, (2) attacking the machinery that makes nucleic acids, (3) attacking the ribosome [22]. One example of an antibiotic that works by inhibiting translation is hygromycin B. Hygromycin b is part of the aminoglycoside family of translation inhibitors that works in both prokaryotic and eukaryotic systems. Although Hygromycin B is a widely used translation inhibitor for studying hygromycin resistant genes, as well as a tool for understanding the translation machinery, its mechanism of action is still not fully understood [23], [24]. It is known that hygromycin B strengthens tRNA binding to the A site, but the most important aspect is the ability for it to prevent translocation from occurring [16], [19]. What is particularly interesting about hygromycin B is that it does not need to be in the presence of elongation factors to function compared to other antibiotics in the same family. This highly suggests that its inhibitory actions are due to interactions with mRNA, tRNA and the ribosome itself [26]. There are no current studies that show aminoglycoside interaction with RNA modifications, or that RNA modifications impact translation inhibition by aminoglycosides.

In this work, we identified the first phenotype for tRNA (uracil-5-)-methyltransferase where yeast lacking the methyltransferase has altered cellular growth under translational

inhibition by aminoglycosides – hygromycin B, cycloheximide, and paromomycin. In particular, we see that *trm2*Δ yeast grow more efficiently and produce more protein than wildtype yeast under hygromycin B stress. Additionally, we find that the wildtype cells have increased m^5U levels under hygromycin B stress. Since hygromycin B inhibits protein synthesis by preventing the translocation of the tRNA, we sought to investigate how $tRNA^{Phe}$ purified from wildtype and *trmA*Δ cells affects amino acid addition and tripeptide synthesis using a well-established fully reconstituted *in vitro* translation system. In $tRNA^{Phe}$ purified from *trmA*Δ *E. coli*, we find that m^5U abundance is significantly decreased as expected; however, we see a significant increase in i^6A and decrease in acp^3U abundances in the *trmA*Δ $tRNA^{Phe}$. Interestingly, we observe a decrease in ms^2i^6A, which is located at A37 in the tRNA, suggesting that m^5U installation is tied to ms^2 installation across the tRNA. We found that the *trmA*Δ purified $tRNA^{Phe}$ does not alter amino acid addition or tripeptide synthesis compared to wildtype $tRNA^{Phe}$ using native conditions. However, in the presence of hygromycin B, *trmA*Δ purified $tRNA^{Phe}$ produces more tripeptide than wildtype $tRNA^{Phe}$. We find that hygromycin B interacts with the ms^2i^6A37 in the $tRNA^{Phe}$ based off a crystal structure, suggesting that ms^2 may be stabilizing the aminoglycoside in the A-site of the ribosome. These findings reveal that the removal of the hypermodification ms^2i^6A37, as observed in the *tRMAΔ* purified $tRNA^{Phe}$, may provide some antibiotic resistance by promoting translocation within the ribosome.

5.2 Results

5.2.1 Trm2 impacts cell growth under translational stress conditions

Despite being studied for over 50 years, the biological role of m^5U remains unclear. While bacterial and eukaryotic cells lacking uracil-5-methyltransferase do not exhibit a growth

defect under normal laboratory conditions [15], [17],cells possessing uracil-5-methyltransferase out compete those lacking the enzyme which suggests that m^5U is advantageous for cellular fitness [16], [17]. This is consequential from the dual function of Trm2 which catalyzes m^5U installation and acts as a tRNA folding chaperone [15]. Nonetheless, conditions under which these individual activities are important are still not known.

To better understand the biological function of Trm2 and m^5U incorporation, we sought to identify situations in which the enzyme impacts cell growth. We conducted spot plating assays with wildtype and *trm2*Δ cells to survey the impact of varying temperature (22ºC, 30ºC, 37ºC), carbon source (glucose, sucrose, galactose), pH (4.5, 6.8, 8.5), salt concentration (NaCl, $MgSO_4$), and proteasome (MG132) and translation inhibitors (hygromycin B, cycloheximide, puromycin, paromomycin) on cell growth (Supplemental Figure 1). Wildtype and *trm2*Δ grew similarly regardless of temperature, carbon source, pH, $MgSO_4$ concentration, or the presence of a proteasome inhibitor. Although the growth of *trm2*Δ cells was unchanged by MgSO4, we observed that deletion of Trm2 resulted in a modest growth enhancement over wildtype under 1 M NaCl salt stress condition. However, the largest effect was observed under the presence of three translation inhibitors: hygromycin B, cycloheximide and paromomycin. Relative to wildtype cells, *trm2*Δ cells were more sensitive cycloheximide, while they were less sensitive to hygromycin B and paromomycin treatment (Figure 1A). These findings were further supported in cellular growth curve assays under the same conditions, where *trm2*Δ grew more robustly in the presence of 1 M NaCl, 50 μg/mL hygromycin B, or 3 mg/mL paromomycin and worse in the presence of 0.1 μg/mL cycloheximide (Supplemental Figure 1). This is the first evidence that uracil-5-methyltransferase and m^5U play a significant biological role.

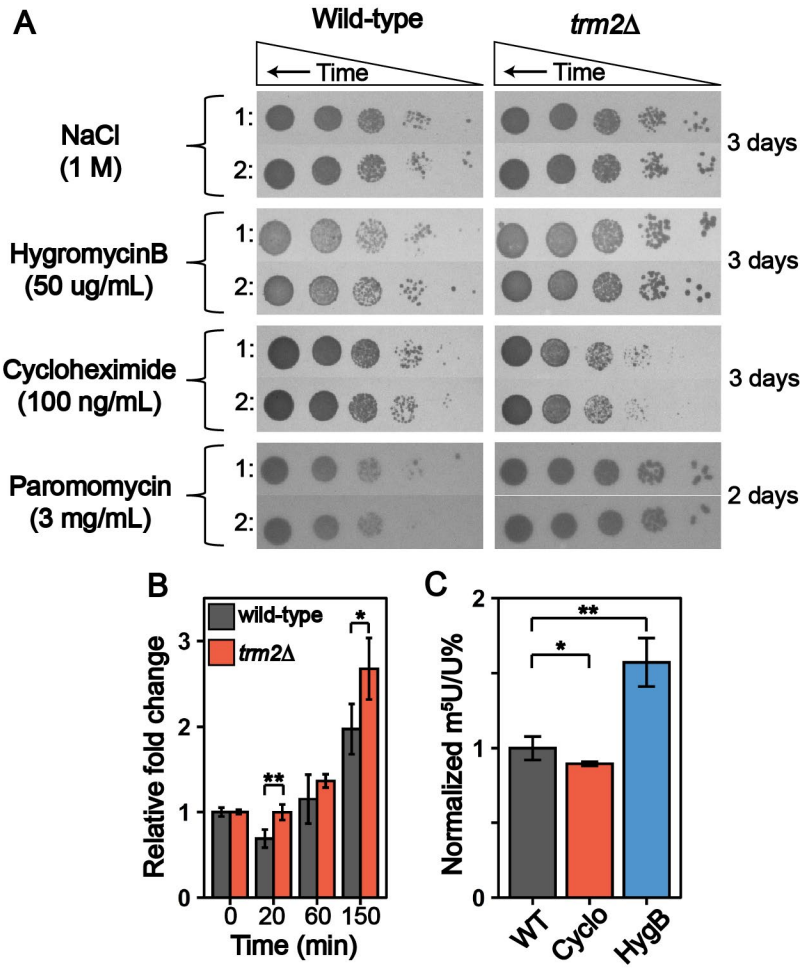

Figure 5.1 *Translational stress response modulated in trm2 KO cell lines.(A) Spot platting assays displaying The growth of trm2Δ was affected in the presence of three translation inhibitors: hygromycin B, cycloheximide, and paromomycin. (B) Luciferase reporter assasys shows that protein level significantly decreased in wild-type than trm2Δ after hygromycin B treatment. (C) m5U levels are higher under hygromycin b stress compared to WT conditions and Cycloheximide stress*

5.2.2 Trm2 influences reporter protein production in cells under translational stress conditions

The influence of the uracil-5-methyltransferase under translational stress cellular fitness could be resultant from altered protein production following the knockout. To investigate this, we tested how hygromycin B and cycloheximide affects protein production in wild-type and

*trm2*Δ cells transfected with luciferase mRNA transcript. Both transfected cell lines were grown to an OD_{600} of 0.5 prior to the Hygromycin B and cycloheximide stress, and the fluorescent intensity was recorded at multiple time points after the stress (0 min, 20 min, 60 min, 120 min). We found that luciferase protein level significantly increased in the *trm2*Δ cells compared to the wildtype after hygromycin B treatment (Figure 1B). Interestingly, we see a decrease in luciferase abundance 20 min following hygromycin B stress in the wild-type cells that is not present in the *trm2*Δ cells. This data corroborates that the presence of uracil-5-methyltransferase influences the impact of hygromycin B and cycloheximide treatment, and the alteration in *trm2*Δ cells cellular fitness could be resultant of altered protein product rates under stress. This further leads us to believe that uracil-5-methltransferase and/or m^5U modification impacts translation under translational inhibition.

5.2.3 m^5U levels in tRNAs fluctuate in response to translational stress

It is well documented that cells modulate RNA modification abundance in response to cellular stress or nutrition to alter their biological function. Accordantly, yeast tRNA m^5U abundance was previously shown to be altered under oxidative and alkylative stress [27]. Since m^5U addition by Trm2 displayed an impact under translational translocation stress, we tested how m^5U abundance is affected following hygromycin B and cycloheximide exposure using a previously reported UHPLC-MS/MS methodology [28]. The $m^5U/U\%$ levels of yeast total RNA were altered under both stress conditions where hygromycin B- and cycloheximide-stress resulted in an upregulation and downregulation of m^5U, respectively (Figure 1C and Supplemental Figure 2).

This alteration in $m^5U/U\%$ can come from multiple different factors – a change in total RNA distribution, altered stoichiometry of m^5U modified sites, or newly modified locations. While the tRNA:rRNA distribution does not drastically change following cycloheximide-stress when compared to the WT, the 18S rRNA expression is downregulated from approximately 20% of the total RNA electropherogram signal to approximately 16% (Supplemental Figures 3). This is consistent with a previous study that detected a decrease in mature 16S rRNA in *E. coli* following hygromycin B treatment [29]. Since m^5U is not present in *S. cerevisiae* rRNA and the bioanalyzer electropherogram signal > 200nt remains approximately 70% of the overall signal for all three conditions, this would not result in the large increase in m^5U signal we detect under this condition [7]. Additionally, since m^5U is present in almost all *S. cerevisiae* tRNA, it is unlikely that the altered m^5U signals detected under each antibiotic stress is coming from a change in individual tRNA abundance. Instead, we posit the altered abundance is arising from an altered stoichiometry of m^5U at position 54 or additional modification sites within the *S. cerevisiae* tRNA or rRNA. This suggests that m^5U enzymatic incorporation in tRNA plays an important role during translational inhibition by hygromycin B and cycloheximide.

Since the UHPLC-MS/MS assay we utilized can be multiplexed to detect up to 50 ribonucleosides in a single analysis, we also identified that translational inhibition affects the abundance of other total and mRNA modifications. Similar to m^5U, most total RNA modifications are upregulated following hygromycin treatment and downregulated following cycloheximide treatment (Supplemental figure 4). Contrarily, mRNA modifications are preferentially upregulated following treatment by both translational inhibitors (Supplemental figure 2). Messenger RNA was purified using a previously described three-stage purification pipeline, and the mRNA purity was confirmed using Bioanalyzer, RNA-seq, RT-qPCR, and LC-

MS/MS (Supplemental figures 2-5). While the total RNA modifications distribution remains similar following translational inhibition, small mRNA (~500 nt) is enriched following both hygromycin and cycloheximide treatment (Supplemental figure 3). Thus, the alteration in mRNA modification abundance could be resulting from a modulation in prevalence or even enrichment in highly modified mRNA transcripts. Nonetheless, this suggests that a multitude of these modifications are important for translation and adds an additional layer of evidence of the translational inhibitor mechanism of action. While we know how these translational inhibitors interact with the ribosome, this suggests that there are further downstream effects on the cellular biology which ultimately affects the translational machinery in more than one way.

5.2.4 trmAΔ changes the modification landscape of E. coli phenylalanine tRNA

Thus far, we identified that m^5U levels increase and *trm2*Δ cell lines grow more efficiently and produce more protein than wildtype cells under hygromycin B stress, while the opposite is true for cycloheximide stress. We posit these alterations could be resultant from the following factors: (1) altered amino acid addition rates under native conditions, (2) altered amino acid addition rates during translational stress, (3) altered ability for translocation to occur during the translational stress. Thus, we sought to use a well-established fully reconstituted *in vitro* translation system to interrogate these two phenomena. Within these assays, we can assess translation using *E. coli* $tRNA^{Phe}$ purified from either WT or *trmA*Δ cell lines. For tRNAs purified from *trmA*Δ cells we confirmed that m^5U was not included by a targeted ribonucleoside LC-MS/MS assay (Figure 2A). In these assays were screened over 51 nucleosides. During the same analysis, we surprisingly found a significant alteration in the overall modifications landscape of *E. coli* $tRNA^{Phe}$ when purified from *trmA*Δ cell lines. In the *trmA*Δ tRNA, we detected a significant upregulation of i^6A (~12-fold, Supplemental figure 2), which could be

resultant from the depletion of the hypermodification ms^2i^6A within the anticodon. The i6A abundance could be estimated to be approximately 0.8 modifications per the *trmA*Δ $tRNA^{Phe}$. The low abundance selenocysteine tRNA is the only *E. coli* tRNA that contains i6A within the tRNA and our $tRNA^{Phe}$ charging efficiency was approximately the same (700pmol/A260), so we posit that this change is coming from an altered $tRNA^{Phe}$ modification landscape. We also detected a moderate decrease in acp^3U in the *trmA*Δ $tRNA^{Phe}$ (~1.7-fold, Supplemental figure 2), a modification within the variable loop.

Our studies both confirmed that *trmA*Δ $tRNA^{Phe}$ lacks m^5U, and revealed that the lack of TrmA further alters the modifications landscape of $tRNA^{Phe}$, suggesting that cooperativity may exist between the modifying enzymes and the tRNA structure or current modification landscape. These findings highlight why it is so difficult to study the biological significance of RNA modifications because the removal of RNA modifying enzymes could have further downstream biological consequences. Nonetheless, these results provide a more comprehensive picture of the tRNA landscape, and we utilize this data along with *in vitro* translation assays to piece together why *E. coli trmA*Δ cell line displays a phenotype under translational inhibition.

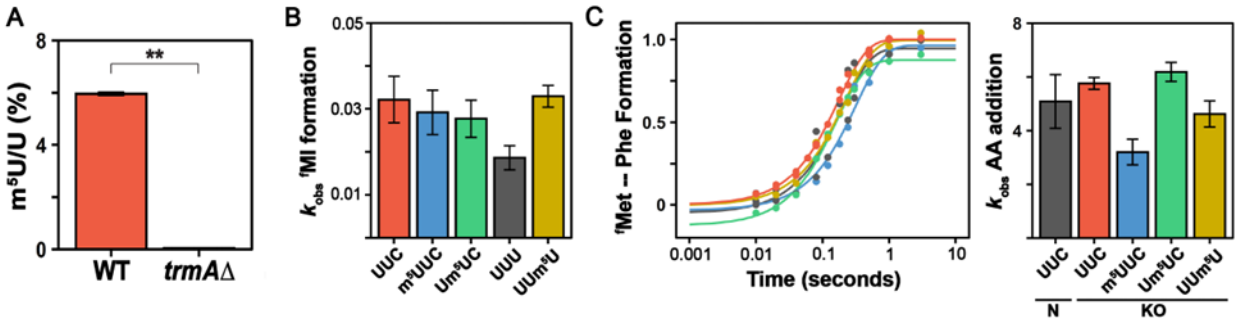

Figure 5.2 *m5U has a minor affect on translationin a position dependent manner in mRNA and no major observed affectt in tRNA. (A) LC-MS/MS analysis showing that our tRNAphe purified from trmA KO cells does not contain m5U modfications. (B) Bar graph showing the formation of misocded Met-Ile product. (C) Kobs Curves and bar plots showing observered rates constant for met-phe dipeptide formation using the KO tRNAphe.*

5.2.5 Translational fidelity is impacted on m^5U-containing codons in a position dependent manner

After successfully purifying our KO phenylalanine tRNA, and analyzing its modification landscape, we were able to perform translation assays using our *in vitro* reconstituted system to test our proposed hypothesis of the effect of m^5U on translation. In previously published work we assessed the impact of m^5U containing codons on translation rates using the same *in vitro* translation system. In our assays, 70S ribosome initiation complexes were formed on messages encoding Met-Phe peptides programmed with ^{35}S-^{f}Met-tRNA^{fmet} bound to AUG in the P site, and UUC or m5U in the 1st, 2nd, or 3rd position in the A site. Initiation complexes (140 nM) were reacted with Phe-tRNA^{Phe}•EF-Tu•GTP (ternary complex; 2uM) at 37^{o} C. These reactions were stopped at discrete time points with KOH, and the resulting products were visualized by electrophoretic TLC. We measured k_{obs} on UUU and UUC codons because the observed rate constants for Phe addition are well established. We observed that amino acid addition rates are impacted on m^5U-containing codons in a position dependent manner, with a 2-fold decrease in the k_{obs}. Following this observations, we were interested in whether or not this phenomenon would have an impact on translation fidelity when m^5U was present on a UUC codon. m^5U has a methyl group on the non-Watson face of the nucleotide and should not affect hydrogen bond base pairing. As previously described, we observed a modest 2-fold change in amino acid addition only at the 3rd position when m^5U is present, therefore we hypothesized fidelity would not be affect by the addition of m^5U on a codon. To investigate the difference between unmodified Phe codons and m^5U codons in regards to allow the addition of near-cognate amino acids, we chose Ile-tRNA^{Ile} which is a small aliphatic near cognate amino acids. To try and

obtain a kinetic understanding on how near-cognate amino acid addition is changing when m^5U is present, we performed kinetic assays with the near-cognate Ile-$tRNA^{Ile}$. These assays utilized an established regenerative mix[30] and contain EfTs. We observed that translation fidelity is slightly affected when m^5U is present at the 3rd position. (Figure 2B) This result is unsurprising due to the fact that we saw a rate defect in amino acid addition when m^5U was present in the 3rd position.

5.2.6 trmAΔ Phe tRNA does not alter amino acid addition

m^5U is one of the most abundant eukaryotic and bacterial modifications and m^5U is speculated to have an impact in tRNA structure, maturation, and thermal stability [14], [31], [32]. However, its impact regarding translation has not been studied. Since *trm2*Δ yeast displayed a growth phenotype and produces more protein than wildtype yeast under translational inhibition, we sought to determine whether m^5U54 in $tRNA^{Phe}$ affects amino acid addition under native conditions. We investigated this using a well-established fully reconstituted *in vitro* translation system where we input $tRNA^{Phe}$ purified from either *trmA*Δ or wildtype *E. coli*. Despite the tRNA changes in modification landscape that we observed in the *trmA*Δ purified $tRNA^{Phe}$, the rate constant for Phe incorporation on an unmodified UUC codon was comparable to wildtype purified $tRNA^{Phe}$ at a k_{obs} of ~ $5s^{-1}$ (Fig 2C). Therefore, we found that *trmAΔ* Phe tRNA does not affect the rate of amino acid addition and cannot explain the increased reported production in *trm2*Δ cells displayed previously.

Recently, m^5U was detected at low abundances in eukaryotic mRNA and reasoned that there could be a cooperative affect between m^5U containing mRNA codons and tRNA [28], [33]–[35.]Thus, we sought to interrogate how amino acid addition on m^5U-containing codons

(1st, 2nd, and 3rd position modified UUU or UUC codons) is affected when decoded by a *trmA*Δ $tRNA^{Phe}$ using the our fully reconstituted *in vitro* translation system. While the rate constants for amino acid was not impacted when m^5U was incorporated at 2nd and 3rd position modified codons, there was a small defect (~2-fold decrease at ~3 s^{-1}) when m^5U-deplete $tRNA^{Phe}$ translated an m^5UUC codon. We previously detected a 2-fold rate defect at the 3rd position modified codon with wildtype $tRNA^{Phe}$ (Figure 2C), which was not present with *trmA*Δ $tRNA^{Phe}$ [28]. This data collectively demonstrate that *trmA*Δ $tRNA^{Phe}$ does not significantly alter amino acid addition of both unmodified and modified codons under unstressed conditions.

5.2.7 trmAΔ $tRNA^{Phe}$ increases tripeptide synthesis under hygromycin B translation inhibition

Hygromycin B prevents translocation to block translation by interacting with the RNA species in the A site within the ribosome, resulting in the cessation of translation. While we that *trmA*Δ $tRNA^{Phe}$ does not alter amino acid addition, this does not interrogate whether this tRNA alters translocation. Thus, we utilized our *in vitro* translation system to synthesize a MFK tripeptide without the presence of hygromycin B. Under these conditions, we found that tripeptide synthesis was not significantly altered when *trmA*Δ $tRNA^{Phe}$ was used instead of wildtype $tRNA^{Phe}$. We found that the k_1 (^fM disappearance) was approximately 5.2 s^{-1} for both $tRNA^{Phe}$ species while the k_2 (^fMFK formation) was 0.34 s^{-1} and 0.19 s^{-1} for wildtype and *trmA*Δ $tRNA^{Phe}$, respectively (Figure 3. We found that *trmA*Δ $tRNA^{Phe}$ does not alter tripeptide synthesis and amino acid addition both unmodified and m^5U modified codons. This corroborates previous studies that did not detect a phenotype for cells lacking tRNA (uracil-5-)-methyltransferase.

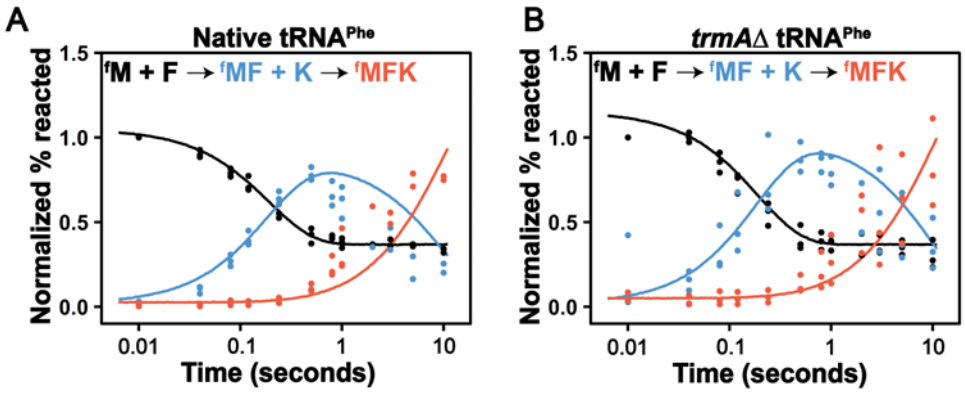

Figure 5.3 *Time courses displaying the formation of fMet-Phe-lys tripeptide on unmodified phenylalanine codons reacting with 1uM Phe+lLys TC complex using either Native phe tRNA and Native Lysine (left) or TrmA KO phe tRNA absent of m5U and Native Lysine. (right) All similuaiton aligned raw data with good fit, R2 then .9.*

In the presence of hygromycin B, *trm2*Δ yeast grow more efficiently and produced more protein (Figure 1). While we did not identify any significant differences in translation assays performed with wildtype and *trmA*Δ $tRNA^{Phe}$ under unstressed conditions, we posited that the presence of hygromycin B would Reveal if there are differences in translocation using both tRNA species. We investigated this by synthesizing the same ^{f}MFK peptide described above, but hygromycin B was included in the reaction mix to inhibit protein synthesis. Since hygromycin B inhibits translation by preventing translocation, we theorized that any differences would be resultant from the ^{f}MFK peptide formation since ^{f}MF formation does not require translocation in the ribosome. While overall tripeptide synthesis was slower using both wildtype and *trmA*Δ $tRNA^{Phe}$, the formation of the ^{f}MF dipeptide was still rapid, as expected because hygromycin should exhibit an effect after the first peptide bond is formed (Figure 4). However, we find that tripeptide synthesis is greatly increased with *trmA*Δ $tRNA^{Phe}$ compared to wildtype (Figure 4). This result is consistent with our observation that *trm2*Δ yeast cells produce more protein than wildtype cells in the presence of hygromycin B (Figure 1).

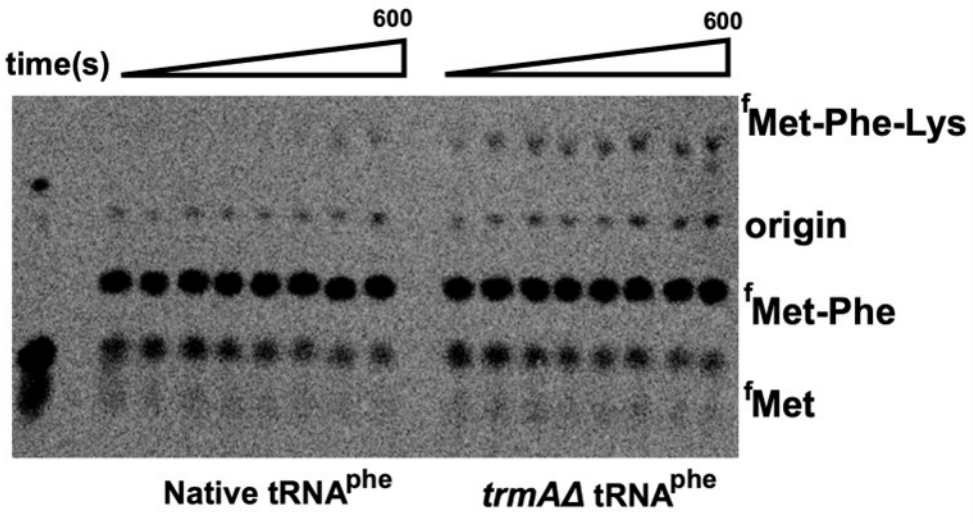

Figure 5.4 *eTLC displaying peptide products of fMet-Phe-lys tripeptide on unmodified phenylalanine codons reacting with 1uM Phe+lLys TC complex using either Native phe tRNA and Native Lysine (left) or TrmA KO phe tRNA absent of m5U and Native Lysine (right) under hygromycin B (50ug/mL final) stress conditions.*

5.3 Discussion

In previously published literature, we discovered that Trm2 was the methyltransferase responsible for incorporating m^5U into yeast mRNA. With its installation understood, we decided to explored the potential role of m^5U in mRNA in translation events only to discover no-to-moderate change. In fact, observable rates of amino acid addition had no changes when m^5U is installed in a UUC codon save a 2-fold rate defect detected only at the 3rd position of a phenylalanine codon[28]. In this work, we investigated the biological relevance/role of Trm2 and m^5U in RNA and discovered that *trm2*Δ yeast grow differently under antibiotic induced translation stress. In fact, we identified the first phenotype for tRNA (uracil-5-)-methyltransferase where yeast lacking the methyltransferase has altered cellular growth under translational inhibition by aminoglycosides – hygromycin B, cycloheximide, and paromomycin. In particular, we see that *trm2*Δ yeast grow more efficiently and produce more protein than wildtype yeast under hygromycin B stress (Figures 1 A and B). This phenotype suggests that

m^5U in mRNA (UUC/UUU codon) may be spatially/stereochemically important in the hygromycin mechanism of action and that removal of m^5U disrupts this mechanism. Furthermore, the increase in m^5U abundance observed during our UHPLC-MS/MS analyses supported this idea. However, our *in vitro* reconstituted translation assays showed us that m^5U in mRNA has no major impact on amino acid addition, suggesting that the m^5U and *trm*2 may be important in other targets/aspects of translation. The next logical target was tRNA, since it carries m^5U modifications and is a key player in protein translation. Interestingly, we saw no apparent change in translation kinetics for both amino acid addition and translocation. Nevertheless, we consistently saw decrease in efficacy of hygromycin B in the absence of m^5U/*trm*2. Our *trmA*Δ $tRNA^{Phe}$ displayed a moderate change in its modifications landscape, and this increase resistance to hygromycin B could be due other modifications or lack thereof.

While *trmA*Δ $tRNA^{Phe}$ provides some resistance to hygromycin B translation inhibition, this effect could be caused by a few different factors– the deletion of m^5U54 in $tRNA^{Phe}$, the alteration in i^6A and acp^3U abundance in *trmA*Δ $tRNA^{Phe}$, or the remodeling of $tRNA^{Phe}$ structure without tRNA (uracil-5-)-methyltransferase present. Previous, structural analysis revealed that hygromycin b binds to the RNA helix 44 (h44) in 30S rRNA small subunit, this position happens to be right next to the aminoacyl-tRNA binding site [23], [24]. It is currently hypothesized that hygromycin works by (1) causing nucleotide A 1493 to flip outwards into a position between the P and A site tRNAs, which could explain the tRNA affinity increase in the A site; (2) A1493 could be causing steric blockage stopping the tRNA from moving to from the p site to the a site; (3) the binding site of hygromycin B allows its second ring to make contact with backbone of the P site mRNA, therefore locking it in position [36]. We speculate that i^6A may the factor contributing to hygromycin B resistance, instead of m^5U. In the *trmA*Δ tRNA, we detected a

significant upregulation of i^6A at position 37 tRNA. In the native *E. coli* and yeast $tRNA^{phe}$, this position is frequently modified to harbor a ms^2i^6A modification. The 37 position in tRNA is adjacent to the anticodon in the ASL, and are known to stabilize codon:anticodon interactions. In this work, a crystal structure with $tRNA^{Phe}$ and hygromycin present in the A-site of the ribosome and indeed, Hygromin B orients and interfaces with the ms^2i^6A modification (Figure 5). Further structural work will be needed to see how hygromycin B interacts with the *trmA*Δ tRNA in the A-site of the ribosome with the hypomodified i^6A at position 37. We hypothesize that i^6A destabilizes the codon:anticodon interactions relative to the fully-modified ms^2i^6A and that hygromycin infers its antibiotic function, to some extent, by interacting with the ms^2 modificiation.

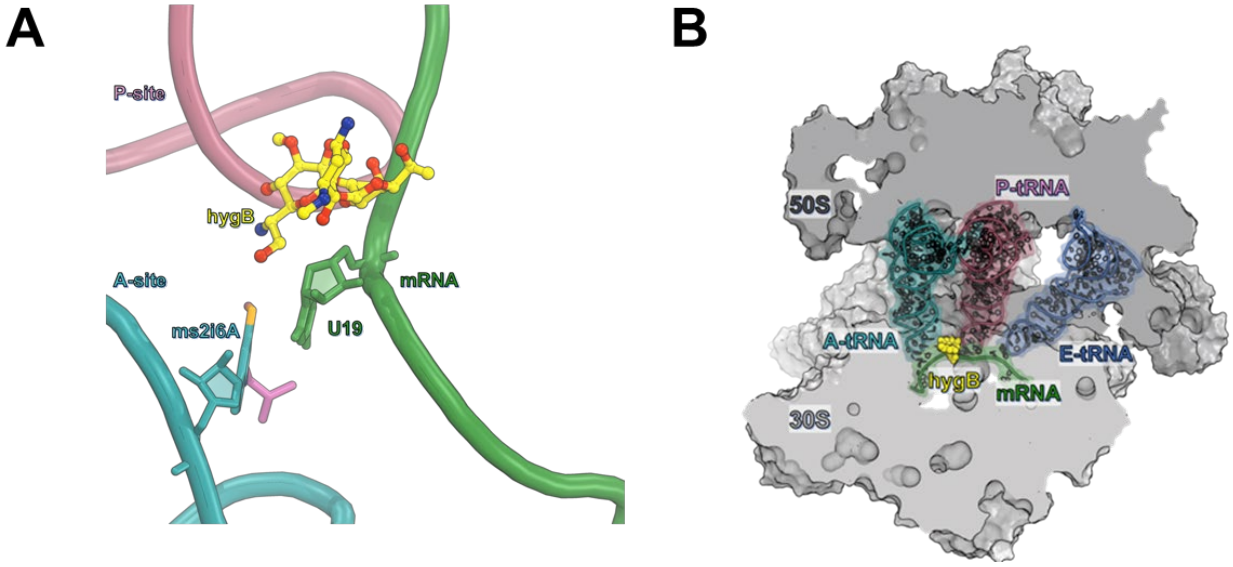

Figure 19 *Crystal structure of 80S S. cerevisiae ribosome with $tRNA^{Phe}$ and hygromycin B programmed in the A-site of the ribosome.*

Antibiotic resistance has become an increasingly prominent public health concern internationally. One mechanism to combat bacterial resistance mechanism is to create new drugs or modify the current antibiotics at our disposal. Therefore, it is important to understand how current translation-targeted drugs work at a molecular level Additionally, in the last few years, it

has been discovered that RNA modifications could play a role in antibiotic resistance. This work contributes to the growing body of literature discussing the impact that tRNA modifications may have on antibiotics, in particular hygromycin induced translational stress control. Here we clearly see that a change in the modification landscape of $tRNA^{phe}$ allowed translocation to continue under hygromycin B induced stress. Furthermore, our data indicates there was no apparent change in translation of this tRNA itself, demonstrating an antibiotic specific response.

5.4 Methods

5.4.1 Spot plating and growth curves

For growth curves, wild-type and *trm2Δ* cells were inoculated into 5 mL YPD and grown overnight at 30˚C. Cultures were then diluted to a starting OD_{600} = 0.05 – 0.1 in 100 mL YPD media containing either 1 M NaCl, 0.1 µg/mL cycloheximide, 50 µg/mL hygromycin B, or 3 mg/mL paromomycin. Cultures were grown in duplicate at 30˚C with shaking unless indicated.

5.4.2 Reporter assay

Plasmid was transformed into wild-type and *Δtrm2 S. cerevisiae* using previously published protocol. The cells were streaked onto CSM-URA agar plates to isolate single colonies [37]. CSM-URA media (30 mL) was inoculated with a single colony and allowed to grow overnight at 30℃ and 250 RPM. The cells were diluted to an OD_{600} of 0.05 with 500 mL of CSM-URA medium and were grown to an OD_{600} of 0.5 at 30℃ and 250 RPM. At this point, the cells were stressed with hygromycin B or cycloheximide and were allowed to continue to grow. At time points of 0 min, 20 min, 60 min, and 150 min after the translational stress, 10 mL of culture was pelleted at 8,000 x g for 10 min. The cell pellet was washed with 1 mL of water prior to storage at -80℃ until the assay was performed.

5.4.3 Yeast Cell Growth and mRNA Purification

Wild-type and *Δtrm2 Saccharomyces cerevisiae* were grown in YPD medium as previously described [38]. *Δtrm2 Saccharomyces cerevisiae* were grown in the presence of 200 μg/mL Geneticin. Briefly, 10 mL of YPD medium was inoculated with a single colony selected from a plate and allowed to grow overnight at 30℃ and 250 RPM. The cells were diluted to an OD_{600} of 0.1 with 200 mL of YPD medium and were grown to an OD_{600} between 0.6 and 0.8 at 30℃ and 250 RPM. Translational stress *S. cerevisiae* were grown with 50 μg/mL hygromycin B or 100ng/mL cycloheximide. Hygromycin B *S. cerevisiae* were grown to an OD_{600} of 0.4 to ensure cells were in mid-log phase growth. This cell culture was pelleted at 15,000xg at 4℃ and used for the RNA extraction.

Yeast cells were lysed as previously described with minor alterations [39]. The 200 mL cell pellet was resuspended in 8 mL of lysis buffer (60 mM sodium acetate pH 5.5, 8.4 mM EDTA) and 800 μL of 10% SDS. One volume (8.8 mL) of phenol was added and vigorously vortexed. The mixture was incubated at 65℃ for five minutes and was again vigorously vortexed. The incubation at 65℃ and vortexing was repeated once. Then, the mixture was rapidly chilled in an ethanol/dry ice bath and centrifuged for 15 minutes at 15,000xg. The total RNA was extracted from the upper aqueous phase using a standard acid phenol-chloroform extraction. The extracted total RNA was treated with 140 U RNase-free DNase I (Roche, 10U/μL) at 37℃ for 30 min. The DNase I was removed through an acid phenol-chloroform extraction. The resulting total RNA was used for our UHPLC-MS/MS, bioanalyzer, and RNA-seq analyses.

mRNA was purified through a three-step purification pipeline [28]. First, small RNA (tRNA and small rRNA) was diminished using the MEGAclear Transcription Clean-Up Kit (Invitrogen) to purify RNA >200nt. Then, Dynabeads oligo-dT magnetic beads (Invitrogen, USA) were used to purify poly(A) RNAs twice from 140 μg of small RNA depleted RNA. The resulting RNA was ethanol precipitated and resuspended in 14 μL. Following, we used the commercial riboPOOL rRNA depletion kit (siTOOLs Biotech, Germany) to remove residual 5S, 5.8S, 18S, and 28S rRNA. The Bioanalyzer RNA 6000 Pico Kit (Agilent, USA) was used to evaluate the purity of the mRNA prior to UHPLC-MS/MS analysis.

5.4.4 qRT-PCR

The RevertAid First Strand cDNA Synthesis Kit (Thermo Scientific, USA) was used to reverse transcribe DNase I treated total RNA and three-stage purified mRNA (200 ng) using the random hexamer primer. The resulting cDNA was diluted 5000-fold and 1 μL of the resulting mixture was analyzed using the Luminaris Color HiGreen qPCR Master Mix (Thermo Scientific, USA) with gene-specific primers.

5.4.5 RNA -seq

The WT *S. cerevisiae* mRNA was analyzed by RNA-seq as previously described by paired-end sequencing using 2.5% of an Illumina NovaSeq (S4) 300 cycle sequencing platform flow cell (0.625% of flow cell for each sample) [28]. All sequence data are paired-end 150 bp reads

5.4.6 RNA enzymatic digestion and UHPLC-MS/MS ribonucleoside analysis

Total RNA and mRNA (125 ng) was digested for each condition. The RNA was hydrolyzed to composite mononucleosides using a two-step enzymatic reaction and quantified using LC-MS/MS as previously described with no alterations [28]

5.4.7 E.coli Ribosomes, and translation factors tRNA and mRNA for in vitro assay

Ribosomes were purified from *E. coli* MRE600 as previously described [40]. All constructors for translation factors were provided by the Green lab unless specifically stated otherwise. Expression and purification of translation factors were carried out as previously described [40]. Unmodified transcripts were prepared using run-off transcription of a DNA template. Modified mRNA sequences containing 5-methyl uridine were purchased from Dharmacon. The mRNA was HPLC purified at Dharmacon. The mRNA sequenced used GGUGUCUUGCGAGGAUAAGUGCAUU AUG UUC UAA GCCCUUCUGUAGCCA, with the coding sequence underline. In these experiments, the modified position was always the first position in the UUC phenylalanine codon.

Method was previously published [41] . Bulk *E. coli* transfer RNA were either bought in bulk from Sigma, or purified in *E. coli* form an HB101 strain containing pUC57-tRNAphe that we obtained from Yury Polikanov. 2 liter cultures containing Terrific Broth (TB) media (TB, 4 mL glycerol/L, 50 mM NH_4Cl, 2 mM $MgSO_4$, 0.1 mM $FeCl_3$, 0.05% glucose and 0.2% lactose (if autoinduction media was used)) were inoculated with 1:400 dilution of a saturated overnight culture and incubated with shaking at 37°C overnight with 400mg/ml of ampicillin. Cells were harvested the next morning by 30 minute centrifugation at 5000 rpm and then stored at -80 C. Extraction of tRNA was done by first responding the cell pellet in 200ml of resuspension buffer (20mM Tris-Cl, 20 mM $Mg(OAc)_2$ pH 7.) The resuspended cells were then placed in Teflon

centrifuge tubes with ETFE o-rings with an acid phenol/chloroform mixture. The cell to phenol/chloroform ratio was approximately 1:1.25 respectively. The tubes were placed in a 4C incubator and left to shake for 1 hour. After incubation cells were spun down for 60 minutes at 4000 rpm at 4C. The supernatant was transferred to another container and the first organic phase was then back-extracted with resuspension buffer and centrifuged down for 60 minutes at 4000 rmp. Aqueous solutions were then combined and a 1/10 volume of 3M NaOAc ph5.2 was added and mixed well. Isopropanol was added to 20% and after proper mixing was centrifuged to remove DNA at 13,700g for 60 minutes at 4C. The supernatant was collected and isopropanol was added to 60% and was left to precipitate at -20C overnight. Precipitation was centrifuged at 13,700 g for 60 minutes at 4C. The pellet was then resuspended with approximately 10 mL 200 mM Tris-Acetate, pH 8.0, and incubate at 37 C for at least 30 minutes. After incubation $1/10^{th}$ volume of 3 M NaOAc and 2 volumes of ethanol was added and mixture was centrifuged at 16,000 g for 60 mins at 4 C. The pellet was washed with 70% ethanol and resuspended in water and desalted on amincon concentrator.

Next the tRNA was isolated on FPLC using buffer A (50 mM NH_4OAc, 300 mM NaCl, 10 mM $MgCl_2$) and buffer B (50 mM NH_4OAc, 800 mM NaCl, 10 mM $MgCl_2$). Resuspended pellet was filtered and loaded on the FPLC. It was eluted with a linear gradient from 0- 50% B over 18 column volumes on a Resource Q column. Fractions were pulled and precipitated overnight.

Pellet was resuspended in water and filtered before being put on the HPLC for further isolation and clean up. The column that was used was a Waters XBridge BEH C18 OBD Prep wide pore column (10x250, ~20 mL column volume, 5 μm). Column was stored in acetonitrile so before any buffers were added, the column was washed with 10 column volumes of water and

then equilibrated with HPLC buffer A (20 mM NH_4OAc, 10 mM $MgCl_2$, 400 mM NaCl at pH 5). 400ul of volume was injected. A linear gradient of buffer B from 0-35% was done over 35 minutes. After 35 mins, the gradient was increased to 100% buffer B over 5 minutes and held at 100% for 10 mins, column was then equilibrated for 10 column volumes before next injection with Buffer A. TCA precipitations were performed on the fractions to determine tRNA of interested, in this case phenylalanine, as well as also determining the A260 and amino acid acceptor activity.

5.4.8 Formation of E. coli ribosome initiation complexes

Initiation complexes (IC's) were formed in 1X 219-Tris buffer (50 mM Tris pH 7.5, 70 mM NH_4Cl, 30 mM KCl, 7 mM $MgCl_2$, 5 mM ß-ME) with 1 mM GTP as previously described(X). 70s ribosomes were incubated with 1uM mRNA (with or without modification), initiation factors (1,2,3) all at 2uM final and 2uM of radiolabeled ^{F}met-tRNA for 30 mins at 37C. After incubation $MgCl_2$ was added to a final concentration of 12mM. The ribosome mixture was then layered onto 1 mL cold buffer D (20 mM Tris-Cl, 1.1 M sucrose, 500 mM NH_4Cl, 10 mM $MgCl_2$, 0.5 mM disodium EDTA, pH 7.5) and centrifuged at 69,000 rpm for 2 hours at 4C. After pelleting, the supernatant was discarded into radioactive waste, and the pellet was resuspended in 1X 219- tris buffer and stored at -80C.

5.4.9 In vitro amino acid addition assays: dipeptide formation

IC complexes were diluted to 140 nM with 1X 219-Tris buffer. Ternary complexes (TCs) were formed by first incubating the EF-Tu pre-loaded with GTP (1X 219-Tris buffer, 10 mM GTP, 60 µM EFTu, 1 µM EFTs) at 37°C for 10 min. The EF-Tu mixture was incubated with the tRNA mixture (1X 219-Tris buffer, Phe-$tRNA^{Phe}$ (1-10 µM), 1 mM GTP) for another 15 min at

37°C. After TC formation was complete, equal volumes of IC complexes (70 nM) and ternary complex (1 μM) were mixed either by hand or using a KinTek quench-flow apparatus. Discrete time-points (0-600 seconds) were taken as to obtain observed rate constants on m^5U-containing mRNAs. Each time point was quenched with 500 mM KOH (final concentration). Time points were then separated by electrophoretic TLC and visualized using phosphorescence as previously described [40], [42]. Images were quantified with ImageQuant. The data were fit using Equation 1: $Fraction\ product\ = A \cdot (\ 1 - e^{k_{obs}t})$

5.4.10 In vitro assays amino acid misincorporation.

In-vitro translation assays were performed by mixing IC complex (70nM final concertation) and ternary complex (1 μM total tRNA aminoacylated with S100 enzymes or specific synthetases, 40 μM EF-Tu, 10 mM GTP, 1X-219 tris buffer) mixed either by hand at room temperature for 10 minutes. Reactions were quenched with 500 mM KOH (final). Products were then separated on Electrophoretic TLC and visualized with phosphorescence as previously described [40].

5.4.11 In vitro amino acid addition assays: tripeptide formation

IC complexes were diluted to 140 nM with 1X 219-Tris buffer. Ternary complexes (TCs) were formed by first incubating the EF-Tu pre-loaded with GTP (1X 219-Tris buffer, 10 mM GTP, 60 μM EFTu, 1 μM EFTs) at 37°C for 10 min. The EF-Tu mixture was incubated with the tRNA mixture (2 μM aminoacyl-tRNA Phe/Lys(s), 24 μM EF-G, 60 μM EF-Tu) with ICs (140 nM) in 219-Tris buffer (50 mM Tris pH 7.5, 70 mM NH_4Cl, 30 mM KCl, 7 mM $MgCl_2$, 5 mM βME). for another 15 min at 37°C. These experiments are done with both native phenylalanine tRNA or our KO phenylalanine tRNA. After TC formation was complete, equal volumes of IC

complexes (70 nM) and ternary complex (1 μM) were mixed using a KinTek quench-flow apparatus. Discrete time-points (0-600 seconds) were taken as to obtain observed rate constants on non-mortified mRNAs, containing a UUC phenylalanine codon. Each time point was quenched with 500 mM KOH (final concentration). Time points were then separated by electrophoretic TLC and visualized using phosphorescence as previously described [40], [42]. Images were quantified with ImageQuant. The data were fit using Equation 1 as previously described.

5.4.12 In vitro amino acid addition assays: tripeptide formation with Hygromycin B

IC complexes were diluted to 140 nM with 1X 219-Tris buffer. Ternary complexes (TCs) were formed by first incubating the EF-Tu pre-loaded with GTP (1X 219-Tris buffer, 10 mM GTP, 120 μM EFTu, PEP, 12mM, PK .40μM, 40 μM EFTs) at 37℃ for 10 min. The EF-Tu mixture was incubated with the tRNA mixture (20–60 μM aminoacyl-tRNA Phe/Lys(s), 24 μM EF-G, 60 μM EF-Tu) with ICs (140 nM) in 219-Tris buffer (50 mM Tris pH 7.5, 70 mM NH_4Cl, 30 mM KCl, 7 mM $MgCl_2$, 5 mM βME). for another 15 min at 37℃. These experiments are done with both native phenylalanine tRNA or our KO phenylalanine tRNA. After TC formation was complete, 50μg/ml of Hygromycin B was added to the IC complex. Then by haand equal volumes of IC complexes (70 nM) and ternary complex (1 μM) were mixed and discrete time-points (0-600 seconds) were taken as to obtain observed rate constants on non-mortified mRNAs, containing a UUC phenylalanine codon. Each time point was quenched with 500 mM KOH (final concentration). Time points were then separated by electrophoretic TLC and visualized using phosphorescence as previously described [40], [42]. Images were quantified with ImageQuant. The data were fit using Equation 1 as previously described.

5.4.13 Fitting observed rate constants and Global analysis simulations of amino acid addition

Fits for used to obtain observed rate constant k_1 was done using a single differential equation in Kaleidagrpah for products in di peptide formation. When multiple peptide products were formed, the disappearance of FMET product was fit sing a single differential equation in Kaleidagrpah to get an observed rate constant k_1. This value was then used in KinTex Explorer to measure subsequent rate constant k_2 using simulations. Simulations were modeled against the equation:

$$^{f}M + F \rightarrow {}^{f}MF + K \rightarrow {}^{f}MFK$$

5.4.14 Spot plating assay and growth curve characterization under stress

Wild-type and *trm2*Δ cells were inoculated into 3 mL YPD and grown overnight. Then these cultures were diluted to OD_{600}=1 as a starting point, and 7 µl of 10-fold serial dilutions were spotted on fresh YPD agar plates including 0.75-1.0 M NaCl, 250 mM $MgSO_4$, 200 µM puromycin, 100 ng/mL cycloheximide, 25-50 µg/mL hygromycin B, 50 µM MG132 and 1.5-3 mg/mL paromomycin. Growth of the cells were also tested in the presence of different carbon sources including 2% glucose, 2% sucrose, 2% galactose and 3% glycerol in YEP agar media (1% yeast extract and 2% peptone). The plates were incubated for 2-5 days at 30 ºC unless indicated.

For growth curves, wild-type and *trm2Δ* cells were inoculated into 5 mL YPD and grown overnight. Cultures were then diluted to a starting OD_{600} = 0.05 – 0.1 in 100 mL YPD media containing either 1 M NaCl, 0.1 µg/mL cycloheximide, 50 µg/mL hygromycin B, or 3 mg/mL paromomycin. Cultures were grown in duplicate at 30˚C with shaking unless indicated, and growth was monitored by OD_{600}

5.5 References

[1] M. T. Angelova et al., “The emerging field of epitranscriptomics in neurodevelopmental and neuronal disorders,” Frontiers in bioengineering and biotechnology, vol. 6, p. 46, 2018.

[2] M. S. Ben-Haim, S. Moshitch-Moshkovitz, and G. Rechavi, “FTO: linking m 6 A demethylation to adipogenesis,” Cell research, vol. 25, no. 1, pp. 3–4, 2015.

[3] Q. I. Cui et al., “m6A RNA methylation regulates the self-renewal and tumorigenesis of glioblastoma stem cells,” Cell reports, vol. 18, no. 11, pp. 2622–2634, 2017.

[4] T. Du et al., “An association study of the m6A genes with major depressive disorder in Chinese Han population,” Journal of affective disorders, vol. 183, pp. 279–286, 2015.

[5] N. Jonkhout, J. Tran, M. A. Smith, N. Schonrock, J. S. Mattick, and E. M. Novoa, “The RNA modification landscape in human disease,” Rna, vol. 23, no. 12, pp. 1754–1769, 2017.

[6] Y. Bykhovskaya, K. Casas, E. Mengesha, A. Inbal, and N. Fischel-Ghodsian, “Missense mutation in pseudouridine synthase 1 (PUS1) causes mitochondrial myopathy and sideroblastic anemia (MLASA),” Am J Hum Genet, vol. 74, no. 6, pp. 1303–1308, Jun. 2004, doi: 10.1086/421530.

[7] P. Boccaletto et al., “MODOMICS: a database of RNA modification pathways. 2017 update,” Nucleic Acids Res, vol. 46, no. D1, pp. D303–D307, Jan. 2018, doi: 10.1093/nar/gkx1030.

[8] T. D. Price, H. A. Hinds, and R. S. Brown, “Thymine ribonucleotides of soluble ribonucleic acid of rat liver,” Journal of Biological Chemistry, vol. 238, no. 1, pp. 311–317, 1963.

[9] V. Anantharaman, E. V. Koonin, and L. Aravind, “TRAM, a predicted RNA-binding domain, common to tRNA uracil methylation and adenine thiolation enzymes,” FEMS microbiology letters, vol. 197, no. 2, pp. 215–221, 2001.

[10] D. T. Dubin, “Methylated nucleotide content of mitochondrial ribosomal RNA from hamster cells,” Journal of molecular biology, vol. 84, no. 2, pp. 257–273, 1974.

[11] S. Auxilien et al., “Specificity shifts in the rRNA and tRNA nucleotide targets of archaeal and bacterial m5U methyltransferases,” RNA, vol. 17, no. 1, pp. 45–53, Jan. 2011, doi: 10.1261/rna.2323411.

[12] C. W. Chan, B. Chetnani, and A. Mondragón, “Structure and function of the T-loop structural motif in noncoding RNAs,” Wiley Interdisciplinary Reviews: RNA, vol. 4, no. 5, pp. 507–522, 2013.

[13] S. Hur, R. M. Stroud, and J. Finer-Moore, “Substrate recognition by RNA 5-methyluridine methyltransferases and pseudouridine synthases: a structural perspective,” Journal of Biological Chemistry, vol. 281, no. 51, pp. 38969–38973, 2006.

[14] P. Davanloo, M. Sprinzl, K. Watanabe, M. Albani, and H. Kersten, “Role of ribothymidine in the thermal stability of transfer RNA as monitored by proton magnetic resonance,” Nucleic Acids Res, vol. 6, no. 4, pp. 1571–1581, Apr. 1979, doi: 10.1093/nar/6.4.1571.

[15] L. C. Keffer-Wilkes, E. F. Soon, and U. Kothe, “The methyltransferase TrmA facilitates tRNA folding through interaction with its RNA-binding domain,” Nucleic acids research, vol. 48, no. 14, pp. 7981–7990, 2020.

[16] G. R. Björk and F. C. Neidhardt, “Physiological and biochemical studies on the function of 5-methyluridine in the transfer ribonucleic acid of *Escherichia coli*,” Journal of Bacteriology, vol. 124, no. 1, pp. 99–111, 1975.

[17] G. R. Björk and F. C. Neidhardt, “Analysis of 5-methyluridine function in the transfer RNA of *Escherichia coli*,” Cancer Research, vol. 31, no. 5, pp. 706–709, 1971.

[18] A. Babosan, L. Fruchard, E. Krin, A. Carvalho, D. Mazel, and Z. Baharoglu, “Non-essential tRNA and rRNA modifications impact the bacterial response to sub-MIC antibiotic stress,” bioRxiv, 2022.

[19] I. Masuda et al., “tRNA methylation is a global determinant of bacterial multi-drug resistance,” Cell systems, vol. 8, no. 4, pp. 302–314, 2019.

[20] Y.-M. Hou, I. Masuda, and L. J. Foster, “tRNA methylation: an unexpected link to bacterial resistance and persistence to antibiotics and beyond,” Wiley Interdisciplinary Reviews: RNA, vol. 11, no. 6, p. e1609, 2020.

[21] Y. Pan, T.-M. Yan, J.-R. Wang, and Z.-H. Jiang, “The nature of the modification at position 37 of tRNAPhe correlates with acquired taxol resistance,” Nucleic acids research, vol. 49, no. 1, pp. 38–52, 2021.

[22] G. Kapoor, S. Saigal, and A. Elongavan, “Action and resistance mechanisms of antibiotics: A guide for clinicians,” Journal of anaesthesiology, clinical pharmacology, vol. 33, no. 3, p. 300, 2017.

[23] D. E. Brodersen, W. M. Clemons Jr, A. P. Carter, R. J. Morgan-Warren, B. T. Wimberly, and V. Ramakrishnan, “The structural basis for the action of the antibiotics tetracycline,

pactamycin, and hygromycin B on the 30S ribosomal subunit," Cell, vol. 103, no. 7, pp. 1143–1154, 2000.

[24] D. Moazed and H. F. Noller, "Interaction of antibiotics with functional sites in 16S ribosomal RNA," Nature, vol. 327, no. 6121, pp. 389–394, 1987.

[25] A. Gonzalez, A. Jimenez, D. Vazquez, J. E. Davies, and D. Schindler, "Studies on the mode of action of hygromycin B, an inhibitor of translocation in eukaryotes," Biochimica et Biophysica Acta (BBA)-Nucleic Acids and Protein Synthesis, vol. 521, no. 2, pp. 459–469, 1978.

[26] M. J. Cabañas, D. Vázquez, and J. Modolell, "Inhibition of ribosomal translocation by aminoglycoside antibiotics," Biochemical and biophysical research communications, vol. 83, no. 3, pp. 991–997, 1978.

[27] C. T. Y. Chan, M. Dyavaiah, M. S. DeMott, K. Taghizadeh, P. C. Dedon, and T. J. Begley, "A Quantitative Systems Approach Reveals Dynamic Control of tRNA Modifications during Cellular Stress," PLoS Genet, vol. 6, no. 12, Art. no. 12, Dec. 2010, doi: 10.1371/journal.pgen.1001247.

[28] Joshua D. Jones et al., "Methylated guanosine and uridine modifications in *S. cerevisiae* mRNAs modulate translation elongation," Rsc chem biol.

[29] S. M. McGaha and W. S. Champney, "Hygromycin B inhibition of protein synthesis and ribosome biogenesis in *Escherichia coli*," Antimicrobial agents and chemotherapy, vol. 51, no. 2, pp. 591–596, 2007.

[30] J. Choi et al., “N(6)-methyladenosine in mRNA disrupts tRNA selection and translation-elongation dynamics,” Nat Struct Mol Biol, vol. 23, no. 2, Art. no. 2, Feb. 2016, doi: 10.1038/nsmb.3148.

[31] M. J. Johansson and A. S. Byström, “Dual function of the tRNA (m5U54) methyltransferase in tRNA maturation,” Rna, vol. 8, no. 3, pp. 324–335, 2002.

[32] C. A. Powell and M. Minczuk, “TRMT2B is responsible for both tRNA and rRNA m5U-methylation in human mitochondria,” RNA Biol, vol. 17, no. 4, pp. 451–462, Apr. 2020, doi: 10.1080/15476286.2020.1712544.

[33] W. Dai et al., “Activity-based RNA-modifying enzyme probing reveals DUS3L-mediated dihydrouridylation,” Nat Chem Biol, vol. 17, no. 1178–1187, 2021, doi: https://doi.org/10.1038/s41589-021-00874-8.

[34] Q.-Y. Cheng et al., “Chemical tagging for sensitive determination of uridine modifications in RNA,” Chem. Sci., vol. 11, no. 7, Art. no. 7, 2020, doi: 10.1039/C9SC05094A.

[35] J.-M. Carter et al., “FICC-Seq: a method for enzyme-specified profiling of methyl-5-uridine in cellular RNA,” Nucleic Acids Research, vol. 47, no. 19, Art. no. 19, Nov. 2019, doi: 10.1093/nar/gkz658.

[36] M. A. Borovinskaya, S. Shoji, K. Fredrick, and J. H. Cate, “Structural basis for hygromycin B inhibition of protein biosynthesis,” Rna, vol. 14, no. 8, pp. 1590–1599, 2008.

[37] R. D. Gietz and R. H. Schiestl, “High-efficiency yeast transformation using the LiAc/SS carrier DNA/PEG method,” Nature protocols, vol. 2, no. 1, pp. 31–34, 2007.

[38] M. Tardu, J. D. Jones, R. T. Kennedy, Q. Lin, and K. S. Koutmou, "Identification and quantification of modified nucleosides in *Saccharomyces cerevisiae* mRNAs," ACS chemical biology, vol. 14, no. 7, pp. 1403–1409, 2019.

[39] M. E. Schmitt, T. A. Brown, and B. L. Trumpower, "A rapid and simple method for preparation of RNA from *Saccharomyces cerevisiae*.," Nucleic Acids Res, vol. 18, no. 10, Art. no. 10, May 1990.

[40] D. E. Eyler et al., "Pseudouridinylation of mRNA coding sequences alters translation," PNAS, vol. 116, no. 46, pp. 23068–23074, Nov. 2019, doi: 10.1073/pnas.1821754116.

[41] J. G. Monroe, T. J. Smith, and K. S. Koutmou, "Investigating the consequences of mRNA modifications on protein synthesis using in vitro translation assays," in Methods in Enzymology, vol. 658, Elsevier, 2021, pp. 379–406.

[42] J. G. Monroe, T. J. Smith, and K. S. Koutmou, "Chapter Sixteen - Investigating the consequences of mRNA modifications on protein synthesis using in vitro translation assays," in Methods in Enzymology, vol. 658, J. E. Jackman, Ed. Academic Press, 2021, pp. 379–406. doi: 10.1016/bs.mie.2021.06.011.

Chapter 6 Conclusions and Future Directions

6.1 Overview

The work presented in this Dissertation aimed to further elucidate the role that mRNA and tRNA sequence play in altering translation and protein synthesis. Specifically, modifications to the purines adenosine and guanosine which have been found to modulate the rate and accuracy of translation. Modifications to both adenosine and guanosine frequently slow translation when present within the coding sequence of mRNAs In the context of poly(A) I explored a new mechanism of movement and found that mRNA sequence alone is sufficient to drive ribosome movement. I also show that adenosine modifications have the potential to alter frame maintenance of mRNA with m^6A being able to decrease ribosome sliding on poly(A). Additionally, I explored the distribution of tRNA modifications in the ASL region to try and develop a stronger characterization of their impact on translation. Furthermore, my work highlights how modifications may be modulated during times of cellular stress, such as translation inhibition with hygromycin B. While the field has been investigating the individual effects that single mRNA or tRNA modifications have on translation, protein homeostasis, and disease states there is a lack of understanding on how sequence and modifications of the biomolecules affect one another (intermolecular) or even themselves (intramolecular). My work sought to understand the interplay between mRNA and tRNA sequence and modification, and how they impact translation.

6.2 Improving *in vitro* translation systems to characterize single-steps in the mechanism of protein synthesis

Chemical modifications to mRNA residues have the potential to influence the rate and fidelity of protein synthesis. Given the complexity of translation it is hard to identify exactly where and how the rate and accuracy of translation can be influenced. The *in vitro* translation system derived from *E. coli* utilizes highly purified components which allows the direct molecular level investigation into the impacts of mRNA modifications on translation. Advantages of *in vitro* studies are that they can directly and discretely study single variable changes within an experiment. The downside to *in vitro* systems is the extensive material and time commitment required in order to utilize them. The *in vitro* system can be used to gain insights into how individual chemical modifications influence translation on the molecular level. Future directions for this system should include detailed kinetic studies of the selection and accuracy of amino acid addition. Currently the effects of modifications on translation accuracy have only been observed on the k_{obs} level. In order to understand how mRNA modifications alter translation accuracy further investigations should utilize Equation 10.

$$Accuracy\ (A) = (s) \times (p) \tag{10}$$

Where s is the tRNA selectivity during amino acid addition and p is the proofreading ability of the ribosome during amino acid addition. By comparing the ratio between cognate (c) and noncognate (nc) accuracy the kinetic efficiency of peptide bond formation can be established for each species of tRNA, as seen in equation 11.

$$A = \frac{\left(k_{obs}/K_{1/2}\right)^{c}_{dipeptide}}{\left(k_{obs}/K_{1/2}\right)^{nc}_{dipeptide}} \tag{11}$$

The ratio between the k_{obs} *and* $K_{1/2}$ for the cognate can provide an experimental double check on the values obtained from *in vitro* experiments since the ratio should be close to 1 in order to allow rapid and accurate addition of the correct amino acid, while non-cognate decoding ratio should have a relatively small number, which should give a high level of accuracy for the ribosome. These type of measurements by themselves will help to provide insight into relative decoding accuracies of the degenerate tRNA anticodons.

The selection and proofreading steps are separated by the GTPase activation and hydrolysis steps (**Figure 2**, steps 3,4) with selection taking place prior to GTPase activation and hydrolysis and proofreading occurring after. This means that selectivity can be defined as Equation 12.

$$s = \frac{(k_{obs}/K_{1/2})^{c}_{GTP}}{(k_{obs}/K_{1/2})^{nc}_{GTP}} \tag{12}$$

The proof-reading ability of the amino acid selection can then be derived by rearranging Equation 10 and substituting in the selectivity equation (Equation 12) to arrive at Equation 13 [1,2].

$$p = \frac{A}{s} = \frac{(k_{obs}/K_{1/2})^{nc}_{GTP}}{(k_{obs}/K_{1/2})^{nc}_{dipeptide}} \Big/ \frac{(k_{obs}/K_{1/2})^{c}_{GTP}}{(k_{obs}/K_{1/2})^{c}_{dipeptide}} \tag{13}$$

These variables for these equations can all be measured using pre-existing techniques and in fact the rates for cognate addition have already been established for several species of tRNA [2]. Using the *in vitro* system to pick apart the kinetics of chemically modified mRNA will allow elucidation into just how exactly RNA modifications alter accuracy at the A-site of the ribosome. Additionally, it will help to establish the significant factors in codon:anticodon interactions (hydrogen bonding, geometry, base stacking, steric interactions, etc.) during translation [1-4].

Another limitation to this current iteration of the recombinant *in vitro* translation system is that is derived from a single organism, the prokaryote *Escherichia coli*. While there are parallels in elongation between prokaryotic and eukaryotic translation, there are major changes that take place during initiation and even termination stages of the translation pathway. In the field, there are other adaptations being made which have produced successful recombinant translation systems for mammalian mitochondrial translation and yeast translation [5,6]. These systems are not inherently "pure" as they contain high-yield purification factors from multiple organisms in their classification category (i.e. yeast). Improving and expanding these types of *in vitro* systems could ultimately serve two major goals in the field. Firstly, it will allow for expansion to understanding the mechanistic level details of translation across all domains of life, giving more accurate and meaningful findings for the organisms they are observed in. Secondly, improvements can be made to decrease labor, cost, and time necessary for such protocols allowing for faster and cheaper yet just as robust scientific findings.

6.3 RNA modification and interactions during translation impact ribosome movement during translocation events

Translation has long been thought to be a relatively ubiquitous and uniform process, with elongation specifically being a step believed to be well-resolved. However, growing literature has challenged the dogma of elongation and showcased many of both programmed and unprogrammed events that alter how the ribosome moves along the sequence of an mRNA to effect protein synthesis. From single nucleotide frameshifts to large sequence skipping in translational bypassing, a growing number of mechanisms of peptide synthesis and its regulation by the ribosome during elongation are coming to light. Conversely, there lie many problems in these mechanisms as often is unclear which molecular constituents or events cause them making

it difficult to deconvolute molecular details without significantly altering the entire biochemical process (e.g., discretely changing only one component). In addition, many steps of "canonical" translation, particularly during translocation, have yet to be full resolved themselves making it difficult to understand exactly what mechanistic steps are affected by molecular-level modulations, such as mRNA and tRNA modifications.

My work has revealed that the ribosome can move into, or occupy, multiple frames during translation of short poly(A) sequences and describe a mechanism by which it does so. This phenomenon, known as sliding, is a newly characterized type of ribosome movement during translation and suggests that there is still much to be discovered on how the ribosome can behave during its movement along mRNA. I show that this movement, as well as decreased rates of amino acid addition, can be affected by multiple factors such as amino acid charge, mRNA sequence, mRNA modification (m^6A), and $tRNA^{Lys}$ modification landscape with the largest contributor to the newly characterized movement being mRNA sequence. While my work provides a kinetic mechanism for the overview of sliding and that molecular level alterations can alter ribosome movement and speed, there is a deficit in how molecular-level components contribute to this phenomenon.

Steps need to be taken to characterize specific steps of translocation and ribosome rotational states during the ribosome movement on mRNA. Traditionally, methods for studying translocation states rely on ribosome pausing or stalling using antibiotics, EF-G mutations, or the use of non-hydrolysable GTP analogs [7-11]. These types of assays can prove problematic as alterations to translocation could lead to off-states or "false positive" findings – especially during GTP hydrolysis and inorganic peptide release [12]. In order to address this concern, steps have been taken in the right direction by utilizing structural studies such as time-resolved Cryo-EM.

For example, such work has revealed that EF-G-GTP associates with the ribosome and behaves rather rigidly to "drive" mRNA-tRNA translocation from the A-site to P-site and GTP hydrolysis and Pi release lead to EF-G dissociation [13]. This offers a lot of new and exciting insight into translocation, but many of the individual rotational states that occur after EF-G association and during tRNA-mRNA movement are still convoluted. This is interesting to study further, especially when considering how modifications to mRNA and tRNA may be involved in affecting movement during this process. To begin investigating rotational states and individual steps in the translocation mechanism, EF-G bound ribosomes could be used to better rationalize how mRNA-tRNA move prior to GTP-hydrolysis. As current evidence suggests that EF-G remains rigid upon binding and GTPase activity leads to its dissociation, incorporating non-hydrolysable GTP analogs onto EF-G (which can result in up to 50-fold decrease EF-G dissociation) can be done to begin investigating these individual rotation states. This could be done using fluorescence labeled mRNA and/or tRNA species to see if they are remaining stabilized or destabilized during A/P-site shifts. Or, 30S body or "head" units could be fluorescently labeled to probe individual rotational states during "body rotation" and "head swivel" events. Such studies could be performed using a single-molecule fluorescence translation platform with a ZMW approach – which allows for up to four different fluorescently labeled ligands to be studied in a single ribosome [14]. Combing this approach with Cryo-EM studies using EF-G:GTP analogs could better elucidate steps of translocation and would then allow for a platform to study how modifications to mRNA or tRNA could affect such steps through stabilization or destabilization of mRNA:tRNA or rRNA interactions. Such findings may explain why certain modifications suppress or promote frameshift events during translocation.

Modifications to either mRNA or tRNA in poly(A) translation affect the rates of addition for the second lysine and that is driven primarily by mRNA sequence. In fact, structural work has been done to visualize $tRNA^{Lys}$ within the A/P site of the ribosome and that tRNA modifications alter base-pairing and ASL stabilization. Using approaches described above, $tRNA^{Lys}$ could be serve as a strong starting point in resolving structures that show the influence that modifications to either mRNA or tRNA (ASL) have on proper decoding (This is continued in Chapter 6.4 – *Anticodon stem-loop --tRNA modifications influence codon decoding and frame maintenance during translation*) [15-18]. In the context of poly(A), we have found that m^6A is frequently installed in poly(A) stretches within the coding sequence, so elucidating structure with the modification present may help to explain the formation of the helix unmodified poly(A) adopts in the ribosome and how such a structure may influence rates and mechanism of elongation. As poly(A) is adopted in a handful of cancers and diseases, understanding the full effects and mechanism of poly(A) translation would give better insight into if its presence is programmed or not, as well as potential avenues into ways to treat or circumvent such errors [19,20]. While mRNA sequence is clearly the primary determinant for decreased rates in polylysine synthesis the role that peptide sequence has on regulating rates cannot be ignored, as "rafts" of charged peptide invoke ribosome stalling after the ribosome have translocated past and off the encoding sequence. Understanding such phenomena would allow us to parse about the significance that translation constituents have in regulating levels of mRNA – in normal, stress, and disease states – so we could determine how protein homeostasis is affected. Ribosome profiling studies comparing translation efficiency of polybasic peptides, for both instances of mRNA sequence and polybasic "rafts", could be performed under varying stress conditions to see how potential mRNA modifications (such as m^6A in poly(A)) compare other polybasic

peptide synthesis. This has the potential to open many avenues of studying how translation is a pivotal point in gene expression which is influenced by simple modifications or by the peptide product it synthesizes.

6.4 tRNA modification cross-talk exploration through enzyme, stress, and kinetic study

Modifications to tRNA have been long known to be involved in assisting the molecule adopt proper structure and folding, but little work has been done in investigating how such modifications impact decoding or how they may be linked to physiological conditions and disease. While it has been discovered that tRNA modifications can have impact on protein homeostasis and the modification landscape through a "cross-talk" system, it is still very unclear how individual modifications may disrupt both molecular (tRNA) and cellular function [21-25]. Additionally, while modifications have been characterized in tRNAs, how they interact inter- and intra-molecularly are not very well established beyond a handful of examples (primarily that of $tRNA^{Lys}$). Perhaps even more troublesome is that many of the enzymes or pathways responsible for the installation of many of these modifications are poorly understood or unknown altogether. To this end, more targeted studies, both structural and mechanistic, are needed to elucidate the roles that tRNA modifications have in protein homeostasis. Such work will allow us to develop a better understanding of their role in cellular physiology as well as provide insight into how such modifications may have been adapted evolutionarily.

In this vein of thought, it is also necessary to expand our working knowledge of how modifications change in varying populations - whether it be in tissues, individuals, disease states, etc., - as mRNA levels are dynamic though poorly understood as to how they are altered or modulated. Genetic fingerprints in DNA often serve as indicators of certain populations and gene expression levels, sequence context, and epitranscriptomic markers serve as indicators of

variance in genetic populations – with these being affected by disease phenotypes, environmental conditions, or even inherited. As such, it is not beyond reason to suggest that RNA and its modifications levels (whether on tRNA, mRNA, or other species) may also serve as indicators of variance which have been evolved or changed over time due to similar genetic pressures. I think it necessary and exciting to explore how modification levels, states, and sequence context can and have diverged (or not) evolutionarily and how RNA modifications may serve a primary adaptors in evolution among different populations.

6.5 Methylated guanosine and uridine modifications in *S. cerevisiae* mRNAs modulate translation elongation

Over 15 different types of mRNA modifications have been identified by sequencing and liquid chromatography coupled to tandem mass spectrometry (LC-MS/MS) technologies. In this work we are able to quantify 50 different mRNA specific modifications in *S. cerevisiae* at a time, by improving mRNA purity and the LC-MS/MS pipeline. Using this method we were able to detect and quantify 13 different known modifications, as well as, detect four new low level modifications e.g. 1-methyguanosine, N2-methylguanosine, N2, N2-dimethylguanosine, and 5-methyluridine. Furthermore, we were able to identify the enzymes responsible for incorporating these modifications into mRNA: Trm10, Trm11, Trm1, and Trm2. Using an in-vitro reconstituted system we discovered that 1-methyguanosine, N2-methylguanosine and 5-methyluridine impede amino acid addition in a position dependent manner on a mRNA codon.

One of the major limitations to assessing the impact of mRNA modifications in translation is simply that many of the enzymes or pathways responsible for incorporating them are unknown or poorly defined. This is not an easy component to address as many of the

enzymes that incorporate well-known modifications in tRNAs, ncRNAs, and even rRNAs are not well-defined. As some enzymes families and domains can have both tRNA and mRNA substrates, as is the case with Trm1 in *S. cerevisiae* which installs N2,N2-dimethylguanosine on both tRNA and mRNAs. While it is an arduous task to determine substrates of enzymes, and even more so to discover the enzymes responsible for incorporation in some cases, I believe it is important to study the Trm enzymes discussed in more detail. Utilizing binding affinity and structural approaches (such SAXS or X-ray crystallography) we can first determine if the modifications put onto mRNAs have specificity – with enzymes having a consensus sequence or structural motif target – or if potential mRNA modifications are simply a consequence of off-target binding for tRNA modifications. This work can then be expanded into other enzymes known to incorporate tRNA modifications and assess if those enzymes may be responsible for mRNA modifications as well.

This work details how m^1G, m^2G, and m^5U alter translation elongation, but it is unclear exactly how these modifications do so. Utilizing both a structural and *in vitro* translation approach, as described previously, to determine this I believe these examples serve as interesting pivot in our research to delve deeper into the basic mechanism of translation and codon-anticodon interactions through base-pairing. For instance, m^1G and m^2G are modestly incorporated, but their presence would decrease the capable hydrogen bonds able to be formed in a G-C base pair or wobble interface. I would like to see the importance of H-bonding, sterics, and Van der Waals forces explored not only in a codon-anticodon context but also in basic base pair interactions which may offer findings that expand out current knowledge of nucleic acid interactions. Preliminary and continued desired work on such a topic is presented and discussed in Appendix F.

6.6 Modulation of tRNA modification landscape alters efficacy of antibiotics and offer exploration of potential biomarkers

It is well known that non-coding RNA is modified, and this has implications on both structure and function. However, the cooperativity of these modifications both intramolecularly in the tRNA or intermolecular with the surrounding rRNA and mRNA is not well studied. This is to do with the fact that knocking out, or even knocking down, some modifying enzyme results in lethal phenotypes and an inability to study their effects. To bypass this feature, our lab seeks to develop and provide a platform for high-yield expression of tRNAs with the modifications of interest either present or absent. This can be done through either bacterial or yeast platforms to yield the tRNAs of interest. Once harvested, these tRNAs can be used in an *in-vitro* setting to determine the roles individual modifications, as well as the entire modification landscape, can have on translation. In addition, it would allow for the exploration that modifications may have on other aspects of tRNA and the tRNA lifecyle such as tRNA maturation, modification cross-talk, or tRNA fragmentation.

Furthermore, understanding how the modification impact this environment spatially or chemically will unveil more of the important interactions necessary within the ribosome and perhaps how modifications to tRNA may be involved in forming, maintaining, or even disrupting such interactions. As shown in Chapter 5 , a single uptick in modification (i^6A) changes the A-site environment sufficiently enough to either compete with or displace Hygromycin B. Elucidating how and what sites of interaction are important for proper translation opens up more avenues to explore for targeted therapeutics, or conversely – as is becoming more problematic with prokaryotes and viruses on a whole – how modifications may be used to confer drug-resistance.

6.7 References

[1] Indrisiunaite G. Accuracy of protein synthesis and its tuning by mRNA modifications n.d.:46.

[2] Indrisiunaite G, Pavlov MY, Heurgué-Hamard V, Ehrenberg M. On the pH Dependence of Class-1 RF-Dependent Termination of mRNA Translation. Journal of Molecular Biology 2015;427:1848–60. https://doi.org/10.1016/j.jmb.2015.01.007.

[3] Gromadski KB, Rodnina MV. Kinetic Determinants of High-Fidelity tRNA Discrimination on the Ribosome. Molecular Cell 2004;13:191–200. https://doi.org/10.1016/S1097-2765(04)00005-X.

[4] Pape T, Wintermeyer W, Rodnina MV. Complete kinetic mechanism of elongation factor Tu-dependent binding of aminoacyl-tRNA to the A site of the *E. coli* ribosome. EMBO J 1998;17:7490–7. https://doi.org/10.1093/emboj/17.24.7490.

[5] R. Nagai, Y. Xu, C. Liu, A. Shimabukuro, and N. Takeuchi-Tomita, "In Vitro Reconstitution of Yeast Translation System Capable of Synthesizing Long Polypeptide and Recapitulating Programmed Ribosome Stalling," Methods Protoc., vol. 4, no. 3, p. 45, Jul. 2021, doi: 10.3390/mps4030045.

[6] M. Lee, N. Matsunaga, S. Akabane, I. Yasuda, T. Ueda, and N. Takeuchi-Tomita, "Reconstitution of mammalian mitochondrial translation system capable of correct initiation and long polypeptide synthesis from leaderless mRNA," Nucleic Acids Res., vol. 49, no. 1, pp. 371–382, Jan. 2021, doi: 10.1093/nar/gkaa1165.

[7] J. Zhou, L. Lancaster, J. P. Donohue, and H. F. Noller, “Crystal Structures of EF-G-Ribosome Complexes Trapped in Intermediate States of Translocation,” Science, vol. 340, no. 6140, p. 1236086, Jun. 2013, doi: 10.1126/science.1236086.

[8] J. Zhou, L. Lancaster, J. P. Donohue, and H. F. Noller, “How the Ribosome Hands the A-site tRNA to the P Site During EF-G-catalyzed Translocation,” Science, vol. 345, no. 6201, Art. no. 6201, Sep. 2014, doi: 10.1126/science.1255030.

[9] J. Lin, M. G. Gagnon, D. Bulkley, and T. A. Steitz, “Conformational Changes of Elongation Factor G on the Ribosome During tRNA Translocation,” Cell, vol. 160, no. 0, pp. 219–227, Jan. 2015, doi: 10.1016/j.cell.2014.11.049.

[10] Y.-G. Gao, M. Selmer, C. M. Dunham, A. Weixlbaumer, A. C. Kelley, and V. Ramakrishnan, “The structure of the ribosome with elongation factor G trapped in the post-translocational state,” Science, vol. 326, no. 5953, pp. 694–699, Oct. 2009, doi: 10.1126/science.1179709.

[11] A. F. Brilot, A. A. Korostelev, D. N. Ermolenko, and N. Grigorieff, “Structure of the ribosome with elongation factor G trapped in the pretranslocation state,” Proc. Natl. Acad. Sci. U. S. A., vol. 110, no. 52, pp. 20994–20999, Dec. 2013, doi: 10.1073/pnas.1311423110.

[12] W. Holtkamp, C. E. Cunha, F. Peske, A. L. Konevega, W. Wintermeyer, and M. V. Rodnina, “GTP hydrolysis by EF-G synchronizes tRNA movement on small and large ribosomal subunits,” EMBO J., vol. 33, no. 9, pp. 1073–1085, May 2014, doi: 10.1002/embj.201387465.

[13] C. E. Carbone, A. B. Loveland, H. B. Gamper, Y.-M. Hou, G. Demo, and A. A. Korostelev, “Time-resolved cryo-EM visualizes ribosomal translocation with EF-G and GTP,” Nat. Commun., vol. 12, p. 7236, Dec. 2021, doi: 10.1038/s41467-021-27415-0.

[14] A. Prabhakar, E. V. Puglisi, and J. D. Puglisi, “Single-Molecule Fluorescence Applied to Translation,” Cold Spring Harb. Perspect. Biol., vol. 11, no. 1, p. a032714, Jan. 2019, doi: 10.1101/cshperspect.a032714.

[15] S. Vangaveti, S. V. Ranganathan, and P. F. Agris, “Physical Chemistry of a Single tRNA-Modified Nucleoside Regulates Decoding of the Synonymous Lysine Wobble Codon and Affects Type 2 Diabetes,” J. Phys. Chem. B, vol. 126, no. 6, pp. 1168–1177, Feb. 2022, doi: 10.1021/acs.jpcb.1c09053.

[16] R. Klassen, P. Grunewald, K. L. Thüring, C. Eichler, M. Helm, and R. Schaffrath, “Loss of Anticodon Wobble Uridine Modifications Affects tRNALys Function and Protein Levels in *Saccharomyces cerevisiae*,” PLoS ONE, vol. 10, no. 3, Mar. 2015, doi: 10.1371/journal.pone.0119261.

[17] M. Sundaram, P. C. Durant, and D. R. Davis, “Hypermodified Nucleosides in the Anticodon of tRNALys Stabilize a Canonical U-Turn Structure,” Biochemistry, vol. 39, no. 41, Art. no. 41, Oct. 2000, doi: 10.1021/bi0014655.

[18] A. Rozov, N. Demeshkina, I. Khusainov, E. Westhof, M. Yusupov, and G. Yusupova, “Novel base-pairing interactions at the tRNA wobble position crucial for accurate reading of the genetic code,” Nat. Commun., vol. 7, Jan. 2016, doi: 10.1038/ncomms10457.

[19] L. L. Arthur, S. Pavlovic-Djuranovic, K. S. Koutmou, R. Green, P. Szczesny, and S. Djuranovic, “Translational control by lysine-encoding A-rich sequences,” Sci. Adv., vol. 1, no. 6, Jul. 2015, doi: 10.1126/sciadv.1500154.

[20] F. Supek, B. Miñana, J. Valcárcel, T. Gabaldón, and B. Lehner, “Synonymous Mutations Frequently Act as Driver Mutations in Human Cancers,” Cell, vol. 156, no. 6, pp. 1324–1335, Mar. 2014, doi: 10.1016/j.cell.2014.01.051.

[21] V. de Crécy-Lagard and M. Jairoch, “Functions of bacterial tRNA modifications: from ubiquity to diversity,” Trends Microbiol., vol. 29, no. 1, pp. 41–53, Jan. 2021, doi: 10.1016/j.tim.2020.06.010.

[22] L. Pollo-Oliveira et al., “Loss of Elongator- and KEOPS-Dependent tRNA Modifications Leads to Severe Growth Phenotypes and Protein Aggregation in Yeast,” Biomolecules, vol. 10, no. 2, p. 322, Feb. 2020, doi: 10.3390/biom10020322.

[23] C. T. Y. Chan et al., “Reprogramming of tRNA modifications controls the oxidative stress response by codon-biased translation of proteins,” Nat. Commun., vol. 3, p. 937, Jul. 2012, doi: 10.1038/ncomms1938.

[24] A. Dannfald, J.-J. Favory, and J.-M. Deragon, “Variations in transfer and ribosomal RNA epitranscriptomic status can adapt eukaryote translation to changing physiological and environmental conditions,” RNA Biol., vol. 18, no. Suppl 1, Art. no. Suppl 1, May 2022, doi: 10.1080/15476286.2021.1931756.

[25] J. Li, W.-Y. Zhu, W.-Q. Yang, C.-T. Li, and R.-J. Liu, “The occurrence order and cross-talk of different tRNA modifications,” Sci. China Life Sci., vol. 64, no. 9, pp. 1423–1436, Sep. 2021, doi: 10.1007/s11427-020-1906-4.

Appendix A: Chapter 2 Supplemental Material

This Appendix contains supplemental figures and tables information for Chapter 2.

A.2.1 Supplementary Figures

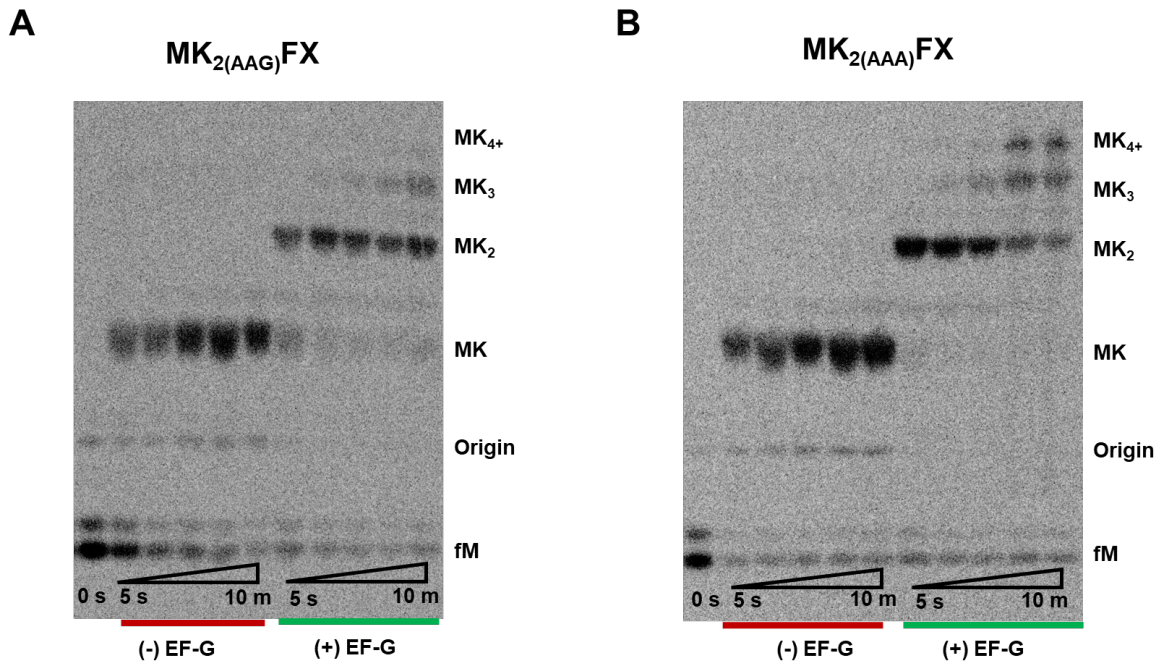

Figure A.2.1 *(A) Phosphorimage eTLC of timecourse reactions of lysine addition and ribosome sliding on MK2(AAG)FX mRNA incubated with Lys-tRNALys TCs in the absence or presence of translation factor EF-G:GTP. Ribosome sliding, as well as synthesis of products longer than di-peptide, require EF-G:GTP with sliding occurring during steps of translocation. (B) Phosphorimage eTLC of timecourse reactions of lysine addition and ribosome sliding on MK2(AAA)FX mRNA incubated with Lys-tRNALys TCs in the absence or presence of translation factor EF-G:GTP. Ribosome sliding, as well as synthesis of products longer than di-peptide, require EF-G:GTP with sliding occurring during steps of translocation. In addition, sliding product is formed more robustly compared to AAG codons.*

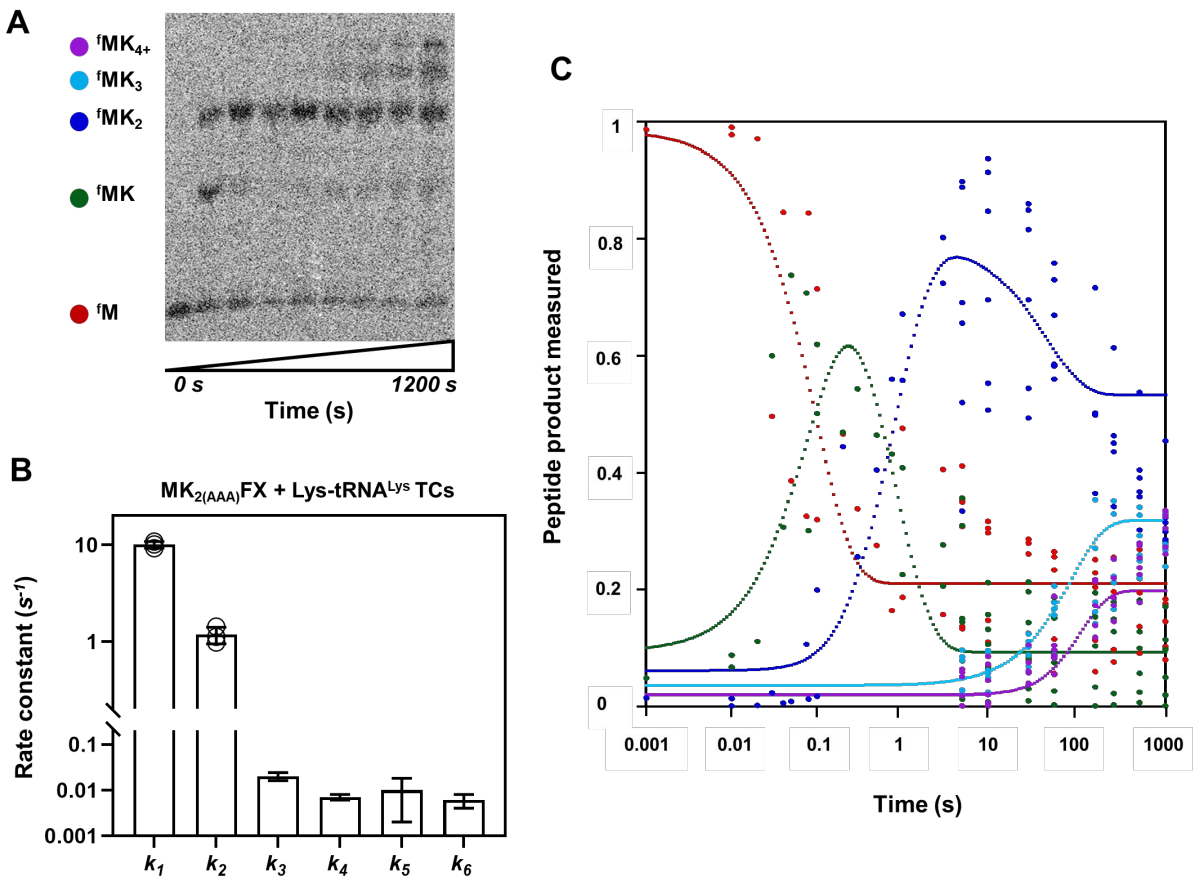

Figure A.2.2 *(A) Phosphorimage eTLC of time course reaction of ribosome sliding on MK2(AAA)FX mRNA incubated with Lys-tRNALys TCs, as displayed in Figure 3C. Peptide products, indicated by color, were quantified with ImageQuant and then data sets used for global analysis in KinTek Explorer as seen in panel C, with corresponding colors. This eTLC is represented again here as these panels offer a representative flowthrough of the methodology used in the main text from which mechanism and rate constants are derived. (B) Rate constants of ribosome sliding on MK2(AAA)FX mRNA using Lys-tRNALys TCs (in the presence of EF-G:GTP), as defined by the proposed mechanism presented in Supplemental Scheme 3A. Rate constants for sliding or unproductive ribosome states (k3, k4, k5, and k6) were obtained via global analysis simulated fitting (as seen in panel C) to determine single rate constants for each step in the proposed Scheme in S3A. Rate constants k1 and k2 were obtained by fitting triplicate data sets of fM disappearance and fMK formation/disappearance in Kaleidagraph software [fM = a1*(1 – (e -k1 (t)) + b ; fMK = a1*(1 – (e -k1 (t)) + a2*(1 – (e -k2 (t)) + b]. (C) Raw data plot time courses (normalized to peptide end-points) of peptide products synthesized during ribosome sliding as exampled in panel A. Global analysis was performed on such data sets to obtain rate constants for lysine addition and ribosome sliding on MK2(AAA)FX mRNA (panel B) as described by the mechanism in Scheme S3A.*

A – *Proposed mechanism for ribosome sliding*

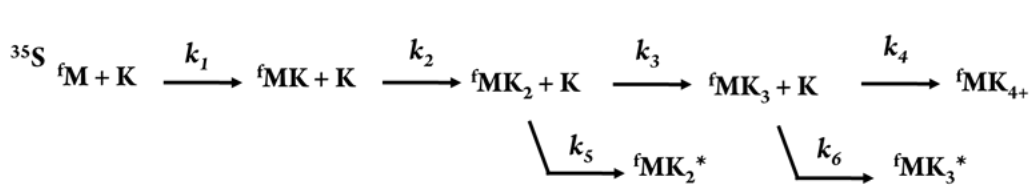

Dipeptide formation: k_1
Tri-peptide formation: k_2
Ribosome sliding and frameshift:
- -3 sliding/frameshift event: k_3, k_4
- Unproductive sliding event(s): k_5, k_6

fMK_2* and fMK_3* represent the first and second unproductive states during sliding, respectfully.

B – *Proposed mechanism for ribosome sliding: Reaction steps with TC substrate concentration subject to consumption*

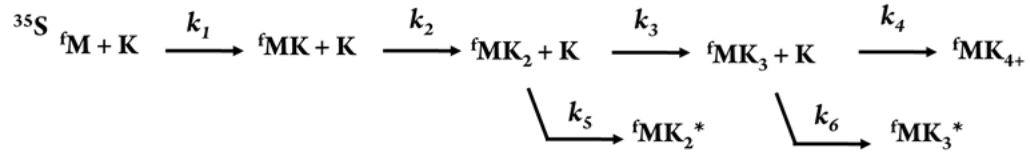

Dipeptide formation: k_1
Tri-peptide formation: k_2
Ribosome sliding and frameshift:
- -3 sliding/frameshift event: k_3, k_4
- Unproductive sliding event(s): k_5, k_6

fMK_2* and fMK_3* represent the first and second unproductive states during sliding, respectfully.
Mechanism tested to see if high concentration [30 uM] of Lys-tRNA^{Lys} TCs in assays kept saturating conditions for all lysine addition steps, or if lysine was being consumed more strongly making reaction steps bi-substrate first-order reactions.

C – *Proposed mechanism for ribosome sliding: Pseudo-first order reaction steps with saturating TC substrate (non-productive state formation)*

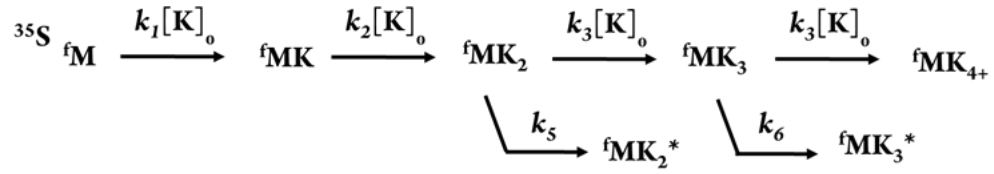

fMK_2* and fMK_3* represent the first and second unproductive states during sliding, respectfully.
Mechanism tested to when high concentration [30 uM] of Lys-tRNA^{Lys} TCs in assays is in fact saturating conditions for all lysine addition steps.

D – *Proposed mechanism for ribosome sliding: Pseudo-first order reaction steps with saturating TC substrate (non-productive state formation)*

Mechanism tested to when high concentration [30 uM] of Lys-tRNA^{Lys} TCs in assays is in fact saturating conditions for all lysine addition steps, but no non-productive state products are formed.

Figure A.2.3 *Tested schemes for ribosome sliding on poly(A) from in vitro translation assays. (A-D) These schemes describe tested schemes/mechanisms for subsequent amino acid additions by a ribosome translating on a poly(A) containing mRNA – as displayed in Figure S2. The scheme contains parameters obtainable from the experiments presented here with sets of conditions and parameters used in each scheme tested as detailed above.*

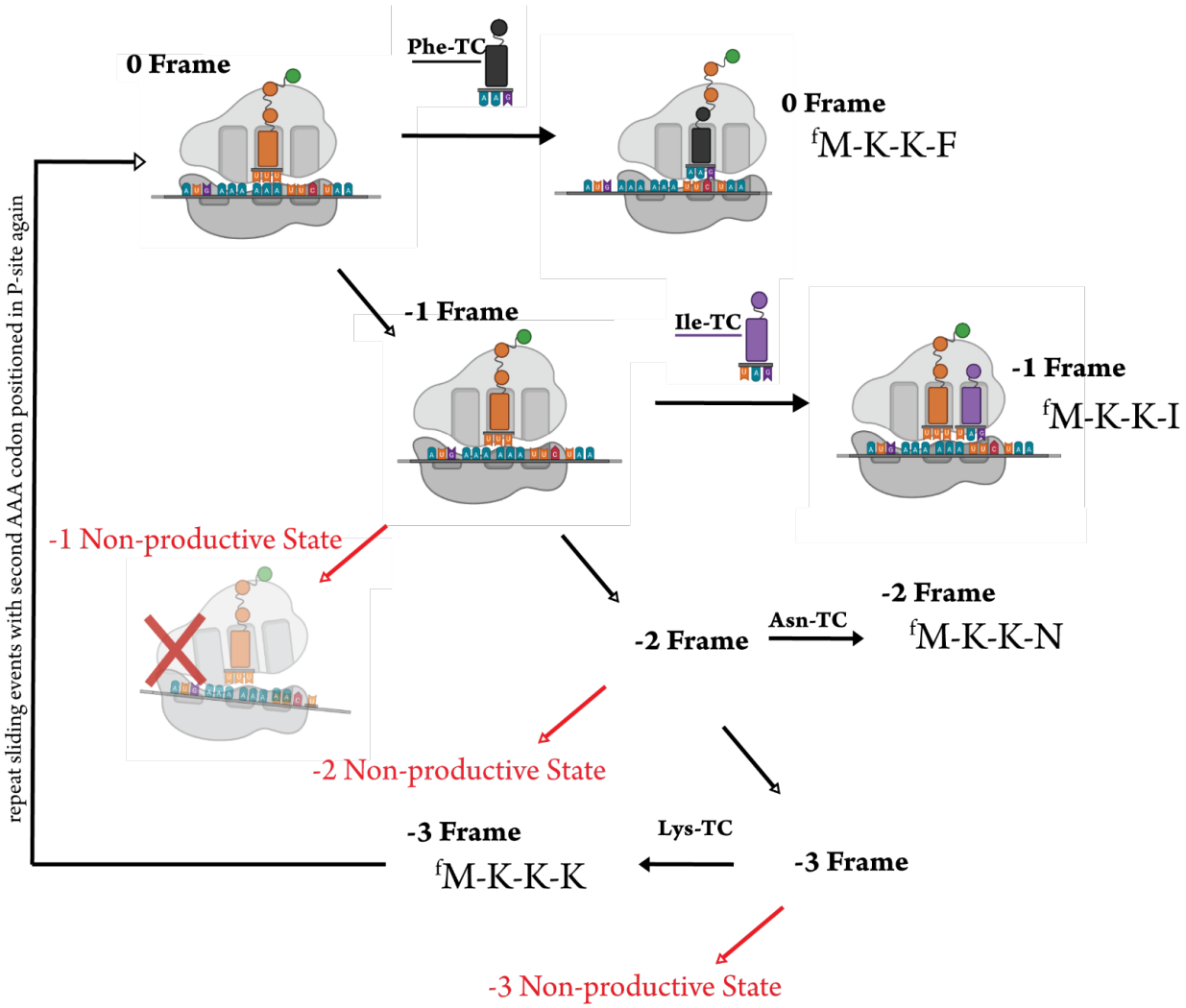

Figure A.2.4 *Scheme of ribosome sliding on poly(A) (example given on MK2(AAA)FX encoding mRNA template). After successfully decoding two AAA codons and incorporating two lysine amino acids, the ribosome is positioned with the next codon in the A-site (UUC). If the cognate amino acyl-tRNA is available (Phe-tRNAPhe) it is incorporated, making product in the 0-frame. In the absence of this available aa-tRNAaa, the ribosome will shift upstream 1 nucleotide into the -1 frame after a period idling on poly(A) and this will change the identity of the codon in the A site (now AUU). This has the potential to code for a new aa-tRNAaa and, if present, will accommodate the aa-tRNAaa and the ribosome will continue translating in the -1 frame. Similarly, absence of the -1 frame aa-tRNAaa (Ile-tRNAIle) will allow the ribosome to continue moving upstream, in a single nucleotide interval (-2 frame). In addition, the ribosome has the potential to enter a non-productive state during the movement into or from the -1 frame in which the ribosome may enter a rotational state that is unable to accommodate a cognate aa-tRNAaa. Similar to the -1 frame event, the ribosome having a now -2 codon in the A-site (now AAU) will code for a new aa-tRNAaa (Asn-tRNAAsn) or enter a non-productive state. Once again, if the aa-tRNAaa is absent and the ribosome idles on the poly(A) it will move another nucleotide upstream (now 3 nucleotides, or full codon) in which AAA will be positioned in the A-site. As Lys-tRNALys is present in such assays, the ribosome will add another lysine or will enter a non-productive state. If lysine is added in this manner, the ribosome will be in the 0-frame once again and can repeat the cycle as described.*

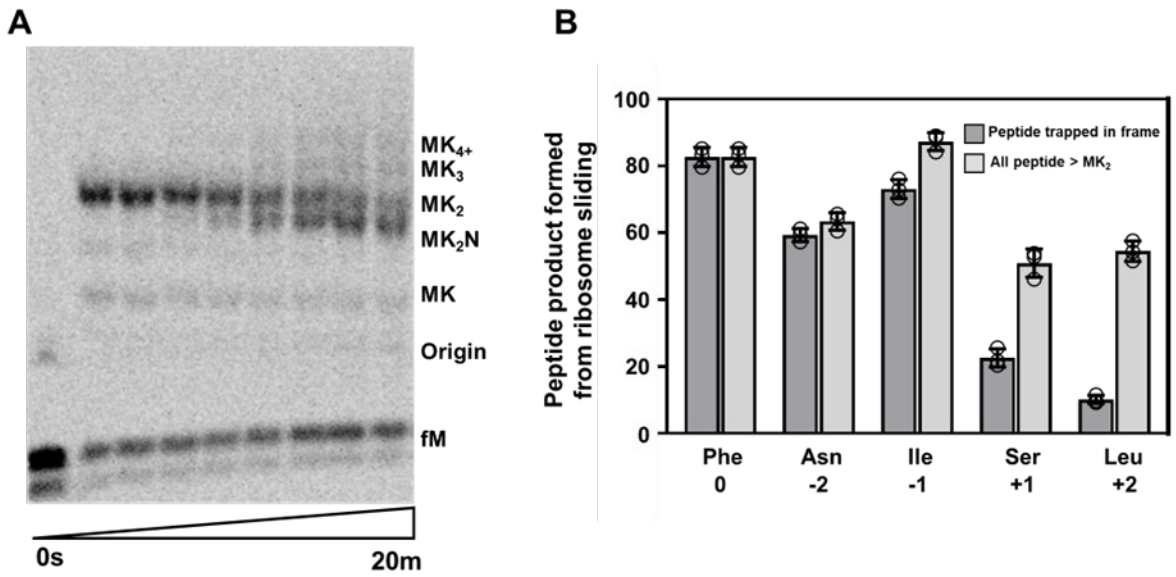

Figure A.2.5 *(A) Representative phosphorimage eTLC of time course reaction of ribosome sliding and frameshift on MK2(AAA)FX mRNA incubated with transcribed Lys-tRNALys and Asn-tRNAAsn TCs, indicating trapped frameshift products in the -2 frame (MK2N). (B) Each frameshift study reported compared levels of peptide synthesized from frameshifting events to fraction of peptide synthesized from ribosome sliding (greater than tripeptide [MK2]) from ICs made with MK2(AAA)FX mRNA after 20 minutes. This was done to assess propensity of frameshift into specific frames versus normal amino acid addition or general ribosome sliding on MK2(AAA)FX mRNA. For instance, in the case of the 0 Frame encoding for Phe to form MK2F tetrapeptide it was observed that ~80% of peptide species synthesized in the assays were longer than MK2. Of these extended products all peptide synthesized was MK2F tetrapeptide, indicating normal and efficient Phe addition in the 0 frame. In the case of the -2 frame, adding Asn (as observed in panel A), there was ~62% of sliding peptide product observed versus total peptide species observed ([MK3 + MK2N + MK4+] / [MK + MK2 + MK3 + MK2N + MK4+]). However MK2N was the predominant species synthesized as it comprised ~60% of total peptide product synthesized ([MK2N] / [MK + MK2 + MK3 + MK2N + MK4+]). This indicates a strong preference to frameshift into, and be trapped in, the -2 frame when Asn-tRNAAsn is available. A similar trend is observed for Ile and the -1 frame, although there is a stronger sliding phenotype observed for -1 frameshifting and sliding. Ser (+1 frame) and Leu (+2 frame) resulted in very little frameshift product as well as extended sliding peptide product.*

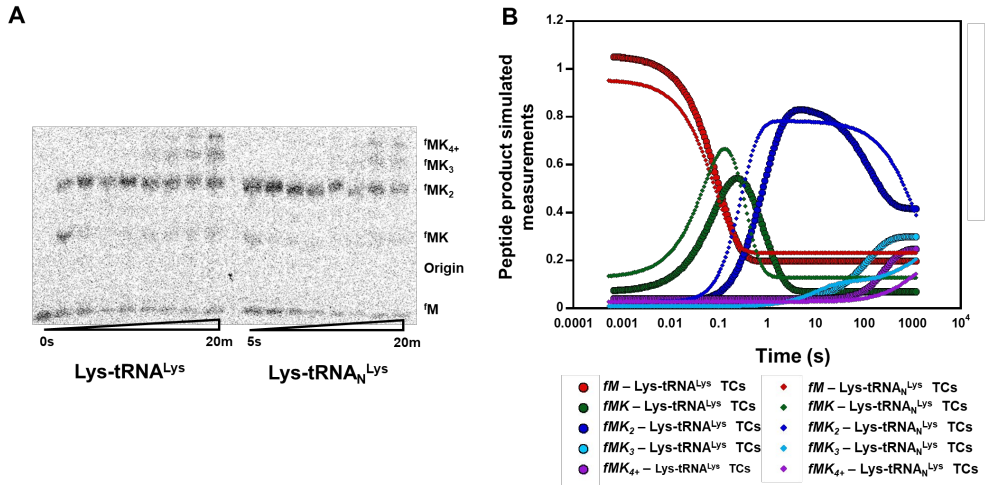

Figure A.2.6 *(A) Full representative phosphorimage eTLC of time course reaction of ribosome sliding on MK2(AAA)FX mRNA incubated with Lys-tRNALys and Lys-tRNANLys TCs (as shown in Figure 3C and Figure S2A). (B) Global analysis was performed on all data sets for assays described in panel A (discussed in methods and Figure S2) and subsequent simulated fits were then overlayed and compared here to view the effect native tRNA modifications have on poly-lysine synthesis when the ribosome reads mRNA containing two iterative AAA codons. Each data set for peptide species was normalized to endpoint (or total peptide product synthesized in the assays) as reflected in the y-axis scale. Synthesis of MK and MK2 is faster on MK2(AAA)FX when Lys-tRNANLys TCs are used although there is a clear sliding defect with much less MK3 and MK4+ peptide formed compared to when Lys-tRNALys TCs are used.*

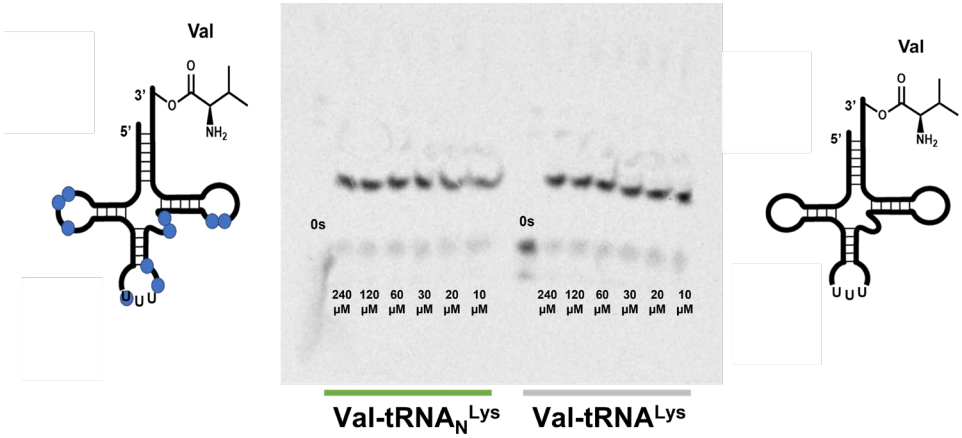

Figure A.2.7 *(A) To assess if translation factor EF-Tu:GTP would be selective against incorporating mis-acylated tRNALys, translation assays were performed to 5 minute endpoints with varying concentrations of EF-Tu:GTP. Assays used in this main work of this study had final concentrations of 30 uM EF-Tu:GTP which was more than sufficient to incorporate mis-acylated tRNALys, regardless of modification status (Val-tRNALys on the left representing Native tRNALys with example sites in which modified nucleosides are located for E. coli tRNALysUUU). The phosphorimage eTLC was analyzed using ImageQuant and all samples resulted in at least 88.9% 35SfMet turnover to synthesize 35SfMet-Val on a MK2(AAA)FX mRNA, regardless of EF-Tu:GTP concentration. These results suggest that EF-Tu:GTP does not select against incorporating Val-tRNALys variants in our assays for this study.*

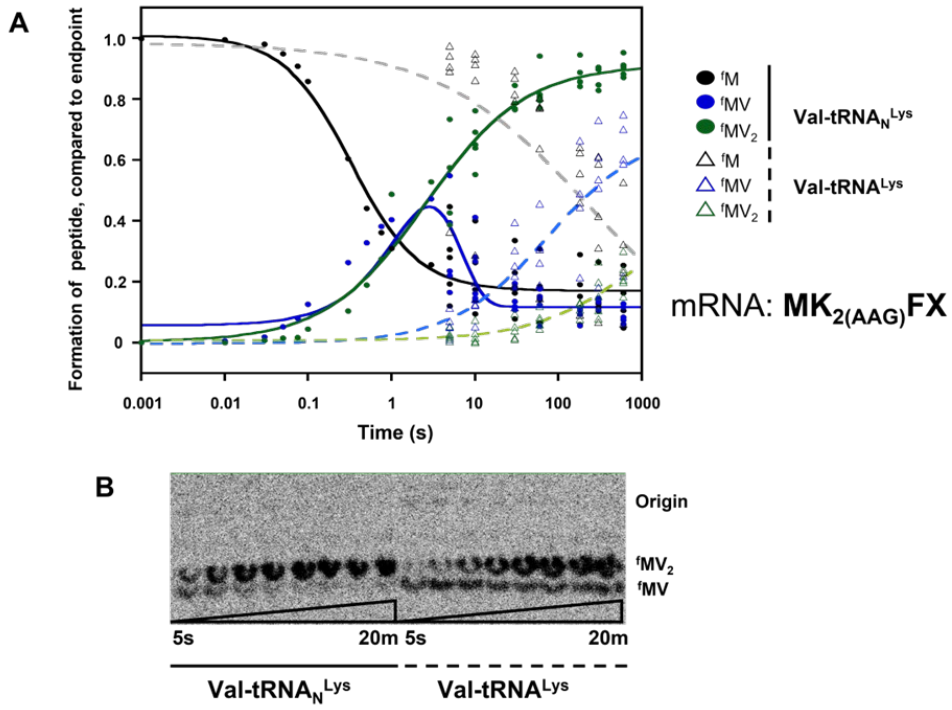

Figure A.2.8 *(A) Analysis performed on all data sets for assays using AUG-AAG-AAG-UUC-UAA mRNA, using either transcribed (Val-tRNALys) or native (Val-tRNANLys) mis-acylated lysyl TCs. Simulated fits from global analysis are overlaid onto data sets with each tRNA species used, and peptide species formed over time in the translation reactions, indicated. (B) Representative phosphorimage eTLC of time course reaction of valine addition on MK2(AAG)FX mRNA incubated with Val-tRNALys or Val-tRNANLys TCs. Lack of modifications to tRNALys results in significantly slowed formation of MV and MV2 peptides from mis-acylated Val-tRNALys compared to Val-tRNANLys. In addition, as also seen in panel A, there is a drastic decrease in endpoints of di- and tri-peptide products formed when Val-tRNALys is used to decode the AAG lysine encoding codon.*

A.2.2 SUPPLEMENTARY TABLES

Table A.2.1 *Rate constants for valine addition on lysine encoding mRNAs*

mRNA construct	$MK_{2(AAA)}FX$		$MK_{2(AAG)}FX$		MV_2FX
tRNA TCs	$Val\text{-}tRNA^{Lys}$	$Val\text{-}tRNA_N^{Lys}$	$Val\text{-}tRNA^{Lys}$	$Val\text{-}tRNA_N^{Lys}$	$Val\text{-}tRNA^{Val}$
Rate constant (s^{-1})					
k_1	2.5± 0.3	2.9 ± 0.6	0.06 ± 0.001	4.4 ± 0.07	7.3 ± 0.9
k_2	0.4 ± 0.1	1.7 ± 0.4	0.0003 ± 0.00002	1.2 ± 0.02	1.9 ± 0.4
$k_{3,obs}$	0.002± 0.00005	0.0002 ± 0.00002	-	-	-

Table A.2.2 *Rate constants for lysine addition during ribosome sliding on m6A containing mRNAs*

m^{6}A containing mRNA	AAm^{6}A-AAA	AAA-m^{6}AAA	AAA-Am^{6}AA	AAA-AAm^{6}A
Rate constant (s^{-1})				
k_1	3.0 ± 0.2	3.2 ± 0.003	11.6 ± 0.8	18.0 ± 2.3
k_2	0.7 ± 0.1	0.2 ± 0.003	0.2 ± 0.003	0.46 ± 0.006
k_3	0.0005 ± 0.0001	0.0006 ± 0.0002	0.0009 ± 0.0003	0.001 ± 0.0001
k_4	0.003 ± 0.0002	0.09 ± 0.02	0.02 ± 0.004	0.1 ± 0.06
k_5	0.0002 ± 0.0001	0.0005 ± 0.0002	0.0007 ± 0.0002	0.001 ± 0.0001
k_6	0.009 ± 0.002	0.1 ± 0.03	0.07 ± 0.02	0.08 ± 0.008

Table A.2.3 *Frequency of m6A installation in coding sequences‡*

Number of consecutive nucleotides (As)	Instances of consecutive Adenosines (A)	Instances with m^{6}A installed‡‡
4	385832	165
5	125346	60
6	34207	15
7	9237	5
8	2286	2

‡ Frequency of consecutive adenosines as exist in the human hg37.75_cds coding sequence reference genome.

‡‡ Frequency of m6A installation in consecutive adenosines as reported in human embryonic kidney cells (HEK293) (53) and human liver, brain, and lung tissues (54).

A.2.3 REFERENCES

53. Linder, B., Grozhik, A. V., Olarerin-George, A. O., Meydan, C., Mason, C. E., and Jaffrey, S. R. (2015) Single-nucleotide resolution mapping of m6A and m6Am throughout the transcriptome. Nat. Methods. 12, 767–772

54. Zhang, Z., Chen, L.-Q., Zhao, Y.-L., Yang, C.-G., Roundtree, I. A., Zhang, Z., Ren, J., Xie, W., He, C., and Luo, G.-Z. (2019) Single-base mapping of m6A by an antibody-independent method. Sci. Adv. 5, eaax0250

Appendix B: Chapter 4 Supplemental Material

This Appendix contains supplemental figures and tables information for Chapter 4.

B.4.1 Supplementary Figures

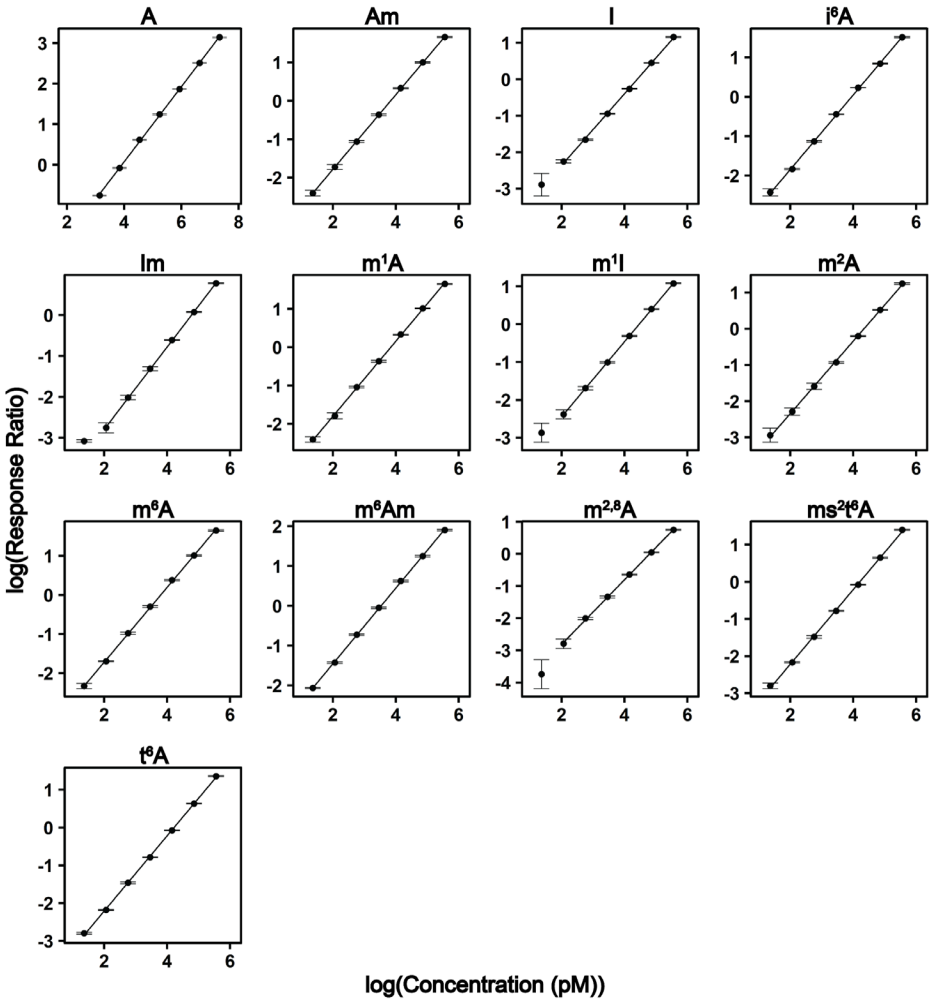

Figure B.4.1 *Calibration curves used to quantify adenosine modification concentrations. Calibration curves of adenosine ribonucleoside modifications plotted in log(response ratio) vs. log(concentration (pM)). The linear regression, limit of detection, and R2 are displayed in Supplemental Table S1 (B.4.1).*

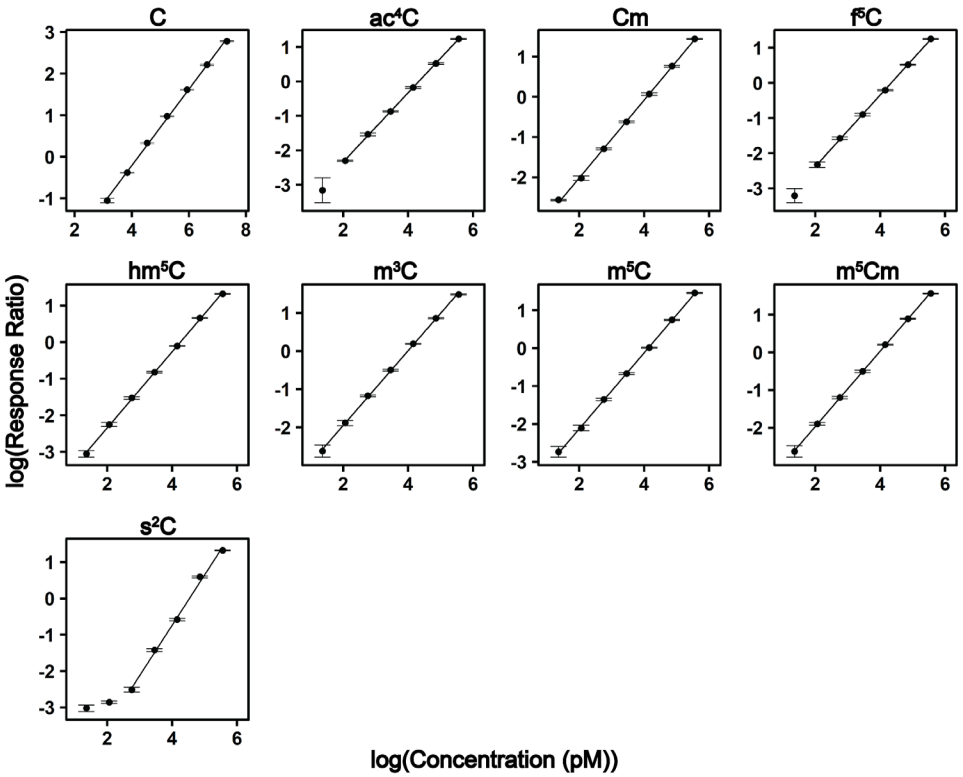

Figure B.4.2 *Calibration curves used to quantify cytidine modification concentrations. Calibration curves of cytidine ribonucleoside modifications plotted in log(response ratio) vs. log(concentration (pM)). The linear regression, limit of detection, and R2 are displayed in Supplemental Table S1 (B.4.1).*

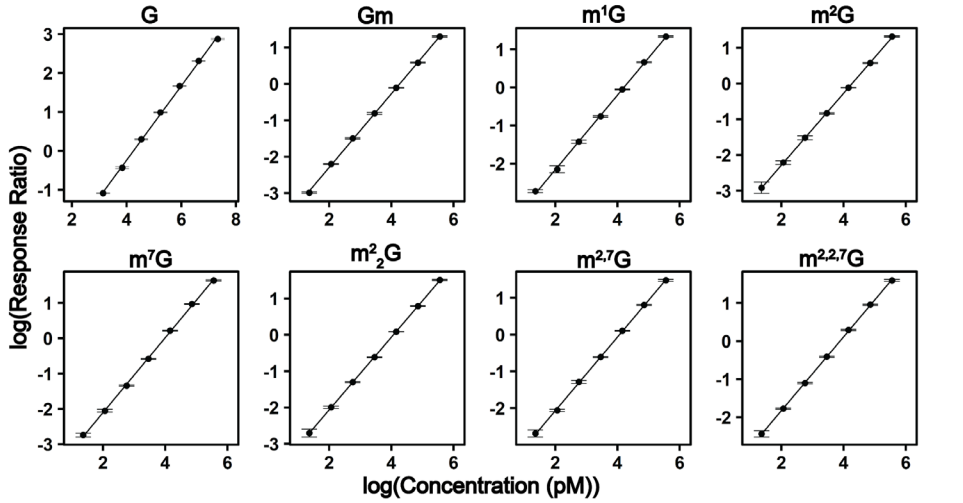

Figure B.4.3 *Calibration curves used to quantify guanosine modification concentrations. Calibration curves of guanosine ribonucleoside modifications plotted in log(response ratio) vs. log(concentration (pM)). The linear regression, limit of detection, and R2 are displayed in Supplemental Table S1 (B.4.1).*

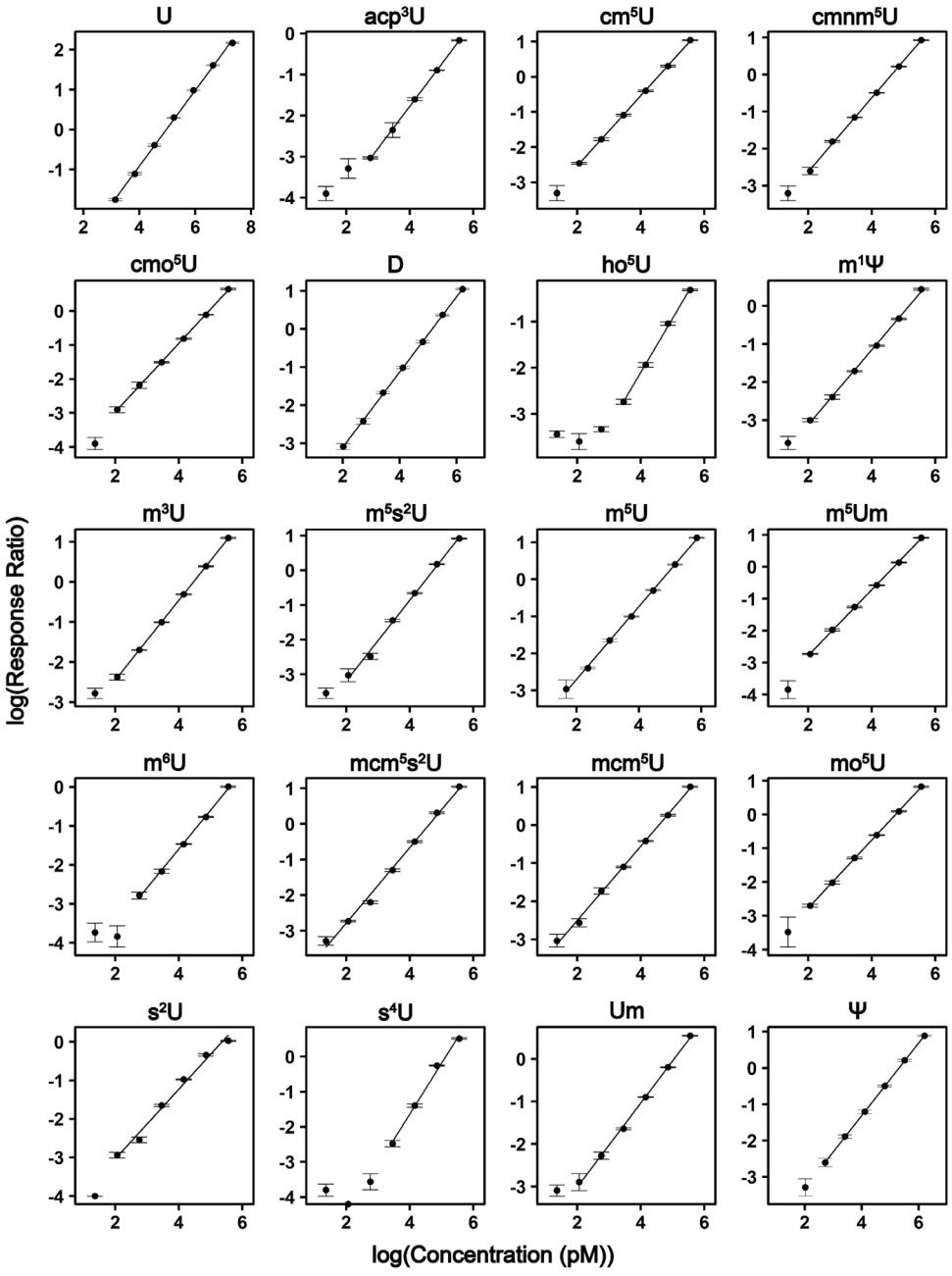

Figure B.4.4 *Calibration curves used to quantify uridine modification concentrations. Calibration curves of uridine ribonucleoside modifications plotted in log(response ratio) vs. log(concentration (pM)). The linear regression, limit of detection, and R2 are displayed in Supplemental Table S1 (B.4.1).*

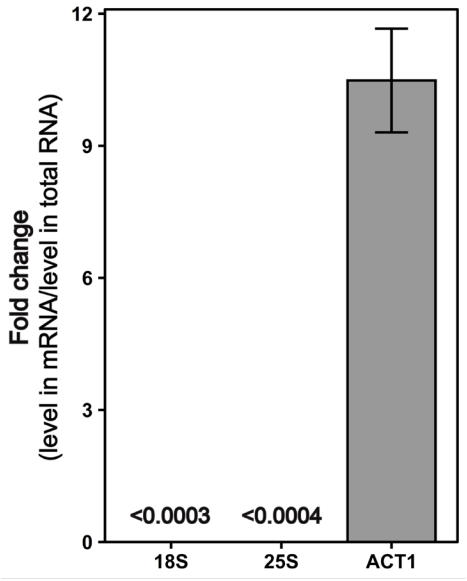

Figure B.4.5 *Ribosomal RNAs are depleted in three-stage purified mRNA. qRT-PCR demonstrates that the 18S and 25S rRNAs are depleted by greater than 3000-fold in the purified mRNA. Contrarily, ACT1 is enriched by greater than 10-fold. This data in addition to the Bioanalyzer electropherograms, RNA-seq, and LC-MS/MS proves that our three-stage purified mRNA is highly pure.*

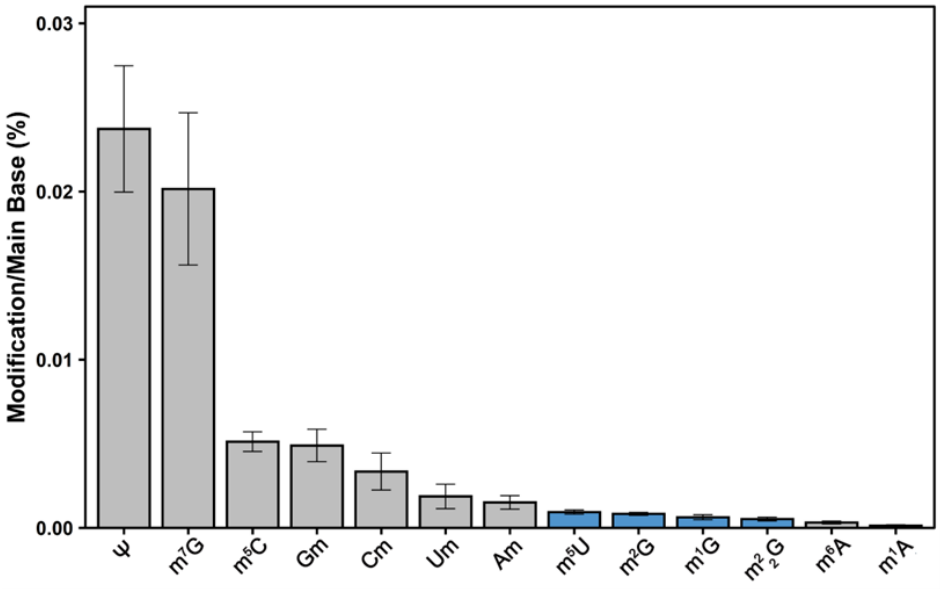

Figure B.4.6 *Ribonucleoside modification abundance in the three-stage purified mRNA. The ribonucleoside abundance is represented as modification/main base% (i.e., m7G/G%) where pseudouridine was the most abundant modification detected. All modifications detected were previously detected in purified mRNA besides for the three methylated guanosine modifications displayed in blue (m1G, m2G, and m22G). Our improvements regarding LC-MS/MS sensitivity and mRNA purity enables us to confidently claim these modifications exist with S. cerevisiae mRNA.*

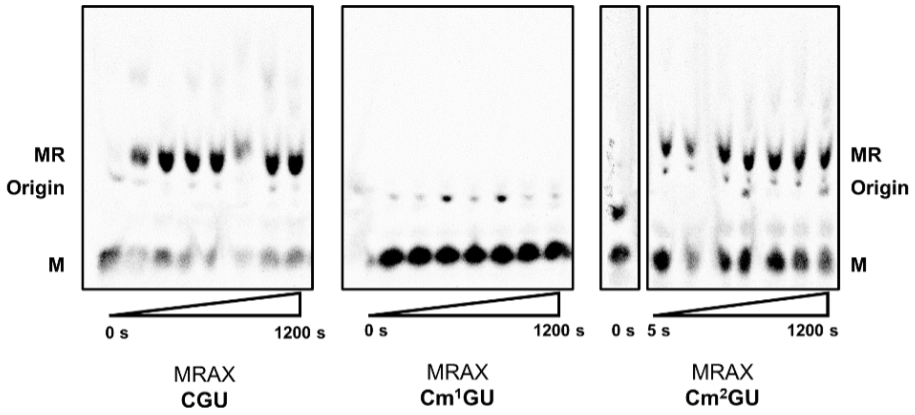

Figure B.4.7 *Electrophoretic TLC displaying the translation products of CGU, Cm1GU, and Cm2GU codons in the presence of arginine tRNA (ArgTC), forming MR dipeptide over the span of 1200 seconds.*

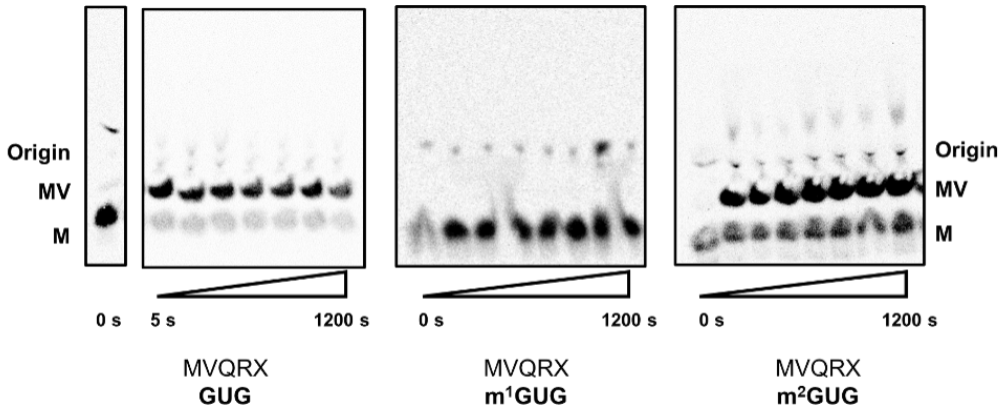

Figure B.4.8 *Electrophoretic TLC displaying the translation products of GUG, m1GUG, and m2GUG codons in the presence of valine tRNA (ValTC), forming MV dipeptide over the span of 1200 seconds.*

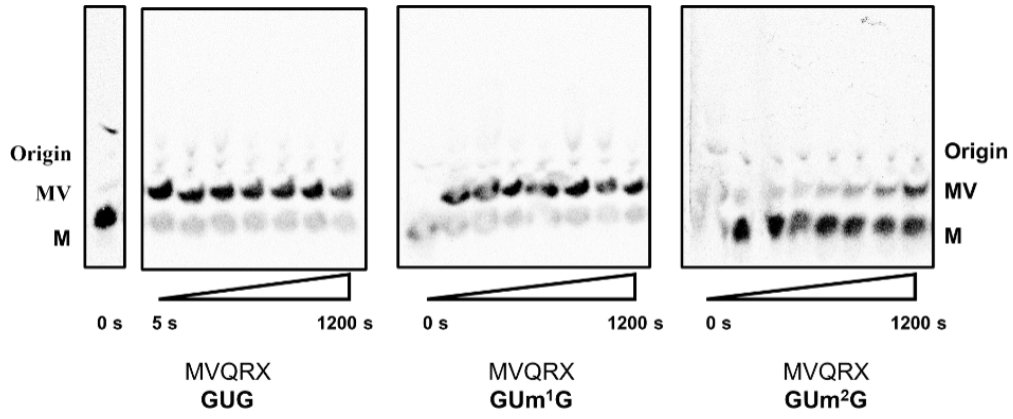

Figure B.4.9 *Electrophoretic TLC displaying the translation products of GUG, GUm1G, and GUm2G codons in the presence of valine tRNA (ValTC), forming MV dipeptide over the span of 1200 seconds.*

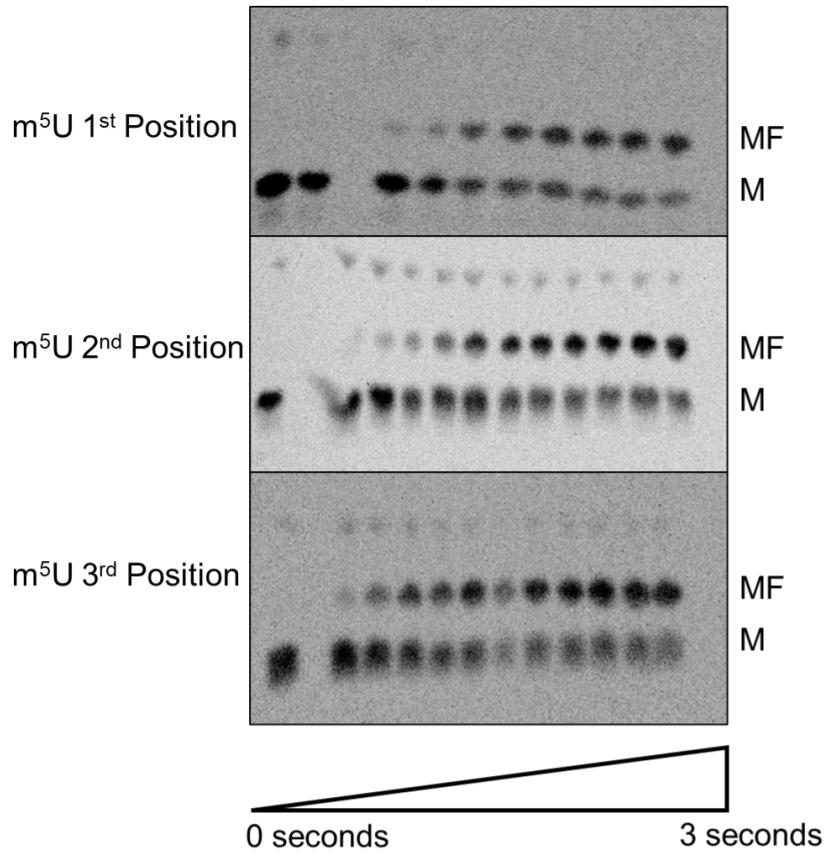

Figure B.4.10 *Electrophoretic TLC displaying the translation products of m5U messages in the presence of phenylalanine tRNA (PheTC), forming MF dipeptide over the span of 3 seconds*

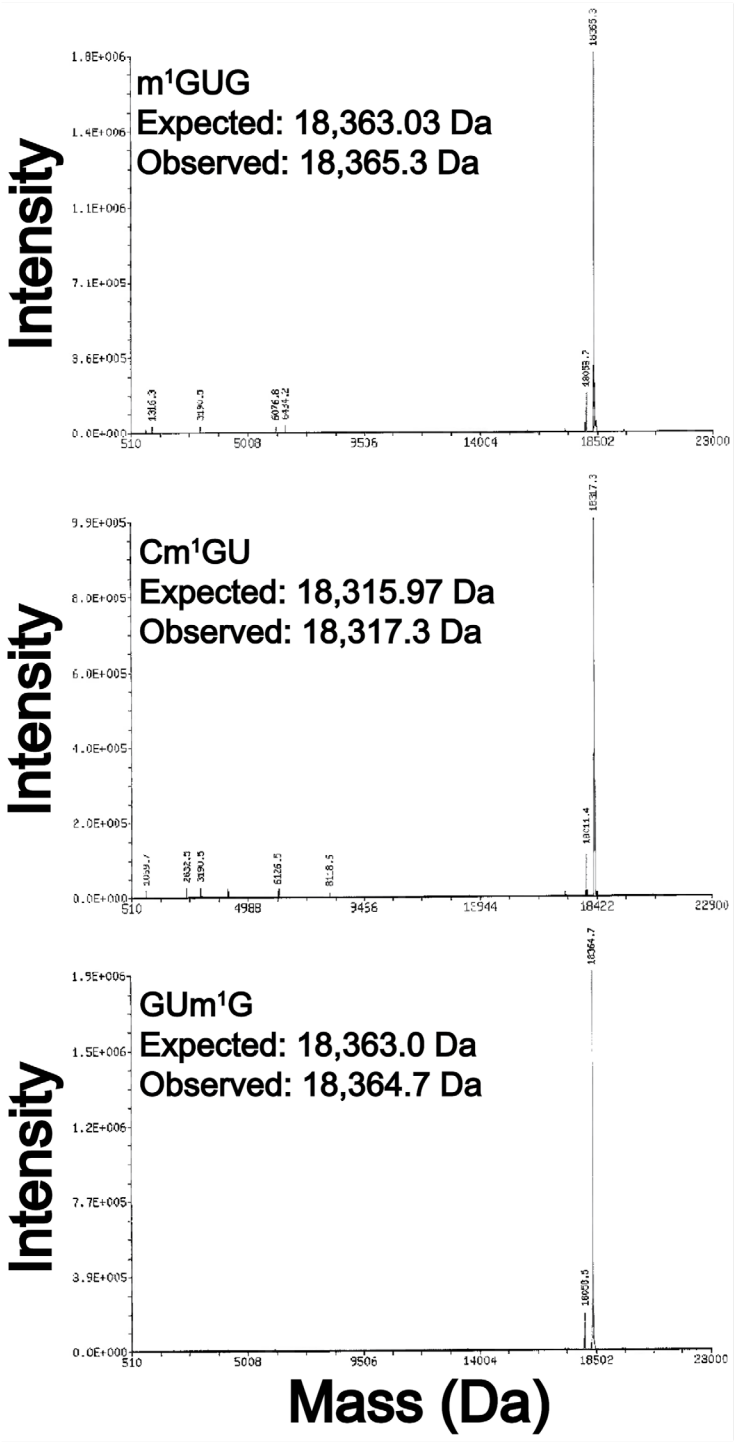

Figure B.4.11 *Deconvoluted ESI-MS spectra of modified oligonucleotides provided by Dharmacon to confirm purity. The expected and observed masses of the m1GUG, Cm1GU, and GUm1G modified codon oligonucleotides are found in the top, middle, and bottom panels, respectively. Minor n-1 oligonucleotides products were detected, but they would not affect the in vitro translation assays because the nucleotide loss occurs in the non-coded region of the purchased mRNA transcript.*

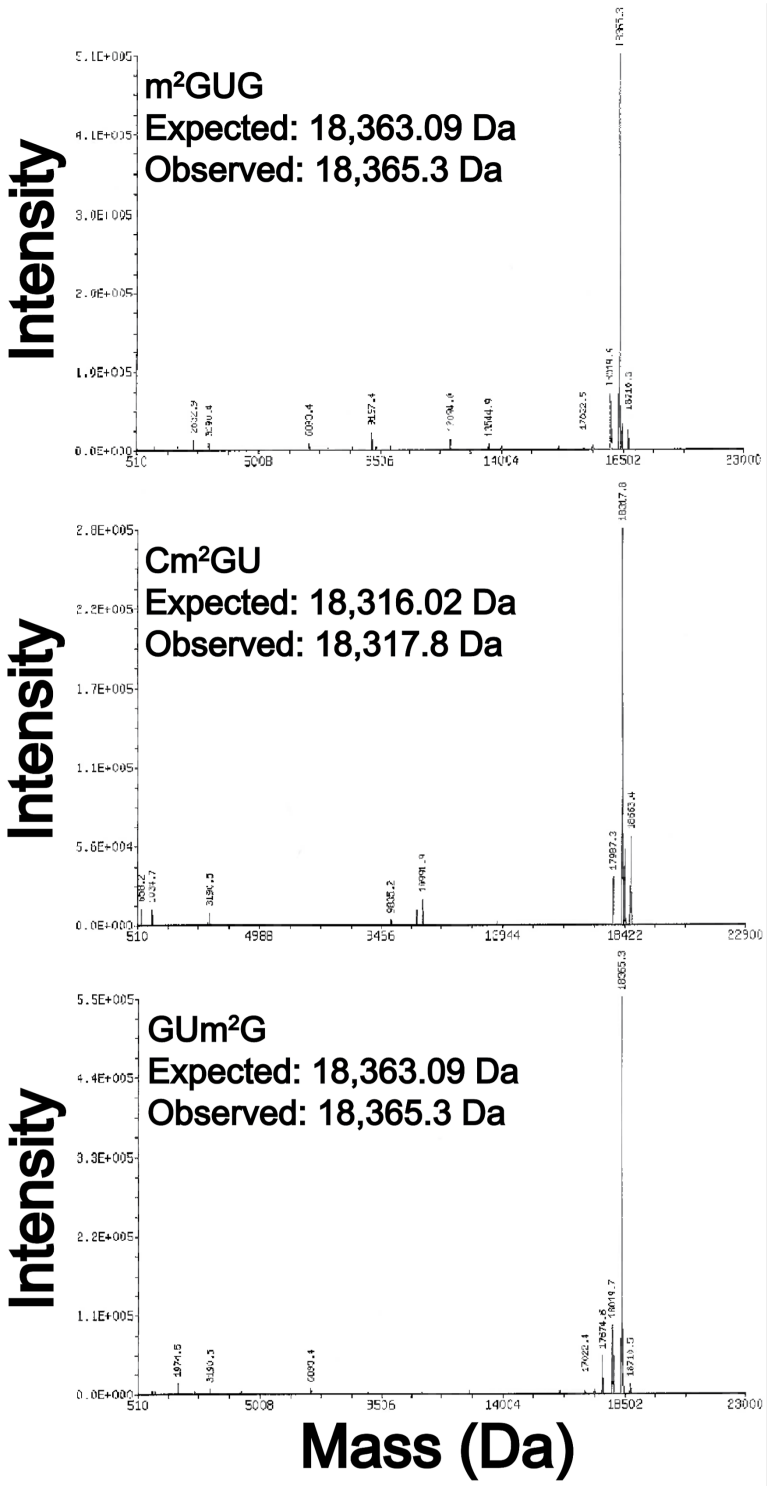

Figure B.4.12 *Deconvoluted ESI-MS spectra of modified oligonucleotides provided by Dharmacon to confirm purity. The expected and observed masses of the m2GUG, Cm2GU, and GUm2G modified codon oligonucleotides are found in the top, middle, and bottom panels, respectively. Minor n-1 oligonucleotides products were detected, but they would not affect the in vitro translation assays because the nucleotide loss occurs in the non-coded region of the purchased mRNA transcript*

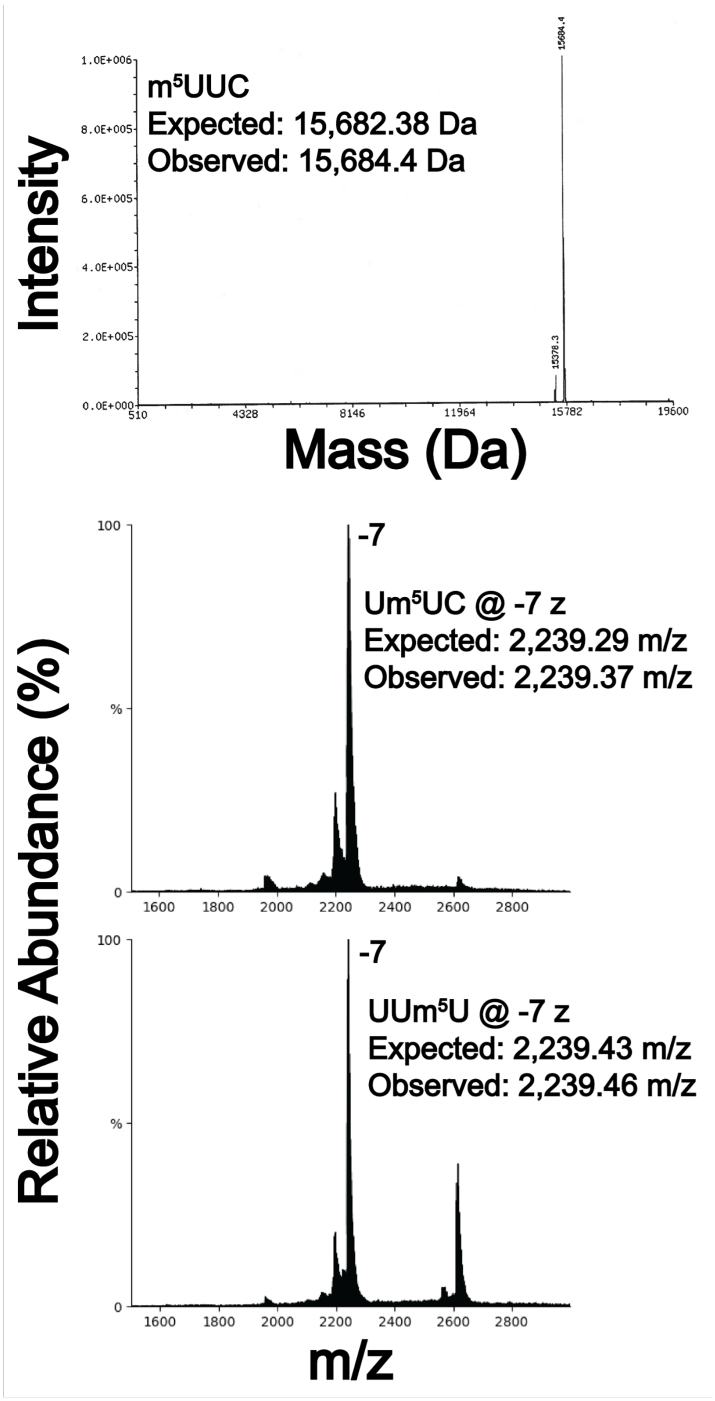

Figure B.4.13 *Deconvoluted ESI-MS spectra of m5UUC modified codon oligonucleotides provided by Dharmacon to confirm purity (top panel). Full scan spectra of Um5UC (middle) and UUm5U (bottom) modified codon oligonucleotide. The corresponding expected and observed mass (Da) or mass-to-charge (m/z) is displayed for each spectrum. Minor n-1 oligonucleotides products were detected, but they would not affect the in vitro translation assays because the nucleotide loss occurs in the non-coded region of the purchased mRNA transcript.*

B.4.2 SUPPLEMENTARY TABLES

Table B.4.1 *Linear regression, limit of detection, and R2 calculated from calibration curves made from nucleoside standards. Y corresponds to log(response ratio) and X corresponds to log(concentration(pM)).*

Nucleoside	Linear Regression	Limit of Detection (amol)	R^2
A	**Y** = 0.9264**X** - 3.632	Not Determined	>0.999
ac^{4}C	**Y** = 1.005**X** - 4.344	43	>0.999
acp^{3}U	**Y** = 1.027**X** - 5.882	1000	0.995
Am	**Y** = 0.972**X** - 3.727	7	>0.999
C	**Y** = 0.9185**X** - 3.884	Not Determined	0.998
Cm	**Y** = 0.9685**X** - 3.953	41	0.998
cm^{5}U	**Y** = 0.998**X** - 4.53	21	>0.999
cmnm^{5}U	**Y** = 0.9981**X** - 4.62	160	0.998
cmo^{5}U	**Y** = 1.007**X** - 4.982	67	0.998
D	**Y** = 0.9866**X** - 5.073	530	>0.999
f^{5}C	**Y** = 1.017**X** - 4.412	21	>0.999
G	**Y** = 0.956**X** - 4.061	Not Determined	0.998
Gm	**Y** = 1.012**X** - 4.319	18	>0.999
hm^{5}C	**Y** = 1.04**X** - 4.424	18	>0.999
ho^{5}U	**Y** = 1.168**X** - 6.776	3300	0.997
I	**Y** = 0.9827**X** - 4.325	170	>0.999
i^{6}A	**Y** = 0.946**X** - 3.735	44	>0.999
Im	**Y** = 1.007**X** - 4.808	150	0.998
m^{1}A	**Y** = 0.9792**X** - 3.76	4	0.999
m^{1}G	**Y** = 0.9791**X** - 4.117	9	0.999
m^{1}I	**Y** = 0.9922**X** - 4.429	50	0.999
m$^1\Psi$	**Y** = 0.9835**X** - 5.088	250	0.998
m$_3$G	**Y** = 0.9686**X** - 3.761	4	>0.999
m$^2{}_2$G	**Y** = 1.001**X** - 4.064	10	>0.999
m^{2,7}G	**Y** = 1.002**X** - 4.073	8	>0.999
m^{2,8}A	**Y** = 1.004**X** - 4.822	79	0.998
m^{2}A	**Y** = 0.9996**X** - 4.341	24	0.997
m^{2}G	**Y** = 1.004**X** - 4.29	26	0.998
m^{3}C	**Y** = 0.9792**X** - 3.906	8	0.998
m^{3}U	**Y** = 0.9944**X** - 4.439	45	>0.999
m^{5}C	**Y** = 1.005**X** - 4.139	21	0.998
m^{5}Cm	**Y** = 1.00**X** - 3.97	14	0.999
m^{5}s^{2}U	**Y** = 1.164**X** - 5.52	250	0.993
m^{5}U	**Y** = 0.9825**X** - 4.665	72	0.996

m^5Um	**Y** = 1.029**X** - 4.836	40	>0.999
m^6A	**Y** = 0.9558**X** - 3.629	3	>0.999
m^6Am	**Y** = 0.9503**X** - 3.356	4	>0.999
m^6U	**Y** = 0.9981**X** - 5.588	640	0.997
m^7G	**Y** = 1.06**X** - 4.22	11	>0.999
mcm^5s^2U	**Y** = 1.061**X** - 4.909	83	0.993
mcm^5U	**Y** = 0.9751**X** - 4.457	29	0.995
mo^5U	**Y** = 1.007**X** - 4.786	67	>0.999
ms^2t^6A	**Y** = 1.004**X** - 4.223	21	>0.999
Ψ	**Y** = 1.00**X** - 5.313	930	0.998
s^2C	**Y** = 1.386**X** - 6.284	1100	0.995
s^2U	**Y** = 0.9031**X** - 4.843	120	0.986
s^4U	**Y** = 1.448**X** - 7.433	2000	0.992
t^6A	**Y** = 0.9956**X** - 4.201	21	>0.999
U	**Y** = 0.9492**X** - 4.714	Not Determined	0.999
Um	**Y** = 0.9891**X** - 4.993	170	0.995

Table B.4.2 *Ribonucleoside standard concentrations displayed in Figure 1A extracted ion chromatogram*

Nucleoside	Peak Label	Concentration (nM)
A	26	6.9
ac^4C	39	14.4
acp^3U	10	72
Am	40	2.9
C	1	6.9
Cm	15	14.4
cm^5U	16	14.4
$cmnm^5U$	5	14.4
cmo^5U	18	72
D	2	64.8
f^5C	23	14.4
G	20	6.9
Gm	34	14.4
hm^5C	3	14.4
ho^5U	9	360
I	19	14.4
i^6A	50	2.9
Im	32	14.4

m^1A	7	2.9
m^1G	33	14.4
m^1I	35	14.4
$m^1\Psi$	14	72
m_3G	36	2.9
$m^2{}_2G$	45	2.9
$m^{2,7}G$	25	2.9
$m^{2,8}A$	43	14.4
m^2A	30	14.4
m^2G	38	14.4
m^3C	6	2.9
m^3U	31	14.4
m^5C	8	2.9
m^5Cm	21	2.9
m^5s^2U	41	14.4
m^5U	22	32
m^5Um	42	14.4
m^6A	44	2.9
m^6Am	47	0.58
m^6U	17	72
m^7G	12	2.9
mcm^5s^2U	46	14.4
mcm^5U	37	14.4
mo^5U	24	14.4
ms^2t^6A	49	2.9
Ψ	4	64.8
s^2C	13	14.4
s^2U	27	72
s^4U	29	72
t^6A	48	2.9
U	11	34.6
Um	28	72

Table B.4.3 *Average Modification Percentage of UHLPC-MS/MS analysis WT and KO cell types. Measurements were averaged between the two biological replicates and three technical replicates of each biological replicate. Each measurement represents modification percentage (modification/canonical base %).*

Nucleoside	**Abbrevi**	**Foun**	**PT**	**WT tota**	**Δtrm1**	**Δtrm2**	**Δtrm10**	**Δtrm11**	**WT mR**	**Δtrm1**	**Δtrm2**	**Δtrm10**	**Δtrm**

	ation	d in S. cerevisiae	MC lass	l RNA	total RNA	total RNA	total RNA	total RNA	NA	mRNA	mRNA	mRNA	11 mRNA
Dihydrouridine	D	Yes	r, t	1.88617182 3	2.00469037 3	1.99118947 8	2.05319471	2.04294477 6	N.D.	N.D.	N.D.	N.D.	N.D.
5-hydroxymethylcytidine	hm5C	No	m, r	N.D.	N.D.	N.D.	N.D.	N.D.	N.D.	N.D.	N.D.	N.D.	N.D.
Pseudouridine	Ψ	Yes	m, r, sn, sno, t	4.79816861 8	5.00988432 6	4.65682032 8	4.95165033 6	5.05488164 4	0.02372314 7	0.01944457 9	0.02475 26	0.02191125 6	0.0204144
3-methylcytidine	m^3C	Yes	m, t	0.04248235 4	0.04256740 3	0.06554411 9	0.04911339 6	0.04483600 8	N.D.	N.D.	0.00045098 8	N.D.	N.D.
1-methyladenosine	m^1A	Yes	m, r, t	0.22235762 6	0.23325342 8	0.35110335	0.23494119 5	0.22448584	0.00013545 5	0.00017155 5	0.00013927	0.00015797 9	0.000139
5-hydroxyuridine	ho^5U	No	t	N.D.	N.D.	N.D.	N.D.	N.D.	N.D.	N.D.	N.D.	N.D.	N.D.
5-methylcytidine	m^5C	Yes	m, r, t	0.79748402 5	0.81129611 6	0.68296682 1	0.85577728 9	0.82305980 6	0.00512690 4	0.00475011 6	0.00449423 1	0.00388942 1	0.003624
1-methylpseudouridine	$m^1\Psi$	Yes	r, t	0.00357684 4	0.00402319 2	0.00430904	0.00371891 1	0.00433346 3	N.D.	N.D.	N.D.	N.D.	N.D.
7-methylguanosine	m^7G	Yes	m, r, t	0.14193920 6	0.15467844 2	0.17502152 6	0.15205227 2	0.14558261 4	0.02015543 6	0.02459492 8	0.01632834 7	0.02004338 5	0.0200007

2′-O-methylcytidine	Cm	Yes	m, r, s n, t	1.37481105	1.39694531	1.22414204	1.38974958	1.37895704	0.00335076	0.00287794	0.00245616	0.00292403	0.002353
Inosine	I	Yes	m, t	0.13114099	0.11026253	0.11571857	0.10882521	0.10933446	N.D.	N.D.	0.00081302	N.D.	N.D.
5-methyluridine	m^5U	Yes	m, r, t	0.46416817	0.49341869	0.03267948	0.52310229	0.50613699	0.00094245	0.00082182	0.00036956	0.00078190	0.000803
5-formylcytidine	f^5C	Yes	m, t	N.D.	N.D.	N.D.	N.D.	N.D.	N.D.	N.D.	N.D.	N.D.	N.D.
2′-O-methyluridine	Um	Yes	m, r, s n, s no, t	0.63934344	0.65275162	0.59783841	0.64708832	0.65350272	0.00187048	0.00103638	0.00188174	0.00138293	0.001403
2-methyladenosine	m^2A	No	r, t	N.D.	N.D.	N.D.	N.D.	N.D.	N.D.	N.D.	N.D.	N.D.	N.D.
1-methylguanosine	m^1G	Yes	m, r, t	0.38074368	0.43596958	0.39662782	0.15137225	0.40785217	0.00063379	0.00061411	0.00072848	0.00036004	0.000046
2′-O-methylguanosine	Gm	Yes	m, r, s n, t	1.15401153	1.16267441	1.00039686	1.18684482	1.15348592	0.00048899	0.00043798	0.00052637	0.00039237	0.003879
1-methylinosine	m^1I	Yes	t	0.02876658	0.02965615	0.02602036	0.03090472	0.02898468	N.D.	N.D.	N.D.	N.D.	N.D.
N2-methylguanosine	m^2G	Yes	r, s n,	0.34426496	0.34800389	0.37324236	0.36284867	0.00464219	0.00083352	0.00071819	0.00125783	0.00067256	0.000038

			t	1		3	7	4	1	7	5	8	7
N4-acetylcytidine	ac^4C	Yes	m,r,t	0.222729013	0.232420258	0.26948754	0.231514162	0.230090178	N.D.	N.D.	N.D.	N.D.	N.D.
2′-O-methyladenosine	Am	Yes	m,r,sn,snot	1.22688889	1.222204138	1.231461536	1.218063628	1.210793776	0.000151562 9	0.000114517 1	0.000154674 9	0.000139292 5	0.001132
N6-methyladenosine	m^6A	Yes	m,r,sn,t	0.123004859	0.12120245	0.105370665	0.123656336	0.120896487	0.000320663	0.000273258	0.000339818	0.000252738	0.00021 3
N2,N2-dimethylguanosine	$m^2{}_2G$	Yes	r,t	0.303458244	0.000474115	0.343770202	0.323715647	0.315705241	0.000527431	0.000147851	0.000669436	0.000466072	0.000513
N6,2′-O-dimethyladenosine	m^6Am	No	m,sn	N.D.	N.D.	N.D.	N.D.	N.D.	N.D.	N.D.	N.D.	N.D.	N.D.
N6-isopentenyladenosine	i^6A	Yes	t	0.078715478	0.082177174	0.067788394	0.085166534	0.083556586	N.D.	N.D.	N.D.	N.D.	N.D.
N2,N7-dimethylguanosine	$m^{2,7}G$	Yes	sn,snso	N.D.	N.D.	N.D.	N.D.	N.D.	N.D.	N.D.	N.D.	N.D.	N.D.
6-methyluridine	m^6U	No	NF	N.D.	N.D.	N.D.	N.D.	N.D.	N.D.	N.D.	N.D.	N.D.	N.D.
5,2'-O-dimethylcytidine	m^5Cm	No	NF	N.D.	N.D.	N.D.	N.D.	N.D.	N.D.	N.D.	N.D.	N.D.	N.D.
5-carboxymethyluridine	cm^5U	Yes	t	0.00179788	0.00202788	0.00182129	0.00219957	0.00200830	N.D.	N.D.	N.D.	N.D.	N.D.

				2	7	5	8	6					
2-thiocytidine	s^2C	No	t	N.D.	N.D.	N.D.	N.D.	N.D.	N.D.	N.D.	N.D.	N.D.	N.D.
2′-O-methylinosine	Im	No	r	N.D.	N.D.	N.D.	N.D.	N.D.	N.D.	N.D.	N.D.	N.D.	N.D.
5-methoxycarbonylmethyluridine	mcm^{5}U	Yes	t	0.02143793 4	0.02384683 5	0.02672345 2	0.02673782	0.02455736 6	N.D.	N.D.	N.D.	N.D.	N.D.
5-carboxymethylaminomethyluridine	cmnm^{5}U	Yes	t	0.00027672	0.00032096 8	0.00060468 5	0.00017227 7	0.00025361 1	N.D.	N.D.	N.D.	N.D.	N.D.
5-methoxyuridine	mo^{5}U	No	t	N.D.	N.D.	N.D.	N.D.	N.D.	N.D.	N.D.	N.D.	N.D.	N.D.
3-(3-amino-3-carboxypropyl)uridine	acp^{3}U	No	r, t	N.D.	N.D.	N.D.	N.D.	N.D.	N.D.	N.D.	N.D.	N.D.	N.D.
uridine 5-oxyacetic acid	cmo^{5}U	No	t	N.D.	N.D.	N.D.	N.D.	N.D.	N.D.	N.D.	N.D.	N.D.	N.D.
2,8-dimethyladenosine	m^{2,8}A	No	r	N.D.	N.D.	N.D.	N.D.	N.D.	N.D.	N.D.	N.D.	N.D.	N.D.
5-methoxycarbonylmethyl-2-thiouridine	mcm^{5}s^{2}U	Yes	t	0.02889898 4	0.02839637 7	0.04372151 8	0.02570161 5	0.02887603	N.D.	N.D.	N.D.	N.D.	N.D.
N2,N2,N7-trimethylguanosine	m$_3$G	Yes	sn, sno	N.D.	N.D.	N.D.	N.D.	N.D.	N.D.	N.D.	N.D.	N.D.	N.D.
5,2′-O-dimethyluridine	m^{5}Um	No	t	N.D.	N.D.	N.D.	N.D.	N.D.	N.D.	N.D.	N.D.	N.D.	N.D.
2-methylthio-N6-threonylcarbamoyladenosine	ms^{2}t^{6}A	No	t	N.D.	N.D.	N.D.	N.D.	N.D.	N.D.	N.D.	N.D.	N.D.	N.D.

4-thiouridine	s^4U	No	t	N.D.	N.D.	N.D.	N.D.	N.D.	N.D.	N.D.	N.D.	N.D.	N.D.
N6-threonylcarbamoyladenosine	t^6A	Yes	t	0.08298883	0.089210315	#DIV/0!	0.091570552	0.087321215	N.D.	N.D.	N.D.	N.D.	N.D.
2-thiouridine	s^2U	Yes	t	N.D.	N.D.	N.D.	N.D.	N.D.	N.D.	N.D.	N.D.	N.D.	N.D.
5-methyl-2-thiouridine	m^5s^2U	No	t	N.D.	N.D.	N.D.	N.D.	N.D.	N.D.	N.D.	N.D.	N.D.	N.D.
3-methyluridine	m^3U	Yes	r	0.00432787 3	0.00250571 4	0.07966519 3	0.00152024 7	0.00172727 4	N.D.	N.D.	N.D.	N.D.	N.D.

Table B.4.4 *Percent retention of modification in purified mRNA. Values were calculated by comparing the mod/main% of the mRNA and the total RNA ((mRNA mod/main%)/total RNA mod/main% *100)*

Nucleoside	Abbreviation	% Retention in WT mRNA
Pseudouridine	Ψ	0.49
1-methyladenosine	m^1A	0.06
5-methylcytidine	m^5C	0.64
7-methylguanosine	m^7G	14.2
2′-O-methylcytidine	Cm	0.24
5-methyluridine	m^5U	0.20
2′-O-methyluridine	Um	0.29

1-methylguanosine	m^1G	0.17
2′-O-methylguanosine	Gm	0.42
N2-methylguanosine	m^2G	0.24
2′-O-methyladenosine	Am	0.12
N6-methyladenosine	m^6A	0.26
N2,N2-dimethylguanosine	m^2_2G	0.17

Table B.4.5 *qRT-PCR primer sequences*

Gene ID	Gene Name	Forward sequence (5'-3')	Reverse sequence (5'-3')
YFL039C	ACT1	GCCTTCTACGTTTCCATCCA	GGCCAAATCGATTCTCAAAA
RDN18-2	18S rRNA	GAGTCCTTGTGGCTCTTGGC	AATACTGATGCCCCCGACC
RDN25-1	25S rRNA	ATGTGATTTCTGCCCAGTGC	AATCCATTCATGCGCGTCAC

Table B.4.6 *UPLC gradients for analytical separation and wash methods. %B corresponds to the percentage of B mobile phase (acetonitrile + 0.01% formic acid)*

Wash Method	
Time (min)	**B (%)**
0	0
1	60
2	0
2.5	0
3.5	60
4.5	0
5	0
6	60
7	0
7.5	0
8.5	60
9.5	0

10	0
11	60
12	0
12.5	0
13.5	60
14.5	0
15	0
16	100
17.8	100
18.3	0
27.8	0

Table B.4.7 *Multiple reaction monitoring parameters of nucleosides*

Nucleoside	**Precursor Ion (m/z)**	**MS1 Resolution**	**Product Ion (m/z)**	**MS2 Resolution**	**Fragmentor (V)**	**Collision Energy (V)**	**Cell Accelerator Voltage (V)**	**Retention Time (min)**	**Delta Retention Time (min)**	**Polarity**
$^{15}N_4$-I	273.2	Wide	141	Unit	90	5	2	6.64	2.5	Positive
A	268.2	Wide	136	Unit	80	15	2	7.66	2.5	Positive
ac^{4}C	286.2	Wide	154	Unit	70	5	2	9.98	2.5	Positive
acp^{3}U	346.1	Wide	214.1	Unit	60	13	4	2.75	2.5	Positive
Am	282.2	Wide	136	Unit	80	15	2	10.07	2.5	Positive
C	244.2	Wide	112	Unit	70	12	3	1.62	2.5	Positive
Cm	258.1	Wide	112	Unit	70	10	3	4.45	2.5	Positive
cm^{5}U	303	Wide	171.1	Unit	80	5	1	5.56	2.5	Positive
cmnm^{5}U	332.1	Wide	125	Unit	70	13	3	1.97	2.5	Positive
cmo^{5}U	319	Wide	187.1	Unit	60	7	1	5.75	2.5	Positive
D	247.2	Wide	115.1	Unit	70	5	3	1.76	2.5	Positive
f^{5}C	272.2	Wide	140	Unit	70	10	2	7.31	2.5	Positive
G	284.1	Wide	152	Unit	70	10	2	6.86	2.5	Posit

										ive
Gm	298.1	Wide	152	Unit	80	5	2	9.18	2.5	Positive
hm^{5}C	274.2	Wide	142	Unit	60	5	2	1.83	2.5	Positive
ho^{5}U	261.2	Wide	129	Unit	80	5	3	2.44	2.5	Positive
I	269.2	Wide	137	Unit	80	10	2	6.64	2.5	Positive
i^{6}A	336	Wide	204.1	Unit	90	17	4	15.14	2.5	Positive
Im	283.1	Wide	136.9	Unit	90	1	2	9.14	2.5	Positive
m^{1}A	282.2	Wide	150	Unit	100	15	2	2.41	2.5	Positive
m^{1}G	298.2	Wide	166.1	Unit	80	5	2	9.15	2.5	Positive
m^{1}I	283	Wide	151	Unit	100	5	2	9.19	2.5	Positive
m^{1}Ψ	259.1	Wide	139	Unit	80	15	2	3.69	2.5	Positive
m$_{3}$G	326.1	Wide	194	Unit	60	15	1	9.89	2.5	Positive
m^{2}$_{2}$G	312.3	Wide	180.1	Unit	80	10	2	11.44	2.5	Positive
m^{2,7}G	312.1	Wide	180.1	Unit	60	10	1	7.82	2.5	Positive
m^{2,8}A	296.1	Wide	164.1	Unit	80	15	1	11.25	2.5	Positive
m^{2}A	282.1	Wide	150	Unit	100	20	2	8.6	2.5	Positive
m^{2}G	298.1	Wide	166.1	Unit	70	10	2	9.77	2.5	Positive
m^{3}C	258.1	Wide	126.1	Unit	60	5	3	2.09	2.5	Positive
m^{3}U	259	Wide	127	Unit	70	5	3	8.47	2.5	Positive
m^{5}C	258.2	Wide	126	Unit	60	5	3	2.61	2.5	Positive
m^{5}Cm	272.1	Wide	126.1	Unit	80	8	3	7.19	2.5	Positive
m^{5}s^{2}U	275	Wide	143	Unit	70	5	2	10.85	2.5	Positive
m^{5}U	259.1	Wide	127	Unit	70	5	3	7.1	2.5	Positive

m^5Um	273.1	Wide	127	Unit	60	5	3	11.06	2.5	Positive
m^6A	282.2	Wide	150	Unit	80	15	2	11.3	2.5	Positive
m^6Am	296.1	Wide	150	Unit	90	15	2	12.5	2.5	Positive
m^6U	259	Wide	127.1	Unit	50	5	2	5.74	2.5	Positive
m^7G	298.2	Wide	166	Unit	80	5	2	3.8	2.5	Positive
mcm^5s^2U	333	Wide	201.1	Unit	60	6	4	12.26	2.5	Positive
mcm^5U	317.1	Wide	185.1	Unit	80	6	1	9.64	2.5	Positive
mo^5U	275	Wide	143.1	Unit	90	1	6	7.38	2.5	Positive
ms^2t^6A	459.2	Wide	327.1	Unit	80	12	2	14.56	2.5	Positive
Ψ	245.1	Wide	209	Unit	70	5	4	1.81	2.5	Positive
s^2C	260	Wide	128	Unit	90	6	3	3.67	2.5	Positive
s^2U	261	Wide	129	Unit	40	3	3	7.61	2.5	Positive
s^4U	261.1	Wide	129	Unit	60	11	3	8.21	2.5	Positive
t^6A	413.1	Wide	281.1	Unit	70	5	5	13.24	2.5	Positive
U	245.2	Wide	113	Unit	50	5	3	3.36	2.5	Positive
Um	259.2	Wide	113	Unit	70	5	3	8.13	2.5	Positive

Table B.4.8 *Concentrations of ribonculeosides in calibration curves standards after the addition of internal standard*

Standard Level	Canonical Nucleosides (nM)	Ψ and DHU (pM)	m5U (pM)	All other modifcations (pM)
1 (highest)	21600	1620000	800000	360000
2	4320	324000	160000	72000
3	864	64800	32000	14400
4	172.8	12960	6400	2880

5	34.56	2592	1280	576
6	6.912	518.4	256	115.2
7	1.3824	103.68	51.2	23.04
8 (lowest)	0	0	0	0

Table B.4.9 *Suppliers of ribonucleoside standards used in LC-MS/MS analyses*

Nucleoside	**Supplier**
$^{15}N_4$-I	Cambridge Isotope Laboratories
A	ACROS Organics
ac^{4}C	Santa Cruz Biotechnology
acp^{3}U	Biosynth Carbosynth
Am	Santa Cruz Biotechnology
C	ACROS Organics
Cm	Alfa Aesar
cm^{5}U	Biosynth Carbosynth
cmnm^{5}U	Biosynth Carbosynth
cmo^{5}U	Biosynth Carbosynth
D	MedChemExpress
f^{5}C	Berry & Associates, Inc.
G	ACROS Organics
Gm	Alfa Aesar
hm^{5}C	Berry & Associates, Inc.
ho^{5}U	Aurum Pharmatech
I	Santa Cruz Biotechnology
i^{6}A	Cayman Chemical
Im	Biosynth Carbosynth
m^{1}A	Cayman Chemical
m^{1}G	Aurum Pharmatech
m^{1}I	Toronto Research Chemicals
m$^1\Psi$	Abcam
m_3G	Biosynth Carbosynth
m$^2{}_2$G	Santa Cruz Biotechnology
m^{2,7}G	Biosynth Carbosynth
m^{2,8}A	Biosynth Carbosynth
m^{2}A	Santa Cruz Biotechnology
m^{2}G	MedChemExpress
m^{3}C	Santa Cruz Biotechnology
m^{3}U	Toronto Research Chemicals
m^{5}C	Santa Cruz Biotechnology
m^{5}Cm	Biosynth Carbosynth

m^5s^2U	Santa Cruz Biotechnology
m^5U	Santa Cruz Biotechnology
m^5Um	Biosynth Carbosynth
m^6A	Berry & Associates, Inc.
m^6Am	Toronto Research Chemicals
m^6U	Biosynth Carbosynth
m^7G	Santa Cruz Biotechnology
mcm^5s^2U	Biosynth Carbosynth
mcm^5U	Toronto Research Chemicals
mo^5U	Biosynth Carbosynth
ms^2t^6A	Santa Cruz Biotechnology
Ψ	Berry & Associates, Inc.
s^2C	Biosynth Carbosynth
s^2U	Cayman Chemical
s^4U	Cayman Chemical
t^6A	Toronto Research Chemicals
U	ACROS Organics
Um	Alfa Aesar

Table B.4.10 *Suppliers of ribonucleoside standards used in LC-MS/MS analyses*

Nucleoside	**Supplier**
$^{15}N_4$-I	Cambridge Isotope Laboratories
A	ACROS Organics
ac^4C	Santa Cruz Biotechnology
acp^3U	Biosynth Carbosynth
Am	Santa Cruz Biotechnology
C	ACROS Organics
Cm	Alfa Aesar
cm^5U	Biosynth Carbosynth
$cmnm^5U$	Biosynth Carbosynth
cmo^5U	Biosynth Carbosynth
D	MedChemExpress
f^5C	Berry & Associates, Inc.
G	ACROS Organics
Gm	Alfa Aesar
hm^5C	Berry & Associates, Inc.
ho^5U	Aurum Pharmatech
I	Santa Cruz Biotechnology
i^6A	Cayman Chemical
Im	Biosynth Carbosynth

m^1A	Cayman Chemical
m^1G	Aurum Pharmatech
m^1I	Toronto Research Chemicals
$m^1\Psi$	Abcam
m_3G	Biosynth Carbosynth
$m^2{}_2G$	Santa Cruz Biotechnology
$m^{2,7}G$	Biosynth Carbosynth
$m^{2,8}A$	Biosynth Carbosynth
m^2A	Santa Cruz Biotechnology
m^2G	MedChemExpress
m^3C	Santa Cruz Biotechnology
m^3U	Toronto Research Chemicals
m^5C	Santa Cruz Biotechnology
m^5Cm	Biosynth Carbosynth
m^5s^2U	Santa Cruz Biotechnology
m^5U	Santa Cruz Biotechnology
m^5Um	Biosynth Carbosynth
m^6A	Berry & Associates, Inc.
m^6Am	Toronto Research Chemicals
m^6U	Biosynth Carbosynth
m^7G	Santa Cruz Biotechnology
mcm^5s^2U	Biosynth Carbosynth
mcm^5U	Toronto Research Chemicals
mo^5U	Biosynth Carbosynth
ms^2t^6A	Santa Cruz Biotechnology
Ψ	Berry & Associates, Inc.
s^2C	Biosynth Carbosynth
s^2U	Cayman Chemical
s^4U	Cayman Chemical
t^6A	Toronto Research Chemicals
U	ACROS Organics
Um	Alfa Aesar

Table B.4.11 *The DNA template and the resulting RNA sequence following run-off T7 transcription*

Amino Acid	Codon	DNA template for transcription	RNA Sequence
Phe	**UUU**	TGGCTACAGAAGGGCTTAGAACATAATGCACTTATCCTCGCAAGACACCCTATAGTGAGTCGTATTA	GGGUGUCUUGCGAGGAUAAGUGCAUUAUGUUUUAAGCCCUUCUGUAGCCA
Phe	**UUC**	TGGCTACAGAAGGGCTTAGAACATAATGCACTTATCCTCGCAAGACACCCTATAGTGAGTCGTATTA	GGGUGUCUUGCGAGGAUAAGUGCAUUAUGUUCUAAGCCCUUCUGUAGCCA
Val	**GUG**	TGGCTACAGAAGGGCTTTTATCGTTGCACCATAATGCACTTATCCTCGCAAGACACCCTATAGTGAGTCGTATT	GGUGUCUUGCGAGGAUAAGUGCAUUAUGGUGCAACGAUAAAAGCCCUUCUGUAGCCA
Arg	**CGU**	TGGCTACAGAAGGGGTCACTTTATGCACGCATAATGCACTTATCCTCGCAAGACACCCTATAGTGAGTCGTATT	GGUGUCUUGCGAGGAUAAGUGCAUUAUGCGUGCAUAAAGUGACCCCUUCUGUAGCCA

Table B.4.12 *Modified RNA transcriptions purchased from Dharmacon*

Amino Acid	Codon	Modified codon	RNA Sequence
Phe	**UUU**	**UUm^{5}U**	GGGUGUCUUGCGAGGAUAAGUGCAUUAUGUUm^{5}UUAAGCCCUUCUGUAGCCA
Phe	**UUC**	**m^{5}UUC**	GGGUGUCUUGCGAGGAUAAGUGCAUUAUGm^{5}UUCUAAGCCCUUCUGUAGCCA
Phe	**UUC**	**Um^{5}UC**	GGGUGUCUUGCGAGGAUAAGUGCAUUAUGUm^{5}UUCUAAGCCCUUCUGUAGCCA
Val	**GUG**	**m^{1}GUG**	GGUGUCUUGCGAGGAUAAGUGCAUUAUGm^{1}GUGCAACGAUAAAAGCCCUUCUGUAGCCA
Val	**GUG**	**m^{2}GUG**	GGUGUCUUGCGAGGAUAAGUGCAUUAUGm^{2}GUGCAACGAUAAAAGCCCUUCUGUAGCCA
Val	**GUG**	**GUm^{1}G**	GGUGUCUUGCGAGGAUAAGUGCAUUAUGGUm^{1}GCAACGAUAAAAGCCCUUCUGUAGCCA
Val	**GUG**	**GUm^{2}G**	GGUGUCUUGCGAGGAUAAGUGCAUUAUGGUm^{2}GCAACGAUAAAAGCCCUUCUGUAGCCA
Arg	**CGU**	**Cm^{1}GU**	GGUGUCUUGCGAGGAUAAGUGCAUUAUGCm^{1}GUGCAUAAAGUGACCCCUUCUGUAGCCA
Arg	**CGU**	**Cm^{2}GU**	GGUGUCUUGCGAGGAUAAGUGCAUUAUGCm^{2}GUGCAUAAAGUGACCCCUUCUGUAGCCA

Appendix C: Chapter 5 Supplemental Material

This appendix contains all supplemental discussion, and data/supporting figures for the paper titled “Modulation of tRNA modification landscape alters the efficacy of Hygromycin B translation inhibition." This work has yet to be published.

C.5.1 Supplementary Figures

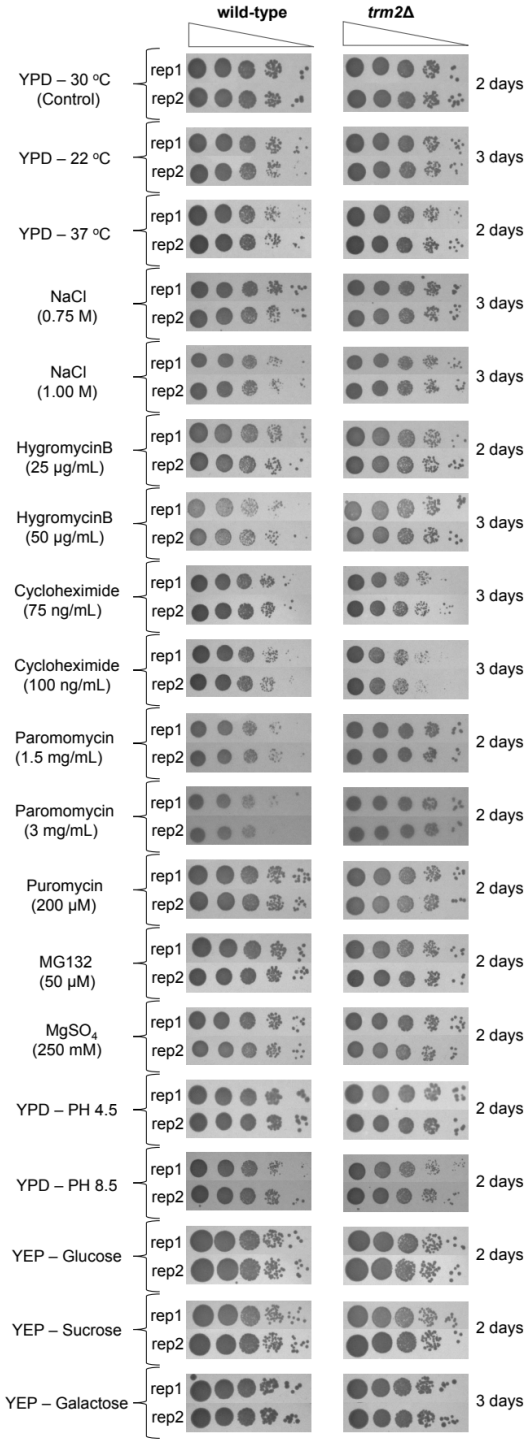

Figure C.5.1 *Spot platting for both native cells and cells with trm2 KO under different growth conditions.*

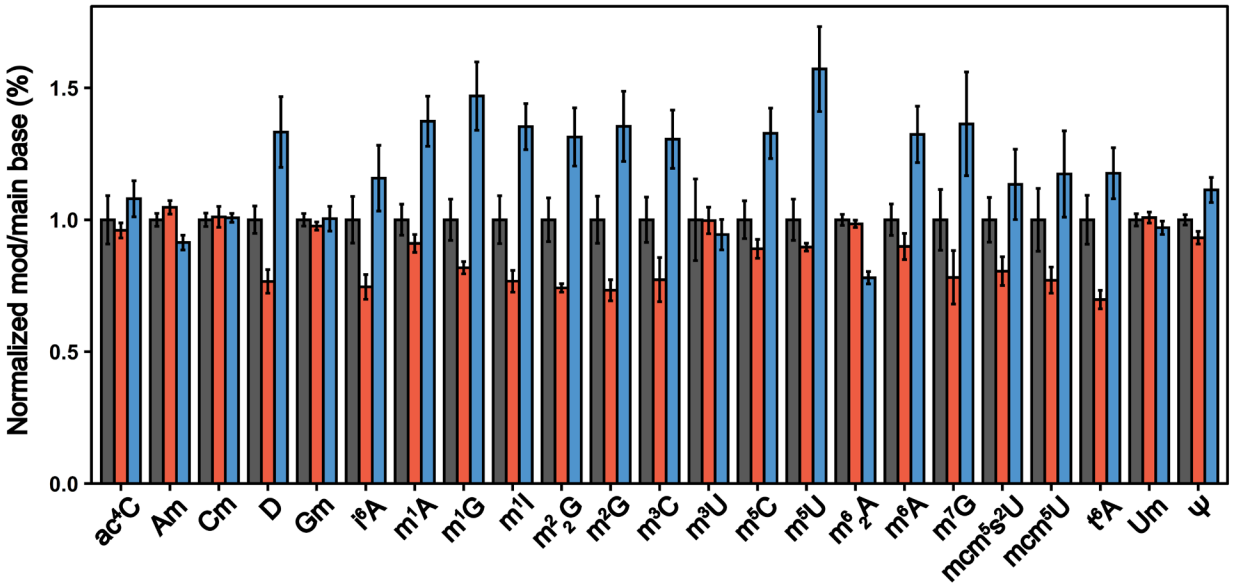

Figure C.5.2 *Bar plot displaying modification levels under different stress conditions Wild type-black, Cycloheximide-red, Hygromycin-blue.*

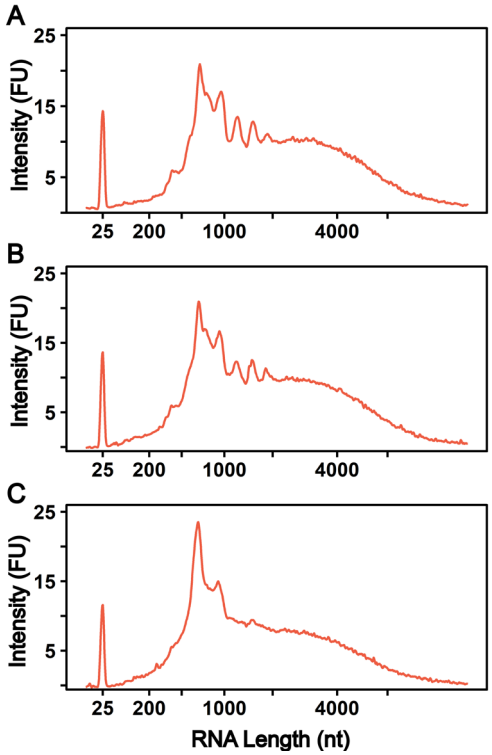

Figure C.5.3 *Bioanalyzer for total tRNA A – wild type, B-cyclohexamide, C-hygromycin B*

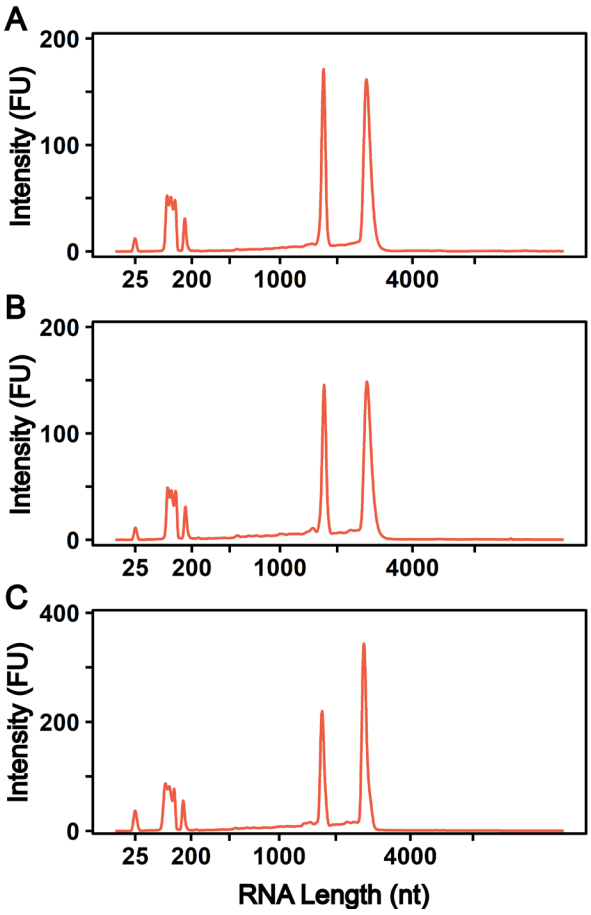

Figure C.5.4 *Bioanalyzer for rRNA A – wild type, B-cyclohexamide, C-hygromycin B*

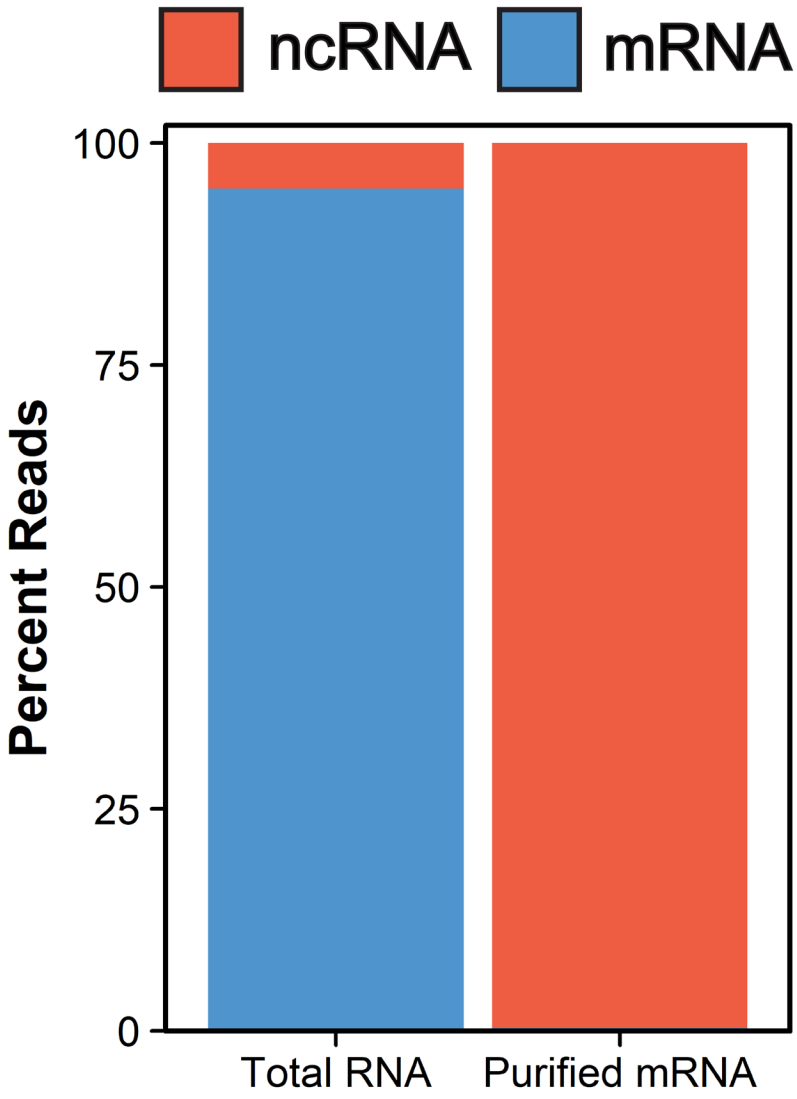

Figure C.5.5 *RNA-sequencing results showing depletion of non-coding RNA's.*

Appendix D: A Humanized Yeast Model Reveals Dominant-Negative Properties of Neuropathy-Associated Alanyl-tRNA Synthetase Mutations

This Appendix contains supplemental material for the currently prepint (as of 7-13-2022) article titled above by the following authors:

Rebecca Meyer-Schuman[1], Sheila Marte[1], Tyler Smith[2], Shawna Feely[3], Marina Kennerson[4,5,6], Garth Nicholson[4,5,6], Mike Shy[3], Kristin Koutmou[2], and Anthony Antonellis[1,7,]*

[1]Department of Human Genetics, University of Michigan Medical School, Ann Arbor, Michigan, USA; [2]Department of Chemistry, University of Michigan, Ann Arbor, Michigan; [3]Department of Neurology, Carver College of Medicine, University of Iowa, Iowa City, Iowa; [4]Northcott Neuroscience Laboratory, ANZAC Research Institute, Sydney, NSW, Australia; [5]Sydney Medical School, University of Sydney, Sydney, NSW, Australia; [6]Molecular Medicine Laboratory, Concord General Repatriation Hospital, Sydney, NSW, Australia; and [7]Department of Neurology, University of Michigan Medical School, Ann Arbor, Michigan, USA.

D.1 Abstract

Aminoacyl-tRNA synthetases (ARSs) are ubiquitously expressed, essential enzymes that ligate tRNA molecules to their cognate amino acids. Heterozygosity for missense variants or small in-frame deletions in five ARS genes causes axonal peripheral neuropathy, a disorder characterized by impaired neuronal function in the distal extremities. These variants reduce enzyme activity without significantly decreasing protein levels and reside in genes encoding homo-dimeric enzymes. These observations raise the possibility of a dominant-negative effect, in which non-functional mutant ARS subunits dimerize with wild-type ARS subunits and reduce overall ARS activity below 50%, breaching a threshold required for peripheral nerve axons. To test for these dominant-negative properties, we developed a humanized yeast assay to co-express pathogenic human alanyl-tRNA synthetase (AARS1) mutations with wild-type human AARS1. We show that multiple loss-of-function, pathogenic AARS1 variants repress yeast growth in the presence of wild-type human AARS1. This growth defect is rescued when these variants are placed in cis with a mutation that reduces dimerization with the wild-type subunit, demonstrating that the interaction between mutant AARS1 and wild-type AARS1 is responsible for the repressed growth. This demonstrates that neuropathy-associated AARS1 variants exert a dominant-negative effect, which supports a common, loss-of-function mechanism for ARS-mediated dominant peripheral neuropathy.

D.2 Discussion of Results

The yeast model serves as a useful system to assess the activity of AlaRS and its various mutations forms tested throughout the study. However, the expression of the enzyme in the dual-vector has the potential to be impacted by cellular conditions enforced or biased as consequence of the model's design. To investigate if the observed decreased activity of ARS may in fact be a consequence of R329H mutation, *in vitro* amino-acylation assays were performed of purified WT and R329H mutant human AARS1. It should be noted that these enzymes were expressed in an *E. coli* system and while the sequence is accurate, there may be discrepancies in modification landscape of the proteins expressed in a prokaryotic system. Despite this, the *in vitro* assays (*Appendix Figure D.1*) showcase that when the R329H mutant is presence, there is approximately a 50% decrease in amino-acylation efficiency. Such findings support the idea that the mutant is responsible for the decreased activity observed in cells and that this, and perhaps other mutants, are significant enough to repress growth in the model system used in this study.

When a pGAL1(R329H) or pGAL(R329H-GDMI) vector is present in the ptetO7-ALA1 yeast strain (after being "turned off"), there is a clear phosphorylation defect of eIF2α (at Ser51). It appears that strains that do not contain a pGAL1(AARS mutant) have similar eIF2α expression, and subsequent Ser-51 phosphorylation, at both 0 and 8 hours (before and after the vector is 'turned on'). Interestingly, the expression of eIF2α is increased in both pGAL1 vectors which harbor a AARS1 R329H mutation while phosphorylation of eIF2α in these cases does not scale as observed in the Wild type AARS 1 containing pGAL1 vector. In fact, it appears that level of phosphorylation is similar to 0 hour growth conditions in all strains. This suggests that when the AARS1 R329H mutation is present, there is a defect in phosphorylation and eIF2α is seemingly overexpressed in attempt to overcome the lack of Ser51 phosphorylation. Normally,

physiological conditions that result in eIF2α phosphorylation stem for stress responses, such as virus infection or heat shock, prevent recycling of eIF2α and thus limit rounds of protein synthesis [1]. This data suggests that presence of the AARS1 R329H mutation may signal a translation defect or deficit in which the cell is attempting to express or overexpress eIF2α and prevent its phosphorylation (or kinase targeting) to improve/increase protein synthesis of the gene product.

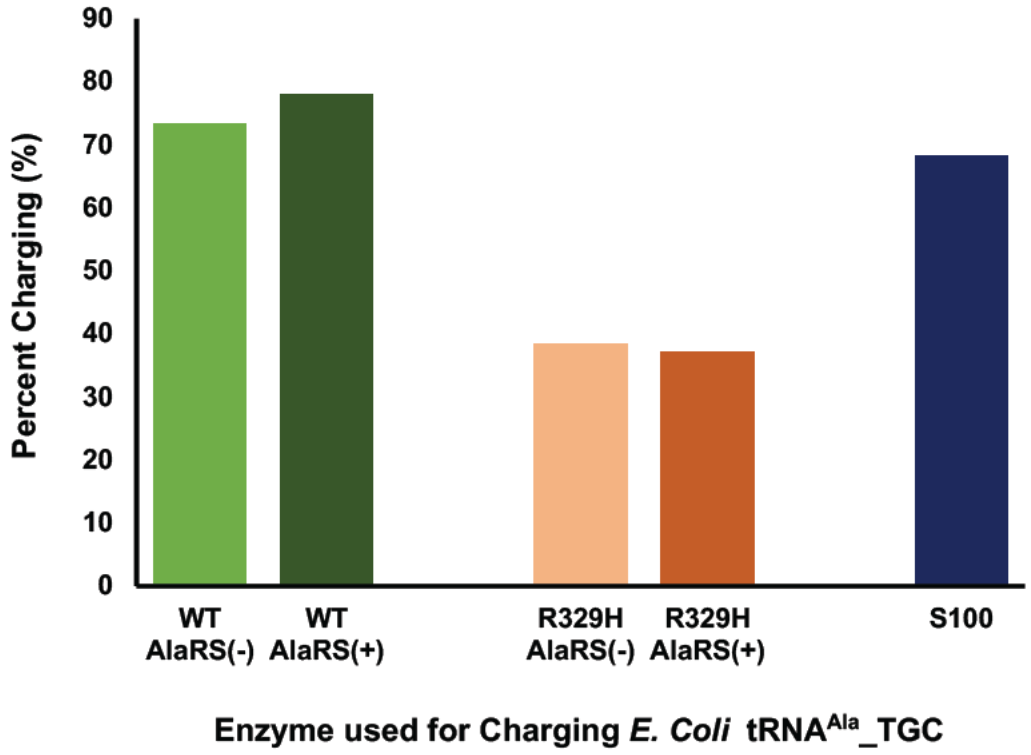

Figure D.2.1 *Charging efficiencies of WT and R329H Alanyl tRNA synthetase, and S100 extract, for amino-acylation of E. coli tRNAAla (TGC isoacceptor). Presence of "-" or "+" indicates absence or presence of 6X His-tag, respectively. His-tag does not appear to affect charging efficiency.*

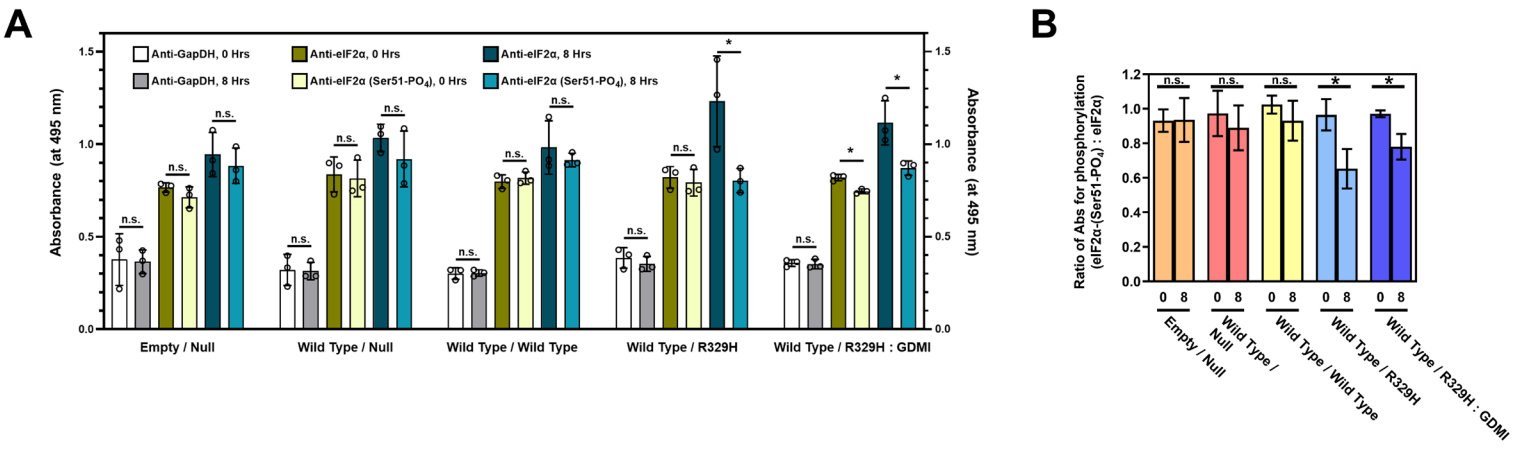

Figure D.2.2 *Detection of phosphorylation of eIF2α in mutant AARS1 containing yeast strains A) ptetO7-ALA1 yeast strains transfected with pADH1(A) and pGAL1(B) vectors, where A and B indicate gene inserts for the H. sapiens AARS, were assayed for phosphorylation of eIF2α-Ser51 during cell growth in the absence or presence of a homolog containing the R329H AARS1 mutation using colormetric cell-based ELISA. Primary antibodies used in the assay were Anti-GAPDH, Anti-eIF2 α, and Anti-eIF2α (Phospho-Ser51). Transfected yeast strains study are abbreviated in the following format: A / B, in which A refers to the gene insert of CEN-bearing pADH1 which expressed in the presence of glucose and B refers to the gene insert of pGAL1 which expresses in the presence of galactose (e.g. Wild Type / R329H represent pADH1(Wild Type AARS1) and pGAL1(AARS1 R329H)). All strains were incubated in glucose containing media to an OD600 of 0.4 before being resuspended in galactose containing media and incubated for either 0 or 8 hours. Error bars represent standard deviation of biological replicates. A ' * ' represented a significant alteration with a p-value <0.05 using a unpaired student t-test comparing absorbance of biological samples treated with indicated primary antibodies at a given time point of growth. B) The ratio of absorbances of biological samples, as shown in panel A, comparing phosphorylation of eIF2α. Presence of AARS1 R329H mutation results in a phosphorylation defect of eIF2α during growth, as seen comparing ratios at 0 and 8 hours. Error bars represent standard deviation of biological replicates. A ' * ' represented a significant alteration with a p-value <0.05 using a unpaired student t-test comparing absorbance of biological samples treated with indicated primary antibodies at a given time point of growth. n.s. indicates not significant.*

D.3 References

[1] Clemens, M. J. Initiation factor eIF2 alpha phosphorylation in stress responses and apoptosis.

Prog Mol Subcell Biol 27, 57–89 (2001). DOI: 10.1007/978-3-662-09889-9_3

Appendix E: Codon and tRNA Evolution in *Lactobaccilales* Impact on Translation Speed and Accuracy: a Directed Study of Leucine Incorporation

This Appendix contains data for a manuscript in preparation that was performed in collaboration with the Tao Pan lab at the University of Chicago.

E.1 Discussion of Results

There has been an observed evolutionary divergence in the prokaryote families within the *Lactobacillales* order regarding codon usage and distribution. This is highly apparent when comparing leucine codon usage of four of the families within the order: *Carnobacteriaceae* (C), *Enterococcaceae* (EF), *Lactobacillaceae* (L), and *Streptococcaceae* (SP). Despite their genomes being highly A/T rich (~65%) and having representation of A and T containing leucine-encoding DNA codons (TTG, TTA, CTT, CTG, CTC, and CTA), there is a shift in codon usage such as with SF having selection against CTT while selecting for TTA (*Appendix Figure E.1*). Interestingly, while SF does indeed have codon usage the family also has changes to its tRNAs which may explain the evolutionary expansion/alteration of their genetic code. For instance, the tRNAs in EF which recognize the CUC mRNA codon is the isoacceptor $tRNA_{GAG}^{Leu}$, which has undergone mutation in SP resulting in the isoacceptor $tRNA_{IAG}^{Leu}$. Due to the wobble property at position 34 of tRNAs, in which this I34 is positioned in the SF tRNA, the $tRNA_{IAG}^{Leu}$ should be able to recognize both the CUC and CUU mRNA codons. In fact, while to a significantly lower degree compared to EF,I find that this tRNA isoacceptor can successfully recognize these codons in an *in vitro* system (*Appendix Figure E.2*).

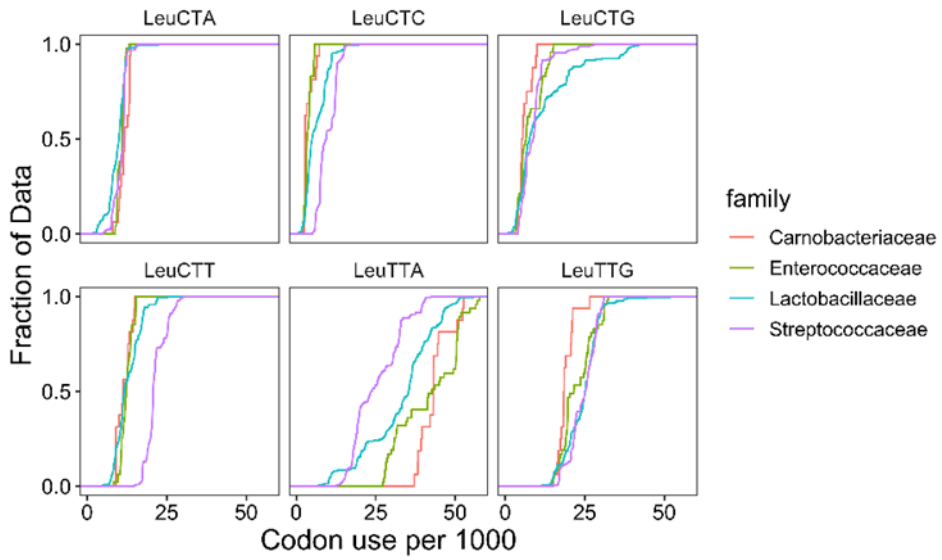

Figure E.1.1 *Codon usage of prokaryote families in the Lactobacillales order.*

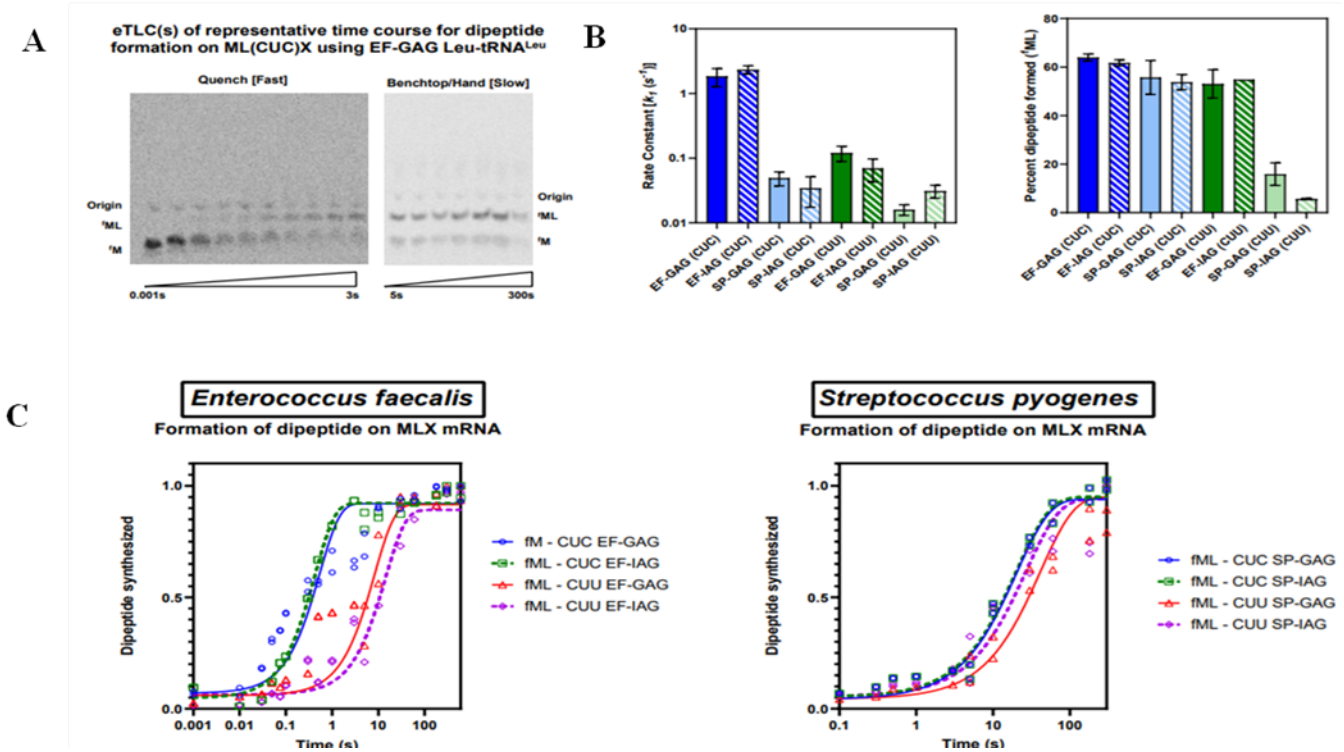

Figure E.1.2 *(A) Representative eTLCs of quench and benchtop assays incorporating leucine onto an MLX encoding mRNA, using Leu-tRNA^{Leu}. (B) Rate constants and percent peptide formation for peptide synthesis on MLX mRNA codons using I34 containing transcript leucine tRNAs. (C) Peptide synthesis curves for reactions detailed in panel B.*

The results on Inosine containing tRNAs explain why SP may have had the mutation in its tRNAs, but it ultimately only part of the puzzle for the evolutionary divergence. While this explains that SP uses one tRNA species to recognize the selected against CTC and CTT codons in regards to Leu usage, it does not answer why the family uses TTA so much more frequently. What makes this more concerning is that certain genes within SP, despite having selection for TTA, instead have high representations of CTT and TTG codons. This suggests that there may be 1, or potentially 2, evolutionary pathways that SP and similar families have undergone to allow for expanded codon recognition. There are three potential hypotheses as to why this may occur.

First is that the there is a difference in the tRNA abundance for the codons TTA and TTG, which are recognized by leucine tRNAs with the TAA and CAA anticodons, respectively. If there is an overall increase in ratio for CAA/TAA in SP compared to EF, the increased expression may explain why SP is able to "flop" between TTA and TTG codons. The second hypothesis postulates that there is an evolutionary change to the tRNA sequences themselves which may alter amino acid fold, stability, and/or activity. The TAA and CAA tRNAs have variability in their V-loops that change the base-pairing number and strength of the region and may then change the aforementioned properties of the tRNAs. The third and final hypothesis is that, similar to the I34 modification highlighted in SP $tRNA_{IAG}$, is that there are different modifications throughout the tRNAs or within the anticodon stem-loop that would change or expand codon recognition.

The final work I will contribute to this work regards the second hypothesis and the remainder of the work needed to assess the importance of the I34 modification. This will require

additional codon studies, such as the CUA codon, to fully explore the effects of the modification and its importance in the evolutionary pathway.

Appendix F: Guanosine mRNA Modifications Influence Translation Elongation and Termination

This appendix contains work for a manuscript in progress by the following authors:

Smith, T., Wan, Z., Giles, R., and Koutmou, K.

F.1 Introduction

Proper base-pairing and base-pair interactions confer structure function among various RNA species, such as ribosomal RNA (rRNA), messenger RNA (mRNA) and transfer tRNA (tRNA). Efficient translation is based upon Watson-Crick base-pairing and is thought to be necessary for proper decoding between tRNA and mRNA within the ribosome [1]. While in the A-site of the ribosome, W-C base pairs are required for proper mRNA-tRNA interactions and accurate decoding at the first two nucleotides of a codon there is more leniency at the third nucleotide with this "wobble" position which has more chemical and regioselective flexibility in its base-pair interaction [2],[3]. Even with the prospect of forming non-W-C interactions at the wobble, formation of hydrogen bonds are still considered to be required for proper codon recognition but this may not always be the case [4]. Recent work has shown that while H-bond between the N1 of purines and N3 of pyrimidines are at least necessary for base-pairing and successful decoding at the first and second base-pairs between mRNA and tRNA, adequate base-stacking alone is sufficient and critical at the third position [5]. While fascinating, many nucleotides studied are non-naturally occurring prosthetic nucleobases and it is unclear how loss of H-bonding potential may be impactful in organisms.

A common way RNA alters it potential to base-pair or form structure is through RNA base modifications, which are abundant throughout tRNA and rRNA [6]–[8]. In addition, there is a growing number of modifications found within mRNAs [9]. Of interest, the adenine/guanosine derivative 2,6-diaminopurine (DAP) has been found to replace adenine in the genetic sequence of the bacteriophage Cyanophage S-2L, an example of nucleobase substitution which is a common mechanism that bacteria viruses use to bypass host defense systems [10]. Using high-throughput LC-MS/MS other H-bonding altering purine bases, N1-methylguanosine (m1G), N2-methylguanosine (m2G), and N2,N2-dimethylguanosine (m2,2G), have recently been discovered to exist at low levels in *S. cerevisiae* mRNAs [11]. While it is uncertain if these modifications exist within the coding sequence, lysate and in vivo translation studies of mRNAs containing modified purines, such as O6-methylguanosine (m6G) , N1-methyladenosine (m1A), m1G, and m2G, impede translation and can even promote miscoding [11], [12]. Changes to the modification landscape of the ASL of tRNAs can affect ribosome frame maintenance and fidelity with position 34, which serves as the base-pairing partner to the mRNA codon's wobble position, serving a pivotal role in the processes [13] (Smith, In Review).

While it is known that modifications to purines, such as guanosine, of both mRNA and tRNAs can influence the addition of amino acids during translation, there is currently no strong kinetic or structural insight into the importance of regioselectivity and H-bonding of base-pairs interacting in the A-site of the ribosome during translation [14, p.]. To address this, we utilize a bacterial in vitro translation system to investigate the roles of modified guanosine nucleosides in mRNAs and their individual hydrogen bonds in the addition of a single amino acid, valine or arginine, or recognition of release factors, RF1 and RF2 (Appendix F, Figure 1). In addition, we

can gain insight into how such modifications and H-bonds are involved in proper decoding, expanded base-pair interactions beyond W-C, ribosome fidelity, and ribosome frame maintenance at a more discrete level.

F.2 Discussion of Results

Current work has revealed that either the N1 and N6 guanosine H-bond donor or acceptor, respectively, are both integral for proper base-pair formation and amino-acid addition, with N1 appearing to be the most important. As expected, these bonds are not necessary at the third position codon. Strikingly, introduction of a methyl group, with two degrees of rotational freedom, as is the case in m2G is sufficient to drastically slow amino acid addition when positioned at the third nucleotide of the codon (Appendix F, Figure 2). This suggests that hydrophobic and stereochemical interactions are important at this position but have the potential to be disrupted by modifications to the mRNA. This is more interesting when we consider that both tRNAVal and tRNAArg harbor modifications at position 34 (cmo5U34 and m2A34, respectively), suggesting that there is an important interplay and communication between modified mRNA and tRNA. This could open up exploration of a new avenue of decoding mechanisms that tRNAs and the ribosome use to recognize mRNA substrates [15], [16].

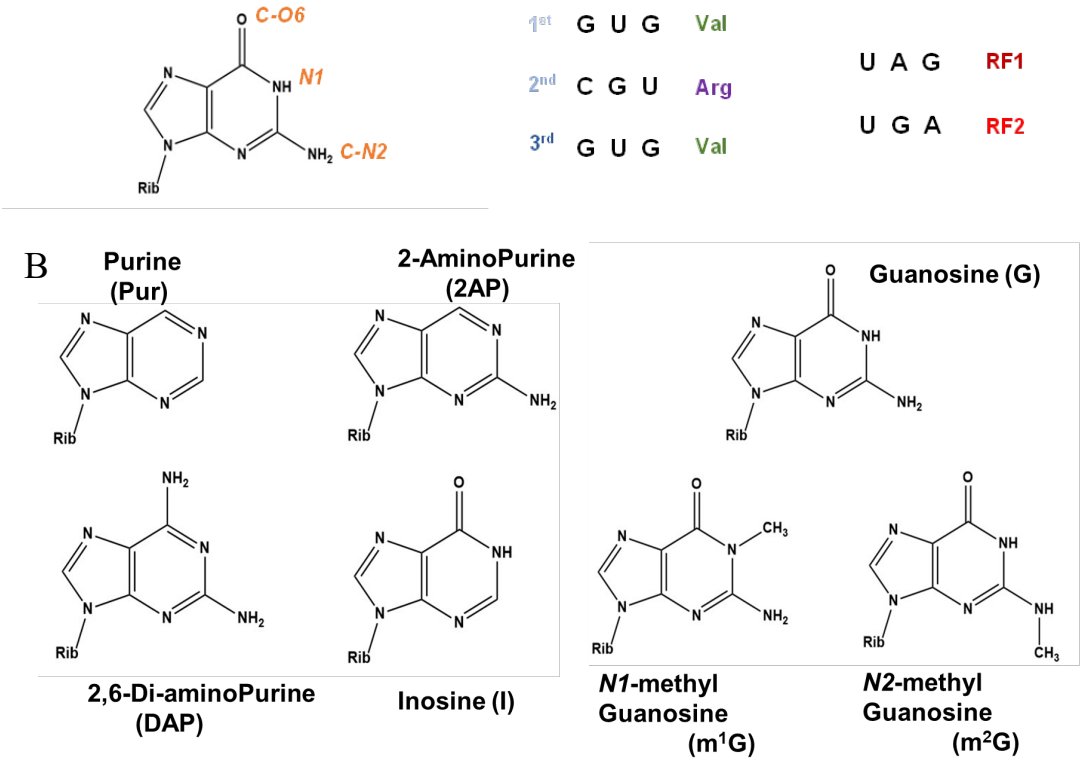

Figure F.2.1 *(A) The guanosine purine nucleobase has three potential Watson-Crick face H-bonds with either a ketone H-bond acceptor or amino group H-bond donor. In this study the valine, arginine, and release factor codons will be used to assess both codon and molecule position dependence of modification. (B) Examples of modifications to guanosine which are found naturally within mRNAs or in nucleotide biosynthesis pathways which are to be studied in this work.*

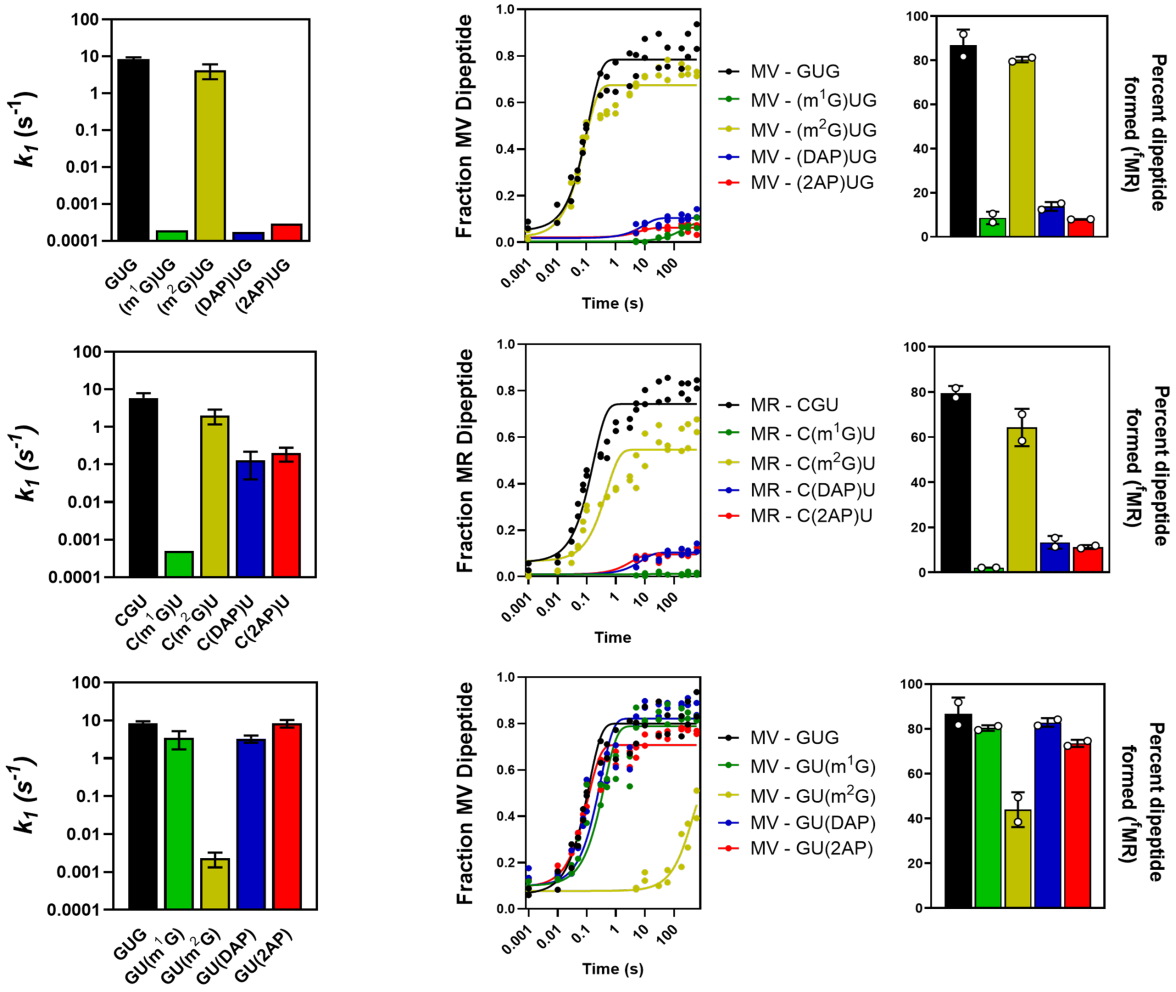

Figure F.2.2 *The rate constants, peptide formation curves, and final peptide percent formed for peptide synthesis or mRNAs encoding for either Met-Val (AUG-GUG) or Met-Arg (AUG-CGU) with guanosine modifications positioned at either the first, second, or third position of the codon.*

F.3 References

[1] N. Demeshkina, L. Jenner, E. Westhof, M. Yusupov, and G. Yusupova, "A new understanding of the decoding principle on the ribosome," Nature, vol. 484, no. 7393, Art. no. 7393, Apr. 2012, doi: 10.1038/nature10913.

[2] P. F. Agris, E. R. Eruysal, A. Narendran, V. Y. P. Väre, S. Vangaveti, and S. V. Ranganathan, "Celebrating wobble decoding: Half a century and still much is new," RNA Biol., vol. 15, no. 4–5, pp. 537–553, Sep. 2017, doi: 10.1080/15476286.2017.1356562.

[3] F. H. C. Crick, "Codon—anticodon pairing: The wobble hypothesis," p. 8.

[4] A. Rozov, N. Demeshkina, I. Khusainov, E. Westhof, M. Yusupov, and G. Yusupova, "Novel base-pairing interactions at the tRNA wobble position crucial for accurate reading of the genetic code," Nat. Commun., vol. 7, Jan. 2016, doi: 10.1038/ncomms10457.

[5] T. P. Hoernes et al., "Translation of non-standard codon nucleotides reveals minimal requirements for codon-anticodon interactions," Nat. Commun., vol. 9, Nov. 2018, doi: 10.1038/s41467-018-07321-8.

[6] P. Boccaletto et al., "MODOMICS: a database of RNA modification pathways. 2021 update," Nucleic Acids Res., vol. 50, no. D1, pp. D231–D235, Dec. 2021, doi: 10.1093/nar/gkab1083.

[7] M. D. Berg and C. J. Brandl, "Transfer RNAs: diversity in form and function," RNA Biol., vol. 18, no. 3, pp. 316–339, doi: 10.1080/15476286.2020.1809197.

[8] K. E. Sloan, A. S. Warda, S. Sharma, K.-D. Entian, D. L. J. Lafontaine, and M. T. Bohnsack, "Tuning the ribosome: The influence of rRNA modification on eukaryotic ribosome biogenesis and function," RNA Biol., vol. 14, no. 9, pp. 1138–1152, Dec. 2016, doi: 10.1080/15476286.2016.1259781.

[9] M. K. Franco and K. S. Koutmou, "Chemical modifications to mRNA nucleobases impact translation elongation and termination," Biophys. Chem., vol. 285, p. 106780, Jun. 2022, doi: 10.1016/j.bpc.2022.106780.

[10] D. Czernecki, P. Legrand, M. Tekpinar, S. Rosario, P.-A. Kaminski, and M. Delarue, "How cyanophage S-2L rejects adenine and incorporates 2-aminoadenine to saturate hydrogen bonding in its DNA," Nat. Commun., vol. 12, p. 2420, Apr. 2021, doi: 10.1038/s41467-021-22626-x.

[11] J. D. Jones et al., "Methylated guanosine and uridine modifications in *S. cerevisiae* mRNAs modulate translation elongation." bioRxiv, p. 2022.06.13.495843, Jun. 13, 2022. doi: 10.1101/2022.06.13.495843.

[12] C. You, X. Dai, and Y. Wang, “Position-dependent effects of regioisomeric methylated adenine and guanine ribonucleosides on translation,” Nucleic Acids Res., vol. 45, no. 15, pp. 9059–9067, Sep. 2017, doi: 10.1093/nar/gkx515.

[13] V. de Crécy-Lagard and M. Jaroch, “Functions of Bacterial tRNA Modifications: From Ubiquity to Diversity,” Trends Microbiol., vol. 29, no. 1, pp. 41–53, Jan. 2021, doi: 10.1016/j.tim.2020.06.010.

[14] Y. Zhang et al., “A Semi-Synthetic Organism that Stores and Retrieves Increased Genetic Information,” Nature, vol. 551, no. 7682, pp. 644–647, Nov. 2017, doi: 10.1038/nature24659.

[15] D. Arango et al., “Acetylation of cytidine in mRNA promotes translation efficiency,” Cell, vol. 175, no. 7, Art. no. 7, 2018.

[16] A. Kintanar, D. Yue, and J. Horowitz, “Effect of nucleoside modifications on the structure and thermal stability of *Escherichia coli* valinetRNA,” Biochimie, vol. 76, no. 12, pp. 1192–1204, Jan. 1994, doi: 10.1016/0300-9084(94)90049-3.